

On the colonisation and alteration of stony meteorites by microorganisms from the Nullarbor Plain, Australia: Applications for future astrobiology exploration on Mars

By
Alastair William Tait
BSc(Hons)

A thesis submitted for the degree of
Doctor of Philosophy

Main Supervisor: Dr. Siobhan A. Wilson
Associate Supervisor: Dr. Andrew G. Tomkins

School of Earth, Atmosphere and Environment
Monash University, Clayton, Victoria, Australia



MONASHUniversity

Copyright Notice

© Alastair W. Tait (2017), except as provided in the Copyright Act 1968, this thesis may not be reproduced in any form without the written permission of the author.

Thesis Declaration

I hereby declare that this thesis contains no material which has been accepted for the award of any other degree or diploma at any university or equivalent institution and that, to the best of my knowledge and belief, this thesis contains no material previously published or written by another person, except where due reference is made in the text of the thesis.

This thesis includes two original papers accepted for publication in peer reviewed journals; one currently under review, and one un-published publication. The core theme of the thesis is to investigate the potential microbial habitability of meteorites sitting on planetary surfaces to expand the search for life in the solar system. The ideas, development and writing up of all the papers in the thesis were the principal responsibility of myself, the student, working within the School of Earth, Atmosphere and Environment under the supervision of Dr. Siobhan A. Wilson and Dr. Andrew G. Tomkins.

The inclusion of co-authors reflects the fact that the work came from active collaboration between researchers and acknowledges input into team-based research.

In the case of chapters 2, 3, 4 and 5 my contribution to the work involved the following:

Thesis chapter	Publication title	Status	Nature and % of student contribution	Co-author name(s) nature and % of co-author's contributions
2	Evaluation of meteorites as habitats for terrestrial microorganisms: Results from the Nullarbor Plain, Australia, a Mars analogue site	Accepted for Publication	80% - Conceptualisation, data collection, experimental design, field work, data interpretation, writing.	5% - S. Wilson, Supervisor. 5% - A. Tomkins, Supervisor. 5% - E. Gagen, Experimental Design. 2.5% - G. Southam, Advisor. 2.5% - S. Fallon, Radiocarbon data analysis.
3	Growth of naturally occurring chasmoendolithic microorganisms within chondritic meteorites recovered from the Nullarbor Plain, Australia: Applications to microhabitat discovery on Mars	In Preparation	82.5% - Conceptualisation, data collection, experimental design, field work, data interpretation, writing.	5% - S. Wilson, Supervisor. 5% - E. Gagen, Experimental Design. 5% - A. Tomkins, Supervisor. 2.5% - G. Southam, Advisor.
4	Microbial populations of stony meteorites: Substrate controls on first colonisers	Accepted for Publication	75% - Conceptualisation, data collection, experimental design, field work, data interpretation, writing.	5% - S. Wilson, Supervisor. 5% - A. Tomkins, Supervisor. 10% - E. Gagen, Experimental Design, DNA extraction. 5% - G. Southam, Advisor.
5	Laboratory induced $\delta^{34}\text{S}$ biosignature in the Chelyabinsk LL5 chondrite: Using terrestrial microorganisms to refine tools for exobiology discovery on the surface of Mars	Submitted for Publication	77% - Conceptualisation, data collection, experimental design, field work, data interpretation, writing.	5% - S. Wilson, Supervisor. 5% - A. Tomkins, Supervisor. 5% - E. Gagen, Experimental Design. 2% - G. Southam, Advisor. 2% - S. Golding, CF-IRMS analysis. 2% - B. Morgan, Sulfate analysis. 2% - A. Liu, FIB user and data interpretation.

I have renumbered sections of submitted or published papers in order to generate a consistent presentation within the thesis.

Student signature:



Date: 01/06/2017

The undersigned hereby certify that the above declaration correctly reflects the nature and extent of the student's and co-authors' contributions to this work. In instances where I am not the responsible author I have consulted with the responsible author to agree on the respective contributions of the authors.

Main Supervisor signature:



Date: 01/06/2017

Table of Contents

Copyright NoticeIII
General Declaration	V
List of Figures	XIII
List of TablesXXI
AcknowledgementsXXII
AbstractXXVII

Chapter 1 1

Introduction to exogenic meteorites as refuge habitats for life on Mars.

1.1 Introduction	3
1.1.1 A quick note on nomenclature.4
1.1.2 Panspermia versus microbial colonisation of exogenic meteorites4
1.1.3 Motivation for microbial habitation of exogenic meteorites5
1.1.4 Meteorite flux to the martian surface6
1.1.5 Meteorite Residence Times on Earth and Mars9
1.1.6 Weathering Products of Stony Meteorites.	10
1.1.7 The Possibility of Microbial Life at or near the Martian Surface	12
1.1.8 Possible Microbial Metabolisms on Mars	12
1.1.9 Bioavailable Nutrient and Energy Sources in Stony Meteorites	15
1.1.10 Sources of Water on the Surface of Mars	16
1.1.11 Inclusion into the MEPAG “Special Regions” Framework	18
1.2 Conclusions	19
1.3 Thesis Structure	19
1.4 Chapter 1 References	22

Chapter 2 33

Evaluation of meteorites as habitats for terrestrial microorganisms: Results from the Nullarbor Plain, Australia, a Mars analogue site.

2.1 Introduction	35
2.2 Methods	39
2.2.1 Meteorite Sample Description.	39
2.2.2 Powder X-ray Diffraction	40

2.2.3	Stable and Radiogenic Isotope Geochemistry	41
2.2.4	Water Sorption Isotherms	42
2.2.5	Scanning Electron Microscopy	42
2.3	Results	43
2.3.1	Stable and Radiogenic Isotopes	43
2.3.2	Mineralogy and Sorption Behavior of Vein Material	43
2.3.3	Mineral–Microbe Associations	47
2.4	Discussion	47
2.4.1	Fingerprinting the Origin of Carbonate Veins	47
2.4.2	Hygroscopic Vein Minerals and Water Cycling	48
2.4.3	Generation of Veins and Porosity within Meteorites	49
2.4.4	Colonization of Veins and Pore Networks by Contaminant Microorganisms	50
2.4.5	Practicality of Finding Meteorites on Mars	51
2.5	Implications	53
2.5.1	Robotic Investigation of Meteorites to Assess Merit of Sample Return	53
2.5.2	A Model for Microbial Colonization and Habitation of Chondrites on Earth and Mars	54
2.6	Conclusions	56
2.7	Chapter 2 References	57

Chapter 3

67

Growth of naturally occurring chasmoendolithic microorganisms within chondritic meteorites recovered from the Nullarbor Plain, Australia: Applications to microhabitat discovery on Mars.

3.1	Introduction	69
3.2	Methods	70
3.2.1	Meteorite Specimens	70
3.2.2	Experiment 1: Infiltration of meteorites by microorganisms	71
3.2.2.1	Media Modification and Culturing.	71
3.2.3	Experiment 2: Biofilm Exhumation	72

3.2.3.1. Acid Etch	72
3.2.3.2 Scanning Electron Microscopy (SEM)	73
3.3 Results	73
3.3.1 Cellular Penetration Experiment	73
3.3.2 Biofilm Exhumation Experiment	78
3.4 Discussion	80
3.4.1 Microbial Penetration	80
3.4.2 Fossilization Potential	83
3.4.2.1. Exhumation of Biomorphic Features From Alteration Minerals	83
3.4.2.2 Alternate Techniques and Follow up Studies	85
3.5 Conclusions	86
3.6 Chapter 3 References	87

Chapter 495

Microbial populations of stony meteorites: Substrate controls on first colonisers.

4.1 Introduction	97
4.2 Methods	101
4.2.1 Field Sampling	101
4.2.2 Meteorite Sample Description.	102
4.2.3 DNA extraction and sequencing	103
4.2.4 Sequence Processing	105
4.2.5 Sequence Analysis	105
4.3 Results	106
4.3.1 Major OTU Classification	106
4.3.2 Alpha Diversity Indices	108
4.3.3 Beta Diversity	108
4.3.4 OTU Abundance	109
4.3.5 OTU Correlations.	110
4.4 Discussion	110
4.4.1 Meteorite Colonisation	110

4.4.2 Comparison to Other Soils	114
4.4.3 Comparison to Volcanic Rocks	115
4.5 Conclusions	117
4.6 Chapter 4 References	118

Chapter 5129

Laboratory induced $\delta^{34}\text{S}$ biosignature in the Chelyabinsk LL5 chondrite: Using terrestrial microorganisms to refine tools for astrobiological exploration on the surface of Mars.

5.1 Introduction	131
5.2 Methods	135
5.2.1 Experimental Design	135
5.2.1.1. Experimental Overview.	135
5.2.1.2. Meteorite and Sulfide Mineral Substrates	135
5.2.1.3. Model Organism	136
5.2.1.4. Experimental Setup	137
5.2.1.5. Media and Culturing	138
5.2.1.6. Sulfur Mixing	139
5.2.2 Analytical Methods	140
5.2.2.1. Cell Counting.	140
5.2.2.2 Dissolved Sulfate Concentrations	140
5.2.2.3 Scanning Electron Microscopy	140
5.2.2.4 Focused Ion Beam - Scanning Electron Microscopy	141
5.2.2.5 Powder X-ray Diffraction	142
5.2.2.6 Continuous Flow - Isotope Ratio Mass Spectrometry (CF-IRMS) for $\delta^{34}\text{S}$	142
5.3 Results	145
5.3.1 Cell-Counting and UV-Microscopy	145
5.3.2 Aqueous sulfate concentration.	145
5.3.3 Scanning Electron Microscopy on Mineral and Meteorite Surfaces	147
5.3.4 Cross Sections Through Meteorite Samples	150

5.3.5	Focused Ion Beam - Scanning Electron Microscopy	152
5.3.6	Powder X-Ray Diffraction	153
5.3.7	Stable Sulfur Isotopes	155
5.4	Discussion	156
5.4.1	Fossilisation of Bacteria During Sulfide Oxidation	156
5.4.2	Elemental and Mineralogical Biosignatures in Biotic Experiments	158
5.4.3	Stable Sulfur Isotope Mixing in Abiotic Experiments	160
5.4.4	Isotopic $\delta^{34}\text{S}$ Biosignatures	160
5.4.4.1.	The Null Hypothesis	161
5.4.4.2.	Sulfur Assimilation	162
5.4.4.3.	Degassing of Isotopically Light $^{32}\text{SO}_2$, Build up of Ferrous Iron and a Switch Metabolic Mode	162
5.4.4.4.	Reduction of Native Sulfur in Anoxic Microenvironments	164
5.4.5	Comparisons of Experimental Meteorite Results to Nullarbor Finds	164
5.4.6	Using Meteorites on Mars for Biomarker Detection	166
5.5	Conclusions	167
5.6	Chapter 5 References	169

Chapter 6

177

Meteorites as a universal habitat: A summary of microbial colonisation on Earth and applications for Mars and beyond.

6.1	Introduction	179
6.1.1	Summary of Terrestrial Microbial Colonisation of Chondrites	179
6.1.2	Application to the Search for Life on Mars	182
6.1.3	Future Research Directions and Applications	185
6.1.3.1.	Functional Gene Analysis	185
6.1.3.2.	Putative Heterotrophic Metabolisms on Mars	186
6.1.3.3.	Carbonaceous Meteorites on Mars	186
6.1.3.4.	Iron Meteorites on Mars	187
6.1.3.5.	Application to the Study of Life on Early Earth	187

6.1.3.6. Applications to Asteroid Mining	188
6.2 Concluding Remarks	189
6.3 Chapter 6 References	190

Appendix I 199

Data processing and analysis commands used in MOTHUR for Chapter 4.

Appendix II 207

Additional data tables from Chapter 5.

Chapter 1

Figure 1.1 | ALH84001 Biomorphs. These Scanning Electron Images (SEI) are taken from (McKAY *ET AL.*, 1996). They show claimed nano-scale “microfossils” from the ALH84001 martian meteorite. These tubular structures are smaller than any known on Earth bacteria, and below the lower limit for what is considered feasible for terrestrial life. The most likely explanation is that they are coating artefacts. (Images used with permission from copyright holder). 4

Figure 1.2 | Meteor Entry. This diagram is taken from (CHAPPELOW & GOLOMBEK 2010). Numbers (0–4) correspond to the possible fates of meteoroids entering a planetary atmosphere (for a detailed description of each see text). On Mars Types 2, 3 in this diagram are most likely to produce meteoroids. “H” is the horizon from the point of entry of the meteoroid. (Images used with permission from copyright holder) 7

Figure 1.3 | Examples of Iron Meteorites on Mars. (A) An iron meteorite, named ‘Block Island’ found by the MER rover Opportunity in 2009 at Meridiana Planum measuring 67 cm in length. **(B)** Three iron meteorites likely from the same fall found by MSL rover Curiosity, Sol 640, at Gale crater 2014. The larger of the three is 2 m wide. 8

Chapter 2

Figure 2.1 | Suitability of astromaterials for detection of biological $\delta^{34}\text{S}$ signatures. The left hand side shows $\delta^{34}\text{S}$ ranges of sulfur-bearing phases in astromaterials. The right hand side plots predicted $\delta^{34}\text{S}$ ranges of secondary minerals (alteration) in ordinary chondrites (OC) affected by some common sulfur oxidising/reducing organisms and abiotic processes. Isotopic fractionation by terrestrial organisms far exceeds the range of $\delta^{34}\text{S}$ values found in ordinary and enstatite chondrites, but is largely within the range found in SNC meteorites. See (FARQUHAR *ET AL.*, 2007; GREENWOOD *ET AL.*, 1997) and references therein for astromaterial values and (BALCI *ET AL.*, 2007; BRABEC *ET AL.*, 2012; CANFIELD, 2001; PISAPIA *ET AL.*, 2007) for values pertaining to fractionation processes. . . . 36

Figure 2.2 | Vein-carbonate Origin and Potential Contamination. Values of $\delta^{13}\text{C}$ versus F_m (^{14}C) are plotted here for meteorite vein material and Nullarbor limestone. $\delta^{13}\text{C}$ values for calcite precipitating in equilibrium with atmospheric CO_2 gas (grey box), are calculated over the typical range of temperatures recorded in the Nullarbor using the fractionation factors of Deines and others (1974). The estimated proportion of contamination (c), from windblown dust and limestone, is given for each meteorite analysed. 40

Figure 2.3 | Adsorption Isotherms for Vein Material. Green = *Ooldea* 002 (L5, W4), orange = *Watson* 015 (H4, W4), purple = *Ooldea* 007 (H3, W4). Filled circles denote sorption steps and empty circles denote desorption. 40

Figure 2.4 | Humidity Oasis. This figure is a stitch of a reflected light image from a petrographic microscope, of the *Ooldea* 009 (H6, S3, W3) chondrite. Phases and voids were determined by scaling the LUT (Look up table), and then artificially colored. **(A)** Original reflected light image. **(B)** Processed image shows void spaces (red) in the centre of *Ooldea* 009. The reduced rim contains unoxidised troilite (yellow) and FeNi alloy (blue). 42

Figure 2.5 | Jarosite in Corrosion Cavity. The above Backscattered Electron (BSE) image and inset Energy Dispersive Spectroscopy (EDS) maps of S and K $K\alpha$ show a corrosion cavity inside the *Ooldea* 005 ordinary chondrite. FeNi and FeS have been oxidised and removed from the system along cracks, leaving behind Fe-(oxy)hydroxides and jarosite (Jrs). 43

Figure 2.6 | Chasmoendolithic Biofilm and Calcite Etching. FEG-SEM micrographs of **(A)** carbonate vein material in *Ooldea* 007 hosting a bacterial biofilm, composed of several, morphologically distinct prokaryotes (highlighted in circles). **(B)** At higher magnification, we see bacteria (arrows) with a fuzzy surface, this is either a mineral precipitate or folded gram-negative cell envelopes. The appearance of pitted and etched scalenohedral calcite suggests that the bacteria are promoting the dissolution of carbonate. **(C)** Heavily etched scalenohedral calcite was particularly visible where the sample dehydration process had peeled the exopolymer (EPS) off of the surface, e.g., *Watson* 017. 44

Figure 2.7 | Cryptoendolithic Biofilm. Continued growth of biofilm (within *Ooldea* 007) has resulted in the formation of corrosion cavities. **(A)** Note the ‘soft texture’ of the inside of the corrosion pit, which is consistent with the presence of exopolymer. Energy dispersive spectroscopy demonstrated the presence of iron oxide proximal to a carbonate vein, which may have aided corrosion. Representative high magnification images (boxes ‘B’ and ‘C’) reveal the presence of bacteria undergoing cell division (arrows) lining the corrosion pit. 45

Figure 2.8 | Biologically-mediated Silicate Etching. FEG-SEM micrograph of *Watson* 017 highlighting the occurrence of diopside, overlain by EPS and bacteria, possessing a ‘sawtooth’ dissolution texture (GIBSON *ET AL.* 1983) demonstrating that bacterial biofilms are also linked to silicate weathering. 46

Figure 2.9 | Meteorite Habitat Model for Mars. This model shows the key properties of a meteorite habitat on Mars. 55

Chapter 3

Figure 3.1 | Penetration of Microbes Into Meteorites. Back Scatter Electron (BSE) images from meteorites incubated in acidophilic sulfur oxidizing enrichment medium for three months. **(a)** Meteorite *Ooldea 003* shows a colony of ~5 μm cocci in a corrosion cavity. This cavity appears cut off from the surface of the meteorite, but microbes probably infiltrated from a crack above or below the plain of the polished cross section. The colony is ~400 μm from the edge of the meteorite fragment. The diffuse Os-stained rim and cell shape are likely products of non-ideal Os and resin penetration at depth within the sample. **(b)** Meteorite *Watson 015*, which is moderately brecciated (S3), also contains ~5 μm cocci within a crack at least 250 μm from the surface of the meteorite. Many of the cocci show what appears to be a nucleus/organelle (arrows in insert). Their large size suggests that they may be eukaryotic. 74

Figure 3.2 | Cell Morphologies in Penetration Experiments. High magnification BSE micrographs revealing microbial structural diversity. **(A)** *Watson 015* shows a variety of morphological types for chasmoendoliths including cocci and bacilli that are ~5 μm in diameter. Microcolonies of 0.5 μm cocci (contrast scaled insert) are also present. **(B)** This image is of *Watson 014* and it shows cryptoendolithic coccobacilli and cocci inside the meteorite. **(C)** An epilithic colony of cocci (or tangentially cut rods) on *Watson 015*. **(D)** Lastly, this image of *Watson 015* shows more chasmoendolithic communities of ~5 μm cocci. These are large for bacteria suggesting that many of these microorganisms are eukaryotic. Arrows point to possible nucleolus/organelles. Poor cell-wall contrast is due to the non-ideal distribution of the Os stain at depth inside the meteorite. 75

Figure 3.3 | Biofilm Acid Etch and Control. These secondary electron images (SEI) show meteorite *Ooldea 007*. The images are of a control sample that was not acid etched (A,B), and a sample that was acid etched (C,D). **(A)** This image shows cells and their biofilm on the carbonate–gypsum surface. **(B)** This image shows a single cell in the centre of the image with dried EPS forming struts around the cell. Above this is a cell in the process of cellular division. **(C)** Here we see the modern biofilm (MB) pulling away from the carbonate–gypsum substrate in response to the acid etch and fixation. **(D)** This image also shows the modern biofilm pulling away from the carbonate–gypsum admixture, as well as a curled over segment of the EPS. 76

Figure 3.4 | Exhumed Biofilm. These secondary electron images (SEI) show the results of acid etching on meteorite *Ooldea 007*. **(A)** Multiple layers of modern biofilm (MB), carbonate–gypsum admixture and a paleobiofilm (PB) overlaying Fe-(oxy)hydroxide. Dotted lines demark the borders of the key layers. Arrows point to cocci (~3–5 μm) and rod-shaped (~3 μm) biomorphs on suspected paleobiofilm. Biomorphs are covered in wisps of calcite and gypsum. **(B)** An acid etched

carbonate-gypsum admixture. Exhumed micrometre-scale cocci and rods are coated in a web of undissolved calcite, resistant gypsum and EPS, whereas detrital microbes that have fallen in from the modern biofilm do not possess such features. This colony has also pulled away and shrunk from the surrounding calcite–gypsum admixture during the fixation process, leaving an imprint around the top of the feature. **(C)** This image shows the base of a layer of carbonate–gypsum that broke off during acid etching, an exhumed rod covered in detritus, and the Fe-(oxy)hydroxide surface beneath. 76

Figure 3.5 | Diatom. This secondary electron image (SEI) shows a pennate diatom on the vein material inside the meteorite, *Watson 015*. **(A)** (5 kV SEI) Extensive biofilm of environmental microorganisms covers ~90% of the surface area of this diatom (as well as other surface material). **(B)** (15 kV SEI) Many rows of puncta can be seen beneath the microbes, including where a dorsal raphe would be indicating this diatom is most likely a member of the order Fragilariophyceae. 78

Chapter 4

Figure 4.1 | Nullarbor Plain Map. This figure shows the Watson location in the Nullarbor Plain, Australia. Circles indicate the locations from which the four meteorites and associated soils were collected. 99

Figure 4.2 | Meteorite Samples This figure shows two meteorites used in the experiment and depicts field-based sub-sectioning methods. **(a)** Sample *Watson 021* in situ. **(b)** Sample *Watson 019* in situ after being flipped over during collection. **(c)** Sample *Watson 019* being sub-sectioned over autoclaved aluminium foil. 100

Figure 4.3 | Heatmap of OTU Abundance. Heatmap analysis of OTU abundance in meteorites and soil samples. Analysis performed for OTUs at a distance of ≤ 0.03 . The scale bar represents the fractional abundance of each OTU within each sample. The identity score, accession number, and the name of the nearest named isolate according to NCBI BLAST are indicated on the righthand side of the heatmap. OTUs that were classified no deeper than bacteria in the Silva database are also noted. 103

Figure 4.4 | Phyla and Actinobacteria Abundance of Meteorites and Soil This figure shows the relative abundance of different phyla and classes. **(a)** The major phyla classified according to the Silva taxonomy identification. ‘Other’ phyla include all phyla present at abundances less than 3%. ‘Bacteria Unclassified’ were OTUs that could not be classified below the domain Bacteria. **(b)** Taxonomic composition of the important soil phylum, Actinobacteria. 104

Figure 4.5 | Community Structure Dissimilarity. This calculation was made using Yue and Clayton (2005) indices at a clustering distance of ≤ 0.03 . The colours are scaled to the highest level of similarity between any two samples (red) and the lowest level of similarity (black). The white outline represents the direct comparison between the meteorite and its underlying soil. 105

Figure 4.6 | Rarefaction Curve. Rarefaction analysis of all samples at a clustering distance of ≤ 0.03 . Warm colours are soil samples, cool colours are meteorites. 106

Figure 4.7 | Non-metric Multidimensional Scaling. NMDS plot for Nullarbor meteorite (MA, MB, MC, MD) and soil (SB, SC SD) samples based on the Yue and Clayton (2005) community structure. The stress value is 0.146 (a measure of fitness < 0.2 is considered good (LEVSHINA, 2015)). 106

Chapter 5

Figure 5.1 | UV Microscopy of *A. ferrooxidans*. These two fluorescent light micrographs fluorescent light micrographs were taken on a UV petrographic microscope using a Petroff-Hausser counting chamber. Microbes were stained with Syto 9, and were photographed at the 1-week time step. **(A)** This image is from the supernatant of a meteorite slice experiment. Notice *A. ferrooxidans* cells (white arrowheads) colonizing a large suspended sulfate grain (XRD inferred mineralogy). **(B)** This image is of the supernatant collected from a pyrite experiment. It shows *A. ferrooxidans* cells attached to grains of pyrite (white arrows). The dim cells in this image are due to prolonged UV bleaching during counting. 142

Figure 5.2 | Cell Counts in Supernatant. These four graphs show the concentration of cells mL^{-1} in the supernatant at each time step. Dashed lines represent a missing time step. The dotted line at the bottom of each graph is the minimum number of cells that can be counted in the chamber. . . . 143

Figure 5.3 | Sulfate Concentration in Supernatant. Dissolved sulfate concentrations in each treatment throughout the experiments. The top four subfigures show the relative change in sulfate concentration compared to starting concentrations (biotic = 183.3 ppm, abiotic = 2006.3 ppm). Dotted lines represent missing data between measurements. The four upper subfigures plot average sulfate concentration for replicate experiments at each time step. The four bottom subfigures show the absolute concentration of sulfate for all experiments. Not all samples have week 4 data due to drying out. 144

Figure 5.4 | Fe-(oxy)hydroxide Efflorescence and Surface Variation. These BSE and petrographic microscope images show polished sections of the Chelyabinsk meteorite from abiotic and biotic experiments at different time steps. **(A)** BSE image of an efflorescence at 24 hrs on *Meteorite 09*, an abiotic sample. The efflorescence is characterized by platy and botryoidal Fe-(oxy)hydroxides covering a FeS or FeNi grain. **(B)** An efflorescence on *Meteorite 12*, a biotic experiment, at one week. It is much thicker than the abiotic efflorescence and characterized by a core of predominantly platy material, surrounded by botryoidal Fe-(oxy)hydroxides and a halo of Fe-bearing nanoparticles. **(C)** A petrographic image of *Meteorite 11*, an abiotic experiment, at 2 weeks. Detrital Fe-(oxy)hydroxides and Fe-phosphates cover the thick section. What were once discrete efflorescences, have grown to coat most of the surface. **(D)** A petrographic image from the biotic *Meteorite 06* experiment at 2 weeks. The surface is relatively clear of efflorescences except for at the surfaces of FeNi-alloy and troilite grains, which bear extensive efflorescences. Although efflorescences are more numerous in biotic experiments, they are smaller than the abiotic ones. **146**

Figure 5.5 | SEM Images of Meteorite Cross-Sections. These BSE images were taken at the 4-week time step from biotic and abiotic samples that were Os stained and impregnated with resin. They show cross-sections through the meteorites and their weathering products. **(A, B)** Both images are of *Meteorite 20*. They show epilithic micro-colonies of *A. ferrooxidans* encased and fossilized within a layer of Fe-(oxy)hydroxide minerals. Arrows point to cells. **(C)** This image shows an efflorescence in cross section from *Meteorite 04*, a biotic experiment. Notice the efflorescence formed on a troilite grain that later was etched away to leave an empty space that is now filled with resin. **(D)** This is an image of *Meteorite 05*, an abiotic experiment. It shows troilite and FeNi-alloy grains that have been etched by the acidic media. As in the biotic samples, efflorescence can be seen forming over the grain, which is being etched away to leave a void. **148**

Figure 5.6 | Bacteria-Mineral Spatial Relationships. These secondary electron images (SEI) are of *Meteorite 08*, from a biotic experiment, after 4 weeks. **(A)** A large FeS grain (dotted line) is covered in EPS, which has peeled back in places. This EPS does not extend to the silicate minerals surrounding the troilite grain. The sulfide grain is extensively etched. **(B)** This micrograph is from the same sulfide grain in (A). It shows the EPS peeling back to expose the troilite underneath. *A. ferrooxidans* cells can be seen embedded in the mineralized biofilm. **(C)** This shows a pitted and weathered FeNi-alloy grain surrounded by silicate minerals. From the polished surface of the silicate grain it is clear that the metal alloy grain has become recessed by ~2 μm . The grain is covered in Fe-(oxy)hydroxide grains and bacteria that are covered in the same material. **(D)** This shows a troilite grain with etched [001] planes. It is covered by a thin film of EPS and bacteria.. . . . **149**

Figure 5.7 | Focused-Ion-Beam Cross-Section and SEM EDX Maps. These images show meteorite samples from one biotic and one abiotic experiment. Each sample had a Focused Ion Beam (FIB) trench cut through an efflorescence into the underlying substrate. Both images were tilted to 38° from the EDX detector. These BSE images were horizontally compressed to adjust for the 50° tilt used on the SEM whilst EDX mapping. Displayed in both images are quantitative element maps of elements (i.e., O, S, Fe, P, N, and K) that include a semi-quantitative measure of elemental abundance in wt.%. Both 5 kV and 15 kV accelerating voltages were used; images collected at 5 kV were binned twice. Vertical striations are FIB cutting artefacts due to the uneven specimen surface. **(A)** This image shows the biotic sample, *Meteorite 12*, at 1 week. The underlying substrate is FeNi-alloy. A distinct gap can be seen at the interface between the FeNi-alloy grain and efflorescence, indicated by a sulfur- and oxygen-rich interlayer (insert: arrows). A thin layer containing elevated phosphorus, potassium and nitrogen is also observed at this interface. **(B)** SEM micrograph of the abiotic sample, *Meteorite 17*, at 48 hrs. The underlying substrate is troilite. There is no gap at the interface between the FeS grain and the efflorescence and the contact between them is very sharp. There is no oxidized interlayer (insert: arrowheads). The efflorescence in the abiotic sample is more phosphorus-rich than the biotic sample. No noticeable potassium or nitrogen layer exists in the abiotic efflorescence. . . .151

Figure 5.8 | $\delta^{34}\text{S}$ Results. This figure shows the $\delta^{34}\text{S}$ results from the CF-IRMS analysis. Not all samples gave results due to their small size. **(a)** The bottom row of values shows the starting isotopic reservoirs, whereas the upper rows show results from biotic (Green) and abiotic (orange) experiments. The abiotic values in the meteorite experiment plot close together, the symbols are efflorescence (Square), BaSO_4 (triangle with white outline). The biotic meteorite experiment produces positive fractionation away from the starting reservoir (chondritic troilite), indicating biological sulfur assimilation. In all abiotic experiments, abiotic oxidation of the substrate resulted in a negative fractionation. Linear mixing trends between reservoirs and fractional contributions to sulfate in alteration minerals are indicated. **(b)** Isotopic differences between alteration products and substrates used in experiments (e.g., meteoritic troilite, synthetic troilite powder, pyrite powder). The green shaded fields are the fractionation ranges of sulfates produced during the ‘initial’ and ‘main’ stages of biotic pyrite leaching experiments in Brunner et al. (2008). The orange field is the abiotic oxidation of pyrite by O_2 (BALCI ET AL. 2007). Note that the abiotic fractionations do not plot in the field for abiotic sulfide oxidation. This is the result of reservoir mixing with ‘contaminant’ sulfate (i.e., melanterite in the medium). . . .

Chapter 2

Table 2.1 Abundances of Minerals in Vein Material by Rietveld Refinement.	38
---	----

Chapter 4

Table 4.1 Sample List and Alpha Diversity.	101
--	-----

Chapter 5

Table 5.1 $\delta^{34}\text{S}$ Values for Experimental Precipitates and Substrates.	153
---	-----

Appendix I

Appendix I: Table 1 Indicator Species list and Iron/Sulfur Cycling Species	200
---	-----

Appendix II

Appendix II: Table 1 Substrate Sample Weights and Initial Sulfur Content.	209
--	-----

Appendix II: Table 2 Powder XRD Phase Analysis Results.	210
--	-----

Acknowledgements

I have been extremely fortunate to have had Sasha and Andy as supervisors during my candidacy. Sasha has taught me so much about environmental geochemistry over the years. There is no technique she doesn't know, but it's what she has taught me about being a mentor and a future academic that I've found most significant. From day one she has had an open door policy and her enthusiasm for teaching encouraged me to follow my own learning path to see where it led. I have found that so important. Sasha is the nicest, smartest person I know and a great friend who is always there to help. It has been a privilege.

I have come to the conclusion that a PhD is the fastest way to spend three and a half years. It does not seem all that long ago that Andy shouted me lunch on the first day of my PhD. Andy was my honours and third year research project supervisor before being my associate PhD supervisor, so I knew what to expect. Like Sasha, Andy is a mentor that always has time for his students; someone enthusiastic about not only his research but also that of his students – a real renaissance styled teacher. Andy has been very much a mentor to me over the last few years, regularly offering advice and direction. My only regret will be missing out on settling down to a plate of his Nullarbor desert spag-bowl and a healthy serving of his geology-themed dad jokes after a long day hunting for meteorites.



Within three months of starting my candidacy, I took three months off to undertake an internship at The Lunar Planetary Institute and NASA. It is uncommon for the university to grant leave during the first year of candidacy, so I must thank Sasha and Andy for supporting my application of leave. Their faith in my abilities allowed me to undertake a once in a lifetime opportunity, and their encouragement upon my return led to the writing of an additional paper based on my experiences, which is now published. As such I would also like to thank my NASA supervisor Dr. Justin Simon



for his wisdom and patience as I juggled my PhD research and the internship research we worked on together. Although the time was short, the skills and experiences I gained working at NASA were life affirming.

At this point I would like to thank my University of Queensland collaborators, especially Dr. Emma Gagen, who effectively taught me microbiology and 16S sequencing, which I did not study during my undergraduate years. Being a geologist, this new science was very daunting, and with no microbiologist in the school of EAE at Monash Emma was my go-to

expert. She was instrumental in helping me come up with experimental design in Chapter 4 and field sampling throughout the research. She was also responsible for data collection in Chapter 3. Without her, this research would not have happened. I thank her for all the hard work she put in teaching me and collecting data, as well as all the little things like lending me a public transport travel card and shouting me lunch when I was visiting UQ. Also at UQ was Professor Gordon Southam, who was an unofficial supervisor to my microbiology work. His enthusiasm for my research was greatly appreciated and his bite-sized nuggets of knowledge were as profound as they were educational. Both Gordon and Emma helped keep me on course with regards to the biology throughout my candidacy, and were also great role models to emulate.

For five years I have ventured out to the Nullarbor Plain to collect meteorites. Every trip was the highlight of the year and every trip was different. Every trip had memories, and every trip had different characters: Kim, Rick, Eleanor, Andy, Andrew, Sophie, Sarah, Lara and Jeff. Thanks to all of you, but especially those who collected samples for me in the scorching sun. For me the Nullarbor Plain is more than a desert; it is an alien place to wander and ponder. Each night, bellies full from an amazing dinner, we sat around the campfire, gazed at the starlit sky, and found a place of pedagogical enlightenment. At the end of every trip I was amazed by my experience and smarter



thanks to Andy's enthusiastic insights about the formation of the solar system.

Our last expedition was only possible because of the generosity of 150 people. Sarah, Andrew and myself ran a successful Pozible crowdfunding campaign to raise funds for the expedition, during which I recovered samples vital to all of my chapters. Without the support of these generous strangers but also many family and friends I would not have been able to complete my PhD. Thank you to all the backers of that crowd funding campaign.

Over the duration of my research, my experiments have been spread out over the whole campus; as such there are many laboratory heads and technical staff I would like to thank. First and foremost is Associate Professor David McCarthy, who runs the Environmental & Public Health Microbiology Laboratory in the Department of Civil Engineering. He graciously let me use facilities in his laboratory that were instrumental in chapter 4. I would also like to extend a big thanks to his fellow lab hands Christelle Schang, Rebekah Henry and Gayani Chandrasena whose collective training enabled me to use the autoclave to find the pesky pH probe. I would also like to thank Dr. Georg Ramm from the School of Biomedical Sciences and his lab-tech Adam Costin, for allowing me to use their critical point dryer, and for embedding samples, often at moments notice. I would also like to thank Jana Habsuda from the Faculty of Engineering for teaching me to use the Cisorp water sorption analyzer, and for handling all the paperwork that goes along with its use. I would also like to thank Dr. Judy Callaghan from the Monash Micro Imaging platform, for setting me up to use their facilities. I would also like to thank Dr. Craig Forsythe from the School of Chemistry, for allowing me to use the XRD D8 in the chemistry laboratory as well as teaching me how to safely pour a dewar of liquid nitrogen. Also from chemistry I would like to thank Karen Little for the use of her plate-reader and Finlay Shanks for his help with the Raman spectroscopy, even if the results didn't make it into my final thesis.





A big thanks goes to the team at Monash Centre for Electron Microscopy who have been instrumental throughout my PhD. In particular I would like to thank Dr. Xi-Ya Fang, Dr. Flame Burgmann, Mr. Renji Pan and Dr. Amelia Liu, who have all had a hand in preparing my samples, teaching me how to use equipment, running jobs for me or troubleshooting.

A big thanks goes to the staff of the School of Earth, Atmosphere and Environment. In particular I would like to thank the admin staff of Tien Chin Chen, Silvana Cifaratti, Robert Oakleigh and Caroline Venn, who have all helped make my time at Monash as smooth as possible. Thanks to the technical staff Massimo Raveggi and Rachelle Pierson for running my stable isotope samples, and Junnel Alegado for teaching me how to make a thin section, even if I still manage to wedge them four years on. Thanks also to Chris Pierson who came in to help fix the wire saw and make custom mounts for it.

A big thanks goes to my office mates Andrew Langendam and Nikk Hunter. While it may not have been the most productive room to do a PhD in, it was certainly the funniest. Many a prank and champion joke has come out of our procrastinations. Thanks for the memories guys. Thanks to my friends and housemates outside of university that have had to deal with last minute cancelations and piled up dishes. You guys are the best. Thanks for being so understanding.

I would also like to acknowledge the work and suggestions made by my two thesis examiners Lisa Pratt and Phill Bland, whose feedback greatly improved my thesis.

Lastly thanks to my parents. You guys are my rock and have supported me every step of the way. More than anybody else, if it wasn't for you both I would not have been able to undertake this journey. Thanks for always being there for me. I love you both to bits.

Abstract

Ordinary chondrite meteorites represent undifferentiated planetary embryos from the beginning of the solar system. They comprise ~87% of meteorites collected on Earth. From over a century of study, we know that these meteorites have narrow ranges of isotopic, chemical, and mineralogical compositions, which is why meteorites are commonly used as geochemical standards. Our geochemical knowledge of Mars by comparison is still being established. This lack of detailed characterisation makes recognising putative biosignature on Mars difficult to impossible. By using the well established knowledge of chondritic meteorites, which fall to both Earth and Mars, it could be possible to circumvent the ambiguity associated with our limited knowledge of Mars to detect biological signatures on that planet.

This thesis presents a series of chapters that establish a terrestrial baseline for recognising microbial colonisation of chondritic meteorites, using samples collected on the arid Nullarbor Plain, Australia. Results are presented, which show that chondrite meteorites are colonised by niche soil biota. These microorganisms colonise microhabitats characterised by alteration minerals that reflect variable pH conditions (e.g., acidic to circumneutral). The alteration minerals in meteorites are found to be hygroscopic, allowing microorganisms to use these minerals as a source of water in an otherwise desiccating environment. Such minerals provided opportunities for microorganisms to be entombed fossilising and preserving their presence. Microbes found hundreds of micrometers within the meteorites themselves indicating a deep level of colonisation of the meteorite. Experiments are reported whereby a fresh chondritic meteorite was inoculated with *Acidithiobacillus ferrooxidans* to induce a biologically-mediated sulfur isotopic fractionation in the oxidative weathering products of troilite (FeS). This experiment produces a positive $\Delta^{34}\text{S}$ value that is indicative of biogenic fractionation and is distinct from the signature of abiotic oxidation of troilite. This isotopic signature was also discovered in the Nullarbor Plain meteorites, indicating that unambiguous sulfur isotope biosignatures can develop and be detected in Mars-like environments.

The concepts developed in this thesis can be used to reduce ambiguity in biomarker detection on Mars. Similar (yet slower) oxidative weathering of meteorites and basalt occurs on Mars, which also produces hygroscopic alteration products. Given the long residence times of meteorites on the martian surface (e.g., 10^9 years), it is possible that meteorites on the surface today could have sampled a putative biosphere on Mars at the Hesperian–Noachian transition (3.7 billion years ago) when the surface is thought to have been habitable. Unlike other possible habitats proposed on Mars, chondritic meteorites are the only one where the plausible biosignatures are divorced from the ambiguity associated with our incomplete understanding of martian geochemistry.

Chapter 1

Introduction to exogenic meteorites as refuge habitats for life on Mars

Alastair W. Tait¹

¹School of Earth, Atmosphere & Environment, Monash University, Australia

1.1 Introduction

The search for extraterrestrial life in our solar system has undergone a renaissance in the past 20 years. This renewed interest in astrobiology has been motivated by the concurrent discovery of diverse extremophile organisms on Earth, and environments in which these organisms would survive on various planets. Extremophile microorganisms live in conditions beyond those of mesophilic organisms, thriving in high/low temperatures, pressures, pH ranges, ionising-radiation, and scarce nutrient and/or water availability. Because of its past climactic similarity to Earth, Mars has received the most attention from astrobiologists and has been the recent focus of several robotic sampling missions.

Mars had an early history almost identical to that of Earth (CARR AND HEAD 2010), but due to its smaller size it is thought that the planet's outer core cooled more quickly than Earth's core, resulting in the cessation of its magnetic dynamo at ~3.6 Ga (MILBURY *ET AL.* 2012). Removal of the protective magnetosphere then allowed the martian atmosphere to be eroded by the solar wind, and its surface to be sterilised by ultraviolet (UV) light and other forms of ionising radiation (MILBURY *ET AL.* 2012). Mars thus lost much of its atmosphere shortly after life developed on Earth (the earliest life detected to date formed stromatolites at 3.7 Ga; (MICHALSKI *ET AL.* 2013; MILBURY *ET AL.* 2012; NUTMAN *ET AL.* 2016). This has led some scientists to suggest that if life ever existed on Mars, evidence for its presence would mostly likely be found in shallow aquifers (10s to 100s of metres deep), or in deep serpentinite systems 5 km below the surface (MCMAHON *ET AL.* 2013; MICHALSKI *ET AL.* 2013). Despite these factors, no biology-focused exploration of the martian subsurface is planned for the foreseeable future. The modern surface of Mars is a hostile environment for life, due to its cold temperatures, ionising-radiation and low-pressure leading to a scarcity of liquid water. Nonetheless, the surface of Mars still presents some environments where extremophile microorganisms may have lived, or could plausibly survive today. This thesis proposes the novel idea that exogenic meteorites (i.e., chondritic meteorites) could act as microbial habitats on the surface of Mars. This chapter introduces the reasoning behind the proposal that meteorites could act as microbial habitats on Mars. It provides background information including an evaluation of the flux of meteoritic material to the martian surface and the environmental chemistry of present-day Mars. This is followed by an assessment of (1) the types of life that might be found on Mars, (2) the mineralogy of chondritic meteorites, and (3) potential water sources available to microorganisms living in surficial regolith. This chapter finishes with an

overview of the thesis structure and a description of how each chapter contributes to building the case for exogenic meteorites as possible microbial habitats on Mars.

1.1.1 A quick note on nomenclature

This thesis focuses on colonisation of “exogenic meteorites” by microorganisms. Exogenic meteorites are primordial meteorites – remnant material from the formation of our solar system. They fall to the surfaces of all planets and moons in our solar system, including Mars (ASHLEY 2015). Exogenic meteorites on the martian surface are not to be confused with the shergottite, nakhlite, chassignite (SNC) achondrites, ALH84001 and NWA 7034 meteorites, which are not primordial solar system material. The latter are pieces of martian crust that were ejected from the red planet via impacts and later fell to Earth as meteorites; they are commonly referred to as “martian meteorites”. Where meteorites are discussed in this thesis, unless explicitly stated, these are exogenic meteorites, not SNC or other martian meteorites.

1.1.2 Panspermia versus microbial colonisation of exogenic meteorites

Panspermia, more specifically lithopanspermia is the hypothesis that a rock containing microorganisms from a planet with a biosphere can be ejected from its host planet during an impact event and travel through space to then land on another planet, thereby seeding that new planet with life (OLSSON-FRANCIS AND COCKELL 2010). This theory made global headlines in 1996 when it was suggested that

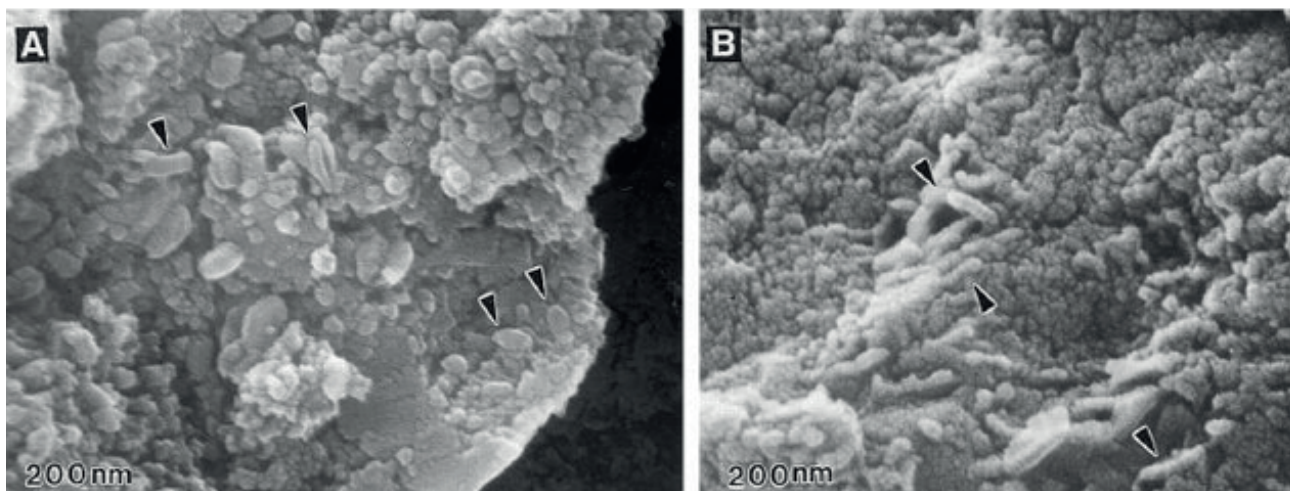


Figure 1.1 | ALH84001 Biomorphs. These Scanning Electron Images (SEI) are taken from (McKAY *ET AL.* 1996). They show claimed nano-scale “microfossils” from the ALH84001 martian meteorite. These tubular structures are smaller than any known on Earth bacteria, and below the lower limit for what is considered feasible for terrestrial life. The most likely explanation is that they are coating artefacts. (Images used with permission from copyright holder)

a meteorite from Mars, ALH84001, contained features resembling microfossils (MCKAY *ET AL.* 1996) (*Figure 1.1*). Although similar in shape to terrestrial bacteria, these “microfossils” were smaller than any known organism previously discovered on Earth at 20 – 100 nm in length.

After 20 years of further study it has been concluded that the “microfossils” described by McKay et al. (1996) are likely to be a coating artefact from the process used to conduct electron microscopy (BRADLEY *ET AL.* 1997). It has also been proposed that the mineralogy of the host rock implied conditions that would have been unfavourable to colonisation by martian life (HARVEY AND MCSWEEN 1996; SCOTT *ET AL.* 1997). Despite these findings many of the original authors still maintain a biological origin for these microfossil-like features. Although many of the features in ALH84001 most likely have an abiotic origin, a biotic origin cannot be fully ruled out, and thus highlights an underlying issue with astrobiology, which is that textural features have perpetual ambiguity. As such, the detection of reported microbial biomarkers in this meteorite remains controversial.

Colonisation and habitation of exogenic meteorites differs from panspermia in several ways. Panspermia deals with transport of crustal materials from one planet through space to introduce life to another planet. Habitation of exogenic meteorites, by contrast, deals with sterile, primordial chondritic material that falls to a planet only then to be inhabited by extant indigenous microorganisms from that planet. As such, this concept does not deal with the questions of how organisms might survive during ejection from a planet, space travel, and atmospheric re-entry. Instead, this research has more in common with the body of work on “first colonisers” (e.g., microbes colonising sterile, recently cooled lava; KELLY *ET AL.* 2014). As such, exogenic meteorites represent the ultimate new real estate.

1.1.3 Motivation for microbial habitation of exogenic meteorites

The possibility that extant life has colonised exogenic meteorites on the martian surface today is slim, but not impossible; it is more likely that meteorites may have been colonised in the past when Mars was more habitable. Consequently, the presence of microorganisms in meteorites would likely be recorded as (1) diagnostic isotopic ratios in alteration minerals and/or (2) microfossils.

One of the current tasks for the Mars Science Laboratory (MSL) rover, Curiosity, is to search for evidence of habitability (SUMMONS *ET AL.* 2011). There are a number of reasons why meteorites are good candidates for microbial habitats on Mars. For instance, all known life requires the following six elements: C, H, N, O, P, and S. These elements exist in varying abundances in stony meteorites, along with bioessential trace elements. These elements are more abundant in chondritic meteorites

than the basalts that dominate the martian surface. Meteorites also provide a shield against UV light and cosmic radiation in the absence of an ozone layer and/or magnetic field (RETTBERG *ET AL.* 2004). Furthermore, meteorites contain energy sources for chemotrophic life, in the form of redox potential contained in ferrous iron and sulfide minerals, and to a lesser extent bioavailable organic carbon in carbonaceous chondrites.

The mass of meteoritic material falling to Earth and Mars during the Hadean (Pre-Noachian) and Archean (Noachian, Hesperian and Paleoamazonian) is thought to have been orders of magnitude greater than today (GOMES *ET AL.* 2005; IVANOV 2001). Mars is also thought to have a greater flux of meteorites to its surface than Earth today due to its proximity to the asteroid belt (BLAND AND SMITH 2000; SHOEMAKER 1977). This would have lead to considerable meteorite scatter on the surface, leaving these exogenic materials susceptible to hydrous alternation. Transient surface brines are thought by some to flow on Mars today (OJHA *ET AL.* 2015), although the evidence for this is debated (DUNDAS *ET AL.* 2015). These brines could precipitate chlorate and perchlorate salts within pore spaces inside meteorites. These salts have the capacity to buffer humidity (LEVY 2012), thus trapping water in an otherwise hostile environment, as well as accelerating the weathering of reduced phases (ZURFLUH *ET AL.* 2013).

1.1.4 Meteorite flux to the martian surface

From the perspective of sample availability during a rover mission, detection of biomarkers of microbial life in meteorites on Mars would require a large amount of meteoritic material to be present on the martian surface. For this to happen, the accumulation rate of meteorites must exceed their weathering rate. On Earth meteorites are rare; our dense atmosphere burns up most meteors, preventing them from reaching the surface, and those that do reach it commonly fall into the oceans or in environments where they are buried or broken down rapidly. Those meteorites that land in “ideal” locations, including Antarctica and hot deserts such as the Nullarbor Plain, are consumed by oxidative weathering on timescales of 10^6 and 10^4 years, respectively (BLAND *ET AL.* 2006).

Calculating the martian meteorite flux is challenging due to the lack of observational data. Because of its proximity to the Asteroid Belt, the meteorite flux to Mars is thought to be 2.6 times that to Earth (estimated using cratering history) (BLAND *ET AL.* 2006; SHOEMAKER 1977). Using estimates from Shoemaker (1977) as a starting point, Bland (2000) estimated the flux of meteoritic material entering

the martian atmosphere based on:

$$\log N = -0.689 \log m + 4.17 \quad (\text{eq.1})$$

Where N is the number of events per 10^6 km^2 (roughly the surface area of Egypt) and m is the mass of the event. There are two factors that influence the survivability of meteoritic material reaching the martian surface: (1) the acceleration of a bolide due to gravity and (2) the ability of the atmosphere to effectively reduce the velocity of the bolide before it hits the surface. Shoemaker (1977) calculates that the low gravity on Mars (about one third of that on Earth) reduces the mean atmospheric entry velocity of meteors to 19 km s^{-1} , but more recent publications put the average entry velocity at 10.2 km s^{-1} (FLYNN AND MCKAY 1990; POPOVA *ET AL.* 2003). This is comparable to the lower end of entry velocities for meteors on Earth, between $11.2 - 72.8 \text{ km s}^{-1}$ (CEPLECHA *ET AL.* 1998). Despite their slower initial velocity, meteors entering Mars' atmosphere are less aerobraked due to the thin atmosphere (pressure at the surface is <1% of that on Earth), and are consequently less likely to survive impact (BLAND AND SMITH 2000). Bland and Smith (2000) also suggested that, for meteorites of 10 – 50 g, only 10 – 20% survive entry, but this assumes an entry angle of 90° . The survivability of meteorites entering the martian atmosphere increases with a lower entry angle, between $7-22^\circ$ (CHAPPELOW AND SHARPTON 2006). This lower angle increases the distance through the atmosphere the meteorite must

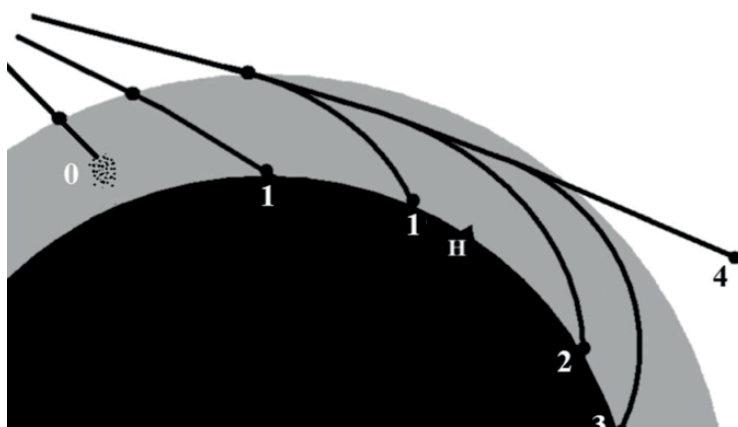


Figure 1.2 | Meteor Entry. This diagram is taken from (CHAPPELOW & GOLOMBEK 2010). Numbers (0 – 4) correspond to the possible fates of meteoroids entering a planetary atmosphere (for a detailed description of each see text). On Mars Types 2, 3 in this diagram are most likely to produce meteoroids. “H” is the horizon from the point of entry of the meteoroid. (Images used with permission from copyright holder)

travel, allowing for greater aerobraking and deceleration. Chappelow and Golombek (2010) identify five possible fates for meteors entering the atmosphere of Mars (*Figure 1.2*): (0) The meteor may burn up due to total ablation, although almost all meteors are thought to survive entry to reach the ground (CHAPPELOW AND SHARPTON 2006). (1) Impact of the meteor with the surface. Approximately 90% of those that hit the ground are hard impacts resulting in destruction of the impactor. The remaining 10% survive as

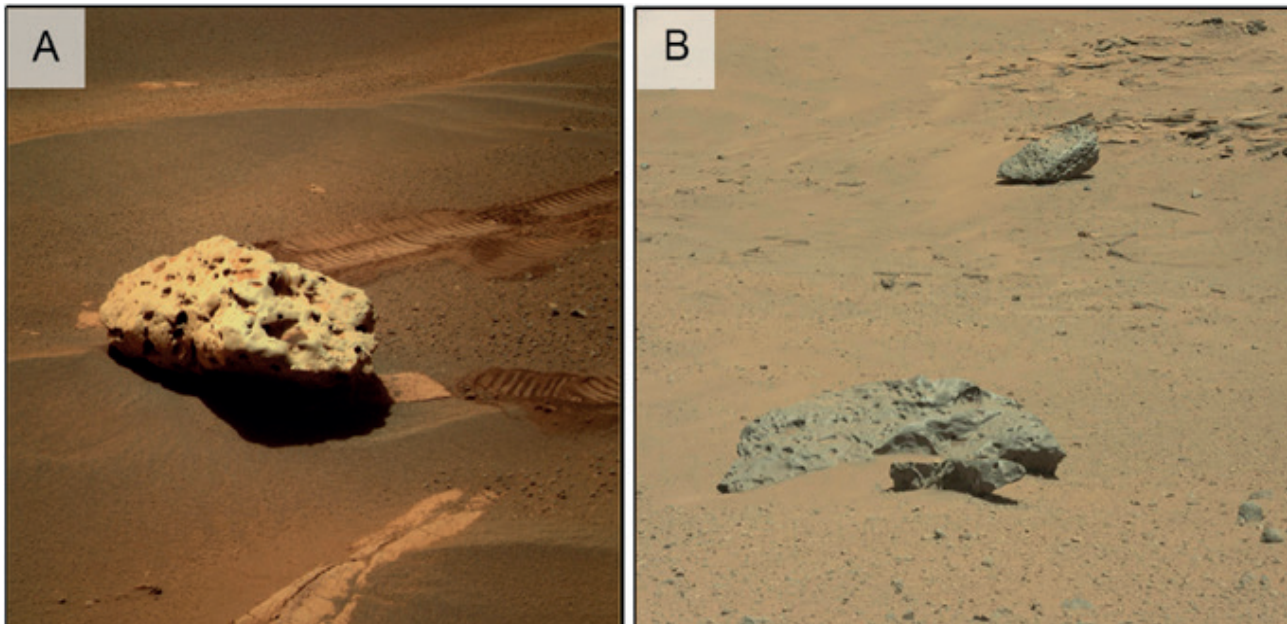


Figure 1.3 | Examples of Iron Meteorites on Mars. (A) An iron meteorite, named ‘Block Island’ found by the MER rover Opportunity in 2009 at Meridiana Planum measuring 67 cm in length. (B) Three iron meteorites likely from the same fall found by MSL rover Curiosity, Sol 640, at Gale crater 2014. The larger of the three is 2 m wide.

meteorites. (2) The meteor has an over-the-horizon trajectory. In this scenario, the meteor travels over the horizon (i.e., the horizon as defined from the point of atmospheric entry), where it impacts with the ground. (3) Fall back of the meteorite, where the meteor travels over the horizon and has its horizontal velocity slowed almost completely by the atmosphere, allowing it to fall to the ground at terminal velocity. (4) The meteor passes through the atmosphere and back out into space without impacting the planet. Only scenarios (2) and (3) are likely to produce the most meteorites under current martian atmospheric densities; (1) would result in the obliteration of 90% of meteorites in hypervelocity impacts (CHAPPELOW AND GOLOMBEK 2010).

Seven iron meteorites have been observed on the martian surface since 2005 (ASHLEY 2015). They have been identified by both of the Mars Exploration Rovers (MER) and MSL (*Figure 1.3*). The identification of iron meteorites is an important discovery because it indicates there are meteorites on Mars and that they can be found by robotic exploration. Iron meteorites make up 2.1% of meteorites that fall to Earth, whereas stony meteorites (the focus of this study) comprise 91.5% (METEORITICAL BULLETIN DATABASE, 2016). Assuming a similar ratio exists for Mars, coupled with a 10% survival rate, the rovers (MER and MSL) should have found, or driven past, ~ 64 stony meteorites (most likely fragments). The reason why these meteorites have not been observed could be (1) that the impact survival rate is lower than expected, (2) the residence time for iron meteorites is longer than for stony meteorites, (3) the introduction of observational bias because stony meteorites have a similar colour to

martian regolith (SCHRÖDER *ET AL.* 2008), or (4) an unknown weathering mechanism preferentially destroys stony meteorites.

1.1.5 Meteorite Residence Times on Earth and Mars

Meteorites contain abundant reduced phases such as metal alloys, and sulfide minerals. These phases are out of equilibrium with the oxidising environment in which they land on Earth, but to a lesser extent on Mars. In oxidising environments, meteorites begin to equilibrate and break apart due to dissolution of silicates (LEE *ET AL.* 2006), oxidation of reduced phases (BLAND *ET AL.* 2006), and formation of veins of alteration minerals (LEE AND BLAND 2004), which induces reaction-driven cracking. Meteorites on Earth are generally found in either the cold deserts of Antarctica or hot deserts such as the Atacama Desert, those in north-west Africa, or the Nullarbor Plain in Australia. Meteorites at these locations have different weathering rates and alteration mineralogy due to their unique environmental conditions. This is important because those meteorites weathering in Antarctica experience temperature conditions closer to those on Mars.

Weathering rates of minerals on Mars are expected to be slower than on Earth (BURNS AND FISHER 1993). Burns and Fisher (1993) calculated that during the end of the Hesperian period on Mars (3.7 to 3 Ga), the concentration of dissolved atmospheric oxygen in equatorial melt waters could only have oxidised 0.3–3 ppm of meteoritic Fe^{2+} to Fe^{3+} per year. This rate is 3–4 orders of magnitude slower than the rate of iron oxidation under ambient terrestrial conditions of 4700 ppm yr^{-1} (BURNS AND FISHER 1993). Given the present lack of atmosphere, the rate of weathering on Mars today would be orders of magnitude slower still, allowing residence times for chondritic material of $>10^9$ years (BLAND, 2000). Thus, in the absence of crustal recycling (i.e., plate tectonics), some meteorites on the martian surface today could have resided there since the Noachian (4.1 to 3.7 Ga) when Mars was warm and had liquid water at its surface (CARR AND HEAD 2010).

On Earth, chondritic material fractures and disintegrates during oxidative weathering and hydrolysis. This is in part the result of the crystallisation pressure created by precipitation of newly formed oxyhydroxides and salts (LEE *ET AL.* 2006). Troilite $[\text{FeS}]$, kamacite $[\text{Fe}_{0.9}\text{Ni}_{0.1}]$ and taenite $[\text{Fe}_{0.8}\text{Ni}_{0.2}]$ have molar volumes (V_m) of 17.90, 7.11 and 7.04 $\text{cm}^3 \text{mol}^{-1}$ respectively. In contrast, their hydrated weathering products, gypsum $[\text{CaSO}_4 \cdot 2\text{H}_2\text{O}]$, goethite $[\text{Fe}^{3+}\text{O}(\text{OH})]$, akaganeite $[\text{Fe}^{3+}_{7.6}\text{Ni}_{0.4}\text{O}_{6.4}(\text{OH})_{9.7}\text{Cl}_{1.3}]$, and jarosite $[\text{KFe}_3^{+3}(\text{SO}_4)_2(\text{OH})_6]$, have larger molar volumes of 74.86, 20.81, 253.79 and 162.07 $\text{cm}^3 \text{mol}^{-1}$ respectively. Note: These molar volumes do not take into

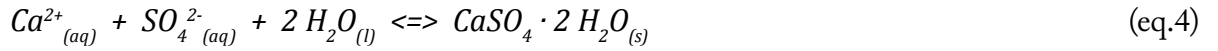
consideration the symmetry of the unit cell volumes (V_{cell}). As addressed by Bland and Smith (2000), stony meteorites have varying degrees of pore space that accommodate some of this volume increase, but after approximately ~50% weathering of the FeNi and FeS (assuming goethite as the product), the pore space in most chondrites would approach zero. Infill of porosity initially hinders penetration of water deep into the interior of meteorites, but eventually results in reaction-driven cracking and mechanical breakdown. Thus, clusters of meteorite fragments are one of the most common finds in hot deserts.

1.1.6 Weathering Products of Stony Meteorites

The weathering products of meteorites on Earth have been studied previously with the goal of understanding the original mineral composition of unaltered meteorites (BLAND *ET AL.* 2006; LEE AND BLAND 2004). Weathering products found in hot desert meteorites include carbonate minerals (e.g., Mg-calcite), sulfates (e.g., gypsum and jarosite), Fe(III) oxides (e.g., goethite), and Mg-rich smectites (*Chapter 2*). The weathering of troilite, as described by Bland et al. (2006) (eq. 2), generates sulfuric acid, which changes the pH of the system, controlling the precipitation of jarosite, goethite and gypsum, as well as the dissolution of calcite and primary silicate phases such as olivine $[(Mg,Fe)_2SiO_4]$, diopside $[CaMg(Si_2O_6)]$ and plagioclase $[(Ca,Na)(Al,Si)_4O_8]$.



The resulting alteration mineralogy is controlled in part by the water–rock ratio during oxidative weathering of Fe-sulfide minerals (ZOLOTOV AND SHOCK 2005). Higher water–rock ratios facilitate the conversion of jarosite into goethite, whereas, under conditions where dehydration and evaporation dominate, lower water–rock ratios facilitate the persistence of jarosite. The latter conditions are important on Mars where liquid water sublimates and only exists transiently at the planet’s surface. Hence, the martian surface environment is expected to have more abundant jarosite, as the surface becomes more acidic over time as the surface dried out (SQUYRES *ET AL.* 2004). Dissolution of calcite (eqs. 3–5), or the weathering of Ca-bearing silicates such as diopside and plagioclase, accounts for the production of gypsum in meteorites:

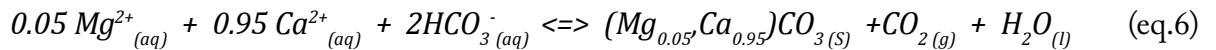


Some of these reactions (i.e., eq. 2) will be slower on Mars due to the lower atmospheric pressure as well as the scarcity of molecular oxygen (~0.13 vol.% of atmosphere; OWEN *ET AL.* 2012) compared to the ~21% abundance of oxygen Earth's atmosphere. Molecular oxygen is produced by photodissociation of CO₂, H₂O and CO in the upper atmosphere of Mars (LEWIS 2004), whereas almost all atmospheric O₂ on Earth is generated by photosynthesis.

CO₂ is a major component of the martian atmosphere (95.97 mol.%) allowing the possibility of carbonate alteration as the dominant weathering mechanism on Mars for stony meteorites. The alteration products of meteorites found in Antarctica are dominated by carbonate minerals (LONG *ET AL.* 1989), suggesting these reactions could be analogous to those on Mars. Under hyper-arid Antarctic and martian conditions, atmospheric CO₂ could dissolve and chemically equilibrate within thin films of water that present themselves on mineral surfaces due to the hygroscopic nature of some minerals (e.g., chlorates, perchlorates, sulfates) to create carbonic acid (eq. 5).



Under weakly acidic to circumneutral conditions, Mg²⁺ and Ca²⁺ cations released during dissolution of meteoritic olivine, pyroxenes and plagioclase react with bicarbonate to precipitate Mg-calcite (LONG *ET AL.* 1989) (eq. 6).



This process has potential to dissolve primary meteoritic minerals and generate more hygroscopic minerals such as gypsum, Fe-oxides and carbonates (*Chapter 2*), which are common weathering products of meteorites. The greater the abundance of hydrated and hygroscopic weathering products, the more water can be stored on or within minerals. These thin films of brine could also be utilised by microscopic organisms (WILSON AND BISH 2011).

1.1.7 The Possibility of Microbial Life at or near the Martian Surface

All life on Earth can trace its heritage back to the Last Universal Common Ancestor (LUCA) (DI GIULIO 2001). This was a single-celled organism that was prokaryote-like and most likely a thermophile or hyper-thermophile, that may have depended on nutrients found near volcanic vents, either in the ocean or on land (DI GIULIO 2001). LUCA is believed to have existed around ~3.7 Ga (BOUSSAU *ET AL.* 2008), although the recent discovery of a 3.7 Ga stromatolite in a shallow marine environment (a possible prototrophic biofilm) implies an alternative age for LUCA (NUTMAN *ET AL.* 2016). Regardless, this timing suggests that LUCA had come into existence on Earth within the timeframe of the warm period that characterised Mars' early history (MICHALSKI *ET AL.* 2013).

If life developed on Mars, and followed a similar path to that of life on Earth, Earth's biosphere had already developed the strategies for living in hostile conditions by the time Mars was becoming inhospitable for surface life. Although there is no clear boundary to when the martian surface became inhospitable, a logical demarcation is when the magnetic dynamo shut down (MILBURY *ET AL.* 2012), allowing the atmosphere to be eroded and bathing the planet in ionizing radiation. This event would almost certainly render any phototrophic life (which derives energy from sunlight) unviable (MICHALSKI *ET AL.* 2013). It has been proposed that these conditions would have resulted in a martian biosphere centred around chemoautotrophs (which use inorganic materials as electron donors and acceptors and are able to fix inorganic carbon for biomass, MICHALSKI *ET AL.* 2013). Michalski et al. (2013) suggested that such organisms could still survive on Mars today in subsurface aquifers. Importantly, groundwater from some aquifers on Mars may reach the surface today (HELDMANN 2005; OJHA *ET AL.* 2015), potentially carrying putative microbes into the environment where meteorites continue to accumulate.

1.1.8 Possible Microbial Metabolisms on Mars

The main group of autotrophs that could survive on Mars today are methanogens, which use H_2 as the electron donor and CO_2 as the electron acceptor, making CH_4 , water and energy (FORMISANO *ET AL.* 2004; MICHALSKI *ET AL.* 2013). Many of Earth's methanogens are autotrophic (meaning that they fix CO_2 for their biomass), but some are heterotrophic and can ferment methyl and acetate compounds in order to make methane (FERRY 1992). Methanogens are anaerobic and tolerate a wide variety of

temperatures and pressures (KRAL AND ALTHEIDE 2013), making them ideal candidates for survival on Mars. Formisano et al. (2004) hypothesised that methanogenic microorganisms could have been the source of trace amounts of methane, which have been found in the martian atmosphere. However, abiotic processes such as serpentinisation are a more likely source of methane, and new measurements by the SAM-TLS instrument on the rover *Curiosity* throw the original finding into doubt (HOUTKOOPER 2013). H_2 would likely only exist in very small quantities in carbonaceous meteorites, as it is highly volatile and would escape easily, giving autotrophic methanogens a poor chance of survival; however, heterotrophic methanogens might have the capacity to metabolise the organic compounds found in carbonaceous meteorites. Other, much more abundant, inorganic electron donors are available to different types of chemoautotrophs in meteorites in the form of various minerals, particularly native and ferrous iron (Fe^0 , Fe^{2+}) in FeNi alloys and troilite (FeS), and reduced sulfur (S^{2-}) in troilite and other sulfides (the highly reduced enstatite chondrites and achondrites contain several additional inorganic electron donors, but these types of meteorite are relatively rare).

The viability of a particular redox reaction for chemoautotrophy is governed by whether or not it is sufficiently energetic to drive production of adenosine triphosphate (ATP) for energy (around $-31.8 \text{ kJ mol}^{-1}$) and CO_2 fixation in biomass (MADIGAN ET AL. 2012). This is best explained using electrode potentials (E_o') from half reactions. Although we do not know the exact biochemistry that could have developed on Mars, redox couples allow predictions to be made about the amount of energy that could be available to microorganisms from common inorganic reactions. Such chemoautotrophic metabolisms can leave a record in the form of stable isotope anomalies in the secondary reaction products, thus recording evidence of life.

One model organism, *Acidithiobacillus ferrooxidans*, is an iron- and sulfur-oxidising species of bacterium that is commonly associated with acid mine drainage environments and can facilitate the production of sulfate minerals such as jarosite (LIU ET AL. 2009). This bacterium uses reduced Fe and S as electron donors and molecular oxygen as an electron acceptor. The standard electrode potential, E_o' , of Fe^{3+}/Fe^{2+} at pH 7 is +0.2 V, or +0.76 V at pH 2, whereas that of $0.5O_2/H_2O$ is +0.82 V (MADIGAN ET AL. 2012), resulting in an idealized energy yield in acidic conditions of $(-32.9 \text{ kJ mol}^{-1})$ (MADIGAN ET AL. 2012). Such calculated energy yields do not reflect the metabolic rates or true energy requirements of environmental microorganisms. Organisms cultured under ideal conditions in a laboratory can have a high carbon turnover, on the order of days to months. In natural systems, energy sources and nutrient resources are scarce, which can slow microbial metabolisms, even to the point that cells will

forgo growth and division when experiencing prolonged unfavourable conditions (HOEHLER AND JORGENSEN, 2013). Many taxa of microorganism can remain dormant, using energy conservation strategies such as sporulation or efficient metabolisms to deal with xerophilic conditions (LENNON AND JONES, 2011). Research into the base power requirements of cells has been done with Sulfate Reducing Bacteria (SRB). SRB cells found ~1 m beneath the surface of deep ocean sediments are reported to have a mean cell specific rate of sulfate utilisation 4×10^{-6} fmol SO_4^{2-} cell⁻¹ day⁻¹ resulting in a biomass turnover of 3000 years (D'HONDT ET AL., 2002; HOEHLER AND JORGENSEN, 2013). By comparison the mean cell specific rate for cultured SRBs is 2 – 47 fmol SO_4^{2-} cell⁻¹ day⁻¹ (PRICE AND SOWERS, 2004). Given the inhospitable conditions, putative microbial life on Mars would likely have a very slow metabolic rate, which would result in slow alteration of rocks, including meteorites. The low oxidation rate of iron (0.3 – 3.0 ppb $\text{Fe}^{2+}/\text{Fe}^{3+}$ yr⁻¹) predicted for Mars (BURNS AND FISHER, 1993) is greater than the mean cell specific rate mentioned above for SRBs (if they metabolised iron), under unfavourable conditions in ocean sediments on Earth, meaning that the weathering of meteoritic troilite alone on Mars could be enough to support a sizeable population of microbes.

Sulfur oxidisers are similar to iron oxidisers in that they oxidise inorganic compounds for energy. Sulfur oxidation is more energetic, yielding larger electrode potentials than iron oxidation; the reactions are also more varied due to the larger number of oxidation states of sulfur. Different oxidation states of sulfur (e.g., S^{2-} , S^0 , S^{2+} , S^{4+}) can either be oxidised directly to sulfate (SO_4^{2-}) by bacteria without intermediaries, or to a series of intermediate sulfur species before making sulfate. Many sulfur-oxidizing organisms are anaerobic (e.g., *Thiobacillus denitrificans*, *Allochromatium vinosum*), and are similar to Fe-oxidisers in that they can use nitrate as an electron acceptor (MADIGAN ET AL. 2012). These anaerobic metabolisms would be advantageous on Mars where there is little free molecular oxygen to drive aerobic respiration. Sulfur is essential not only for microorganisms that use it in metabolic reactions, but to all cells which must assimilate it for use in other biological functions. Assimilatory sulfate reduction requires an investment of energy by a cell to take up sulfate from the environment to produce reduced protein phases such as adenosine-5'-phosphorsulfate (APS) or phosphoadenosine-5'-phosphosulfate (PAPS), which are important to all terrestrial metabolisms (CANFIELD 2001). Thus, enzymatic processes that are not related to energy generation could also be recorded as stable sulfur isotopic fractionations on Mars.

1.1.9 Bioavailable Nutrient and Energy Sources in Stony Meteorites

Because early Earth and Mars shared a similar environmental history, it is commonly assumed that putative martian biochemistry would bear a resemblance to that of Earth (CARR AND HEAD, 2010; MICHALSKI *ET AL.*, 2013). Carbon, hydrogen, nitrogen, oxygen, phosphorus and sulfur are bioessential elements for life on Earth. They are also amongst the most abundant elements in our solar system (LODDERS, 2010). It would not make sense for putative life on Mars to have a biochemistry based on rare transition metals, for example; such organisms would be at an evolutionary disadvantage due to the rarity of their bioessential elements. Instead, it makes more sense that the elements that are most abundant in an environment are of use to organisms. However, on terrestrial planets this can also include elements like silicon. A hypothetical biochemistry based on silicon rather than carbon has been proposed, owing to the identical valence (IV) of these elements and the propensity of silicon to polymerise (BENNETT AND SHOSTAK, 2006). However, carbon is a better candidate because it can bond with a greater variety of non-metals and it forms a variety of bonds, such as double or triple bonds which can store energy (PACE, 2001). Self-replicating carbon-based molecules, such as RNA, are also vital information carrying molecules that are crucial to the replication of life (PASEK, 2013). Furthermore, carbon-based biochemistry provides a basis for the containment of a cell's organelles from the environment in the form of phospholipid membranes. As such it is most likely that an organic biochemistry would occur on Mars, if life ever developed there.

The bioessential nutrients required for life on Earth are available in the martian crust in varying abundances. Meteorites also contain energy sources as well as some macronutrients that are important to terrestrial life and which would likely be important for putative martian organisms. Stony meteorites contain possible energy sources for many chemoautotrophic Bacteria and Archaea in the form of reduced elements in iron-nickel alloys and troilite. The most abundant types of stony meteorites that fall to Earth today are the ordinary chondrites (OC). These contain 5.43–5.79 wt.% of Fe²⁺-bearing troilite and 2.44–15.98 wt.% of Fe²⁺-bearing grains of metal alloy minerals such as kamacite and taenite (JAROSEWICH 1990). Meteorites also contain bioavailable phosphate, which is a major component of cell membranes, RNA and DNA. Phosphate minerals have been measured at abundances between 0.22 and 0.27 wt.% in OCs (JAROSEWICH 1990), existing primarily as chlorapatite [Ca₅(PO₄)₃(Cl)] and merrillite [Ca₁₈Na₂Mg₂(PO₄)₁₄] (PASEK AND LAURETTA 2007). These phosphate minerals are more soluble than those typically found on Earth, potentially providing greater access to phosphorous for bacteria (PASEK *ET AL.* 2013). Phosphorus may also be present in meteorites within FeNi grains or

as the reduced phosphide mineral, schreibersite $[(\text{Fe,Ni})_3\text{P}]$.

Chondritic meteorites are also known to contain organic molecules that may be of use to heterotrophic bacteria. For instance, the Murchison carbonaceous chondrite (CM2), which was a fall over Murchison, Australia in 1969, contains amino acids at a concentration of ~60 ppm (CRONIN AND PIZZARELLO 1983). Of the over 50 amino acids found in this meteorite, some of the common ones are glycine, sacosine, and alanine (PIZZARELLO *ET AL.* 2004). Murchison contains, more importantly, simple monocarboxylic acids (e.g., acetic acid) at >330 ppm, and organic macromolecules at 1.45 wt.% (SEPHTON 2002). The presence of these organics in meteorites implies that they could also support heterotrophic organisms. The organic compounds in meteorites represent a source of bioavailable carbon, which would otherwise need to be fixed from the atmosphere or aqueous solution by autotrophs. Nitrogen, which is used in nucleobases, is another essential element for life. Nitrogen is in low abundance in stony meteorites and may be the limiting nutrient in this environment, with H chondrites containing on average ~50 ppm (MOORE AND GIBSON 1969). However, carbonaceous meteorites, such as the CI chondrites, can have bulk concentrations of nitrogen on the order of ~1500 ppm (KERRIDGE, 1985). Nitrate may also be found in martian regolith, contamination my such regolith could overcome this limitation. The martian polar lander, Phoenix, did not detect NO_3^- as the high levels of perchlorate (ClO_4^-) and chlorate (ClO_3^-) may have masked its presence (KOUNAVES *ET AL.*, 2014A). It has been estimated from charge balance and conductivity measurements made by Phoenix, that the amount of nitrate on Mars (in the polar region) would be present in a ~1:1 mass ratio with the Cl in salts (KOUNAVES *ET AL.*, 2014A). As such, nitrate may be present at comparable abundances to perchlorate (~ 0.6 wt.%) at the Phoenix landing site (KOUNAVES *ET AL.*, 2014B). The high abundance of perchlorate in some martian surface environments may have negative consequences for life because perchlorate is highly oxidising and may contribute to the breakdown of organic molecules.

1.1.10 Sources of Water on the Surface of Mars

Large standing bodies of water do not occur on Mars today due to the low atmospheric pressure compared to that of Earth (< 1.0%) (SOM 2014). This low atmospheric pressure causes liquid water to rapidly boil, posing a problem for organisms that need water to function. However, there are three possible mechanisms that could supply water to meteorites on the surface of Mars today: (1) Seasonal brine seeping from groundwater aquifers or accumulation of this water as thin films on hygroscopic minerals (OJHA *ET AL.* 2015); (2) large meteorite impacts exposing ground ice (KOSSACKI *ET AL.*

2011), the history of which is clearly observable in the rampart craters of the northern lowlands (e.g., WOHLLETZ AND SHERIDAN 1983); (3) hygroscopic adsorption of water vapour from the atmosphere to mineral surfaces as a consequence of diurnal variations in humidity (OJHA *ET AL.* 2015). The recent seasonal observations of Recurring Slope Lineae (RSL) on Mars have been interpreted as brines seeping through regolith (OJHA *ET AL.* 2015). These are not to be confused with gullies, that are thought to be related to dry flow events and to act on longer timescales than RSL (MALIN *ET AL.* 2006). Furthermore, the most recent volcanic eruptions on Mars occurred at approximately 2 Ma (NEUKUM *ET AL.* 2004), well within the timeframe of meteorite survival, and these have been demonstrated to have caused water release from martian glaciers (NEUKUM *ET AL.* 2004).

Post-Noachian impacts on Mars have made fluvial landforms in over 200 craters surveyed thus far (MANGOLD 2012). Residual heat in the ejecta from the impact of these modest craters (20–40 km in diameter) can last for several hundred years (MANGOLD 2012). This residual heat can melt or sublimate near-surface ice that has been blanketed by the ejecta (MANGOLD 2012). Indeed, blanket material may record evidence of excavated hydrothermal systems or saturated zones within regolith that could potentially support a deep putative biosphere. Furthermore, it has been proposed that hydrothermal systems driven by impact-related heating on both Earth and Mars could last up to ~1 m.y. (OSINSKI *ET AL.*, 2013). Small fresh craters (<10 m in diameter) have been observed by the martian orbiter HiRISE, which have exposed the martian cryosphere within the last 10 years. Upon exposure, subsurface ice has been observed to sublimate completely within 100 sols (KOSSACKI *ET AL.* 2011). Initial heat from an impact event could potentially blanket nearby meteorites with water or water ice, potentially contaminating them with putative biota from the sub-surface. Also, fragments of meteorite from a bolide impact could find themselves exposed to water vapour during sublimation of ice.

The martian atmosphere is supersaturated with respect to water, but holds 10,000 times less water than Earth's atmosphere (MALTAGLIATI *ET AL.* 2011). Water vapour is likely to be cycled extensively within the martian regolith, although the majority of water vapour on Mars is in the upper atmosphere (FOUCHET *ET AL.* 2007). Liquid water can exist as thin films from 0.6 to 5 nm in thickness on ice interfaces, thicker still if contaminated with impurities (FOUCHET *ET AL.* 2007). Importantly, terrestrial deliquescence experiments have shown that liquid water can exist on the surfaces of hygroscopic mineral grains as micrometre-thick films (STEIGER *ET AL.* 2007). Diurnal variation in atmospheric humidity on Mars is sufficient to drive cation exchange reactions between minerals and could also feasibly transport nutrients (WILSON AND BISH 2011). Furthermore, laboratory experiments simulating

sublimation of water ice under several centimetres of regolith, conducted at martian atmospheric pressures and temperatures, have shown that the sublimating ice creates a ‘wet’ layer close to the ice allowing for terrestrial microbes to utilise for survival (PAVLOV *ET AL.* 2010).

1.1.11 Inclusion into the MEPAG “Special Regions” Framework

The Mars Exploration Program Analysis Group (MEPAG), under the direction of NASA, has updated and reviewed its position on “special regions” on Mars (RUMMEL *ET AL.*, 2014). Rummel et al. (2014) describe the constraints on known and theoretical life within the martian environment, both to guide exploration for putative, extant life on Mars and for planetary protection (i.e., preventing contamination of Mars with Earth’s biosphere). The previous report on “special-regions” identified three types of environment that are key for astrobiology exploration and planetary protection (BEATY *ET AL.*, 2006): (1) “Special-regions” which are defined as “regions where micro-organisms can propagate”. This is environmentally constrained via the limits of known terrestrial biota to be environments defined by temperatures greater than -18°C and a water activity (a_w) above 0.6 (RUMMEL *ET AL.*, 2014). (2) “Non-special” regions are those where the environmental constraints are below viable conditions for more than 100 years, but should be treated as “special regions” due to the potential of colonisation by organisms. (3) “Uncertain-regions” are where the environmental conditions are poorly constrained but have potential to support life, and thus should also be treated as “special-regions” until such time as more data are available to confirm their environmental conditions.

Although they have been observed on Mars, exogenic meteorites were not considered by Rummel et al. (2014). Meteorites fulfill many of the generic environmental properties that Rummel et al. (2014) have used to define “uncertain regions” [i.e., protection from UV and Galactic Cosmic Rays (GCR)]. It is not possible to classify meteorites as “special regions” with respect to temperature and water activity at this time. Temperature is easier to infer, as meteorites are usually darker than surrounding rocks or soil due to their fusion crust and mafic lithology. The internal temperature of meteorites would be warmer owing to their low albedo, which is consistent with findings from martian analogue sites in terrestrial polar regions where dark rocks are warmer than the surrounding lighter coloured rocks (OMELON *ET AL.*, 2006). The activity of water within exogenic meteorites on Mars is less easy to infer because this would depend on the identities of the weathering products, and the nature of microenvironments, inside meteorites.

This chapter has already discussed a mechanism by which meteorite weathering products could adsorb

water to the surfaces of alteration minerals, and/or control the RH inside this microenvironment. Chapter Two investigates the behaviour of alteration minerals in meteorites collected from Earth's Nullarbor Plain to better address this question. It could be that the water activity inside meteorites is lower than what is possible to support growth of microbial communities. However, this would not necessarily stop meteorites from acting as "life boats" for survival of microbes instead.

1.2 Conclusions

Before meteorites can be considered as possible microbial habitats on Mars, a rationale must be presented for (1) the likelihood of their habitation by microorganisms, and (2) the ease of microbiological detection, past or present. As this chapter has shown, meteorites contain abundant reduced minerals that could be utilised by chemoautotrophic organisms as energy and nutrient sources. Furthermore, meteorites have long residence times on the martian surface, meaning that some meteorites could have sampled a putative biosphere at the martian surface throughout most of the planet's history, even as far back as the Noarchian when Mars and Earth had similar environmental conditions. This makes meteorites a prime environment for astrobiological exploration.

1.3 Thesis Structure

This thesis contains six chapters including the introductory chapter you are presently reading, and is formatted as a thesis by publication. Chapters 2, 3, 4 and 5 are written as stand-alone manuscripts to be submitted to peer-reviewed, international journals. Chapter 2 has already been submitted to the journal *Geochimica et Cosmochimica Acta* (GCA), and has been accepted for publication. Chapter 5 has also been submitted to GCA, and is currently under review. Chapter 4 has also been submitted to *Frontiers in Microbiology*, and has been accepted for publication. Due to this stand-alone structure, some duplication in content is unavoidable, especially in introductory and discussion segments where the research settings and central themes are presented. Chapter 6 is the final chapter, and serves as a synthesis of the material.

Very little previous work has been done on the topic of microbial colonisation and habitation of meteorites; most past research has focused on the idea of panspermia. Because of this, my research aims to distance itself from panspermia research and deal with firm observations of microbial habitation of meteorites at a Mars analogue site on Earth (*Chapter 2 and 3*), ecology of the organisms that inhabit

these meteorites (*Chapter 4*), experimental evidence that these microorganisms can be preserved and detected within meteorites (*Chapter 5*), and a discussion of how my observations could be applied by future astrobiology missions to Mars (*Chapter 6*).

Chapter 2 investigates the viability of meteorites as hosts to terrestrial microbes on the Nullarbor Plain, Australia. If we are to investigate exogenic meteorites on Mars, we must first understand how colonisation of meteorites by an existing biosphere occurs. The aims of this study are to: (1) identify hygroscopic minerals in cracks in meteorites that could be utilised by microorganisms as a source of water. (2) Use radiogenic carbon to determine that the carbonate in the meteorite veins is a product of modern meteorite weathering and not contaminants from the Nullarbor limestone. (3) Identify chasmoendolithic organisms indigenous to the Nullarbor living on the hygroscopic minerals in the veins. (4) Identify cryptoendolithic organisms living in the pore spaces left by the oxidation of metal/sulphide minerals. (5) Identify minerals associated with preserving organic, isotopic and fossil biosignatures, and the spatial relationship with modern biofilm. Understanding where microbes live in the meteorites and their relationship to mineral substrate biosignatures, paints a complex picture of microenvironments within the meteorites.

Chapter 3 expands on the previous chapter by examining the relationships between cracks and chasmoendolithic organisms that inhabit them. More specifically (1) can organisms penetrate new and smaller cracks in the meteorite, and (2) can the efflorescence's found in the established veins hold evidence of paleo-biofilms. The point of the former is to see if microbes can penetrate deep enough into a meteorite to mitigate the effects of UV light, if these were on Mars. The goal of the later is to see if fossilisation is possible in meteorites. The results from this chapter show that (1) microbes penetrated new cracks in excess of 500 μm into the meteorite. (2) That Eukaryotes including diatoms were found in meteorites; diatoms are a product of periodic flooding events on the Nullarbor. (3) Acid etch of existing biofilms showed that biomorphic shapes were found within the carbonate/gypsum efflorescences, and that follow up organic studies would be necessary to ascertain their biogenic origin. This chapter shows that organic preservation is indeed possible in meteorites, opening up another tool for astrobiology discovery.

Chapter 4 is a 16S phylogenetic analysis of the meteorites and the soils from the Nullarbor plain region. The microbial ecology showed that meteorites had low species evenness and low species richness compared to the soils. The meteorites were dominated by a singular OTU (organisation

taxonomic unit) that shared a 98% similarity with the organism *Rubrobacter radiotolerans*. The species is known for its desiccation and ionising radiation resistances. Moreover we found that despite being separated by many kilometres the meteorites shared more in common with each other than the soils they were directly sitting on, indicating that the substrate is more important for controlling a community composition than the location it is found. The application to Mars is that if meteorites were to be colonised by putative organisms, a few specialists, rather than a cross section of the regional community, would be present.

Chapter 5 builds on the direct field observations of the previous three chapters to develop an experiment that test whether alteration minerals in meteorites can record isotopic and microfossil biosignatures. The experiment uses the LL5 Chelyabinsk ordinary chondrite, and several standard Fe-sulfide minerals, as a substrate for culturing the chemolithotrophic organism, *Acidithiobacillus ferrooxidans*.

The stable sulfur isotopic composition of chondritic meteorites falls within a narrow range and has a standard deviation that is smaller than the isotopic fractionation of most known sulfur oxidising organisms (*Chapter 2*). As such, sulfur isotopic biosignatures should be recognisable in the mineral alteration products of meteorites. The results of this experiment showed that microfossils and biological isotope fractionations can be induced by chemolithotrophy, but more importantly it was the sulfur assimilation of the chemolithotrophic organisms that was clearer in nutrient limited conditions. This shows that meteorites are ideal tools for preserving evidence of biosignatures in a clear fashion without ambiguity.

In Chapter 6, the possibility of meteorites on Mars hosting microorganisms is discussed. This chapter draws upon the observations of the previous chapters in establishing a terrestrial baseline for microbial interaction with Earth's biosphere. This chapter discuss how these observations would apply to Mars, and the search for life on the red planet using robotic, sample return, and human exploration. This chapter ultimately lays out a roadmap for future research pertaining to exogenic meteorites on Mars, and their role in astrobiology.

1.4 Chapter 1 References

A

Ashley J. W. (2015) The Study of Exogenic Rocks on Mars — an Evolving Subdiscipline in Meteoritics. In: *Elements*, pp 10-11.

B

Beaty D. W., Carr M., Abell P., Barnes J., Boston P. J., Brinckerhoff W., Charles J., Delory G., Head J. W., Heldmann J. L. and others. (2006) Findings of the Mars Special Regions Science Analysis Group. *Astrobiology*, 6: 677-732.

Bennett J., and Shostak S. (2006) Life in the universe. *Addison - Wesley*.

Bland P., and Smith T. B. (2000) Meteorite accumulations on Mars. *Icarus*, 144: 21-26.

Bland P. A., Zolensky M. E., Benedix G. K., and Sephton M. A. (2006) Weathering of chondritic meteorites. In: *Meteorites and the Early Solar System II*. edited by DS Lauretta and HY McSween, *University of Arizona Press*, Tucson, pp 943.

Boussau B., Blanquart S., Necsulea A., Lartillot N., and Gouy M. (2008) Parallel adaptations to high temperatures in the Archaean eon. *Nature*, 456: 945-946.

Bradley J. P., Harvey R. P., McSween H. Y., Gibson E., Thomas-Keprta K., and Vali H. (1997) No 'nanofossils' in martian meteorite. *Nature*, 390: 454-456.

Burns R. G., and Fisher D. S. (1993) Rates of oxidative weathering on the surface of Mars. *Journal of Geophysical Research*, 98: 3365.

C

Canfield D. E. (2001) Biogeochemistry of sulfur isotopes. In: *Reviews in Mineralogy and Geochemistry*. edited by JW Valley and DR Coles, *Mineralogical Society of America*, Washington, DC, USA, pp 607-636.

Carr M. H., and Head J. W. (2010) Geologic history of Mars. *Earth and Planetary Science Letters*, 294: 185-203.

Cepelcha Z., Borovička J., Elford W. G., Revekke D. O., Hawkes R. L., Porubčan V., Šimek M. (1998) Meteor Phenomena and Bodies. *Space Science Reviews*, 84(3-4): 327-471.

Chappelow J., and Sharpton V. (2006) Atmospheric variations and meteorite production on Mars. *Icarus*, 184: 424-435.

Chappelow J. E., and Golombek M. P. (2010) Event and conditions that produced the iron meteorite Block Island on Mars. *Journal of Geophysical Research: Biogeosciences (2005–2012)*, 115.

Cronin J. R., and Pizzarello S. (1983) Amino acids in meteorites. *Advances in Space Research*, 3: 5-18.

D

- D'Hondt S., Rutherford S., and Spivack A. J. (2002) Metabolic activity of subsurface life in deep-sea sediments. *Science*, 295: 2067-2070.
- Di Giulio M. (2001) The universal ancestor was a thermophile or a hyperthermophile. *Gene*, 281: 11-17.
- Diniega S., Hansen C. J., McElwaine J. N., Hugenholtz C. H., Dundas C. M., McEwen A. S., and Bourke M. C. (2013) A new dry hypothesis for the formation of martian linear gullies. *Icarus*, 225: 526-537.
- Dundas C. M., Diniega S., and McEwen A. S. (2015) Long-term monitoring of martian gully formation and evolution with MRO/HiRISE. *Icarus*, 251: 244-263.

F

- Ferry J. G. (1992) Methane from Acetate. *American Society for Microbiology*: 5489-5495.
- Flynn G. J., and McKay D. S. (1990) An assessment of the meteoritic contribution to the Martian soil. *Journal of Geophysical Research*, 95: 14497.
- Formisano V., Atreya S., Encrenaz T., Ignatiev N., and Giuranna M. (2004) Detection of methane in the atmosphere of Mars. *Science*, 306: 1758-1761.
- Fouchet T., Lellouch E., Ignatiev N. I., Forget F., Titov D. V., Tschimmel M., Montmessin F., Formisano V., Giuranna A., Maturilli A. and others. (2007) Martian water vapor: Mars Express PFS/LW observations. *Icarus*, 190: 32-49.

G

- Gomes R., Levison H. F., Tsiganis K., and Morbidelli A. (2005) Origin of the cataclysmic Late Heavy Bombardment period of the terrestrial planets. *Nature*, 435: 466-469.

H

- Harvey R. P., and McSween Jr H. Y. (1996) A possible high-temperature origin for the carbonates in the martian meteorite ALH84001. *Nature*, 382: 49-51.
- Heldmann J. L. (2005) Formation of Martian gullies by the action of liquid water flowing under current Martian environmental conditions. *Journal of Geophysical Research*, 110: E05004.
- Hoehler T. M., and Jorgensen B. B. (2013) Microbial life under extreme energy limitation. *Nature Reviews Microbiology*, 11: 83-94.
- Houtkooper J. M. (2013) Turnover of Methane in the Martian Atmosphere. *ESPC Abstracts*, 8.

I

Ivanov B. A. (2001) Mars/Moon cratering rate ratio estimates. *Space Science Reviews*, 96: 87-104.

J

Jarosewich E. (1990) Chemical analyses of meteorites: A compilation of stony and iron meteorite analyses. *Meteoritics*, 25: 323-337.

K

Kelly L. C., Cockell C. S., Thorsteinsson T., Marteinson V., and Stevenson J. (2014) Pioneer Microbial Communities of the Fimmvörðuháls Lava Flow, Eyjafjallajökull, Iceland. *Microbial Ecology*, 68: 504-518.

Kossacki K. J., Portyankina G., and Thomas N. (2011) The evolution of exposed ice in a fresh mid-latitude crater on Mars. *Icarus*, 211: 195-206.

Kounaves S. P., Carrier B. L., O'Neil G. D., Stroble S. T., and Claire M. W. (2014a) Evidence of martian perchlorate, chlorate, and nitrate in Mars meteorite EETA79001: Implications for oxidants and organics. *Icarus*, 229: 206-213.

Kounaves S. P., Chaniotakis N. A., Chevrier V. F., Carrier B. L., Folds K. E., Hansen V. M., McElhoney K. M., O'Neil G. D., and Weber A. W. (2014b) Identification of the perchlorate parent salts at the Phoenix Mars landing site and possible implications. *Icarus*, 232: 226-231.

Kral T. A., and Altheide S. T. (2013) Methanogen survival following exposure to desiccation, low pressure and martian regolith analogs. *Planetary & Space Science*, 89: 167-171.

L

Lee M. R., and Bland P. A. (2004) Mechanisms of weathering of meteorites recovered from hot and cold deserts and the formation of phyllosilicates. *Geochimica et Cosmochimica Acta*, 68: 893-916.

Lee M. R., Smith C., Gordon S. H., and Hodson M. E. (2006) Laboratory simulation of terrestrial meteorite weathering using the Bensour (LL6) ordinary chondrite. *Meteoritics & Planetary Science*, 41.

Lennon J. T., and Jones S. E. (2011) Microbial seed banks: the ecological and evolutionary implications of dormancy. *Nature Reviews Microbiology*, 9: 119-130.

Levy J. (2012) Hydrological characteristics of recurrent slope lineae on Mars: Evidence for liquid flow through regolith and comparisons with Antarctic terrestrial analogs. *Icarus*, 219: 1-4.

Lewis J. S. (2004) Physics and Chemistry of the Solar System. *Elsevier/Academic Press*.

- Liu J.y., Xiu X.-x., and Cai P. (2009) Study of formation of jarosite mediated by *Thiobacillus ferrooxidans* in 9K medium. *PROEPS*, 1: 706-712.
- Lodders K. (2010) Solar System Abundances of the Elements. *Principles and Perspectives in Cosmochemistry*, 379-417.
- Long D. T., Velbel M., and Gooding J. I. (1989) Terrestrial weathering of Antarctic stone meteorites: Formation of Mg-carbonates on ordinary chondrites. *Geochimica et Cosmochimica Acta*, 55: 67-76.

M

- Madigan M., Martinko J., Stahl D., and Clark D. (2012) Brock: Biology of Microorganisms. *Pearson*, San Fransisco.
- Malin M. C., Edgett K. S., Posiolova L. V., McColley S. M., and Dobrea E. Z. N. (2006) Present-day impact cratering rate and contemporary gully activity on Mars. *Science*, 314: 1573-1577.
- Maltagliati L., Montmessin F., Fedorova A., Korablev O., Forget F., and Bertaux J. L. (2011) Evidence of water vapor in excess of saturation in the atmosphere of Mars. *Science*, 333: 1868-1871.
- Mangold N. (2012) Fluvial landforms on fresh impact ejecta on Mars. *Planetary and Space Science*, 62: 69-85.
- McKay D. S., Gibson Jr E. K., Thomas-Keprta K. L., Vali H., Romanek C. S., Clemett S. J., Chillier X. D. F., Maechling C. R., and Zare R. N. (1996) Search for Past Life on Mars: Possible Relic Biogenic Activity in Martian Meteorite ALH84001. *Science*, 273: 924-930.
- McMahon S., Parnell J., Ponicka J., Hole M., and Boyce A. (2013) The habitability of vesicles in martian basalt. *Astronomy & Geophysics*, 54: 17-21.
- Michalski J. R., Cuadros J., Niles P. B., Parnell J., Rogers A. D., and Wright S. P. (2013) Groundwater activity on Mars and implications for a deep biosphere. *Nature Geoscience*, 6: 133-138.
- Milbury C., Schubert G., Raymond C. A., Smrekar S. E., and Langlais B. (2012) The history of Mars' dynamo as revealed by modeling magnetic anomalies near Tyrrhenus Mons and Syrtis Major. *Journal of Geophysical Research: Biogeosciences (2005-2012)*, 117: E10007
- Moore C. B., and Gibson E. K. (1969) Nitrogen Abundances in Chondritic Meteorites. *Science*, 163: 174-176.

N

- Neukum G., Jaumann R., Hoffmann H., Hauber E., Head J. W., Basilevsky A. T., Ivanov B. A., Werner S. C., van Gasselt S., Murray J. B. and others. (2004) Recent and episodic volcanic and glacial activity on Mars revealed by the High Resolution Stereo Camera. *Nature*, 432: 971-979.

- Nutman A. P., Bennett V. C., Friend C. R. L., Van Kranendonk M. J., and Chivas A. R. (2016) Rapid emergence of life shown by discovery of 3,700-million-year-old microbial structures. *Nature*, 537: 535-538.

O

- Ojha L., Wilhelm M. B., Murchie S. L., McEwen A. S., Wray J. J., Hanley J., Massé M., and Chojnacki M. (2015) Spectral evidence for hydrated salts in recurring slope lineae on Mars. *Nature Geoscience*, 8: 829-832.
- Olsson-Francis K., and Cockell C. S. (2010) Experimental methods for studying microbial survival in extraterrestrial environments. *Journal of Microbiological Methods*, 80: 1-13.
- Owen T., Biemann K., Rushneck D. R., Biller J. E., Howarth D. W., and Lafleur A. L. (2012) The composition of the atmosphere at the surface of Mars. *Journal of Geophysical Research*, 82: 4635-4639.

P

- Pace N. R. (2001) The universal nature of biochemistry. *Proceedings of the National Academy of Sciences of the United States of America*, 98: 805-808.
- Pasek M., and Lauretta D. (2007) Extraterrestrial Flux of Potentially Prebiotic C, N, and P to the Early Earth. *Origins of Life and Evolution of Biospheres*, 38: 5-21.
- Pasek M. A., Harnmeijer J. P., Buick R., Gull M., and Atlas Z. (2013) Evidence for reactive reduced phosphorus species in the early Archean ocean. *Proceedings of the National Academy of Sciences of the United States of America*, 220: 10089-10094.
- Pavlov A. K., Shelegedin V. N., Vdovina M. A., and Pavlov A. A. (2010) Growth of microorganisms in Martian-like shallow subsurface conditions: laboratory modelling. *International Journal of Astrobiology*, 9: 51-58.
- Pizzarello S., Huang Y., and Fuller M. (2004) The carbon isotopic distribution of Murchison amino acids. *Geochimica et Cosmochimica Acta*, 68: 4963-4969.
- Popova O., Nemtchinov I., Hartmann W. K. (2003) Bolides in the present and past martian atmosphere and effects on cratering processes, *Meteoritics & Planetary Science*, 38(6); 905-925.
- Price P. B., and Sowers T. (2004) Temperature dependence of metabolic rates for microbial growth, maintenance, and survival. *Proceedings of the National Academy of Sciences of the United States of America*, 101: 4631-4636.

R

- Rettberg P., Rabbow E., Panitz C., and Horneck G. (2004) Biological space experiments for the simulation of Martian conditions: UV radiation and Martian soil analogues. *Advances in Space Research*, 33: 1294-1301.

S

- Schorghofer N. (2008) Temperature response of Mars to Milankovitch cycles. *Geophysical Research Letters*, 35.
- Schröder C., Rodionov D. S., McCoy T. J., Jolliff B. L., Gellert R., Nittler L. R., Farrand W. H., R J. J. J., Ruff S. W., Ashley J. W. and others. (2008) Meteorites on Mars observed with the Mars Exploration Rovers. *Journal of Geophysical Research*, 113: 1-19.
- Scott E. R. D., Yamaguchi A., and Krot A. N. (1997) Petrological evidence for shock melting of carbonates in the martian meteorite ALH84001. *Nature*, 387: 377-379.
- Sephton M. A. (2002) Organic compounds in carbonaceous meteorites. *Natural Product Reports*, 19: 292-311.
- Shoemaker E. M. (1977) Astronomically observable crater-forming projectiles. edited by DJ Roddy, RO Pepin and RB Merrills, *Pergamon Press*, New York, pp 617-628.
- Som S. M. (2014) Planetary science: Into thin martian air. *Nature Publishing Group*, 7: 329-330.
- Squyres S. W., Grotzinger J. P., Arvidson R. E., Bell J. F., Calvin W., Christensen P. R., Clark B. C., Crisp J. A., Farrand W. H., Herkenhoff K. and others. (2004) In Situ Evidence for an Ancient Aqueous Environment at Meridiani Planum, Mars. *Science*, 306: 1709-1714.
- Steiger M., Linnow K., Juling H., Gülker G., El Jarad A., Brüggerhoff S., and Kirchner D. (2007) Hydration of $\text{MgSO}_4 \cdot \text{H}_2\text{O}$ and Generation of Stress in Porous Materials. *Crystal Growth and Design*, 8(1): 336-343.
- Summons R. E., Amend J. P., Bish D., Buick R., Cody G. D., Des Marais D. J., Dromart G., Eigenbrode J. L., Knoll A. H., and Sumner D. Y. (2011) Preservation of martian organic and environmental records: Final report of the Mars Biosignature Working Group. *Astrobiology*, 11: 157-181.

W

- Wilson S. A., and Bish D. L. (2011) Formation of gypsum and bassanite by cation exchange reactions in the absence of free-liquid H_2O : Implications for Mars. *Journal of Geophysical Research*, 116: E09010.
- Wohletz K. H., and Sheridan M. F. (1983) Martian rampart crater ejecta - Experiments and analysis of melt-water interaction. *Icarus*, 56: 15-37.

Z

- Zolotov M. Y., and Shock E. L. (2005) Formation of jarosite-bearing deposits through aqueous oxidation of pyrite at Meridiani Planum, Mars. *Geophysical Research Letters*, 32: L21203.
- Zurfluh F. J., Hofmann B. A., Gnos E., and Eggenberger U. (2013) “Sweating meteorites”—Water-soluble salts and temperature variation in ordinary chondrites and soil from the hot desert of Oman. *Meteoritics & Planetary Science*, 48: 1958-1980.



Declaration for Thesis Chapter 2

Declaration by candidate

In the case of Chapter 2, the nature and extent of my contribution is as follows:

<i>Nature of contribution</i>	<i>Extent of contribution (%)</i>
Conceptualisation, sample Collection, sample preparation, SEM analysis, field work, adsorption analysis, data interpretation, manuscript writing	80%

The following co-authors contributed to the work. If co-authors are students at Monash University, the extent of their contribution in percentage terms must be stated:

<i>Name</i>	<i>Nature of contribution</i>	<i>Extent of contribution (%)</i>
Siobhan A. Wilson	Supervisory Role	5%
Andrew G. Tomkins	Supervisory Role	5%
Emma J. Gagen	Experimental Design	5%
Stewart J. Fallon	Radiocarbon Data Collection	2.5%
Gordon Southam	Advisory Role	2.5%

The undersigned hereby certify that the above declaration correctly reflects the nature and extent of the candidate's and co-authors contributions to this work*.

Candidate's signature:

Date: 01/06/2017

Main supervisor's signature:

Date: 01/06/2017

*Note: Where the responsible author is not the candidate's main supervisor, the main supervisor should consult with the responsible author to agree on the respective contributions of the authors.

Chapter 2

Evaluation of meteorites as habitats for terrestrial microorganisms: Results from the Nullarbor Plain, Australia, a Mars analogue site [†]

Alastair W. Tait¹, Siobhan A. Wilson¹, Andrew G. Tomkins¹, Emma J. Gagen², Stewart J. Fallon³ and Gordon Southam²

¹School of Earth, Atmosphere & Environment, Monash University, Australia

²School of Earth & Environmental Sciences, The University of Queensland, Australia

³Research School of Earth Sciences, The Australian National University, Australia

[†] Accepted for publication in *Geochimica et Cosmochimica Acta*

28th May 2017

Unambiguous identification of biosignatures on Mars requires access to well-characterized, long-lasting geochemical standards at the planet's surface that can be modified by theoretical martian life. Ordinary chondrites, which are ancient meteorites that commonly fall to the surface of Mars and Earth, have well-characterized, narrow ranges in trace element and isotope geochemistry compared to martian rocks. Given that their mineralogy is more attractive to known chemolithotrophic life than the basaltic rocks that dominate the martian surface, meteorites may be good places to look for signs of prior life endemic to Mars. In this study, we show that ordinary chondrites, collected from the arid Australian Nullarbor Plain, are commonly colonized and inhabited by terrestrial microorganisms that are endemic to this Mars analogue site. These terrestrial endolithic and chasmolithic microbial contaminants are commonly found in close association with hygroscopic veins of gypsum and Mg-calcite, which have formed within cracks penetrating deep into the meteorites. Terrestrial bacteria are observed within corrosion cavities, where troilite (FeS) oxidation has produced jarosite $[\text{KFe}_3(\text{SO}_4)_2(\text{OH})_6]$. Where terrestrial microorganisms have colonized primary silicate minerals and secondary calcite, these mineral surfaces are heavily etched. Our results show that inhabitation of meteorites by terrestrial microorganisms in arid environments relies upon humidity and pH regulation by minerals. Furthermore, microbial colonization affects the weathering of meteorites and production of sulfate, carbonate, Fe-oxide and smectite minerals that can preserve chemical and isotopic biosignatures for thousands to millions of years on Earth. Meteorites are thus habitable by terrestrial microorganisms, even under highly desiccating environmental conditions of relevance to Mars. They may therefore be useful as chemical and isotopic “standards” that preserve evidence of life, thereby providing the possibility of universal context for recognition of microbial biosignatures on Earth, Mars and throughout the solar system.

2.1 Introduction

One of the greatest hurdles to identifying extra-terrestrial life is the ambiguity inherent to detection of biosignatures in poorly understood geochemical settings, such as the martian surface. Ideally, a well-characterized, sterile geochemical standard could be deployed to the surface of Mars that, if colonized and inhabited by putative martian microorganisms, would give unambiguous signatures of microbial modification. Conveniently, the mineralogical, elemental and isotopic characteristics of chondritic meteorites — which make up 87% of our catalogue of meteorites on Earth — have been carefully constrained by extensive study (FARQUHAR *ET AL.*, 2007; JAROSEWICH, 1990). Chondrites contain sulfide minerals and FeNi alloys that support terrestrial sulfur- and iron-oxidizing microorganisms under laboratory conditions (GRONSTAL *ET AL.*, 2009). Chondritic meteorites (carbonaceous chondrites in particular) also contain soluble organic compounds and minerals that can support heterotrophic microorganisms (MAUTNER, 1997). For instance, bioavailable phosphorus, nitrogen and chromium are found within meteorites in apatite group minerals $[\text{Ca}_5(\text{PO}_4)_3(\text{OH},\text{F},\text{Cl})]$, schriebersite $[(\text{Fe},\text{Ni})_3\text{P}]$

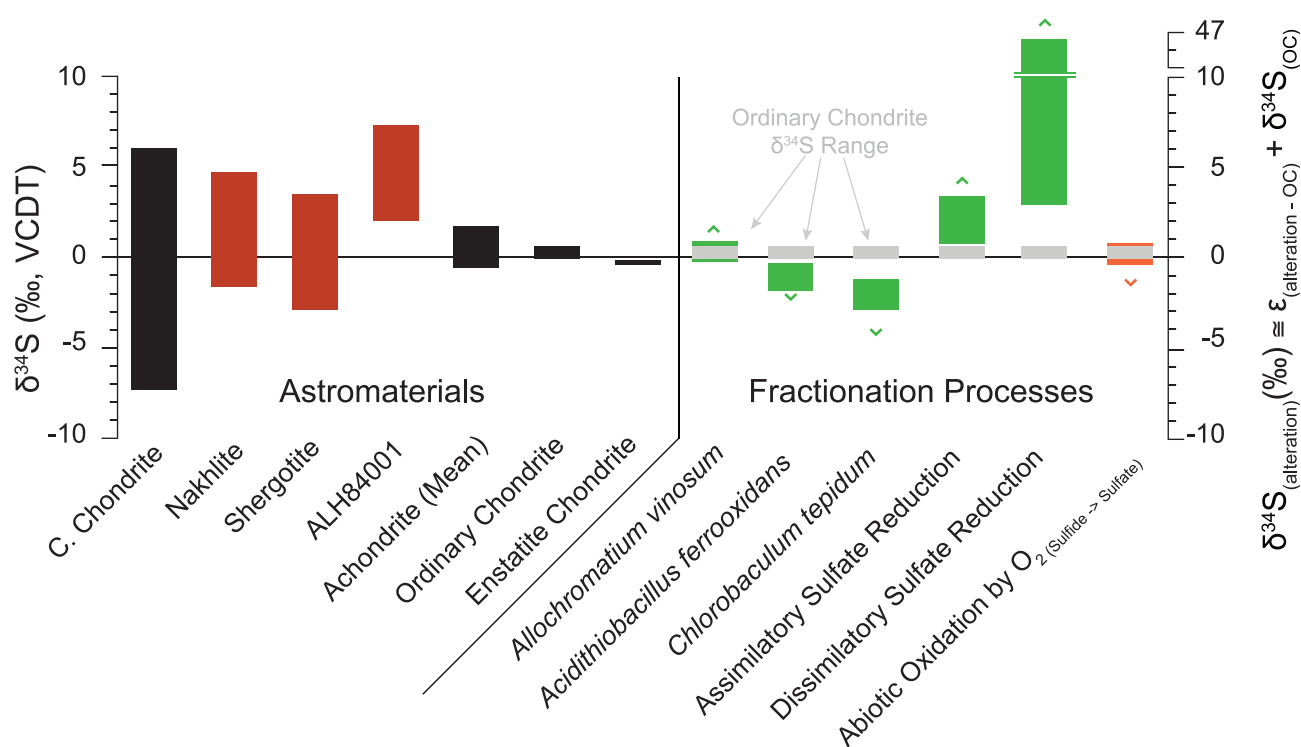


Figure 2.1 | Suitability of astromaterials for detection of biological $\delta^{34}\text{S}$ signatures. The left hand side shows $\delta^{34}\text{S}$ ranges of sulfur-bearing phases in astromaterials. The right hand side plots predicted $\delta^{34}\text{S}$ ranges of secondary minerals (alteration) in ordinary chondrites (OC) affected by some common sulfur oxidising/reducing organisms and abiotic processes. Isotopic fractionation by terrestrial organisms far exceeds the range of $\delta^{34}\text{S}$ values found in ordinary and enstatite chondrites, but is largely within the range found in SNC meteorites. See (FARQUHAR *ET AL.*, 2007; GREENWOOD *ET AL.*, 1997) and references therein for astromaterial values and (BALCI *ET AL.*, 2007; BRABEC *ET AL.*, 2012; CANFIELD, 2001; PISAPIA *ET AL.*, 2007) for values pertaining to fractionation processes.

(PASEK AND LAURETTA, 2008) and carlsbergite (CrN) (HARRIES *ET AL.*, 2015). Microbial sulfur cycling causes stable isotope fractionation and produces alteration minerals with distinctive isotopic signatures (CANFIELD, 2001) that can be readily distinguished from those observed in unaltered meteorites (*Figure 2.1*). Comparatively little is known about the stable sulfur isotope signatures of martian rocks and how the planet's complex history could have affected sulfur isotope fractionation (FARQUHAR *ET AL.*, 2000; FARQUHAR *ET AL.*, 2010). Our understanding of martian sulfur cycling comes from studies of the SNC (Shergottite, Nakhlite, Cassinite) meteorites, which are samples of the martian crust that were ejected during from Mars during impact events. Large differences in $\delta^{34}\text{S}$ values have been reported for the different classes of SNC meteorites (Farquhar et al., 2000). Even within the Nakhlite sub-types there is (1) $\delta^{34}\text{S}_{(\text{means})} = -6.1 - 1.5\text{‰}$ variation of the means (using pyrrhotite and pyrite) in $\delta^{34}\text{S}$ values between meteorites (GREENWOOD *ET AL.*, 2000), (2) $\delta^{34}\text{S}_{(\text{S.Phases})} = 0.93 - 2.03\text{‰}$ variation between different sulfur-bearing phases within a single meteorite (Nakhlite) (FARQUHAR *ET AL.*, 2000), and (3) $\delta^{34}\text{S}_{(\text{Nakhlite})} = -1.7 - 4.9\text{‰}$ variation within grains of the same phase

(pyrrhotite) within one meteorite (Nakhla) (FARQUHAR *ET AL.*, 2007; GREENWOOD *ET AL.*, 2000). This heterogeneity, combined with poor constraints on the evolution of the martian sulfur cycle, could make unambiguous detection of stable sulfur isotopic biomarkers difficult. Given these points, we suggest that chondritic meteorites are ideal standards for the detection of past or present life at planetary surfaces.

However, there must be a compelling case for microbial habitation for a standard to be of use to astrobiologists. In addition to redox sensitive elements, such as carbon, sulfur and iron, which can be harnessed for metabolism and/or biomass production, microorganisms require a source of water. Earth's deserts, such as the Nullarbor Plain in Australia, are valued as Mars analogues because of their aridity. They are also commonly explored for meteorites because the scarcity of water slows weathering, improving preservation of their original composition (BLAND *ET AL.*, 2006). However, the scarcity of bioavailable water in terrestrial deserts poses a challenge to life; it is also likely this would be a problem for theoretical life in the arid martian surface and subsurface.

Hygroscopic minerals such as sulfates, halides, perchlorates, carbonates, Fe-oxyhydroxides and smectites naturally adsorb atmospheric water vapor to crystal surfaces and accommodate H₂O within their crystal structures. It has been speculated that this mineral behavior could provide a source of water to desiccation-resistant microorganisms on Mars (DAVILA *ET AL.*, 2008). Davila et al. (2008) have demonstrated that deliquescence of halite (NaCl) provides sufficient water to sustain endolithic cyanobacteria under the desiccating conditions of the hyperarid Atacama Desert in South America. Furthermore, reactions amongst hygroscopic minerals are known to occur at or below their deliquescence relative humidities (RH), and can thus maintain nutrient cycling in the absence of detectable liquid water even at temperatures much less than 0°C (WILSON AND BISH, 2011, 2012). In this way, hygroscopic minerals may allow survival of putative microorganisms within the shallow martian subsurface (BENISON AND KARMANOCKY, 2014; MOHLMANN AND THOMSEN, 2011). Meteorites commonly contain hygroscopic sulfates, carbonates, Fe-oxyhydroxides and smectites by virtue of weathering of primary sulfides, FeNi alloys and silicate minerals (BLAND *ET AL.*, 2006; ZURFLUH *ET AL.*, 2013). The high porosity of chondritic meteorites and elevated phosphorus concentrations relative to many common rock compositions are also expected to facilitate colonization by contaminant microorganisms. Combined, these traits suggest meteorites may be excellent refuge habitats for microorganisms in environmentally hostile conditions.

Chondritic meteorites are fragments of asteroid parent bodies that formed over 4.5 billion years

ago during the birth of our solar system and which never underwent accretion to form planets. As such, their formation predates the emergence of life on Earth and they are sterile when they fall to the surfaces of Earth, Mars and other solar system bodies. Thus, any microorganisms detected in chondritic meteorites will be endemic to the planet and local environment in which the meteorite fell. This means that the biological study of meteorites is similar to “first colonizer” research from recent basaltic lava flows in Iceland (KELLY *ET AL.*, 2014). Kelly et al. (2014) showed that these lavas were colonized by low diversity microbial colonies, including chemolithotrophic taxa, within 3–5 months post eruption. Basaltic rocks on Earth and Mars are chemically and mineralogically similar to chondritic meteorites. Thus meteorites may represent a more easily colonized refuge on the surface of Mars for theoretical chemolithotrophic organisms adapted to basaltic substrates. The weathering profiles of meteorites can create points of ingress for endolithic microorganisms to take advantage of a diversity of microhabitats. As such, we might expect to find that microorganisms colonize pore spaces or voids (i.e., cryptoendoliths) as well as fissures and cracks (i.e., chasmoendoliths) within meteorites.

Table 2.1| Abundances of Minerals in Vein Material by Rietveld Refinement.

Official Name	Ooldea 002	Watson 015	Ooldea 007	Ooldea Regolith
Type	L5	H4	H3	-
Weathering grade	W4	W4	W4	-
Mineral	Ooldea 002 (wt.%)	Watson 015 (wt.%)	Ooldea 007 (wt.%)	Ooldea Regolith (wt.%)
kaolinite	5.7		8.6	17.4
illite	33.4			11.9
magnesite	0.5			
orthoclase	0.6		0.9	10.6
oligoclase	5.8		2.1	5.7
goethite	2.5	3.8	1.5	0.5
gypsum	0.6	24.6	6.1	
calcite	38.0	60.0	52.4	0.8
quartz	12.8	8.9	28.4	53.2
diopside		2.7		
totals	100.0	100.0	100.0	100.0
Contamination (wt.%)*	18.9	16.7	53.4	-
Rwp (%)	11.4	11.7	11.0	16.7

* Contamination is based on the quartz content in the vein material, scaled to the Ooldea regolith.

We collected fragments of chondritic meteorites from the Nullarbor Plain, an arid Eocene limestone karst in southern central Australia (WEBB AND JAMES, 2006), to examine whether they interact in a detectable way with Earth's biosphere under Mars-like conditions. A subset of meteorite samples was glutaraldehyde-fixed in the field for later imaging of microorganisms endemic to the Nullarbor Plain using a Field Emission Gun Scanning Electron Microscope (FEG-SEM). Secondary minerals were identified, and their abundances quantified, using powder X-Ray Diffraction (XRD). The extent to which these weathering products adsorb atmospheric water vapor was measured using a water sorption analyzer. Stable and radiogenic carbon isotope data were used to determine the origin of Mg-calcite as either a weathering product that could form in any CO₂-rich planetary atmosphere, such as that of Earth or Mars, or contamination from Eocene Nullarbor Limestone. Our results provide confirmation that terrestrial microorganisms commonly colonize and inhabit meteorites in one of the most arid environments on Earth. Furthermore, they leave behind an assemblage of alteration minerals that is ideally suited to preservation of fossil, organic molecular and isotopic biosignatures within ordinary chondrites.

2.2 Methods

2.2.1 Meteorite Sample Description

Meteorites were recovered from the Nullarbor Plain during Monash University's 2013–2015 annual recovery expeditions. Full meteorite descriptions can be found on The Meteoritical Bulletin Database and all samples are curated within the collection of the School of Earth, Atmosphere and Environment at Monash University. For petrological classification methods see Van Schmus and Wood (1967), for shock classification see Stoffler et al. (1991), and for weathering classification see Wlotzka (1993). Meteorites and soil samples were collected aseptically using gloves washed in 70% ethanol, and sterile bags/falcon tubes to prevent contamination by microorganisms other than those endemic to the Nullarbor Plain.

Ooldea 002 is a fragmented 1.3-kg L5 chondrite that was found in nine partially buried pieces. The sample is lightly shocked (S2) and quite weathered exhibiting a W4 weathering profile. *Ooldea 005* is a 144-g H5 chondrite that is broken into blocks with a partial fusion crust. The sample is moderately shocked (S3) with heavy alteration (W3). *Ooldea 007* is a single H3 stone weighing 135 g, exhibiting moderate shock (S3) and complete metal alloy and sulfide alteration (W4). *Ooldea 009* is

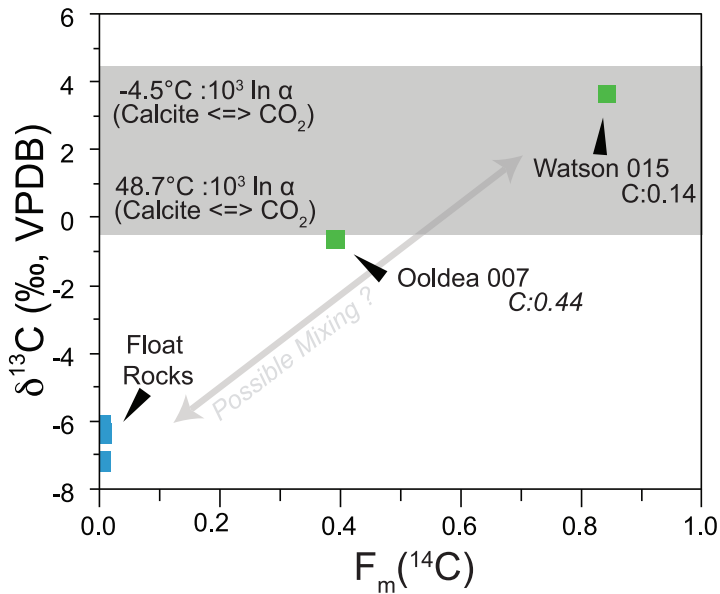


Figure 2.2 | Vein-carbonate Origin and Potential Contamination.

Values of $\delta^{13}\text{C}$ versus $F_m(^{14}\text{C})$ are plotted here for meteorite vein material and Nullarbor limestone. $\delta^{13}\text{C}$ values for calcite precipitating in equilibrium with atmospheric CO_2 gas (grey box), are calculated over the typical range of temperatures recorded in the Nullarbor using the fractionation factors of Deines and others (1974). The estimated proportion of contamination (c), from windblown dust and limestone, is given for each meteorite analysed.

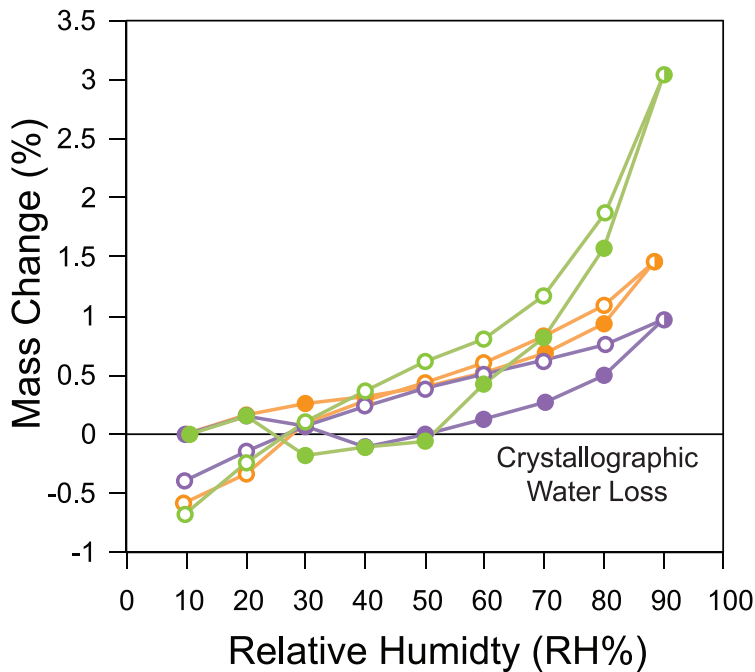


Figure 2.3 | Adsorption Isotherms for Vein Material. Green = *Ooldea 002* (L5, W4), orange = *Watson 015* (H4, W4), purple = *Ooldea 007* (H3, W4). Filled circles denote sorption steps and empty circles denote desorption.

a H6 chondrite consisting of two pieces that jigsaw fit together, with a total mass of 47 g. The sample exhibits light shock (S2) and heavy alteration (W3). *Watson 015* is a 457-g H4 chondrite that was found in two pieces, with 2/3rds coverage by fusion crust. The sample is lightly shocked (S2) and exhibits complete alteration of the metal alloy and sulfide grains (W4). *Watson 017* is a 1.8-kg H5 chondrite that was found in over 100 pieces with two main masses. The meteorite is moderately shocked (S3) and heavily altered (W3). Weathering grade in meteorites reflects terrestrial alteration of the original mineralogical composition since falling to Earth.

2.2.2 Powder X-ray Diffraction

Mineralogical characterization of meteorites focused on alteration products within networks of pores and fractures, which would be accessible to microorganisms endemic to the Nullarbor Plain. An off-white precipitate commonly develops within these fractures, infilling them as veins that can be up to several hundreds of μm in thickness. The mineralogical composition of vein samples from three meteorites, *Ooldea 002*, *Watson 015*, and

Ooldea 007, was determined using powder X-ray Diffraction (XRD), which required breaking the meteorites along existing planes of weakness to expose their interior surfaces. Vein material was mechanically etched from meteorites, homogenized in an agate mortar and pestle under anhydrous ethanol, and dried in a fume hood. Samples were stored under ambient temperatures and relative humidities typical for Melbourne, Australia.

Mineral identification and semi-quantitative phase analysis were carried out in the Monash X-ray Platform using a Bruker D8 Advance X-Ray Diffractometer. Patterns were collected using a Cu X-ray tube (operated at 40 kV and 40 mA) over a 2θ range of $3 - 80^\circ$ with a step size of $0.02^\circ/\text{step}$ and a dwell time of 3 s/step. Due to their small size, samples were mounted as ethanol slurries onto a zero-background silicon plate for analysis. Mineral phases were identified using the Powder Diffraction File 2 (PDF-2) database available from the International Centre for Diffraction Data (ICDD) using the DIFFRACplus EVA v.2 software program (Bruker AXS). Estimates of phase abundances were obtained by Rietveld refinement (BISH AND HOWARD, 1988; HILL AND HOWARD, 1987; RIETVELD, 1969) using the program Topas v.4.2 (Bruker AXS). The resulting Rietveld refinements provide a semi-quantitative measure of phase abundance owing to collection of patterns from thin films of hand-ground powder, mounted on a zero-background silicon plate. XRD patterns collected in this way exhibit the effects of non-ideal particle size statistics and preferred orientation on some phases, which can result in higher Rwp values (see *Table 2.1* for results).

We used the abundance of quartz found within the cracks in meteorites to estimate the amount of terrestrial mineral contamination derived from Nullarbor regolith. This value can be used to estimate contamination because quartz is not an abundant primary phase in chondritic meteorites, and thus must be terrestrial in origin (HEZEL *ET AL.*, 2006). The abundances of all mineral phases found in both the regolith and meteorite samples were scaled, based on the amount of quartz in the sample, to estimate the amount of contamination in each sample. These estimations should only be considered rough guidelines (see *Table 2.1* for results).

2.2.3 Stable and Radiogenic Isotope Geochemistry

Samples of vein material from three meteorites (*Ooldea 002*, *Ooldea 007*, *Watson 015*) and three samples of Nullarbor Limestone were analyzed for their ^{14}C concentrations using the Single Stage Accelerator Mass Spectrometer (SSAMS) at the Australian National University (ANU) (FALLON *ET AL.*, 2010). *Ooldea 002* failed to produce a result. Stable carbon isotopic data were collected from

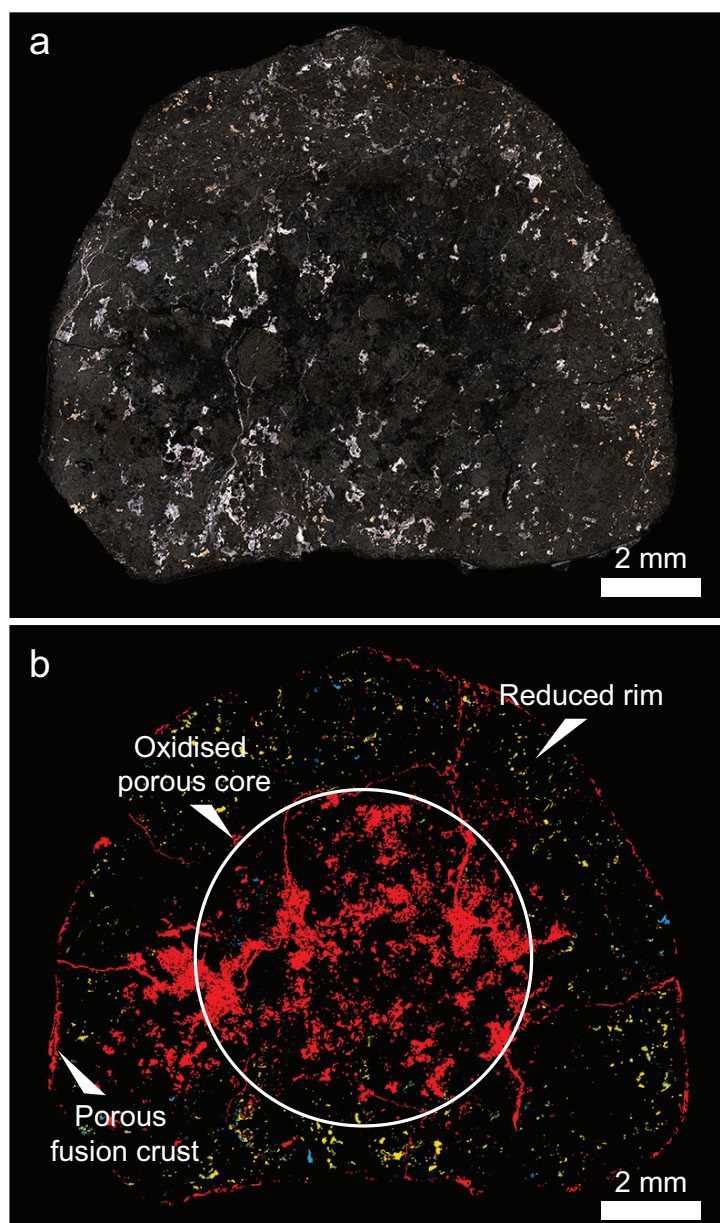


Figure 2.4 | Humidity Oasis. This figure is a stitch of a reflected light image from a petrographic microscope, of the *Ooldea 009* (H6, S3, W3) chondrite. Phases and voids were determined by scaling the LUT (Look up table), and then artificially colored. **(A)** Original reflected light image. **(B)** Processed image shows void spaces (red) in the centre of *Ooldea 009*. The reduced rim contains unoxidised troilite (yellow) and FeNi alloy (blue).

the same six samples by Isotope Ratio Mass Spectrometry (IRMS) at Monash University (MU). The $\delta^{13}\text{C}$ compositions are given relative to Vienna Pee Dee Belemnite (VPDB).

2.2.4 Water Sorption Isotherms

Water sorption isotherm experiments were carried out in the Department of Materials Engineering at MU using a gravimetric CISORP Water Sorption Analyzer (manufactured by CI Electronics; methods modified from Morgan et al. (2015)). Samples were exposed to ambient pressure at a constant temperature of 20°C, which was chosen for overlap between peak equatorial temperatures on Mars and ambient conditions in the Nullarbor Desert. A diurnal cycle of relative humidity (RH) was simulated by increasing RH from 10 to 90% and then allowing it return to 10% RH (in 10% increments). Samples were allowed to equilibrate with atmospheric RH at each step before the instrument automatically began the next humidity

increment. Scales were calibrated to 20°C prior to commencement of the experiment and each of the samples analyzed weighed approximately 100 mg.

2.2.5 Scanning Electron Microscopy

Biological samples for SEM were collected aseptically and field-fixed with filter-sterilized (0.1 μm)

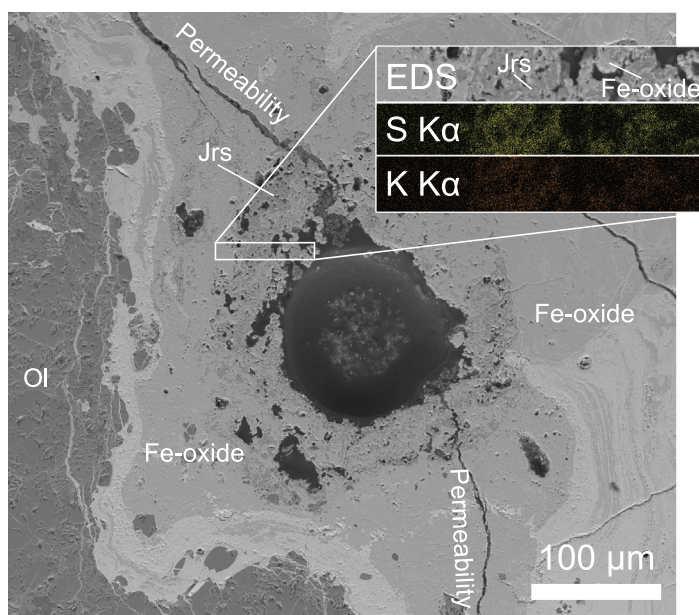


Figure 2.5 | Jarosite in Corrosion Cavity. The above Backscattered Electron (BSE) image and inset Energy Dispersive Spectroscopy (EDS) maps of S and K K α show a corrosion cavity inside the *Ooldea 005* ordinary chondrite. FeNi and FeS have been oxidised and removed from the system along cracks, leaving behind Fe-oxyhydroxides and jarosite (Jrs).

solution of 0.1%_(aq) glutaraldehyde. Samples were then dehydrated using a traditional graded ethanol series (50%, 70%, 90% and 100% x3) and critical point dried using a Bal-Tec CPD 030. Back Scattered Electron (BSE) and Secondary Electron Images (SEI) were collected from Pt-coated samples using a JEOL 7001F FEG-SEM at the Monash Centre for Electron Microscopy. The microscope was operated in BSE, SEI and Energy Dispersive X-ray Spectroscopy (EDX) modes using varying accelerating voltages, ranging from 1–15 kV, with a working distance of 10 mm.

2.3 Results

2.3.1 Stable and Radiogenic Isotopes

Nullarbor Limestone samples (n=3) gave ^{14}C -depleted F_m values between 0.0015 and 0.0034 and $\delta^{13}\text{C}$ values between -7.20 and -6.09‰, (Figure 2.2). Two meteorite vein samples, identified as carbonate-bearing, gave much greater F_m values of 0.8458 ± 0.25 and 0.3967 ± 0.65 that correspond to calibrated ^{14}C ages of 7490 ± 140 cal BP (*Ooldea 007*) and 1410 ± 25 cal BP (*Watson 015*). The meteorite veins gave $\delta^{13}\text{C}$ values of -0.70‰ (*Ooldea 007*) and 3.60‰ (*Watson 015*). No stable or radiogenic isotope results could be obtained for the *Ooldea 002* vein sample because of its small size and relatively low carbonate content (Table 2.1).

2.3.2 Mineralogy and Sorption Behavior of Vein Material

Ordinary chondritic meteorites contain primarily olivine [(Mg,Fe) $_2\text{SiO}_4$], enstatite [(Mg,Fe) SiO_3], diopside [$\text{MgCaSi}_2\text{O}_6$], plagioclase [(Na,Ca)(Al,Si) $_4\text{O}_8$], apatite [$\text{Ca}_5(\text{PO}_4)_3(\text{F,Cl,OH})$], troilite, and taenite/kamacite [FeNi] alloys. Weathering products in crack-filling veins were found to be

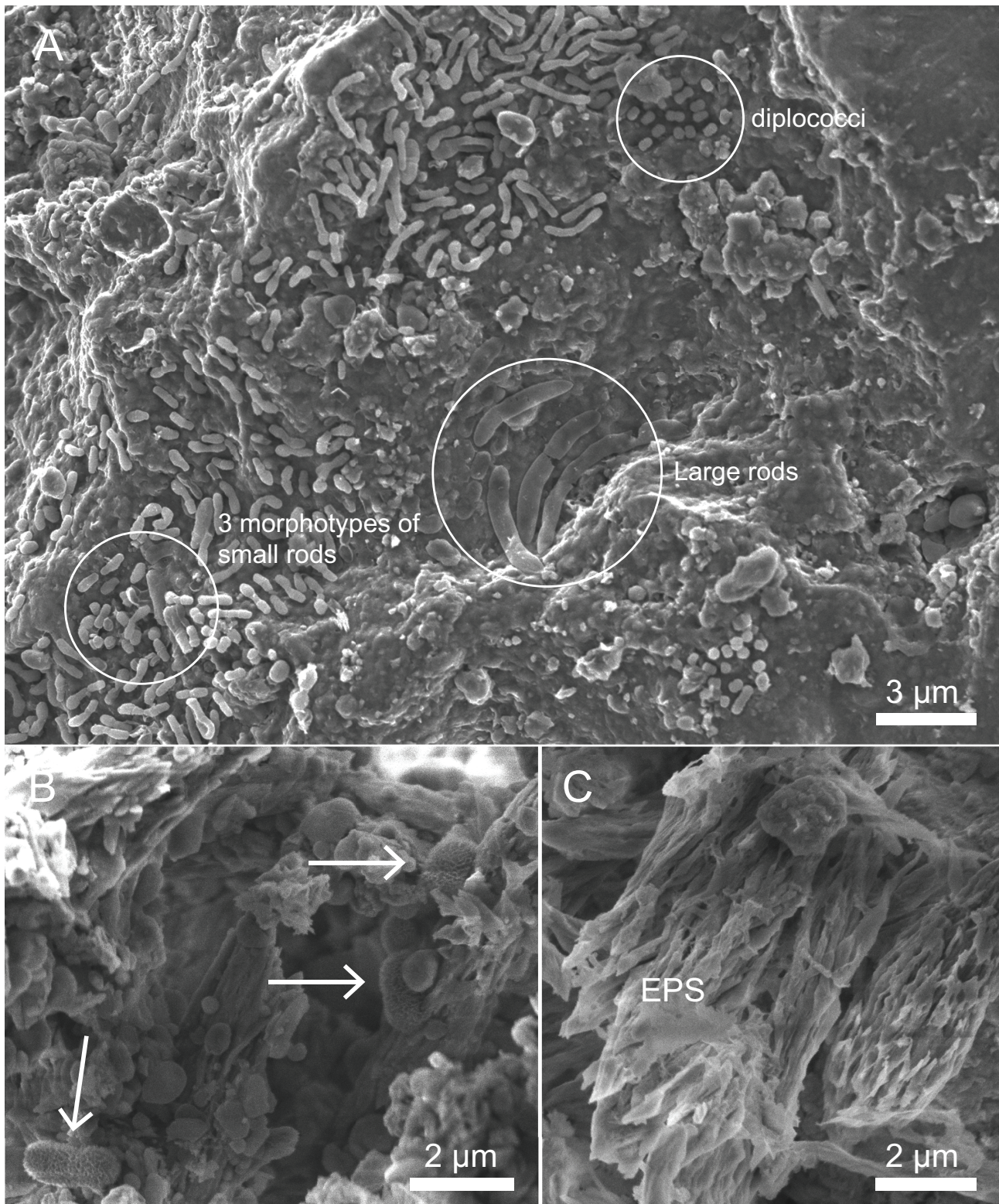


Figure 2.6 | Chasmoendolithic Biofilm and Calcite Etching. FEG-SEM micrographs of (A) carbonate vein material in *Ooldea 007* hosting a bacterial biofilm, composed of several, morphologically distinct prokaryotes (highlighted in circles). (B) At higher magnification, we see bacteria (arrows) with a fuzzy surface, this is either a mineral precipitate or folded gram-negative cell envelopes. The appearance of pitted and etched scalenohedral calcite suggests that the bacteria are promoting the dissolution of carbonate. (C) Heavily etched scalenohedral calcite was particularly visible where the sample dehydration process had peeled the exopolymer (EPS) off of the surface, e.g., *Watson 017*.

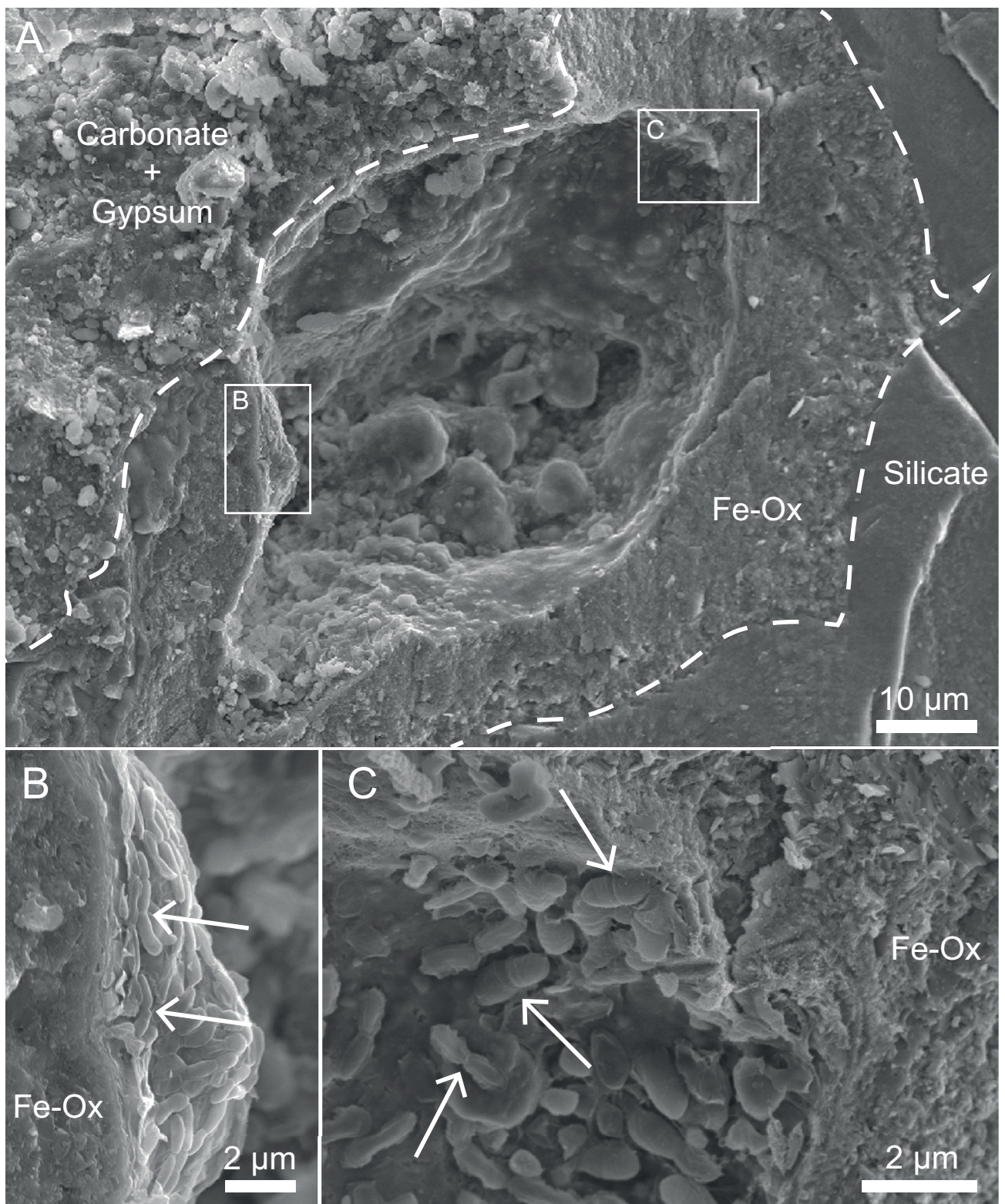


Figure 2.7 | Cryptoendolithic Biofilm. Continued growth of biofilm (within *Ooldea 007*) has resulted in the formation of corrosion cavities. Note the ‘soft texture’ of the inside of the corrosion pit (A), which is consistent with the presence of exopolymer. Energy dispersive spectroscopy demonstrated the presence of iron oxide proximal to a carbonate vein, which may have aided corrosion. Representative high magnification images (boxes ‘B’ and ‘C’) reveal the presence of bacteria undergoing cell division (arrows) lining the corrosion pit.

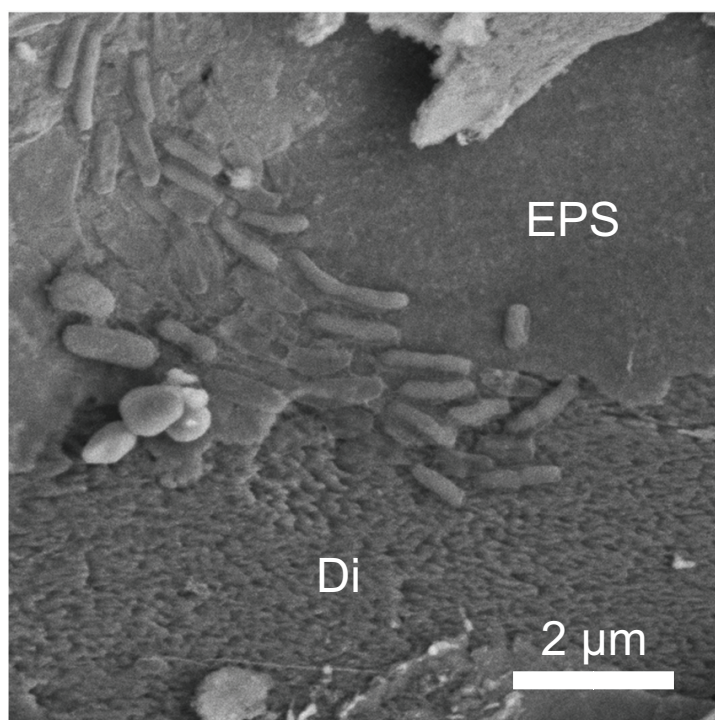


Figure 2.8 | Biologically-mediated Silicate Etching. FEG-SEM micrograph of *Watson 017* highlighting the occurrence of diopside, overlain by EPS and bacteria, possessing a ‘sawtooth’ dissolution texture (GIBSON *ET AL* 1983) demonstrating that bacterial biofilms are also linked to silicate weathering.

predominantly Mg-calcite $[(\text{Ca},\text{Mg})\text{CO}_3]$ and gypsum $[\text{CaSO}_4 \cdot 2\text{H}_2\text{O}]$, with minor goethite $[\alpha\text{-FeO}(\text{OH})]$ and smectites. Aeolian quartz $[\text{SiO}_2]$ and orthoclase $[\text{KAlSi}_3\text{O}_8]$ were found in some fractures (*Table 2.1*). Because quartz is not found in ordinary chondrites, its abundance in each meteorite was used to estimate the relative amount of contamination (as a percentage by weight) introduced from the Nullarbor Plain (*Table 2.1*). This also provides a relative measure of the extent to which contamination by Nullarbor sediment might have provided a mechanism for ingress of terrestrial microorganisms into meteorites along the fracture networks.

Water sorption analyses indicate that vein material extracted from meteorites can gain up to 3.0 % of its mass in sorbed H_2O as humidity increases (*Figure 2.3*). The hysteresis observed in desorption isotherms indicates that these admixtures of hygroscopic minerals tend to retain more H_2O at a given RH than was initially sorbed. Desorption curves cross the paths of adsorption curves for all samples, resulting in a negative mass change at low RH.

Light microscopy and SEM imaging provides further information about the spatial distribution of hygroscopic alteration phases relative to fractures and pores in meteorites. Figures 4A and B show that Fe^0 , Fe^{2+} and S^{2-} in FeNi alloy and troilite near the cores of weathered meteorites have been oxidized to Fe^{3+} - and SO_4^{2-} -bearing minerals, including jarosite $[\text{KFe}_3(\text{SO}_4)_2(\text{OH})_6]$ (*Figure 2.5*). Contrastingly, near the exterior of each meteorite, these primary minerals are typically less weathered. Large cracks, caused by the crystallization pressure of hydrated sulfate minerals, can be seen to increase the permeability of the remainder of the meteorite with respect to this corrosion cavity (*Figure 2.5*).

2.3.3 Mineral–Microbe Associations

In addition to fracture porosity, extensively weathered meteorites possess 50 – 1000 μm diameter voids that are produced by corrosive removal of FeNi alloys and/or troilite. These are commonly found at depths $> 1 - 3$ mm beneath their fusion crusts. Like the fracture networks, these corrosion cavities are also coated with hygroscopic alteration minerals, and biofilms line the interiors of some, but not all voids (*Figures 2.6, 2.7*). Indeed, we found a surprisingly high level of microbial colonization and diversity in meteorite fractures: 10–20 μm thick biofilms, inhabited by a range of morphologically distinct terrestrial microorganisms, commonly cover extensive regions of Mg-calcite veins (*Figure 2.6 A*). Microbial community composition/structure of Nullarbor ordinary chondrites is described in detail in (TAIT *ET AL.*, 2017). Additionally, in the course of our sampling we glutaraldehyde-fixed cells in the process of — or having recently completed — binary cell division (e.g., diplobacilli and diplococci, *Figures 2.6 A* and *2.7 B,C*). The surface of Mg-calcite vein material is commonly obscured by a layer of extracellular polymeric substances (EPS) (*Figure 2.6*), which are commonly generated by microorganisms and consist predominantly of polysaccharides and proteins. The process of chemical fixation and dehydration, combined with exposure to vacuum during electron microscopy work, results in a volume change to the EPS that causes the residual material to appear deflated, torn, and filamentous (DOHNALKOVA *ET AL.*, 2011). The EPS has peeled back in places to reveal strongly degraded and pitted scalenohedral calcite (*Figure 2.6B, C*). Also observed in the Mg-calcite/gypsum veins were microbes that had been covered by a nanocrystalline precipitate, but this feature could also be produced by dehydration of gram-negative cell envelopes (*Figure 2.6B*). *Figure 2.8* in particular shows a close spatial relationship between biofilms (i.e., cells and EPS) and corroded diopside.

2.4 Discussion

2.4.1 Fingerprinting the Origin of Carbonate Veins

The calibrated ^{14}C ages for vein material indicate the minimum amount of time that meteorites have been on the Nullarbor Plain. Based on these values, *Watson 015* and *Ooldea 007* have been interacting with Earth's biosphere for a minimum of 1410 ± 25 to 7490 ± 140 years, respectively. These meteorites were selected for study owing to the outward appearance of cracking (which would indicate the presence of interior vein material). The weathering grade assigned to both meteorites is W4 (on a scale from W1 – W6 (WLOTZKA, 1993)). Weathering grade is commonly used as a proxy for the duration

of time a meteorite spent on Earth's surface; but, in the case of the Nullarbor, weathering rates are thought to be more variable owing to climatic change in the region over time (BLAND *ET AL.*, 2000; JULL *ET AL.*, 2010), thus a residency age based on weathering grade alone is not applicable.

Values of $F_m > 1$ uniquely identify uptake of modern atmospheric carbon into minerals. Additionally, stable carbon isotopic fractionation factors can be used to predict the range of $\delta^{13}\text{C}$ values expected for a mineral forming in isotopic equilibrium with atmospheric CO_2 . Calculated values of $\delta^{13}\text{C}_{\text{calcite}}$ for calcite precipitation in equilibrium with atmospheric CO_2 were obtained using a $\delta^{13}\text{C}_{\text{CO}_2}$ value of -8.31‰ . This value was assumed for the modern atmosphere in the Nullarbor Desert based on data from Kermadec Island (KEELING *ET AL.*, 2005). The stable carbon isotopic fractionation factor, $\Delta^{13}\text{C}_{\text{calcite-CO}_2(\text{g})}$, of Deines and others (1974) was used for this calculation over the range of temperatures relevant to the Nullarbor Plain (-4.5°C to 48.7°C) (DEINES *ET AL.*, 1974; AUSTRALIAN BUREAU OF METEOROLOGY, 2015). The resulting values of $\delta^{13}\text{C}_{\text{Calcite}}$ were used to designate a field for carbonate precipitation from the modern atmosphere in *Figure 2.2*.

The depleted ^{14}C signature of Nullarbor Limestone is consistent with their identification as Eocene in age (15–25 Ma). Contrastingly, the meteorite vein material from *Watson 015* gives $\delta^{13}\text{C}$ and F_m values consistent with equilibrium precipitation of calcite from the modern (or recent) atmosphere (*Figure 2.2*). Thus, the Mg-calcite from meteorite fractures likely formed via reaction between carbonic acid in rainwater with primary Ca- and Mg-bearing minerals such as plagioclase and clinopyroxene that exist within the meteorites. The $\delta^{13}\text{C}$ and F_m values for *Ooldea 007* plot outside the modern equilibrium field. We interpret this as a mixing curve resulting from contamination of the meteorite samples by Nullarbor Limestone. This would indicate most of the carbonate in this sample is derived from weathering of the meteorites by reaction with Earth's atmosphere, and a smaller fraction from externally remobilized limestone. Thus, carbonate alteration, which is hygroscopic and can preserve textural, isotopic and fossil biosignatures, would still form by interaction of ordinary chondrites with a CO_2 -bearing atmosphere, such as that on Mars, in the absence of limestone.

2.4.2 Hygroscopic Vein Minerals and Water Cycling

XRD analysis shows that the vein material contains four hygroscopic minerals: gypsum, a smectite, goethite and Mg-calcite. Carbonate minerals such as Mg-calcite have been found previously within veins in meteorites collected from Antarctica (JULL *ET AL.*, 1988; LONG *ET AL.*, 1989). It is an important observation that carbonate alteration of meteorites can occur under Antarctic temperature conditions

because these more closely reflect the climate on Mars. Each of the hygroscopic phases found in the Nullarbor meteorites exhibits distinct H₂O sorption behavior; however, we have treated them together because they form a hygroscopic admixture within the veins.

As with the surface of Mars (SAVIJÄRVI, 1995), atmospheric RH on the Nullarbor Plain decreases with increasing daytime temperature and increases during the cooler nights. Application of these conditions to the hygroscopic vein material consistently results in a negative mass change in which the desorption isotherm crosses the sorption isotherm at the lowest RH values. This mass loss most likely results from the loss of crystallographic H₂O from gypsum during a partial phase transition to bassanite [CaSO₄·~0.5H₂O] or anhydrite [CaSO₄]. Although neither bassanite nor anhydrite was found during XRD analysis, two possibilities exist that could account for this disparity: (1) bassanite and/or anhydrite did form at low RH, but quickly rehydrated to produce gypsum in Melbourne's more humid atmosphere prior to analysis or (2) the abundances of the lower hydrates of Ca-sulfate were below the detection limits of our XRD under the operating conditions we used.

The samples of vein material gained 1.0 – 3.0 % of their mass in H₂O at a peak RH value of 90 %. Furthermore, under moderate RH conditions the vein material retained as much as 0.5 wt.% of sorbed H₂O under conditions of declining RH. The variation in the sorption behavior of meteorite vein material (*Figure 2.3*) likely results from differences in the relative proportions of hygroscopic minerals (*Table 2.1*). Vein material that forms within meteorites thus attracts atmospheric H₂O vapor to its surface and retains it under most RH conditions. This would serve to buffer atmospheric RH, leading to development of a 'humidity oasis' within the fracture systems in meteorites (i.e., humidity is higher inside meteorites as external humidity drops, providing a source of water for further weathering and support of microbes).

2.4.3 Generation of Veins and Porosity within Meteorites

The creation of veins and porosity in the meteorites is controlled by the removal of FeNi and FeS from the system. This feature probably reflects: (1) uptake of water by capillary action followed by (2) rapid evaporation of water from the exterior during the hot and arid daytime. The greater extent of weathering deep within the meteorites relative to their surfaces (*Figure 2.4*) supports the idea that weathering is driven by capillary transport of water. Oxidative dissolution of FeNi alloy, troilite and silicate minerals would then increase porosity by transfer of mass into fractures (to form the veins), which are widened and extended by the crystallization pressure of hydrous weathering products.

An example can be seen in *Figure 2.5*, where FeNi and FeS have been oxidized and mass has been removed from the system along cracks. This leaves behind Fe-oxyhydroxides and jarosite. Jarosite, which forms in low pH conditions, is known to have the capacity to preserve molecular biosignatures (PRESTON *ET AL.*, 2011).

2.4.4 Colonization of Veins and Pore Networks by Contaminant Microorganisms

Terrestrial contaminant microorganisms have colonized some but not all of the voids left by the weathering of FeNi alloys and troilite; they are also found on hygroscopic vein material. This variability in habitation likely relates to permeability changes during progressive weathering whereby not all cavities would be continuously accessible to environmental microorganisms.

Figure 2.8 shows a close spatial relationship between biofilms and corroded diopside, which is texturally similar to silicate dissolution features observed by Gibson et al. (1983), implying that, as in other environments (JONES, 2010), microbes promote weathering to generate secondary minerals that favor environmental regulation. Coupled weathering of troilite, plagioclase, diopside and forsterite (driven either abiotically or by acidophilic bacteria) provides a mechanism by which SO_4^{2-} , Fe^{3+} , Ca^{2+} , Mg^{2+} and K^+ are mobilized for precipitation of goethite, gypsum, and jarosite beneath biofilms in corrosion cavities (*Figures 2.7*). These minerals indicate a low-pH microenvironment, which is favored by some Fe- and S-oxidizing bacteria, and thus may preserve stable C, O, and S isotope signatures that are indicative of metabolism (*e.g.*, *Figure 2.1*). Other evidence of habitation, detectable even in the absence of cells, comes in the form of pitting on grains of diopside and scalenohedral Mg-calcite. Identical textures have been observed previously in calcite and are known to reflect acid dissolution of the mineral by microorganisms to regulate pH (STEINHAEUER *ET AL.*, 2010). The EPS covering grains of scalenohedral calcite in our samples form drapes of a smooth, semi-transparent (transparent to the electron beam at ~15 kV) material. It peels back in places to reveal filamentous structures within the fixed and dehydrated EPS that remain attached to underlying cells, such filamentous behavior of EPS dehydration is described by Dohnalkova et al. (2011). The EPS appears to begin peeling from the apices of scalenohedral calcite grains, which results in isolated patches of EPS left draped over calcite surfaces (*Figure 2.2 C*). The EPS on the diopside (*Figure 2.8*) had a different morphology than that coating calcite grains, in that it had a mottled surface texture rather than being dominated by filaments, and some cells within the EPS were flattened. The composition of thin layers of EPS was impossible to determine with EDX because the electron beam interacts with both the EPS and the

underlying mineral substrate; however, it is most likely composed of polysaccharides (DONLAN, 2002). One possible function of EPS in chondritic meteorites, other than nutrient cycling, is as a store for water. Retention and adsorption of water vapor by EPS is a valuable property that has previously been reported to be used by hypolithic cyanobacteria in the Atacama Desert (AZUA-BUSTOS *ET AL.*, 2011). Just as alteration minerals in chondritic meteorites adsorb water to their surfaces during periods of high RH, EPS could also help the microbial community retain water in the arid Nullarbor Plain.

Carbonate minerals, such as the Mg-calcite in veins, can form in circumneutral to alkaline microenvironments, even under bulk acidic conditions (FERNÁNDEZ-REMOLAR *ET AL.*, 2012). Also, carbonate minerals are known to preserve organic biomolecules (i.e., phenols associated with lignin) for millions of years in stalagmites from the Nullarbor Plain (BLYTH *ET AL.*, 2010), and by extension, could offer the same preservation potential within meteorites. Of further relevance to biomarker preservation is the observation that the surfaces of some microbes in the Mg-calcite/gypsum veins appear to be covered by a nanocrystalline precipitate (*Figure 2.6B*). Such coatings are thought to play an important role in fossilization and biopreservation of microbial cells within terrestrial settings (WILLIAMS *ET AL.*, 2015) and may be relevant to the search for life on Mars and other planets. However, this feature is ambiguous and could also result from dehydration of gram-negative cell envelopes, which are relatively thin compared to those of gram-positive cells, during the fixation process.

Chondritic meteorites are sterile when they fall to planetary surfaces and weather to produce the ‘trinity’ of biopreservation minerals: (1) carbonates for isotopic, organic molecular and fossil preservation (BLYTH *ET AL.*, 2010; POWER *ET AL.*, 2011), (2) smectites for preservation of organic molecules (Gaines et al., 2005), and (3) sulfates for isotopic, organic and fossil preservation (BENISON AND KARMANOCKY, 2014; SZYNKIEWICZ *ET AL.*, 2012). Thus, in addition to lending themselves to habitation (contamination) by environmental microorganisms under Mars relevant conditions, such as those in the Nullarbor Plain, chondrites also provide ideal conditions to preserve evidence of past life.

2.4.5 Practicality of Finding Meteorites on Mars

Rover missions have identified more than 20 iron and/or stony-iron meteorites on the surface of Mars (ASHLEY *ET AL.*, 2011), as well as some achondrites (SCHRÖDER *ET AL.*, 2016), but as of yet no confirmed chondritic meteorites have been described. This could be related to survival of stony meteorites requiring shallow atmospheric entry ($\sim 10^{\circ}$ – 30°) and masses <100 kg (CHAPPELOW AND SHARPTON, 2006). However, cratering records indicate that the surface of Mars receives 2.6 times

more meteoritic material than that of Earth (SHOEMAKER, 1977). Furthermore, the mean residence time for meteorites during the martian wet period which occurred 2–3 b.y.a. has been estimated to be on the order of 10^9 years (compared to a maximum of $\sim 10^6$ years on modern-day Earth). This is likely to be even longer on Mars today (BLAND AND SMITH, 2000). Consequently, chondritic meteorites should be plentiful on the surface of Mars, particularly given the absence of a planet wide resurfacing mechanism such as tectonics. Thus, it could be that no chondritic meteorites have been reported on Mars owing to difficulties with visual identification and their low mission priority.

The most distinctive feature of meteorites, which provides the best criterion for finding them on Mars, is their fusion crusts. The fusion crust of a chondritic meteorite is a smooth, full or partial covering of quenched silicate melt with thumb-sized divots, called regmaglypts, and is the product of ablation during atmospheric entry (THAISEN AND TAYLOR, 2010). However, chondritic meteorites on Earth — given enough time — lose their distinctive fusion crusts to oxidative weathering, revealing sharp-edged fresh material underneath.

Given similar oxidative weathering pathways on Mars and Earth, finding reddish-brown chondritic meteorites on the reddish-brown surface of Mars may be difficult. There are three additional features, in addition to fusion crusts, that may facilitate identification of chondritic meteorites on Mars. (1) Mg-carbonate efflorescences may protrude from cracks in the surfaces of chondritic meteorites. This is a common feature of meteorites recovered from Antarctica, a better analog to Mars than the Nullarbor Plain. Most of these efflorescences form after collection, a consequence of being stored in warmer atmospheres with higher relative humidities (JULL *ET AL.*, 1988). Given the complex history of the martian water cycle and the impact of Milankovitch cycles, periods of increased water vapor pressures in the martian atmosphere could generate similar efflorescences, and as a consequence also record information about atmospheric evolution on Mars (ASHLEY *ET AL.*, 2011). Such distinctive surface features may be present on martian chondrites, making visual identification easier. (2) The chondritic weathering profile is quite unique. As reduced iron phases oxidize, they create secondary weathering products with higher molecular volumes. This leads to the formation of cracks that cross cut the meteorite resulting in mass wasting of thin flakes of material from the meteorite. It is common on Earth to find flakes of chondritic material spread across a small area (e.g., $< 1 \text{ m}^2$), resulting in tightly grouped paving around the main mass of a meteorite. This weathering pattern may be used to find meteorites on Mars as well as Earth. (3) The prevailing wind on Mars has resulted in aeolian erosion of surface features and rocks, including preferential erosion of softer materials. This process

could expose chondrules and grains of metals and sulfides beneath the fusion crusts of meteorites, which would be visibly different from textural features of surrounding rocks (Ashley et al., 2011). It may be possible to develop a machine learning algorithm to search for these features, or create a citizen science website (e.g., Moon Zoo, Planet Four, Stardust@Home etc.) in order to leverage human pattern recognition on a large scale to search for meteorites on Mars.

2.5 Implications

2.5.1 Robotic Investigation of Meteorites to Assess Merit of Sample Return

There are currently two active rovers on Mars: Mars Exploration Rover (MER) “*Opportunity*” and Mars Science Laboratory (MSL) “*Curiosity*”. More robotic missions are planned, which will lead to robotic and/or human return of martian material to Earth within the next few decades. If chondrites are to be considered among the specimens selected on sample return missions, robotic exploration must first show that: (1) chondritic meteorites are present on Mars, (2) they have merit as past or present habitats for hypothetical microorganisms on Mars, and (3) meteorites are recoverable within the bounds of the engineering constraints placed on sample return missions.

The MER contains a suite of instruments aimed at exploring questions of habitability, including Pancam, Navcam, Mini-TES (Miniature Thermal Emission Spectrometer), APXS (Alpha Particle X-Ray Spectrometer), MB (Mossbauer Spectrometer), and MI (Microscopic Imager). All of these instruments have been employed in tandem for the identification of iron and stony-iron, and howardite–eucrite–diogenite (HED) meteorites on Mars (ASHLEY *ET AL.*, 2011; SCHRÖDER *ET AL.*, 2016).

The Mastcam and ChemCam’s RMI (Remote Micro-Imager) on Curiosity have also been used in identifying iron meteorites at Gale Crater (ASHLEY, 2015). Curiosity also has the ability to vaporize rocks for chemical identification using ChemCam, which may be the easiest method to survey small candidate chondritic meteorites. Curiosity’s SAM (Sample Analysis at Mars), which contains a Gas Chromatograph Quadrupole Mass Spectrometer and a Tunable Laser Spectrometer, could also be used to assess the habitability of meteorites. If a discovered meteorite has visible efflorescences (or is marked by cracks where sulfate and carbonate minerals may be hidden), drilling that material for analysis with the SAM instrument may reveal organic biomolecules produced by putative organisms preserved within alteration minerals inside the meteorite.

The CheMin instrument, which is an XRD/XRF on Curiosity, could be used as we have done in our experiments using XRD to identify chondritic meteorites and their secondary weathering products. However, there remain two operational difficulties to using this instrument with regards to meteorites: (1) if the meteorite is too small, the drill required for sampling may slip and (2) if the meteorite is too large, the “inside out” weathering profile and “humidity oasis” shown by our terrestrial investigations may result in the illusion of an un-weathered rock if only the surface can be sampled. If this weathering mechanism also happens on Mars, and the drill is too short, it may not access the weathered and thus habitable region of a large chondrite, providing a false negative.

The current generation of rovers has the capacity to establish the habitability potential of meteorites on Mars. Once this is established, their potential for sample return can be properly assessed with respect to other sample return priorities.

2.5.2 A Model for Microbial Colonization and Habitation of Chondrites on Earth and Mars

Our SEM results show that terrestrial microorganisms commonly colonize and inhabit ordinary chondrites from the Nullarbor Plain, Australia. This represents an important first step in establishing that chondritic materials on Mars and other planetary surfaces might also support putative microbial communities and provide a robust record of past or present mineral–microbe interactions. Follow up studies should investigate the longevity of preservation of organic biomolecules and stable isotopic biosignatures in ordinary chondrites.

Chondritic meteorites offer a combination of factors favoring microbial life in arid environments: (1) a mineralogical source of energy and nutrients, (2) provision of water, (3) shielding from UV light and ionizing radiation, (4) temperature moderation, (5) humidity regulation, and (6) accessible and chemically regulated microhabitats (cracks and voids). Basalt, which covers most of the surface of Mars, is deficient in all ways relative to meteorites, save for UV shielding, and has a broad range in stable sulfur isotope values (*Figure 2.1*; FARQUHAR *ET AL.* 2007)) that could potentially mask isotopic biosignatures.

We can extrapolate our terrestrial observations of microbial colonization and habitation of meteorites in the Nullarbor Plain to the surface of Mars (*Figure 2.9*). In this model, water vapor and molecular oxygen in the martian atmosphere plus or minus biogeochemical processes oxidize the FeNi alloys and sulfide minerals within a meteorite. This produces hygroscopic minerals such as Fe-oxyhydroxides,

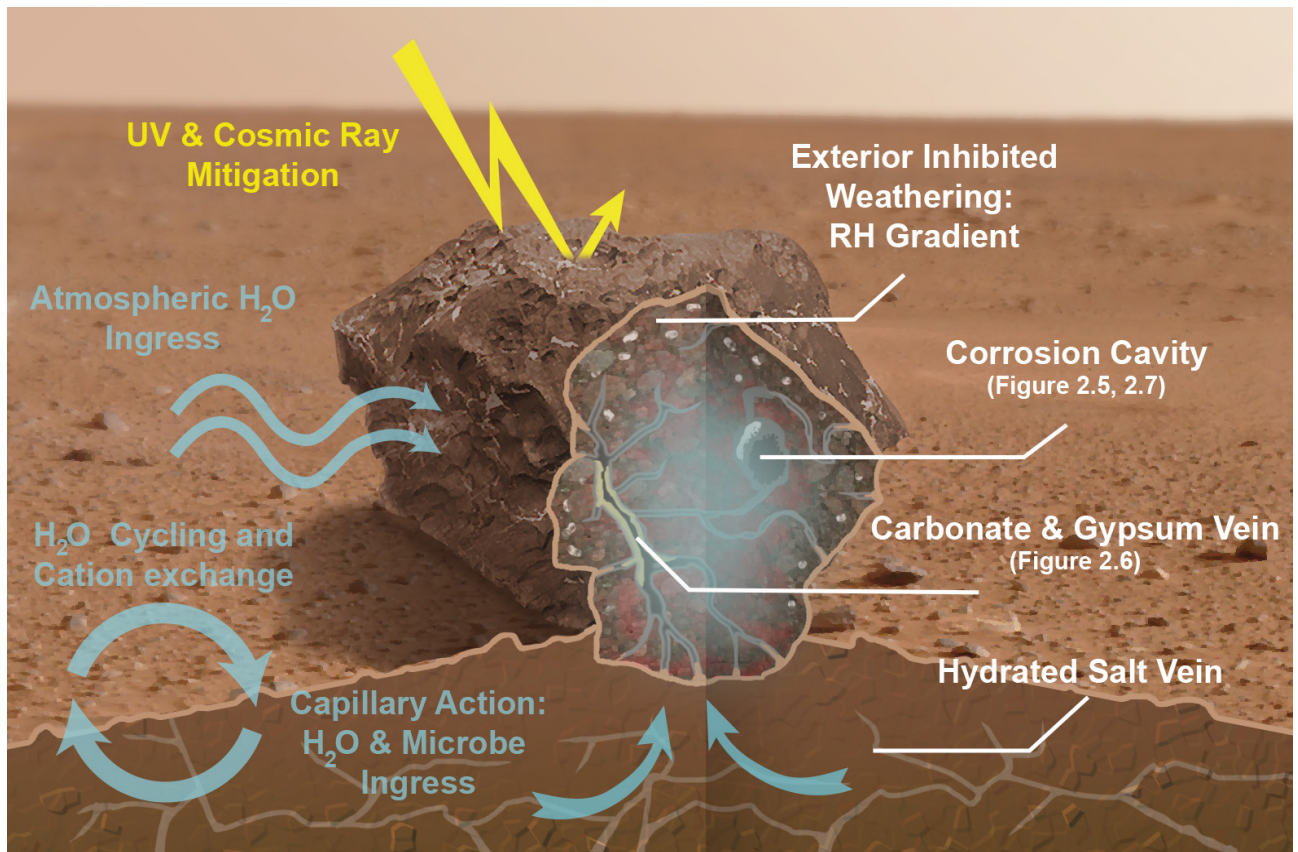


Figure 2.9 | Meteorite Habitat Model for Mars. This model shows the key properties of a meteorite habitat on Mars. sulfates, carbonates and smectites. These in turn buffer the relative humidity inside the meteorite by adsorbing water vapor to mineral surfaces at night and releasing it during the warmer day. This humidity oasis enhances the weathering of primary phases, such as silicates and phosphates, releasing more cations for uptake by any potential biofilms. Microhabitats form over a range of pH conditions putative martian microbes may continue to ingress the meteorite via the regolith, or transient water flow. Should these putative martian microorganisms be chemotrophic and adapted to xerophilic conditions, they could survive within the relatively humid environment inside meteorites. Thus, meteorites have potential to act as a refuge long enough for the microbes to alter the geochemistry of the substrate in a recognizable manner before ultimately succumbing to the hostility of the martian surface.

The most primitive life forms on Earth are believed to be chemolithotrophic. If a martian biosphere exists, or existed, it stands to reason that it would also be chemolithotrophic, but perhaps located deep underground where it is still warm (MICHALSKI *ET AL.*, 2013). Today, oxidative weathering would be slower, and sorption of water of lesser magnitude, on Mars than on the Nullarbor Plain due to the lower partial pressures of water vapor and molecular oxygen (MALTAGLIATI *ET AL.*, 2011). Due to the long residence time of martian meteorites, estimated to be on the order of 10^9 years (BLAND

AND SMITH, 2000), some meteorites presently on the surface of Mars could have sampled a putative surface biosphere during the Amazonian/Hesperian transition at ~3 Ga (CARR AND HEAD, 2010). Furthermore, transient surface brines, such as those suggested to be responsible for the recurring slope lineae within craters (OJHA *ET AL.*, 2015), could vector currently living microorganisms from a near-surface biosphere into the refugia of more recently fallen meteorites, making meteorites prime targets for future sample return missions to Mars.

2.6 Conclusions

Our study has shown that stony meteorites on Earth contain a ‘trinity’ of biopreservation minerals (e.g., smectites, sulfates, and carbonates) that are known to preserve organics and stable isotopic biosignatures for millions of years. We have also shown that the hygroscopic alteration minerals in meteorites adsorb water vapor from the atmosphere to their crystal surfaces and that microorganisms appear to colonize these minerals preferentially, suggesting they are using this hygroscopy to obtain water in the arid Nullarbor Plain. These microorganisms were also found to be dissolving primary silicate and secondary carbonate minerals within the meteorites, showing that biota contribute to the alteration of meteorites. Furthermore, indications of microbially mediated alteration of meteorites is commonly preserved and detectable. Endolithic microbes are known to colonize rocks and soils at Earth’s surface; thus, it is unsurprising that terrestrial microorganisms commonly colonize stony meteorites. Unlike terrestrial rocks, meteorites have unique value as substrates for microbial growth: as remnants of the primordial solar system, they are used extensively as isotopic standards (e.g., VCDT) and geochemical baselines (e.g., CI normalization). The relatively homogeneous composition of meteorites makes them indispensable to understanding geological and environmental processes. This ‘standard’-like property of meteorites makes them ideal ‘witness plates’ for microbially mediated alteration. Consequently, meteorites on Mars could become an invaluable resource for astrobiological exploration, particularly since existing rover missions are capable of sampling and analyzing meteorites for signs of some biomarkers that we have identified. Meteorite residence times can date back to the Hesperian when Mars was warm and wet, potential recording snapshot of a putative martian biosphere from that time. Meteorites represent a readily accessible habitat that is made of a solar-system-wide standard material; thus, they can be used to reduce ambiguity in detecting signs of life on the surface of Mars.

2.7 Chapter 2 References

A

- Ashley J. W. (2015) The Study of Exogenic Rocks on Mars — an Evolving Subdiscipline in Meteoritics. In: *Elements*, pp 10-11.
- Ashley J. W., Golombek M. P., Christensen P. R., Squyres S. W., McCoy T. J., Schröder C., Fleischer I., R J. J. J., Herkenhoff K. E., and Parker T. J. (2011) Evidence for mechanical and chemical alteration of iron-nickel meteorites on Mars: Process insights for Meridiani Planum. *Journal of Geophysical Research*, 116: E00F20.
- Australian Bureau of Meteorology (2015) Cook Weather station - 018110, (Years 1920-2010).
- Azua-Bustos A., González-Silva C., Mancilla R. A., Salas L., Gómez Silva B., McKay C. P., and Vicuña R. (2011) Hypolithic cyanobacteria supported mainly by fog in the coastal range of the Atacama Desert. *Microbial Ecology*, 61: 568-581.

B

- Balci N., Shanks Iii W. C., Mayer B., and Mandernack K. W. (2007) Oxygen and sulfur isotope systematics of sulfate produced by bacterial and abiotic oxidation of pyrite. *Geochimica et Cosmochimica Acta*, 71: 3796-3811.
- Benison K. C., and Karmanocky F. J. (2014) Could microorganisms be preserved in Mars gypsum? Insights from terrestrial examples. *Geology*, 42: G35542.1.
- Bish D. L., and Howard S. A. (1988) Quantitative phase analysis using the Rietveld method. *Journal of Applied Crystallography*, 21: 86-91.
- Bland P., and Smith T. B. (2000) Meteorite accumulations on Mars. *Icarus*, 144: 21-26.
- Bland P. A., Bevan A. W. R., and Jull A. J. T. (2000) Ancient Meteorite Finds and the Earth's Surface Environment. *Quaternary Research*, 53: 131-142.
- Bland P. A., Zolensky M. E., Benedix G. K., and Sephton M. A. (2006) Weathering of chondritic meteorites. In: *Meteorites and the Early Solar System II*. edited by DS Lauretta and HY McSween, *University of Arizona Press*, Tucson, pp 943.
- Blyth A. J., Watson J. S., Woodhead J., and Hellstrom J. (2010) Organic compounds preserved in a 2.9 million year old stalagmite from the Nullarbor Plain, Australia. *Chemical Geology*, 279: 101-105.
- Brabec M. Y., Lyons T. W., and Mandernack K. W. (2012) Oxygen and sulfur isotope fractionation during sulfide oxidation by anoxygenic phototrophic bacteria. *Geochimica et Cosmochimica Acta*, 83: 234-251.

C

- Canfield D. E. (2001) Biogeochemistry of sulfur isotopes. In: Reviews in Mineralogy and Geochemistry. edited by JW Valley and DR Coles, *Mineralogical Society of America*, Washington, DC, USA, pp 607-636.
- Carr M. H., and Head J. W. (2010) Geologic history of Mars. *Earth and Planetary Science Letters*, 294: 185-203.
- Chappelow J., and Sharpton V. (2006) Atmospheric variations and meteorite production on Mars. *Icarus*, 184: 424-435.

D

- Davila A. F., Gómez Silva B., de los Ríos A., Ascaso C., Olivares H., McKay C. P., and Wierzchos J. (2008) Facilitation of endolithic microbial survival in the hyperarid core of the Atacama Desert by mineral deliquescence. *Journal of Geophysical Research: Biogeosciences*, 113: G01028.
- Deines P., Langmuir D., and Harmon R. S. (1974) Stable carbon isotope ratios and the existence of a gas phase in the evolution of carbonate ground waters. *Geochimica et Cosmochimica Acta*, 38: 1147-1164.
- Dohnalkova A. C., Marshall M. J., Arey B. W., Williams K. H., Buck E. C., and Fredrickson J. K. (2011) Imaging hydrated microbial extracellular polymers: comparative analysis by electron microscopy. *Applied and Environmental Microbiology*, 77: 1254-1262.
- Donlan R. M. (2002) Biofilms: Microbial Life on Surfaces. *Emerging Infectious Diseases Journal*, 8: 881-890.

F

- Fallon S. J., Fifield L. K., and Chappel J. M. (2010) The next chapter in radiocarbon dating at the Australian National University: Status report on the single stage AMS. *Nuclear Instruments and Methods in Physics Research Section B: Beam Interactions with Materials and Atoms*, 268: 898-901.
- Farquhar J., Kim S. T., and Masterson A. (2007) Implications from sulfur isotopes of the Nakhla meteorite for the origin of sulfate on Mars. *Earth and Planetary Science Letters*, 264: 1-8.
- Farquhar J., Savarino J., Jackson T. L., and Thiemens M. H. (2000) Evidence of atmospheric sulphur in the martian regolith from sulphur isotopes in meteorites. *Nature*, 404: 50-52.
- Farquhar J., Wu N., Canfield D. E., and Oduro H. (2010) Connections between Sulfur Cycle Evolution, Sulfur Isotopes, Sediments, and Base Metal Sulfide Deposits. *Society of Economic Geologists*, 105: 509-533.

Fernández-Remolar D. C., Preston L. J., Sánchez-Román M., Izawa M. R. M., Huang L., Southam G., Banerjee N. R., Osinski G. R., Flemming R., Gómez-Ortíz D. and others. (2012) Carbonate precipitation under bulk acidic conditions as a potential biosignature for searching life on Mars. *Earth and Planetary Science Letters*, 351–352: 13–26.

G

Gaines R. R., Kennedy M. J., and Droser M. L. (2005) A new hypothesis for organic preservation of Burgess Shale taxa in the middle Cambrian Wheeler Formation, House Range, Utah. *Palaeogeography, Palaeoclimatology, Palaeoecology*, 220: 193–205.

Gibson E. K., Wentworth S. J., and McKay D. S. (1983) Chemical weathering and diagenesis of a cold desert soil from Wright Valley, Antarctica: An analog of martian weathering processes. *Journal of Geophysical Research*, 88: A912–A928.

Greenwood J. P., Riciputi L. R., and McSween H. Y. (1997) Sulfide isotopic compositions in shergottites and ALH84001, and possible implications for life on Mars. *Geochimica et Cosmochimica Acta*, 61: 4449–4453.

Greenwood J. P., Riciputi L. R., McSween H. Y., and Taylor L. A. (2000) Modified sulfur isotopic compositions of sulfides in the nakhlites and Chassigny. *Geochimica et Cosmochimica Acta*, 64: 1121–1131.

Gronstal A., Pearson V., Kappler A., Dooris C., Anand M., Poitrasson F., Kee T. P., and Cockell C. S. (2009) Laboratory experiments on the weathering of iron meteorites and carbonaceous chondrites by iron-oxidizing bacteria. *Meteoritics & Planetary Science*, 44: 233–247–15.

H

Harries D., Hoppe P., and Langenhorst F. (2015) Reactive ammonia in the solar protoplanetary disk and the origin of Earth's nitrogen. *Nature Geoscience*, 8: 97–101.

Hezel D. C., Palme H., Nasdala L., and Brenker F. E. (2006) Origin of SiO₂-rich components in ordinary chondrites. *Geochimica et Cosmochimica Acta*, 70: 1548–1564.

Hill R. J., and Howard C. J. (1987) Quantitative phase analysis from neutron powder diffraction data using the Rietveld Method. *Journal of Applied Crystallography*, 20: 467–474.

J

Jarosewich E. (1990) Chemical analyses of meteorites: A compilation of stony and iron meteorite analyses. *Meteoritics*, 25: 323–337.

Jones B. (2010) Microbes in caves: agents of calcite corrosion and precipitation. *Geological Society*, 336: 7–30.

Jull A. J., Cheng S., Gooding J. L., and Velbel M. A. (1988) Rapid growth of magnesium-carbonate weathering products in a stony meteorite from Antarctica. *Science*, 242: 417–419.

Jull A. J. T., McHargue L. R., Bland P. A., Greenwood R. C., Bevan A. W. R., Kim K. J., LaMotta S. E., and Johnson J. A. (2010) Terrestrial ages of meteorites from the Nullarbor region, Australia, based on ^{14}C and ^{14}C - ^{10}Be measurements. *Meteoritics & Planetary Science*, 45: 1271-1283.

K

Keeling C. D., Piper S. C., Bacastow R. B., Wahlen M., Whorf T. P., Heimann M., and Meier H. A. (2005) Atmospheric CO_2 and $^{13}\text{CO}_2$ exchange with the terrestrial biosphere and oceans from 1978 to 2000: observations and carbon cycle implications. In: A history of atmospheric CO_2 and its effects on plants, animals and ecosystems. edited by JR Ehleringer, TE Cerling and MD Dearing, *Springer Verlag*, New York, pp 83-113.

Kelly L. C., Cockell C. S., Thorsteinsson T., Marteinson V., and Stevenson J. (2014) Pioneer Microbial Communities of the Fimmvörðuháls Lava Flow, Eyjafjallajökull, Iceland. *Microbial Ecology*, 68: 504-518.

L

Long D. T., Velbel M., and Gooding J. I. (1989) Terrestrial weathering of Antarctic stone meteorites: Formation of Mg-carbonates on ordinary chondrites. *Geochimica et Cosmochimica Acta*, 55: 67-76.

M

Maltagliati L., Montmessin F., Fedorova A., Korablev O., Forget F., and Bertaux J. L. (2011) Evidence of water vapor in excess of saturation in the atmosphere of Mars. *Science*, 333: 1868-1871.

Mautner M. N. (1997) Biological potential of extraterrestrial materials—1. Nutrients in carbonaceous meteorites, and effects on biological growth. *Planetary and Space Science*, 45: 653-664.

Michalski J. R., Cuadros J., Niles P. B., Parnell J., Rogers A. D., and Wright S. P. (2013) Groundwater activity on Mars and implications for a deep biosphere. *Nature Geoscience*, 6: 133-138.

Mohlmann D., and Thomsen K. (2011) Properties of cryobrines on Mars. *Icarus*, 212: 123-130.

Morgan B., Wilson S. A., Madsen I. C., Gozukara Y. M., and Habsuda J. (2015) Increased thermal stability of nesquehonite ($\text{MgCO}_3 \cdot 3\text{H}_2\text{O}$) in the presence of humidity and CO_2 : Implications for low-temperature CO_2 storage. *International Journal of Greenhouse Gas Control*, 39: 366-376.

O

- Ojha L., Wilhelm M. B., Murchie S. L., McEwen A. S., Wray J. J., Hanley J., Massé M., and Chojnacki M. (2015) Spectral evidence for hydrated salts in recurring slope lineae on Mars. *Nature Geoscience*, 8: 829-832.

P

- Pasek M., and Lauretta D. S. (2008) Extraterrestrial flux of potentially prebiotic C, N, and P to the early earth. Origins of life and evolution of the biosphere: *The journal of the International Society for the Study of the Origin of Life*, 38: 5-21.
- Pisapia C., Chaussidon M., Mustin C., and Humbert B. (2007) O and S isotopic composition of dissolved and attached oxidation products of pyrite by *Acidithiobacillus ferrooxidans*: Comparison with abiotic oxidations. *Geochimica et Cosmochimica Acta*, 71: 2474-2490.
- Power I. M., Wilson S. A., Dipple G. M., and Southam G. (2011) Modern carbonate microbialites from an asbestos open pit pond, Yukon, Canada. *Geobiology*, 9: 180-195.
- Preston L. J., Shuster J., Fernández-Remolar D., Banerjee N. R., Osinski G. R., and Southam G. (2011) The preservation and degradation of filamentous bacteria and biomolecules within iron oxide deposits at Rio Tinto, Spain. *Geobiology*, 9: 233-249.

R

- Rietveld H. M. (1969) A profile refinement method for nuclear and magnetic structures. *Journal of Applied Crystallography*, 2: 65-71.

S

- Savijärvi H. (1995) Mars boundary layer modeling: Diurnal moisture cycle and soil properties at the Viking Lander 1 Site. *Icarus*, 117: 120-127.
- Schröder C., Bland P. A., Golombek M. P., Ashley J. W., Warner N. H., and Grant J. A. (2016) Amazonian chemical weathering rate derived from stony meteorite finds at Meridiani Planum on Mars. *Nature Communications*, 7: 13459.
- Shoemaker E. M. (1977) Astronomically observable crater-forming projectiles. edited by DJ Roddy, RO Pepin and RB Merrills, *Pergamon Press*, New York, pp 617-628.
- Steinhauer E. S., Omelon C. R., and Bennett P. C. (2010) Limestone corrosion by neutrophilic sulfur-oxidizing bacteria: A coupled microbe-mineral system. *Geomicrobiology Journal*, 27: 723-738.
- Stoffler D., Keil K., and Edward R. D. (1991) Shock metamorphism of ordinary chondrites. *Geochimica et Cosmochimica Acta*, 55: 3845-3867.

Szynkiewicz A., Johnson A. P., and Pratt L. M. (2012) Sulfur species and biosignatures in Sulphur Springs, Valles Caldera, New Mexico—Implications for Mars astrobiology. *Earth and Planetary Science Letters*, 321-322: 1-13.

T

Tait A. W., Gagen E. J., Wilson S. A., Tomkins A. G., and Southam G. (2017) Microbial populations of stony meteorites: Substrate controls on first colonisers. *Frontiers in Microbiology* (Accepted for publication, 19th May 2017).

Thaisen K. G., and Taylor L. A. (2010) Meteorite fusion crust variability. *Meteoritics & Planetary Science*, 44: 871-878.

V

Van Schmus W. R., and Wood J. (1967) A chemical-petrologic classification for the chondritic meteorites. *Geochimica et Cosmochimica Acta*, 31: 747-765.

Webb J. A., and James J. M. (2006) Karst evolution of the Nullarbor Plain, Australia. *Geological Society of America Special Paper*, 404: 65-78.

W

Williams A. J., Sumner D. Y., Alpers C. N., Karunatillake S., and Hofmann B. A. (2015) Preserved filamentous microbial biosignatures in the Brick Flat Gossan, Iron Mountain, California. *Astrobiology*, 15: 637-668.

Wilson S. A., and Bish D. L. (2011) Formation of gypsum and bassanite by cation exchange reactions in the absence of free-liquid H₂O: Implications for Mars. *Journal of Geophysical Research*, 116: E09010.

Wilson S. A., and Bish D. L. (2012) Stability of Mg-sulfate minerals in the presence of smectites: Possible mineralogical controls on H₂O cycling and biomarker preservation on Mars. *Geochimica et Cosmochimica Acta*, 96: 120-133.

Wlotzka F. (1993) A Weathering Scale for the ordinary chondrites. *Meteoritics*, 28: 460.

Z

Zurfluh F. J., Hofmann B. A., Gnos E., and Eggenberger U. (2013) “Sweating meteorites”—Water-soluble salts and temperature variation in ordinary chondrites and soil from the hot desert of Oman. *Meteoritics & Planetary Science*, 48: 1958-1980.

Declaration for Thesis Chapter 3

Declaration by candidate

In the case of Chapter 3, the nature and extent of my contribution is as follows:

<i>Nature of contribution</i>	<i>Extent of contribution (%)</i>
Conceptualisation, sample preparation, SEM analysis, field work, data analysis, data interpretation, manuscript writing	82.5%

The following co-authors contributed to the work. If co-authors are students at Monash University, the extent of their contribution in percentage terms must be stated:

<i>Name</i>	<i>Nature of contribution</i>	<i>Extent of contribution (%)</i>
Emma J. Gagen	Organism Cultivation, Sample Fixation	5%
Siobhan A. Wilson	Supervisory Role	5%
Andrew G. Tomkins	Supervisory Role	5%
Gordon Southam	Advisory Role	2.5%

The undersigned hereby certify that the above declaration correctly reflects the nature and extent of the candidate's and co-authors contributions to this work*.

Candidate's signature:



Date: 01/06/2017

Main supervisor's signature:

Date: 01/06/2017

*Note: Where the responsible author is not the candidate's main supervisor, the main supervisor should consult with the responsible author to agree on the respective contributions of the authors.

Chapter 3

Growth of naturally occurring chasmoendolithic microorganisms within chondritic meteorites recovered from the Nullarbor Plain, Australia: Applications to microhabitat discovery on Mars[†]

Alastair W. Tait¹, Emma J. Gagen², Siobhan A. Wilson¹, Andrew G. Tomkins¹, Gordon Southam²

¹School of Earth, Atmosphere & Environment, Monash University, Australia

²School of Earth & Environmental Sciences, The University of Queensland, Australia

[†] Prepared for submission to *Geobiology*

Chondritic meteorites that have fallen to the surface of Mars represent possible refuge habitats for microorganisms. We find that terrestrial microorganisms preferentially colonise hygroscopic alteration minerals such as sulfates, carbonates, Fe-oxyhydroxides and smectites within weathered ordinary chondrites recovered from the Nullarbor Plain, Australia. Acid etching the interiors of ordinary chondrites revealed entombed microbial biofilms preserved within weathering products. Microorganisms were observed colonizing cracks and pores within chips of these ordinary chondrites that were placed into dilute culture media. Our results demonstrate that microorganisms can quickly colonize pockets of porosity in meteorites, penetrating > 400 μm into a meteorite along ‘fresh cracks’ within a three month period. This would be deep enough within a meteorite to mitigate the effects of harmful ionising radiation on Mars. Here, we describe a continuum from initial colonization of meteorites by terrestrial microorganisms to preservation of well-established biofilms and microorganisms within veins of alteration minerals. Thus, putative microbes could be entombed and preserved within alteration minerals in meteorites for geological timescales, making meteorites ideal candidates for robotic exploration and recovery. Given the recent discovery of stony meteorites on Mars, this material could be examined by rovers on the martian surface today.

3.1 Introduction

Detection and characterization of microbial biosignatures, including fossil, isotopic and organic biosignatures, is currently a major focus of astrobiology and a goal of martian rover science (Cady *ET AL.* 2003; SUMMONS *ET AL.* 2011). Chondritic meteorites on the surface of Mars provide a uniquely useful tool for astrobiologists owing to their long residence times at the Martian surface (BLAND AND SMITH 2000; SCHRÖDER *ET AL.* 2016). Consequently, some meteorites could have sampled a potential biosphere at the Amazonian/Hesperian transition when Mars last had longstanding bodies of liquid water at its surface (CARR AND HEAD 2010; TAIT *ET AL.* 2017B). Meteorites have other beneficial properties, including a well-known and narrow range of stable sulfur isotopic compositions, that allow them to act as standard materials that record environmental histories (ASHLEY 2011) including biological signatures produced by microorganisms that may have interacted with them (TAIT *ET AL.* 2017A; TAIT *ET AL.* 2017B). Using meteorites as standard materials may help to mitigate the ambiguity associated with doing environmental science on planets, such as Mars, where biogeochemical context is still being established.

Tait et al. (2017b) observed terrestrial ‘contaminant’ microorganisms (colonizers) living inside ordinary chondritic meteorites from the Nullarbor Plain, Australia. The colonizers were found inhabiting pore spaces created by corrosion of troilite $[\text{FeS}]$ and iron-nickel alloys $[\text{Fe}_{1-x}\text{Ni}_x]$. They also formed biofilms on admixtures of gypsum $[\text{CaSO}_4 \cdot 2\text{H}_2\text{O}]$ and Mg-calcite $[(\text{Ca},\text{Mg})\text{CO}_3]$ within networks of cracks

that had formed through reaction-driven cracking during precipitation of these minerals (TAIT *ET AL.* 2017B). Such carbonate–gypsum admixtures adsorb water vapour from the atmosphere and provide a source of bioavailable water in the harsh desiccating conditions of the Nullarbor (TAIT *ET AL.* 2017B). They also have the capability to preserve fossil biofilms within carbonate minerals (BOROWITZKA 1982). Given the age (up to $\sim 4 \times 10^4$ years) of meteorites from the Nullarbor region (JULL *ET AL.* 2010), the biofilms reported by Tait et al. (2017b) may have first developed in these meteorites tens of thousands of years ago. Extending these observations to Mars, it is possible that putative biofilms may have been similarly preserved within alteration minerals in exogenic meteorites, potentially for billions of years given the predicted residence times of meteorites on Mars (BLAND AND SMITH 2000; SCHRÖDER *ET AL.* 2016). Carbonate minerals are well-known to provide fossil records of past microbial life on Earth (e.g., (POWER *ET AL.* 2011)) and they may protect organic molecules produced by putative microbes from the highly oxidizing perchlorates that have been discovered on Mars (KOUNAVES *ET AL.* 2014). However, this raises three questions. (1) How do microorganisms penetrate and colonize meteorites without the presence of hygroscopic weathering veins to act as a source of water? (2) Can microorganisms penetrate deep enough within a meteorite to obtain protection from UV light under Martian surface conditions. (3) How readily can potential fossil cells and biofilms be identified and extracted for further organic geochemical analysis from the alteration minerals in meteorites?

This study aims to answer these questions by investigating (1) experimental colonization of ordinary chondritic meteorites by microorganisms and (2) the preservation of cells and biofilms within alteration minerals in meteorites collected from the Nullarbor Plain, Australia. Our results indicate that environmental microbes can penetrate deep into cracks in meteorites and interact with hygroscopic alteration minerals that can preserve them. This suggests meteorites on Mars have similar potential to preserve fossil biosignatures.

3.2 Methods

3.2.1 Meteorite Specimens

This study consists of two experiments that used seven chondritic meteorites. These were collected from 2013–2015 as part of Monash University’s annual meteorite recovery expedition to the Nullarbor Plain. All meteorite samples were collected aseptically using gloves washed with 70%_(aq) ethanol and

were placed into sterile plastic bags.

Watson 014 is a 15.1-g H3 chondrite that was found in three jigsaw fit pieces. It is relatively unweathered (grade W1) with light shock (S2). *Watson 015* is a lightly shocked (S2) H4 chondrite that was recovered in two pieces, with a combined weight of 457 g. Two-thirds of its surface is covered by a fusion crust and sulfide and metal alloy phases have completely weathered away (W4). *Ooldea 002* is a L5 chondrite that was found in nine pieces. It exhibits complete weathering of sulfide and metal alloy phases (W4) and has undergone light shock (S2). *Ooldea 003* is a single, 24.3-g fragment of H4 chondrite that was found with extensive corrosion cavities (W3) and showing light shock (S2). *Ooldea 004* (official classification pending) is an EL3 chondrite that was found in 37 pieces weighing a total of 1043.5 g. Its metal alloy and sulfide grains have completely weathered away (W4) and the meteorite exhibits low shock (S1). *Ooldea 005* is a H5 chondrite that was found in several fragments weighing a total of 144.3 g. It exhibits moderate shock (S3) and heavy weathering (W3). *Ooldea 007* was recovered as a single stone weighing 135 g. The petrological classification of this chondrite is H3. It shows moderate shock (S3) and heavy alteration of the sulfide and metal alloy phases (W3). All meteorites were used in experiment 1, except for *Ooldea 007*, which was used only in experiment 2.

For full meteorite descriptions, refer to The Meteoritical Bulletin Database. All specimens are curated at the School of Earth, Atmosphere and Environment, Monash University. For petrological classification refer to Tait et al. (2014); Van Schmus and Wood (1967). Weathering grade is described by Wlotzka (1993) and shock grade categorization is outlined by Stoffler et al. (1991).

3.2.2 Experiment 1: Infiltration of meteorites by microorganisms

3.2.2.1 Media Modification and Culturing

Several fragments of meteorites (*Watson 014*, *Watson 015*, *Ooldea 003*, *Ooldea 002*, *Ooldea 004* and *Ooldea 005*) that were recovered aseptically from the Nullarbor Plain were wrapped in sterile plastic and crushed into grains with volumes of $\sim 0.3 \text{ cm}^3$. Grains from each meteorite were transferred into 50 mL FalconTM tubes, with each tube containing 20 mL of DSMZ 71 medium. The medium was prepared in two parts: (1) the first part consisted of $(\text{NH}_4)\text{SO}_4$ (3.00 g), $\text{MgSO}_4 \cdot 7\text{H}_2\text{O}$ (0.50 g), KH_2PO_4 (3.0 g), and $\text{CaCl}_2 \cdot 2\text{H}_2\text{O}$ (0.25 g) dissolved in 900 mL of deionized water (DI). The pH of this solution was adjusted to 4.5 using 1 M HCl, before autoclaving at 122° C for 30 min. (2) The

second part of the medium was prepared using $\text{Na}_2\text{S}_2\text{O}_3 \cdot 5\text{H}_2\text{O}$ (5.00 g) dissolved in 100 mL DI. Once again, the pH was adjusted to 4.5 using 1 M HCl. The second solution was filter sterilized (0.45 μm) and combined with the first part once it had cooled. This medium was used to provide a nutritional advantage to any environmental acidophilic sulfur oxidizing organisms in the meteorite fragments. Tait et al. (2017b) proposed that such microorganisms might use troilite or iron-nickel alloys as electron donors; as such, this experiment sought to enrich for these organisms over other metabolic processes. Samples were incubated in 50 mL Falcon™ tubes with loose caps at 25° C for three months and were periodically checked periodically (macroscopically) for growth of biofilms on the substrate.

Samples were prepared for Field Emission Gun - Scanning Electron Microscopy (FEG-SEM) by overnight fixation in 2.0%_(aq) glutaraldehyde. They were then washed twice in a Phosphate-Buffered Saline (PBS) solution before being stained with 1% osmium tetroxide. They were subsequently washed in DI water before undergoing an aqueous-acetone dehydration series (50, 70, 90, 95, 100, 100%). The acetone was then replaced with 50:50 mixture of EPON 'hard' resin that was left overnight to evaporate the acetone. Samples were treated with 100% EPON 'hard' resin for five hours. A final treatment of 100% EPON 'hard' resin and DMP-30 hardener was applied to the samples, which were placed under vacuum to remove bubbles and cured at 60°C for 48 hours. After embedding, the samples were ground down and machine polished to half their volume in order to expose any infiltration by microscopic organisms. These were then mechanically polished to a 0.25 μm finish.

3.2.3 Experiment 2: Biofilm Exhumation

3.2.3.1 Acid Etch

This experiment was designed to investigate whether fossil microorganisms and biofilms are preserved in calcite–gypsum veins in Nullarbor meteorites. Tait et al. (2017b) have shown that this vein material is predominantly Mg-calcite precipitated in isotopic equilibrium with modern or recent atmospheric CO_2 , which confirms it as a weathering product of meteorites, rather than contamination from the Nullarbor limestone. Approximately 10 μm -thick biofilms commonly develop on the surfaces of carbonate–gypsum veins within cracks in meteorites (TAIT *ET AL.* 2017B).

A method modified from (POWER *ET AL.* 2011) was used to exhume any preserved cells and biofilms

from the calcite–gypsum veins. A weak acid solution (0.1 M HCl) was used to etch away carbonate minerals from efflorescent veins extracted from meteorites *Watson 015* and *Ooldea 007*. This acidic solution was applied for 2 minutes before samples were gently washed with 0.45 µm filtered DI to remove acid and loose debris. These samples, along with controls that had not undergone acid treatment, were chemically fixed with 2.0% glutaraldehyde for 24 hrs. These then underwent an ethanol dehydration series (25, 50, 75, 100, 100, 100%) before being critical point dried in a BalTec 030 critical point dryer.

3.2.3.2 Scanning Electron Microscopy (SEM)

Samples from experiments 1 and 2 were coated in Pt and vacuum desiccated before SEM analysis. They were analysed using a JEOL 7001F FEG-SEM at the Monash Centre for Electron Microscopy (MCEM). Energy Dispersive X-ray Spectroscopy (EDX), Back Scattered Electron imaging (BSE) and Secondary Electron Imaging (SEI) modes were used at accelerating voltages ranging from 1–15 kV with a working distance of 10 mm.

3.3 Results

3.3.1 Cellular Penetration Experiment

Samples were inspected at 4, 8, 10 weeks and 3 months for evidence of macroscopic biofilms. The samples *Watson 015* and *Ooldea 004* had a macroscopic black biofilm growing on their exterior surfaces at 4 weeks. These continued to grow over the course of the experiment. At 8 weeks, sample *Watson 014* began to develop a black biofilm. *Ooldea 003* and *Ooldea 002* developed a macroscopic black biofilm within 10 weeks. Sample *Ooldea 005* did not develop a macroscopic black biofilm, although SEM analysis did verify the presence of thin biofilms. All meteorite samples, including *Ooldea 002*, exhibited epilithic films of microorganisms on their exterior surfaces. Microorganisms were easily recognizable under BSE due to the use of an osmium stain that attached to their cell membranes and provided a contrast in mean atomic number. Some heterogeneity in the osmium stain was observed using SEM analysis. This is most likely an artefact of our sample preparation strategy, which required the stain to permeate an already reagent-saturated rock. Staining and embedding organisms deep inside the meteorite chips has resulted in a non-ideal distribution of stain (resulting in less contrast in walls of cells found deeper within meteorites) and resin (resulting in a diffuse stain around the cell

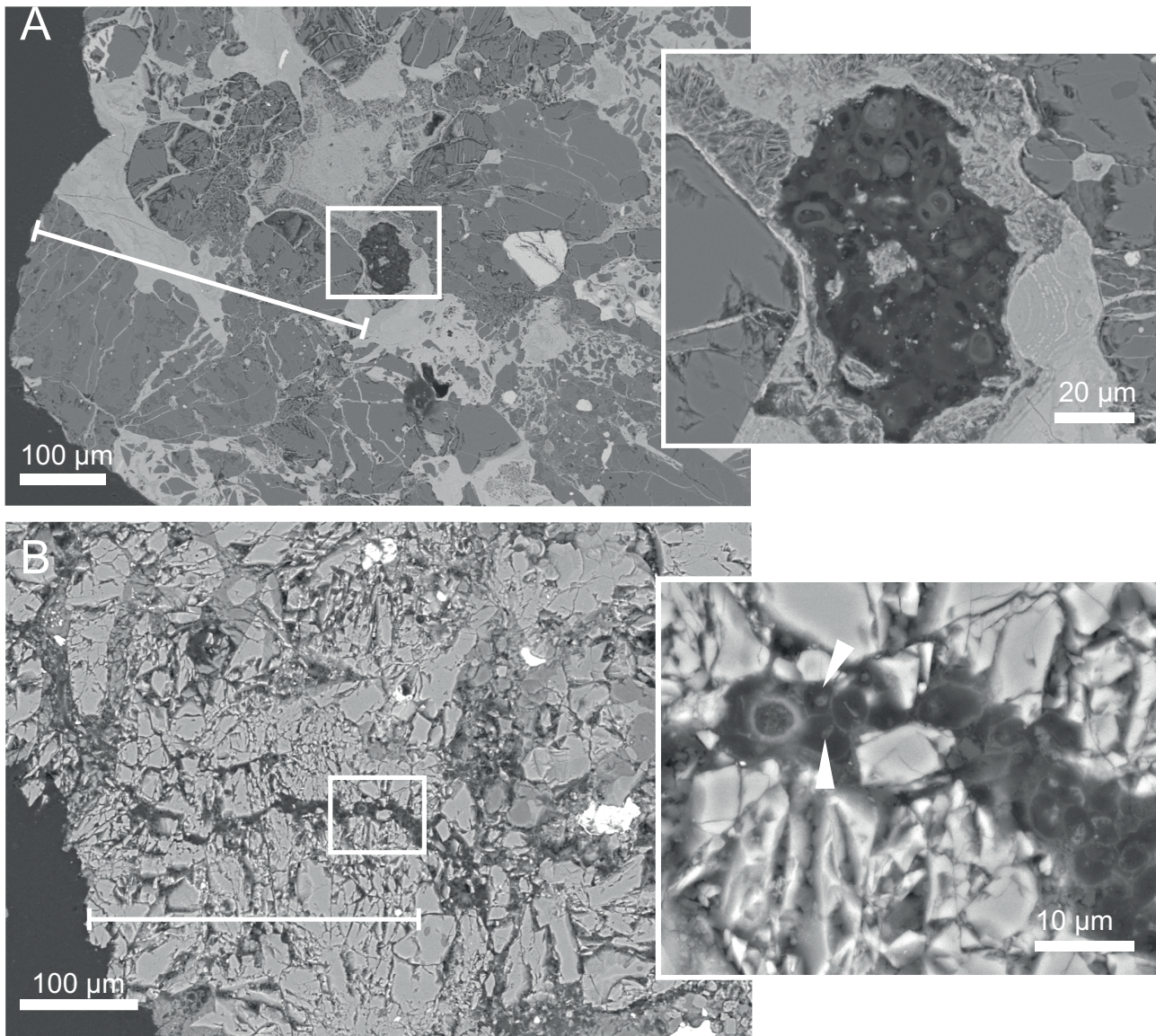


Figure 3.1 | Penetration of Microbes Into Meteorites. Back Scatter Electron (BSE) images from meteorites incubated in acidophilic sulfur oxidizing enrichment medium for three months. **(a)** Meteorite *Ooldea 003* shows a colony of $\sim 5\ \mu\text{m}$ cocci in a corrosion cavity. This cavity appears cut off from the surface of the meteorite, but microbes probably infiltrated from a crack above or below the plain of the polished cross section. The colony is $\sim 400\ \mu\text{m}$ from the edge of the meteorite fragment. The diffuse Os-stained rim and cell shape are likely products of non-deal Os and resin penetration at depth within the sample. **(b)** Meteorite *Watson 015*, which is moderately brecciated (S3), also contains $\sim 5\ \mu\text{m}$ cocci within a crack at least $250\ \mu\text{m}$ from the surface of the meteorite. Many of the cocci show what appears to be a nucleus/organelle (arrows in insert). Their large size suggests that they may be eukaryotic.

walls).

The most commonly observed organisms in the experimental samples were $\sim 5\ \mu\text{m}$ diameter cocci (Figures 3.1, 3.2). Although bacteria of this size exist, these cells are considered large for most bacteria, suggesting that they may be eukaryotic (Figure 3.1 B, 3.2 B, D). Furthermore, the presence of what appear to be nucleolus/organelle near the centre of the cells provides evidence that they are eukaryotes (Figure 3.1 B, Figure 3.2 D). We do not think these are bacterial cells beneath the eukaryotic cell because the alignment of this high contrast feature to the near-centre of the larger cells occurs

frequently. It is statistically unlikely that a bacterium would be found centred beneath every larger cell. The bacteria we have found in cracks within meteorites form micro-colonies and are rarely seen as a single cell. Contrastingly, the smaller features that we have identified as nucleoli are not associated with micro-colonies. The micro-colonies that include small cocci of ($\sim 0.5\ \mu\text{m}$) are more likely to be bacteria (*Figure 3.2 A*). Therefore, we are interpreting the high contrast features in the centre of each of the larger (eukaryotic) cells as an organelle (likely a nucleolus). These cocci could also be rods that have been cut tangentially though $5\text{-}\mu\text{m}$ diameter rods were not observed in any of the sections. Other cell morphologies included coccobacillus and bacillus (*Figure 3.2 B*).

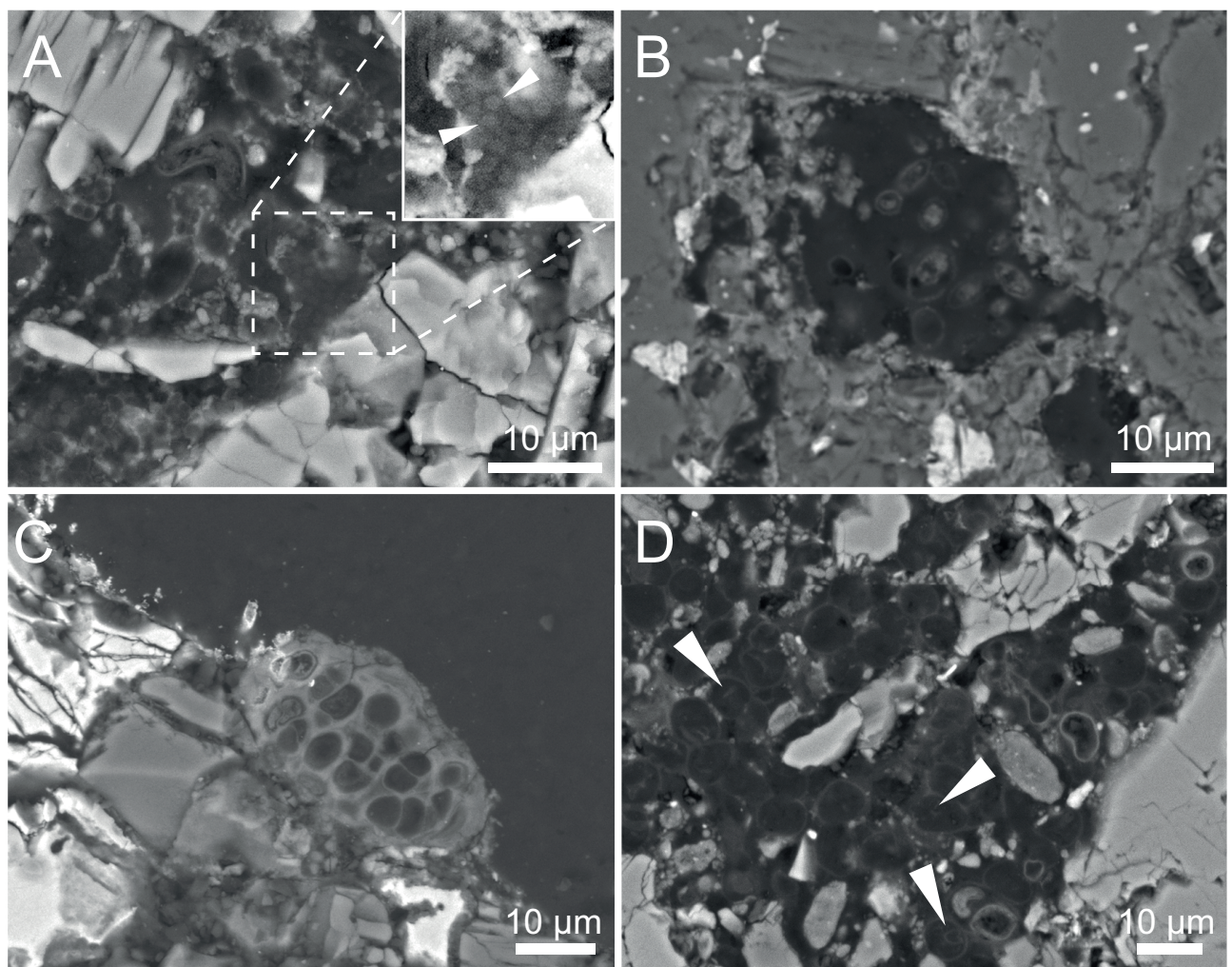


Figure 3.2 | Cell Morphologies in Penetration Experiments. High magnification BSE micrographs revealing microbial structural diversity. (A) *Watson 015* shows a variety of morphological types for chasmoendoliths including cocci and bacilli that are $\sim 5\ \mu\text{m}$ in diameter. Microcolonies of $0.5\ \mu\text{m}$ cocci (contrast scaled insert) are also present. (B) This image is of *Watson 014* and it shows cryptoendolithic coccobacilli and cocci inside the meteorite. (C) An epilithic colony of cocci (or tangentially cut rods) on *Watson 015*. (D) Lastly, this image of *Watson 015* shows more chasmoendolithic communities of $\sim 5\ \mu\text{m}$ cocci. These are large for bacteria suggesting that many of these microorganisms are eukaryotic. . Arrows point to possible nucleolus/organelles. Poor cell-wall contrast is due to the non-ideal distribution of the Os stain at depth inside the meteorite.

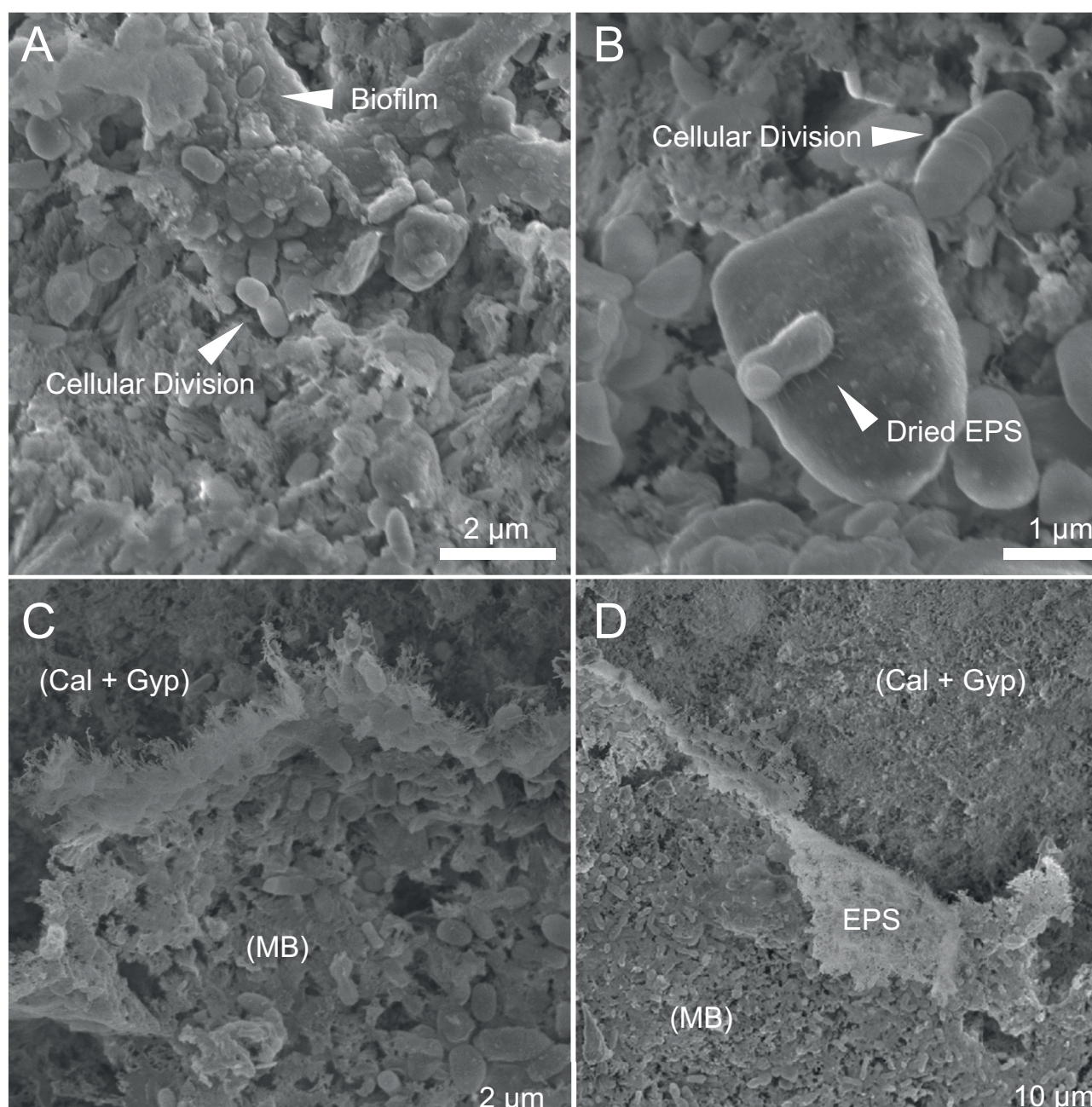


Figure 3.3 | Biofilm Acid Etch and Control. These secondary electron images (SEI) show meteorite *Ooldea 007*. The images are of a control sample that was not acid etched (A,B), and a sample that was acid etched (C,D). **(A)** This image shows cells and their biofilm on the carbonate–gypsum surface. **(B)** This image shows a single cell in the centre of the image with dried EPS forming struts around the cell. Above this is a cell in the process of cellular division. **(C)** Here we see the modern biofilm (MB) pulling away from the carbonate–gypsum substrate in response to the acid etch and fixation. **(D)** This image also shows the modern biofilm pulling away from the carbonate–gypsum admixture, as well as a curled over segment of the EPS.

Microorganisms were found 200–500 μm away from the surface of a fragment of *Ooldea 003*. Infiltration of microorganisms into cracks was more widespread in *Watson 015*, which is a more brecciated meteorite. Microorganisms were found in cracks whose breadths were roughly equal to the cell diameter $\sim 5\ \mu\text{m}$ (Figure 3.1 B). Some clusters of microbes appeared in pores that seemed isolated from the surface (Figure 3.1 A) with no obvious pathway for colonization, which indicates

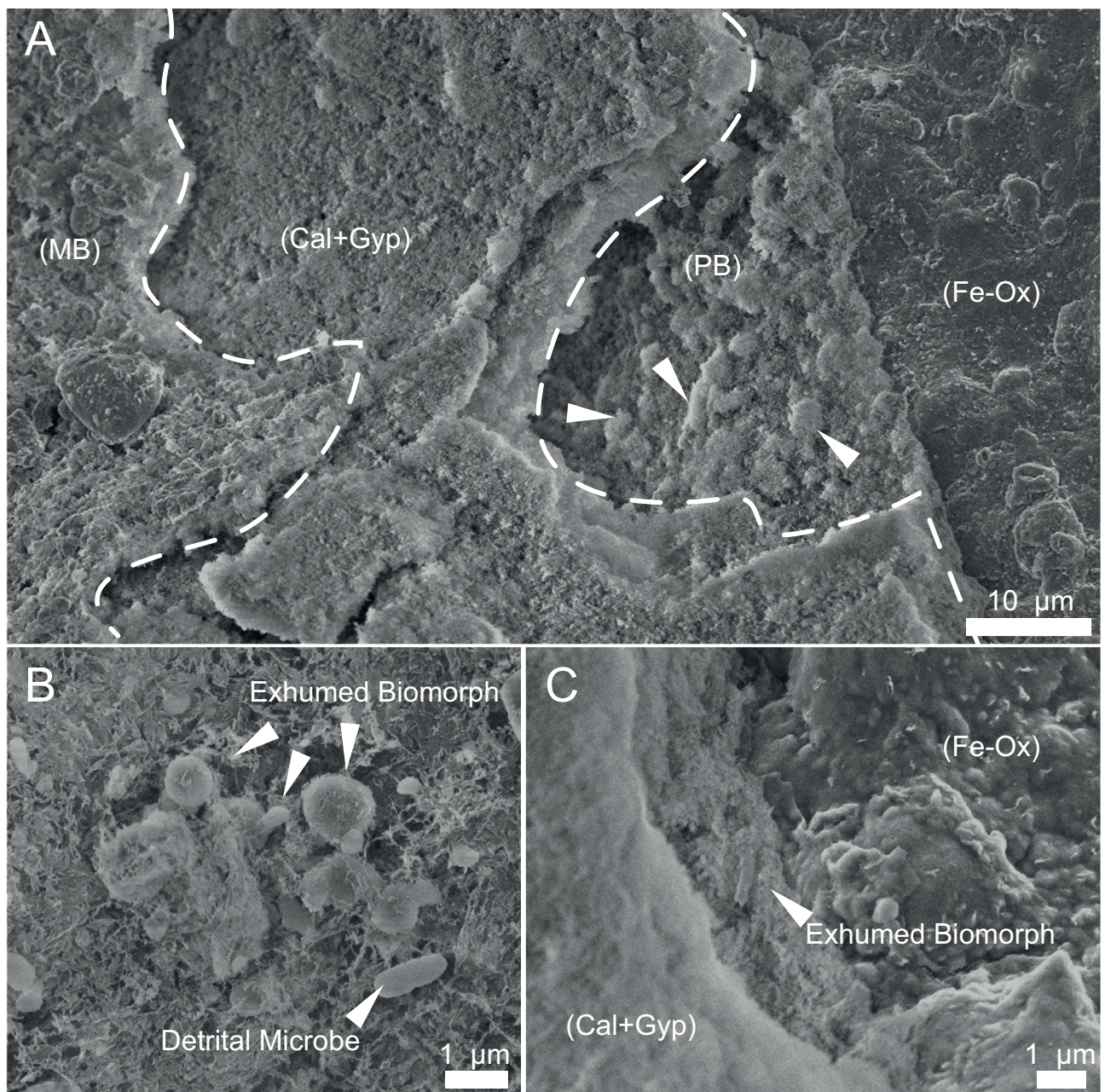


Figure 3.4 | Exhumed Biofilm. These secondary electron images (SEI) show the results of acid etching on meteorite *Ooldea 007*. **(A)** Multiple layers of modern biofilm (MB), carbonate–gypsum admixture and a paleobiofilm (PB) overlaying Fe-(oxy)hydroxide. Dotted lines demarcate the borders of the key layers. Arrows point to cocci (~3–5 µm) and rod-shaped (~3 µm) biomorphs on suspected paleobiofilm. Biomorphs are covered in wisps of calcite and gypsum. **(B)** An acid etched carbonate–gypsum admixture. Exhumed micrometre-scale cocci and rods are coated in a web of undissolved calcite, resistant gypsum and EPS, whereas detrital microbes that have fallen in from the modern biofilm do not possess such features. This colony has also pulled away and shrunk from the surrounding calcite–gypsum admixture during the fixation process, leaving an imprint around the top of the feature. **(C)** This image shows the base of a layer of carbonate–gypsum that broke off during acid etching, an exhumed rod covered in detritus, and the Fe-(oxy)hydroxide surface beneath.

that the infiltration crack they used was not parallel to the cut face. Consistent with our macroscopic observations of biofilm growth on meteorite surfaces, epilithic microcolonies of microorganisms were found on the exteriors of meteorites (*Figure 3.2 C*), as well as extensive biofilms covering pore surfaces.

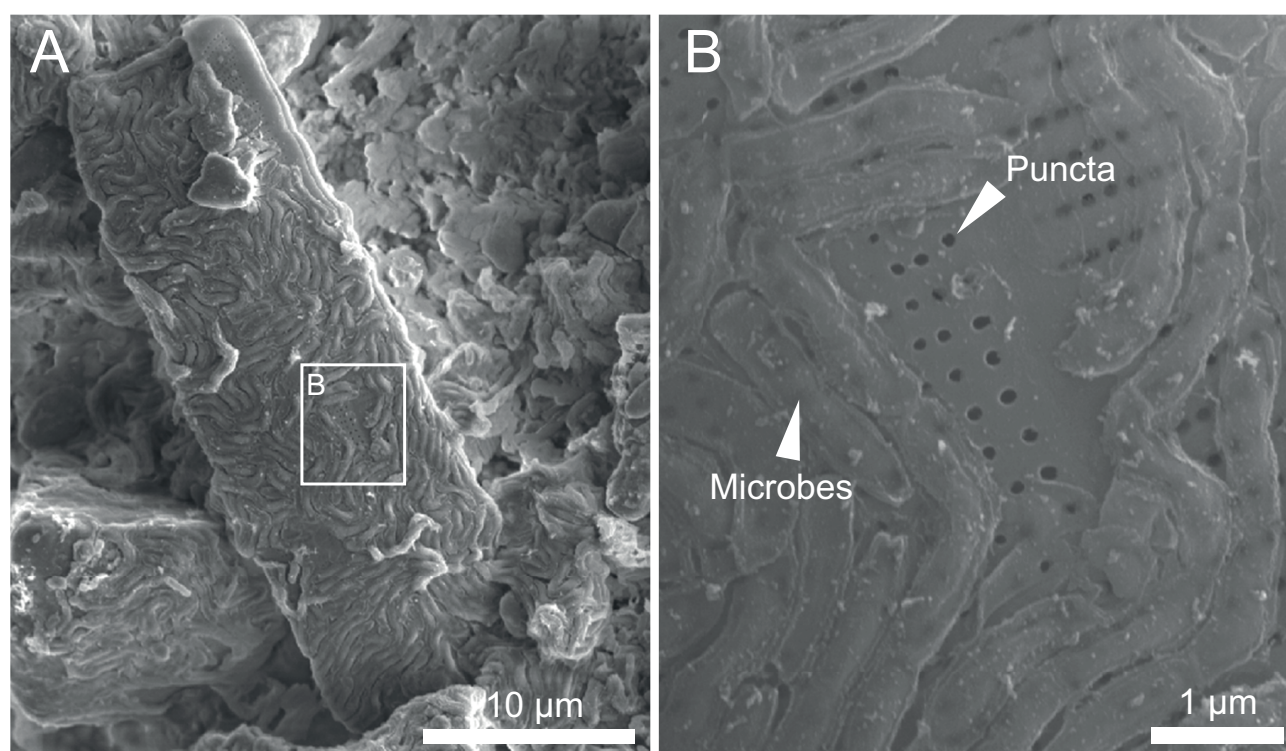


Figure 3.5 | Diatom. This secondary electron image (SEI) shows a pennate diatom on the vein material inside the meteorite, *Watson 015*. **(A)** (5 kV SEI) Extensive biofilm of environmental microorganisms covers ~90% of the surface area of this diatom (as well as other surface material). **(B)** (15 kV SEI) Many rows of puncta can be seen beneath the microbes, including where a dorsal raphe would be indicating this diatom is most likely a member of the order Fragilariophyceae.

3.3.2 Biofilm Exhumation Experiment

As described by Tait et al. (2017b), the carbonate–gypsum admixture found in Nullarbor chondrites typically exhibits a ~2–10 µm-thick modern biofilm. Biofilms are communities of microorganisms associated with surfaces in a matrix of excreted material called Extracellular Polymeric Substances (EPS). The EPS is made out of, but not limited to: polysaccharides, proteins, lipids, and water (DOHNALKOVA ET AL. 2011). When the EPS is dehydrated during sample preparation for Scanning Electron Microscope (SEM) analysis, the EPS can shrink forming dendritic/web-like structures of leftover material (*Figure 3.3 B, C, D*) (DOHNALKOVA ET AL. 2011). Examination of control samples, which did not undergo acid treatment, indicated that the acid-etch had very little effect on the morphology of modern biofilms and cells appeared relatively intact compared to the control (*Figure 3.3*). The acid etch did however dislodge some cells from the substrate (*Figure 3.3 C, D*).

Investigation of the control samples showed that multiple patches of biofilm on multiple samples contained many different morphological shapes including bacillus, diplococcus and coccobacillus

of varying sizes (*Figure 3.3 A, B*). EPS were seen intertwined with occasional crystals of pitted, scalenohedral calcite [CaCO_3]. The EPS in all samples had dried out during the fixation process to form a web of “struts” around individual cells (*Figure 3.3 B*).

The modern biofilm observed across all samples were shallowly rooted (0.5–2 μm) into the substrate as can be seen by EPS that has peeled back (*Figure 3.3 C, D*). Fixation and dehydration of samples aided in peeling back the modern biofilms via shrinkage, which resulted in more exposure of the buried cells beneath at the base of the modern biofilm. Many detrital cells near this peel-back feature may have been removed from the sample or may have fallen onto the exposed substrate; these were easily distinguished from exhumed cells by their smooth surfaces that lacked a covering of detrital minerals (*Figure 3.4 B*). The substrate exposed by the acid etch exhibited a fuzzy texture, most likely a consequence of residual material (e.g., gypsum, smectites) and/or EPS that did not dissolve. Cell shapes were found in situ within this material at the acid-etched surface of the substrate. These included both cocci or bacilli, which were covered in fine grains of detrital material (*Figure 3.4 B*). In addition many of these groupings of these cells have pulled away from the substrate leaving dark gaps, which indicated they were hydrated and shrunk during the fixation process. A fortuitously located crack that crosscut the vein material was exposed showing terraced layers of mineral precipitates and biofilms within an efflorescence (*Figure 3.4 A*). The cross section, where vein material has peeled off in layers, exposes a possible paleobiofilm (PB), a layer of carbonate–gypsum vein material, and detritus-covered cells at the base. In addition, at the base of one of the cross sections through vein material, there is a possible bacillus (~2 μm in size) that is covered in detrital material and extruding from a wall of carbonate–gypsum (*Figure 3.4 C*). The carbonate–gypsum vein material overlays a smooth surface of Fe-oxyhydroxide minerals with little to no botryoidal textures that could be mistaken for cells.

One surprising observation from the surface of the exposed vein material in *Watson 015* was the discovery of a 35 μm x 10 μm pennate diatom frustule. This diatom was found at the surface of the vein material and it was covered in a monolayer of 2- μm long rods that formed a biofilm (*Figure 3.5*). The diatom was tabular in shape and ~90% of its surface area was covered in biofilm (*Figure 3.5A*), which hindered identification beyond order level classification. Higher accelerating voltages were not effective for revealing features obscured by the biofilm. Fortunately, a small clear section was exposed in the middle dorsal region of the diatom (*Figure 3.5 B*). Puncta can be seen under the biofilm and are

located where a dorsal raphe could have been. Because of the lack of this feature it is likely this diatom is a member of the order Fragilariophyceae (ROUND *ET AL.* 1990). The biofilm covering the diatom was too thick to identify further diagnostic features.

3.4 Discussion

3.4.1 Microbial Penetration

Chondrites are porous by nature; however, the amount of porosity is quite variable in ordinary chondrites (0 – 27%) (WILKISON *ET AL.* 2003). Larger variation in porosity exists within carbonaceous chondrites (CONSOLMAGNO *ET AL.* 2008). This variability has been tied to the amount of shock the parent body receives, with higher shock resulting in lower porosity (CONSOLMAGNO *ET AL.* 2008; TAIT *ET AL.* 2016). Porosity should have an impact on the amount of microbes found in a chondritic meteorite because increased porosity should offer greater internal surface area for microbes to colonise. Such porosity can be infilled with weathering products such as goethite, resulting in a slow decrease in porosity while a meteorite is resident on Earth (BLAND *ET AL.* 2006). Infilling of pore space by alteration minerals would decrease the available surface area for microbes to colonise. In some instances, alteration of meteorites can produce porosity in the form of ‘corrosion cavities’. Many of the weathered meteorites we collected from the Nullarbor contain corrosion cavities produced as a result of alloy and sulfide mineral oxidation combined with alteration products migrating into cracks, leaving behind cavernous areas for microbes to colonise (*Chapter 2*). High porosity does not always translate into permeability (PONTEFRACT *ET AL.* 2014). For instance, fissures will form due to reaction-driven cracking during precipitation of alteration minerals such as Fe-(oxy)hydroxides, sulfates, carbonates and smectites (BLAND *ET AL.* 2006), this increase permeability. Over time, these fissures become wider and develop extensive efflorescent coatings (*Chapter 2*), which allows environmental microorganisms to ingress and provides an opportunity for them to scavenge water from hygroscopic minerals.

One meteorite, *Watson 015*, had a 35 µm x 10 µm penate diatom on the surface of efflorescent vein material (*Figure 3.5*). This diatom was covered in a biofilm, which indicates that its presence in the meteorite is not a result of post-recovery contamination, but instead that the diatom became lodged in the crack during the residence of *Watson 015* on the Nullarbor Plain. Diatoms are heterokont algae that form a siliceous outer shell called a frustule (ROUND *ET AL.* 1990). They inhabit most bodies of

water over a range of salinities, and are even found in moist soils. Identification of this diatom was limited to order Fragilariophyceae. It is unknown whether this is a fossil diatom dislodged from the marine Nullarbor Plain limestone karst or if it is a recently living freshwater diatom sourced from a bloom that might have occurred during a flooding event; the latter seems more likely, given the extensive, un-mineralized biofilm observed covering its surface. The Nullarbor Plain is known to flood periodically during storm events (WEBB AND JAMES 2006), which could trigger reproduction of dormant diatoms in the soil and cause bloom events. This periodic flooding could also provide a method for ingress of diatoms and other environmental microorganisms into meteorites. This mechanism has parallels to seasonal groundwater seepage events that occur on Mars given the recent discovery that Recurring Slope Lineae (RSL) are outflowing seeps of brine (OJHA *ET AL.* 2015). It is believed that the RSL travel through the Martian regolith rather than over it, which could allow for capillary rise of brines from regolith into meteorites, allowing mechanisms of ingress for putative Martian microorganisms.

Diatoms are large compared to other microorganisms such as bacteria. Smaller organisms are able to penetrate deeper into newly fallen meteorites especially along fresh cracks that are generated during impact fragmentation or brecciation in chondrites (PONTEFRACT *ET AL.* 2014). The penetration experiments demonstrated that microorganisms can ingress meteorites along fissures to distances > 400 μm from the surface of a meteorite within only three months. An interesting finding from these experiments is that the microorganisms were able to trespass along fissures as narrow as their own diameter, $\sim 5 \mu\text{m}$ (*Figure 3.1 B*). Although the medium used in these experiments was chosen to select for Fe- and S- oxidising bacteria, many of these $\sim 5\text{-}\mu\text{m}$ sized organisms are considered large for bacteria suggesting they may be eukaryotic (*Figure 3.2 B, D*). Bacteria by comparison are much smaller (e.g. typically $0.5\text{--}1 \mu\text{m}$), which would allow them to penetrate even deeper into the meteorite along more narrow fissures. Bacteria observed in this meteorite were only seen in micro-colonies (in association with larger cells) and were not found individually (*Figure 3.2 A*). It is not clear at this time whether all these microorganisms were already present at that penetrative depth at the start of this experiment as they were environmental samples and already colonised, or whether they migrated to that depth during the course of the 3-month experiment. Growth of the macroscopic, black biofilms presumably relates to the acid catalysed disproportionation of thiosulfate (JOHNSTON AND McAMISH 1972), which is accelerated during biooxidation/acid production, producing sulphide, which reacted

with the iron present in the meteorites producing the black colouration.

Biological textures and Os stain heterogeneity between the images are most likely a preparation caveat for trying to permeate an already reagent saturated rock with another liquid reagent. Trying to stain and embed organisms deep inside the meteorite chip has resulted in a non-ideal distribution of stain (resulting in less contrast in rims for deeper cells), and resin resulting in a diffuse stain around the cell walls. Overall uniform size of Eukaryotes, spatial relationships to each other and osmium stained rim (even if weak) are the clear indicators of cells at depth.

On Mars, the depth to which putative martian microbes might penetrate meteorites is an important consideration due to the high flux of UV light to the planet's surface. Because Mars lacks an ozone layer, this radiation would likely result in sterilization of a putative surface biosphere (MANCINELLI AND KLOVSTAD 2000; RETTBERG *ET AL.* 2004). Experiments have been done on *B. subtilis*, on Earth and in Earth-orbit, to determine the minimum thickness of various environmental materials needed to mitigate the sterilizing effects of UV exposure (MANCINELLI AND KLOVSTAD 2000; RETTBERG *ET AL.* 2002). One experiment has shown that as little as 12 μm of dust is sufficient to start mitigating the harmful effects of UV (i.e., allowing for ~10 % survival of *B. subtilis*) (MANCINELLI AND KLOVSTAD 2000). Orbital studies have shown that grains of meteorites (mean diameter of 80–100 μm) also reduce the number of spores killed by UV light in open space (RETTBERG *ET AL.* 2002). It is worth reiterating here that the penetrative depth of the microbes into fresh cracks in our experiment was commonly >400 μm (*Figure 3.1*), which is 4 \times times the thickness of meteorite required to protect against UV exposure on Mars. Although epilithic communities were common in these experiments (*Figure 3.2C*), microbes have previously been found much deeper than 400 μm within cracks in meteorites (TAIT *ET AL.* 2017b). Thus, if chondritic meteorites on Mars were to host putative microorganisms they would provide ample protection from UV radiation, assuming similar endolithic penetration by putative Martian organisms. This study lends support to a finding by Tait et al. (2017b) that microbial colonization “keeps up” with weathering fronts in meteorites and that any connected cracks larger than ~0.5 μm could potentially be a habitat for microorganisms.

3.4.2 Fossilization Potential

3.4.2.1 Exhumation of Biomorphic Features From Alteration Minerals

Fossilization of microbes is likely to occur in the weathering products of meteorites. The alteration minerals in chondrites are known to entomb microbes and preserve fossil evidence of their presence in other terrestrial settings. These minerals include Fe-(oxy)hydroxide and sulfate minerals (WILLIAMS *ET AL.* 2015) and carbonate minerals (POWER *ET AL.* 2011). Preservation of microorganisms in carbonate minerals is useful because they can retain recognizable biomolecules, such as phenols associated with lignin, for millions of years on Earth (BLYTH *ET AL.* 2010). In the martian context, (1) a biomorphic structure that could be a fossil cell or (2) organic biomolecules within carbonate minerals could be useful signposts suggesting that further evidence of biogenicity might be found on closer analysis. As such, in our second experiment we attempted to find a paleobiofilm within carbonate efflorescences inside the meteorites as a proof of concept. Considering that a modern biofilm has already been shown to exist in these meteorites, and that efflorescences may grow slowly over thousands of years (TAIT *ET AL.* 2017B), it stands to reason that some, or all older biofilms may be entombed within or under this material. This entombment may be promoted by calcifying organisms that can nucleate carbonate crystals on their cell membranes (BOROWITZKA 1982), making it likely that the growth of efflorescences in meteorites is accelerated by the presence of microorganisms.

Modern biofilms contracted and peeled away from meteorite surfaces following acid etching and fixation (*Figure 3.3 C, D*). These biofilms appeared to be only one or two cells thick. A fine-grained mass of undissolved calcite, gypsum and other minerals was present underneath the biofilms. Very few obviously detrital organisms from the modern biofilm were observed in this layer and most cells were covered in residue (either EPS or minerals such as gypsum) (*Figure 3.4 B*). Due to the sample of *Ooldea 007* being chipped in places, there were clear cross sections through efflorescent carbonate–gypsum veins as well as terraced layers of undissolved material (*Figure 3.4 A, C*), which gave an unprecedented view across their layered structures. The growth banding can be seen in vein material, indicating periods of faster or compositionally different mineral growth (*e.g. Figure 3.4 A*). Biomorphic shapes, that could be fossilized/entombed cells, were found throughout the efflorescences at different depths below the surface of the vein material.

Employing further analytical techniques for identification of organic or inorganic biomarkers from palaeobiofilms could be complicated by contamination from the modern biofilm and EDX would likely pick up the surrounding carbonate and phosphate minerals instead of relic kerogen (a likely organic breakdown product of cells) (SCHIDLOWSKI *ET AL.* 1983; SOUTHAM 1999). There are several possible traits that suggest these biomorphs are prokaryotic or eukaryotic cells. Most of the acid etched efflorescences were ‘fuzzy’ and homogenous in texture, but there were three areas of interest that could be a possible preserved biofilm in *Ooldea 007*. All of these locations feature ~1–2 μm diameter sized cocci-shaped biomorphs (*Figure 3.4B*) as well as similar sized (~5 μm) microorganisms found in the penetration experiment. Also, environmental cocci are often treated with suspicion in the context of fossil biomarkers because many abiotic materials can also form round, and thus cocci-shaped, features (e.g., aeolian sorted sand particles and botryoidal textures in Fe-(oxy)hydroxide minerals). However, we also observed rod-shaped cells (1–2 μm in length) in association with the biomorphic cocci. These rod-shaped features were found in two locations: (1) associated with the cocci (*Figure 3.4 B*) and embedded at the base of a carbonate–gypsum efflorescence (*Figure 3.4 C*). The cells in both locations were covered in detrital minerals, which is very different from the smooth surfaces of cells from the modern biofilm. The rod-shaped cells were also detected *in situ* based on the observation that they were partially buried within the efflorescence, which confirms they were not sourced from the modern biofilm. Also, in some cases, rod-shaped cells were juxtaposed with smooth Fe-(oxy) hydroxides that showed no botryoidal shapes that could be confused with fossil cells (*Figure 3.4 A, C*). The areas that appeared to host fossil biofilms contained clusters of biomorphs. The presumed paleobiofilm also shrunk away from the surrounding efflorescence, presumably during fixation, which suggests this feature was initially hydrated. This can be seen by the imprint of the original size of the feature prior to shrinking (*Figure 3.4 B*). This behaviour parallels that of the modern biofilm.

These cells may be entombed microorganisms. Bacteria are hard to preserve (DES MARAIS 2000) and harder to identify as life by SEM analysis alone. On Earth, where microbial life is common, it is likely that biomorphic features found in association with a modern biofilm are preserved cells. The existence of a diatom frustule is less ambiguous as life due to its distinctive morphology. We found one full diatom frustule (*Figure 3.5*) in *Watson 015* and a fragment of another in *Ooldea 007*, but none were exhumed from vein material by acid etching. It is possible that diatoms could be entombed within growing bands of carbonate efflorescence in meteorites in a similar fashion to those found in

carbonate microbialites (POWER *ET AL.* 2011). Indeed, we may have caught this process in action, as the diatom frustule was already covered by a modern biofilm. The organisms found on the frustule are most likely heterotrophs utilising the organics in the decaying diatom as a source of nutrients. Organics in ordinary chondrites are less abundant than in carbonaceous meteorites (SEPHTON 2002; ZENOBI *ET AL.* 1992) due to thermal metamorphism on the parent body. This leaves exogenous sources of organics (e.g., lichen, diatoms, other microbes) to support heterotrophic microorganisms under conditions where organic matter is scarce. Indeed, *Chapter 4* shows that Fe- and S-based metabolisms are not a driving force behind community structure inside ordinary chondrites, indicating that other properties of meteorites, such as water retention, temperature control, porosity, and pH regulation, are likely larger drivers of colonisation than specific nutrients and electron donors/acceptors.

3.4.2.2 Alternate Techniques and Follow up Studies

Carbonate–gypsum vein material in meteorites offered the opportunity to study modern biofilms and preserved diatom(s) in more detail. Our observations suggest the presence of entombed biofilms within efflorescences given their punctuated growth and layering. However, modern biofilms are unlikely to exist on Mars. Therefore, evidence of a past putative biosphere would need to be targeted within the meteorite alteration products. For Mars, this morphological triage would subsequently require a dedicated follow up study focusing on organic analysis to evaluate the biogenicity of any cell-like features found within meteorites on Mars (CADY *ET AL.* 2003). Techniques such as Gas Chromatography (GC), Time-of-Flight Secondary Ion Mass Spectroscopy (TOF-SIMS), and Transmission Electron Microscopy (TEM), as well as Infrared Spectroscopy and Raman Spectroscopy (CADY *ET AL.* 2003) could be used in conjunction with SEM to assess spatial associations between biomorphic features and organics. A follow up study could also be done in line with the capabilities of the Curiosity Mars Science Laboratory (MSL) rover. The Science Analysis at Mars (SAM) instrument suite (MAHAFFY *ET AL.* 2012) has the capability to analyse organic molecules by pyrolysis using a Quadrupole Mass Spectrometer (QMS), Gas Chromatograph, and Tunable Laser Spectrometer (TLS). Gas chromatography results for etched material, with the modern biofilm removed, could be used to confirm the presence of organic matter associated with the cells. This could then be compared with the organic molecules inherited from the meteorite to assess biogenicity.

3.5 Conclusions

The following conclusions can be drawn from our experiments:

- 1) Microorganisms can penetrate deep into meteorites along networks of cracks of similar widths to their own diameters (1 to 5 μm). Environmental microbes from the Nullarbor Plain can reach depths of $>400\text{ }\mu\text{m}$ below the surface of a meteorite, which is well beyond the depth required to mitigate the harmful effects of UV light (RETTBERG *ET AL.* 2002) under Martian surface conditions. Previous studies have shown that crystallisation of hygroscopic alteration minerals induces reaction-driven cracking, which widens cracks allowing microbes to penetrate even deeper into the meteorite (TAIT *ET AL.* 2017B). At the same time, these minerals scavenge water vapour from the atmosphere, promoting colonisation of efflorescences by microbes (TAIT *ET AL.* 2017B).
- 2) Vein efflorescences in meteorites recovered from the Nullarbor Plain were acid etched to reveal forms consistent with the presence of entombed biofilms and cells. This same preservation potential, could potentially allow meteorites record the presence of relic biofilms for millions of years.

This work shows that meteorites are complex habitats for terrestrial endolithic and epilithic microorganisms and that they have the capacity to preserve paleo-biofilms and cells within alteration minerals. The observations from this terrestrial study could also apply to preservation of putative biofilms and cells within meteorites on Mars. Given the long residence times of meteorites on Mars, they may record a snapshot of a putative Martian biosphere throughout the planet's history.

3.6 Chapter 3 References

A

Ashley J. W. (2011) Meteorites on Mars as Planetary Research Tools with Special Considerations for Martian Weathering Processes: *Arizona State University*. 343 p.

B

Bland P., and Smith T. B. (2000) Meteorite accumulations on Mars. *Icarus*, 144: 21-26.

Bland P. A., Zolensky M. E., Benedix G. K., and Sephton M. A. (2006) Weathering of chondritic meteorites. In: *Meteorites and the Early Solar System II*. edited by DS Lauretta and HY McSween, *University of Arizona Press*, Tucson, pp 943.

Blyth A. J., Watson J. S., Woodhead J., and Hellstrom J. (2010) Organic compounds preserved in a 2.9 million year old stalagmite from the Nullarbor Plain, Australia. *Chemical Geology*, 279: 101-105.

Borowitzka M. (1982) Mechanisms in algal calcification. *Progress in Phycological Research*: 137-177.

C

Cady S. L., Farmer J. D., Grotzinger J. P., Schopf J. W., and Steele A. (2003) Morphological biosignatures and the search for life on Mars. *Astrobiology*, 3: 351-368.

Carr M. H., and Head J. W. (2010) Geologic history of Mars. *Earth and Planetary Science Letters*, 294: 185-203.

Consolmagno G. J., Britt D. T., and Macke R. J. (2008) The significance of meteorite density and porosity. *Chemie der Erde-Geochemistry*, 68: 1-29.

D

Des Marais D. J. (2000) When Did Photosynthesis Emerge on Earth? *Science*, 289: 1703-1705.

Dohnalkova A. C., Marshall M. J., Arey B. W., Williams K. H., Buck E. C., and Fredrickson J. K. (2011) Imaging hydrated microbial extracellular polymers: comparative analysis by electron microscopy. *Applied and Environmental Microbiology*, 77: 1254-1262.

J

Johnston F., and McAmish L. (1972) A study of the rates of sulfur production in acid thiosulfate solutions using S-35. *Journal of Colloid and Interface Science*, 42: 112-119.

Jull A. J. T., McHargue L. R., Bland P. A., Greenwood R. C., Bevan A. W. R., Kim K. J., LaMotta S. E., and Johnson J. A. (2010) Terrestrial ages of meteorites from the Nullarbor region, Australia, based on ^{14}C and ^{14}C - ^{10}Be measurements. *Meteoritics & Planetary Science*, 45: 1271-1283.

K

Kounaves S. P., Chaniotakis N. A., Chevrier V. F., Carrier B. L., Folds K. E., Hansen V. M., McElhoney K. M., O'Neil G. D., and Weber A. W. (2014) Identification of the perchlorate parent salts at the Phoenix Mars landing site and possible implications. *Icarus*, 232: 226-231.

M

Mahaffy P. R., Webster C. R., Cabane M., Conrad P. G., Coll P., Atreya S. K., Arvey R., Barciniak M., Benna M., Bleacher L. and others. (2012) The Sample Analysis at Mars Investigation and Instrument Suite. *Space Science Reviews*, 170: 401-478.

Mancinelli R. L., and Klovstad M. (2000) Martian soil and UV radiation: microbial viability assessment on spacecraft surfaces. *Planetary and Space Science*, 48: 1093-1097.

O

Ojha L., Wilhelm M. B., Murchie S. L., McEwen A. S., Wray J. J., Hanley J., Massé M., and Chojnacki M. (2015) Spectral evidence for hydrated salts in recurring slope lineae on Mars. *Nature Geoscience*, 8: 829-832.

P

Pontefract A., Osinski G. R., Cockell C. S., Moore C. A., Moores J. E., and Southam G. (2014) Impact-generated endolithic habitat within crystalline rocks of the Haughton impact structure, Devon Island, Canada. *Astrobiology*, 14: 522-533.

Power I. M., Wilson S. A., Dipple G. M., and Southam G. (2011) Modern carbonate microbialites from an asbestos open pit pond, Yukon, Canada. *Geobiology*, 9: 180-195.

R

Rettberg P., Eschweiler U., Strauch K., Reitz G., Horneck G., Wänke H., Brack A., and Barbier B. (2002) Survival of microorganisms in space protected by meteorite material: Results of the experiment 'EXOBIOLOGIE' of the PERSEUS mission. *Advances in Space Research*, 30: 1539-1545.

- Rettberg P., Rabbow E., Panitz C., and Horneck G. (2004) Biological space experiments for the simulation of Martian conditions: UV radiation and Martian soil analogues. *Advances in Space Research*, 33: 1294-1301.
- Round F. E., Crawford R. M., and Mann D. G. (1990) Diatoms: biology and morphology of the genera. *Cambridge University Press*, UK.

S

- Schidlowski M., Hayes J. M., and Kaplan I. R. (1983) Isotopic inferences of ancient biochemistries: Carbon, sulfur, hydrogen and nitrogen. In: *Earth's Earliest Biosphere. Its Origin and Evolution.* edited by JW Schopfs, *Princeton University Press*, Princeton, NJ, USA, pp 149–186.
- Schröder C., Bland P. A., Golombek M. P., Ashley J. W., Warner N. H., and Grant J. A. (2016) Amazonian chemical weathering rate derived from stony meteorite finds at Meridiani Planum on Mars. *Nature Communications*, 7: 13459.
- Sephton M. A. (2002) Organic compounds in carbonaceous meteorites. *Natural Product Reports*, 19: 292-311.
- Southam G. (1999) A structural comparison of bacterial microfossils vs. 'nanobacteria' and nanofossils. *Earth-Science Reviews*, 48: 251-264.
- Stoffler D., Keil K., and Edward R. D. (1991) Shock metamorphism of ordinary chondrites. *Geochimica et Cosmochimica Acta*, 55: 3845-3867.
- Summons R. E., Amend J. P., Bish D., Buick R., Cody G. D., Des Marais D. J., Dromart G., Eigenbrode J. L., Knoll A. H., and Sumner D. Y. (2011) Preservation of martian organic and environmental records: Final report of the Mars Biosignature Working Group. *Astrobiology*, 11: 157-181.

T

- Tait A. W., Fisher K. R., Srinivasan P., and Simon J. I. (2016) Evidence for impact induced pressure gradients on the Allende CV3 parent body: Consequences for fluid and volatile transport. *Earth and Planetary Science Letters*, 454: 213-224.
- Tait A. W., Tomkins A. G., Godel B. M., Wilson S. A., and Hasalova P. (2014) Investigation of the H7 ordinary chondrite, Watson 012: Implications for recognition and classification of Type 7 meteorites. *Geochimica et Cosmochimica Acta*, 134: 175-196.
- Tait A. W., Wilson S. A., Tomkins A. G., Gagen E. J., Liu A. C. Y., Morgan B., Golding S. D., and Southam G. (2017a) Bacterially-generated $\delta^{34}\text{S}$ biosignature in the Chelyabinsk LL5 chondrite: Using terrestrial microorganisms to refine tools for astrobiological exploration on the surface of Mars. *Geochimica et Cosmochimica Acta* (Under Review, 17th February 2017).

- Tait A. W., Wilson S. A., Tomkins A. G., Gagen E. J., Stewart F. J., and Southam G. (2017b) Evaluation of meteorites as habitats for terrestrial microorganisms: Results from the Nullarbor Plain, Australia, a Mars analogue site. *Geochimica et Cosmochimica Acta* (Accepted for publication 28th May 2017).

V

- Van Schmus W. R., and Wood J. A. (1967) A chemical-petrologic classification for the chondritic meteorites. *Geochimica et Cosmochimica Acta*, 31: 747-765.

W

- Webb J. A., and James J. M. (2006) Karst evolution of the Nullarbor Plain, Australia. *Geological Society of America Special Paper*, 404: 65-78.
- Wilkison S. L., McCoy T. J., McCamant J. E., Robinson M. S., and Britt D. T. (2003) Porosity and density of ordinary chondrites: Clues to the formation of friable and porous ordinary chondrites. *Meteoritics & Planetary Science*, 38: 1533-1546.
- Williams A. J., Sumner D. Y., Alpers C. N., Karunatillake S., and Hofmann B. A. (2015) Preserved filamentous microbial biosignatures in the Brick Flat Gossan, Iron Mountain, California. *Astrobiology*, 15: 637-668.
- Wlotzka F. (1993) A Weathering Scale for the ordinary chondrites. *Meteoritics*, 28: 460.

Z

- Zenobi R., Philippoz J.-M., Zare R. N., Wing M. R., Bada J. L., and Marti K. (1992) Organic compounds in the Forest Vale, H4 ordinary chondrite. *Geochimica et Cosmochimica Acta*, 56: 2899-2905.

Declaration for Thesis Chapter 4

Declaration by candidate

In the case of Chapter 4, the nature and extent of my contribution is as follows:

<i>Nature of contribution</i>	<i>Extent of contribution (%)</i>
Conceptualisation, field work, sample collection, sequence data analysis, data interpretation, manuscript writing	77.5%

The following co-authors contributed to the work. If co-authors are students at Monash University, the extent of their contribution in percentage terms must be stated:

<i>Name</i>	<i>Nature of contribution</i>	<i>Extent of contribution (%)</i>
Emma J. Gagen	DNA Extraction, Sequencing	10%
Siobhan A. Wilson	Supervisory Role	5%
Andrew G. Tomkins	Supervisory Role	5%
Gordon Southam	Advisory Role	2.5%

The undersigned hereby certify that the above declaration correctly reflects the nature and extent of the candidate's and co-authors contributions to this work*.

Candidate's signature:  Date: 01/06/2017

Main supervisor's signature: _____ Date: 01/06/2017

*Note: Where the responsible author is not the candidate's main supervisor, the main supervisor should consult with the responsible author to agree on the respective contributions of the authors.

Chapter 4

Microbial populations of stony meteorites: Substrate controls on first colonisers[†]

Alastair W. Tait¹, Emma J. Gagen², Siobhan A. Wilson¹, Andrew G. Tomkins¹, Gordon Southam²

¹School of Earth, Atmosphere & Environment, Monash University, Australia

²School of Earth & Environmental Sciences, The University of Queensland, Australia

[†] Accepted for publication in *Frontiers in Microbiology*
19th May 2017

Finding fresh, sterilised rocks provides ecologists with a clean slate to test ideas about first colonisation and the evolution of soils *de novo*. Lava has been used previously in first coloniser studies due to the sterilising heat required for its formation. However, fresh lava typically falls upon older volcanic successions of similar chemistry and modal mineral abundance. Given enough time, this results in the development of similar microbial communities in the newly erupted lava due to a lack of contrast between the new and old substrates. Meteorites, which are sterile when they fall to Earth, provide such contrast because their reduced and mafic chemistry commonly differs to the surfaces on which they land; thus allowing investigation of how community membership and structure respond to this new substrate over time. We conducted 16S rRNA gene analysis on meteorites and soil from the Nullarbor Plain, Australia. We found that the meteorites have low species richness and evenness compared to soil sampled from directly beneath each meteorite. Despite the meteorites being found kilometres apart, the community structure of each meteorite bore more similarity to those of other meteorites (of similar composition) than to the community structure of the soil on which it resided. Meteorites were dominated by sequences that affiliated with the Actinobacteria with the major Operational Taxonomic Unit (OTU) classified as *Rubrobacter radiotolerans*. Proteobacteria and Bacteroidetes were the next most abundant phyla. The soils were also dominated by Actinobacteria but to a lesser extent than the meteorites. We also found OTUs affiliated with iron/sulfur cycling organisms *Geobacter spp.* and *Desulfovibrio spp.*. This is an important finding as meteorites contain abundant metal and sulfur for use as energy sources. These ecological findings demonstrate that the structure of the microbial community in these meteorites is controlled by the substrate, and will not reach homeostasis with the Nullarbor community, even after ca. 35,000 years. Our findings show that meteorites provide a unique, sterile substrate with which to test ideas relating to first-colonisers. Although meteorites are colonised by microorganisms, the microbial population is unlikely to match the community of the surrounding soil on which they fall.

4.1 Introduction

The Nullarbor Plain is a 20-million year old and ~200,000 km² area dominated by limestone karst that spans the southern regions of South Australia (SA) and Western Australia (WA) (WEBB AND JAMES, 2006). It is a semi-arid environment characterised by an extreme average summer UV-index of 12.0 and a moderate average UV-index of 3.3 in the winter (AUSTRALIAN BUREAU OF METEOROLOGY, 2015). The Nullarbor Plain has high evaporation rates (2000 – 3000 mm yr⁻¹) with low rainfall (150 – 400 mm yr⁻¹) and occasional flooding on its flat topographic profile. This is a deflationary surface made up of aeolian sediments and a ~1-m thick calcrete cap covers much of the region (WEBB AND JAMES, 2006). The Nullarbor is named for its lack of trees; it is a sparse shrub-land dominated by the shrubs *Antiplex* and *Maireana*, which are colloquially known as ‘salt bush’ (GILLIESON *ET AL.*, 1994). The Nullarbor reached its present aridity ~1 m.y.a (WEBB AND JAMES, 2006) and the presence of evaporates in its cave systems indicates this aridity has been a stable climatic feature throughout

the Pleistocene (GOEDE *ET AL.*, 1992). Palynology and cave excavation also indicate that a period of prolonged aridity existed between 20 ka – 10 ka, at the end of the last ice age (MARTIN, 1973). Aridity has been a constant feature of this region, making the Nullarbor Plain one of the most homogenous terrains on the planet. Very few microbial studies have been done on the Nullarbor; although distally related research includes the ecology of cryptogammic crusts from the region (ELDRIDGE AND GREENE, 1994; ELDRIDGE, 1998). Research more relevant to molecular studies includes analysis of novel chemolithoautotrophic microbial communities inside cave environments deep under the Nullarbor Plain (HOLMES *ET AL.*, 2001; TETU *ET AL.*, 2013). The microbial ecology of the Nullarbor topsoil remains unknown; however, microbial ecology studies of soils from other desert regions in Australia, such as the Sturt National Park, New South Wales, have been conducted using the 16S rRNA gene marker (HOLMES *ET AL.*, 2000). Holmes et al. (2000) found that a novel *Rubrobacter* species (a member of the Actinobacteria) dominated desert soil samples from that region at a relative abundance of 2.6 – 10.2%. Studies from the Atacama Desert have previously shown that Acidobacteria and Proteobacteria are less common in soils from hyperarid regions (NEILSON *ET AL.*, 2012). Although these two phyla are more abundant in forested and pastoral soils (JANSSEN, 2006), the Actinobacteria seem to dominate in arid environments.

One area of research tackling how communities develop over time is that surrounding “pioneer organisms” in fresh volcanic material (ENGLUND, 1976; KELLY *ET AL.*, 2014). The primary goals such studies are to identify the first organisms to colonise lava flows post eruption, and to follow changes in community structure with time (KELLY *ET AL.*, 2010; KELLY *ET AL.*, 2011; KELLY *ET AL.*, 2014). Cooled lava flows represent sterile environments with which to test colonisation hypotheses; however, new lavas commonly overprint past eruptive successions. Thus, given sufficient time, the pioneering communities of successive lavas (whilst initially different from those of past successions due to localised heterogeneities in the soil (KELLY *ET AL.*, 2014)) will eventually increase their community diversity until the populations begin to look similar to the microbial populations of previous units. This process has also been observed in arctic soils (SCHÜTTE *ET AL.*, 2010). Such studies raise the following questions about the role of a substrate in controlling the composition of its microbial community: (A) Is the endolithic microbial community controlled by the substrate (i.e., does the rock itself provide an environmental/nutritional advantage or does a level of ‘plasticity’ in microbial communities shape bulk rock environments into distinct microenvironments (Los Ríos *ET AL.*, 2003)?). (B) Is it inevitable that

all rocks, independent of their elemental and mineralogical composition, converge on an ecological community ‘fingerprint’ characterised by an increase in species richness and structure over time within a given region? The latter case has been seen in Icelandic lava fields (KELLY *ET AL.*, 2014). It is difficult to answer these questions in settings, such as lava flows, that produce sterile rocks of homogeneous composition. However, the introduction of sterile rocks into a non-sterile and petrologically different setting could be used to examine whether community structure is controlled by substrate composition or by stochastic processes. Ideally, such an experiment could be conducted over a long period of time (i.e., centuries to tens of millennia).

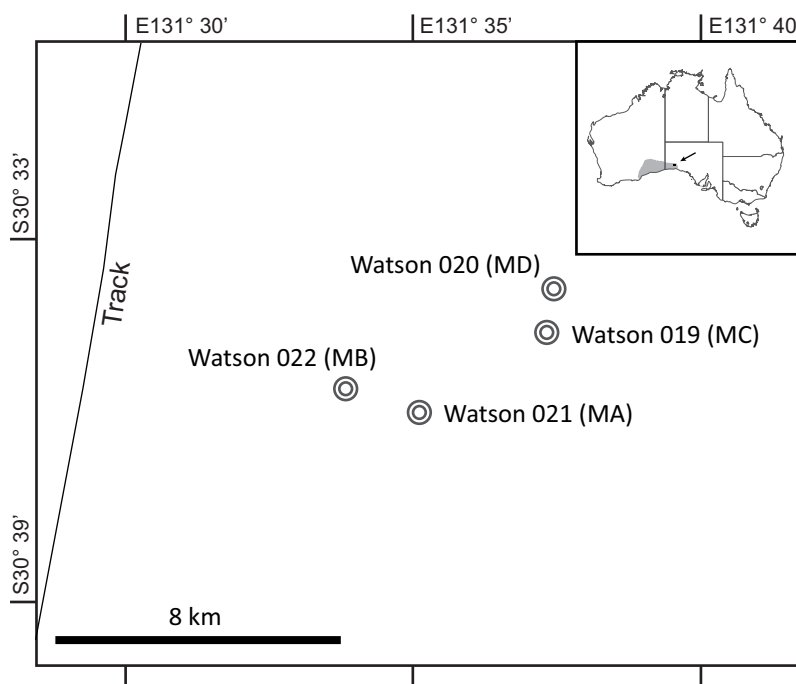


Figure 4.1 | Nullarbor Plain Map. This figure shows the Watson location in the Nullarbor Plain, Australia. Circles indicate the locations from which the four meteorites and associated soils were collected.

Here, we employ chondritic meteorites that have fallen to the limestone Nullarbor Plain over the past ~35 ka (JULL *ET AL.*, 2010) to test these ideas. Chondritic meteorites are sterile owing to their formation in the proto-planetary disk before the accretion of Earth (MINSTER AND ALLÈGRE, 1979; BENNETT AND MCSWEEN, 2012). Meteoroids enter Earth's

atmosphere at speeds of 11.2 – 72.8 km s⁻¹ (CEPLECHA *ET AL.*, 1998), compressing atmospheric gasses to

produce a plasma that oblates the meteoroids to produce a ~1-mm thick layer of molten silicate glass called a ‘fusion crust’. This process is often preceded or followed by meteoroids experiencing one or more high-energy air blasts (BROWN *ET AL.*, 2013). Such conditions should destroy any microorganisms encountered in Earth's upper atmosphere and render the meteorites sterile. During ‘dark flight’, in which bolide fragments fall at terminal velocity (>400 km hr⁻¹) through the troposphere, they may encounter atmospheric microorganisms. However, fallen meteorites continually interact with troposphere, which is the lowest layer of Earth's atmosphere. Thus, atmospheric contamination of a meteorite during its fall to Earth is unlikely to have a significant effect on community development.

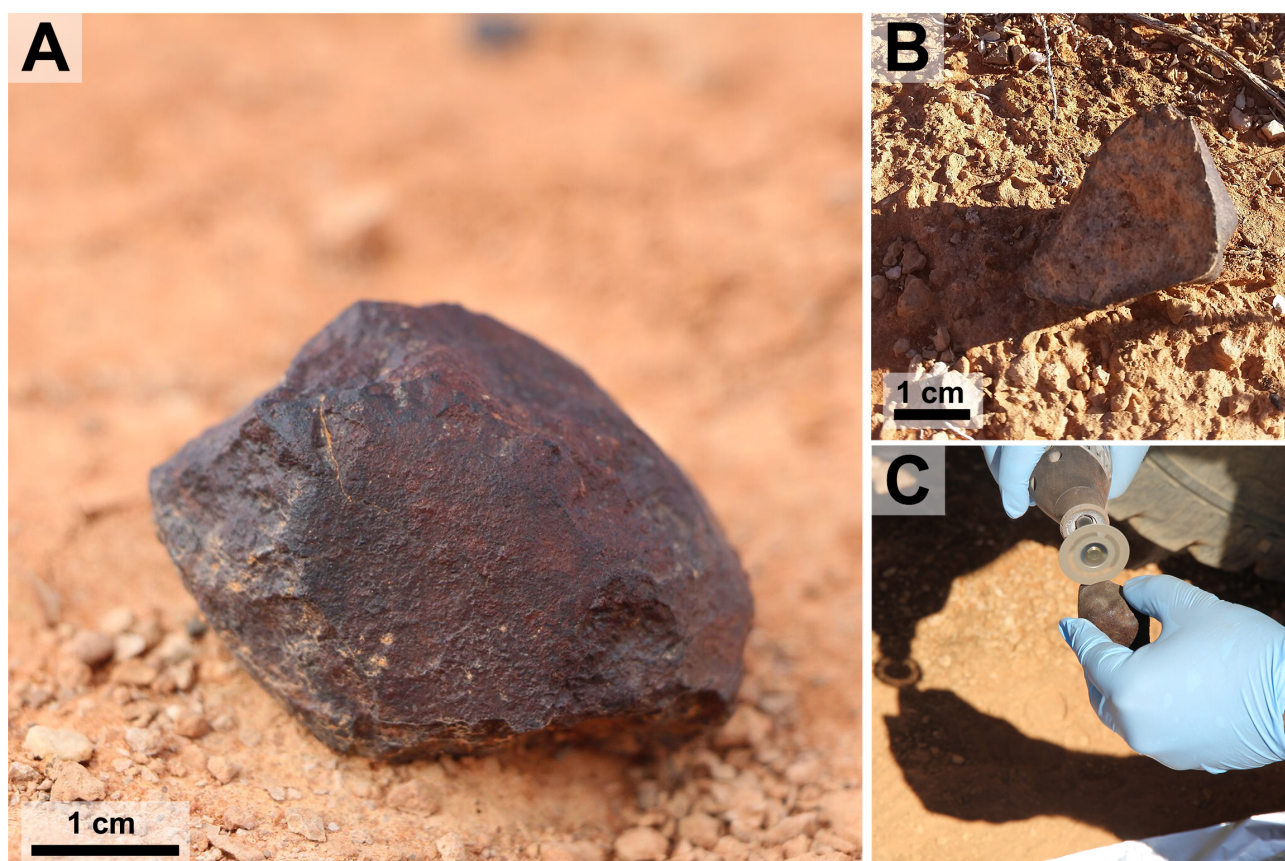


Figure 4.2 | Meteorite Samples This figure shows two meteorites used in the experiment and depicts field-based sub-sectioning methods. (a) Sample *Watson 021* in situ. (b) Sample *Watson 019* in situ after being flipped over during collection. (c) Sample *Watson 019* being sub-sectioned over autoclaved aluminium foil.

Chondrites are also mafic to ultramafic in composition, which provides a contrast in composition relative to the more common continental lithologies at Earth's surface. Chondritic meteorites are similar in elemental and mineralogical composition to mafic rocks on Earth [e.g., they contain olivine $[(\text{Mg},\text{Fe})_2\text{SiO}_4]$, plagioclase $[(\text{Na},\text{Ca})(\text{Si},\text{Al})_4\text{O}_8]$, and enstatite $[\text{Mg}_2\text{Si}_2\text{O}_6]$ (DUNN *ET AL.*, 2010)]; thus, results of first coloniser studies on chondrites can be directly compared to previous results from volcanic settings.

Lastly, meteorites contain troilite $[\text{FeS}]$ and FeNi alloys $[\text{Fe}_{1-x}\text{Ni}_x]$ that can be used as electron donors by iron and sulfur oxidising organisms (e.g., *Acidithiobacillus ferrooxidans*). This provides a suitable contrast to the fossiliferous limestone of the Nullarbor Plain, which predominantly contains calcite $[\text{CaCO}_3]$ and quartz $[\text{SiO}_2]$ (WEBB AND JAMES, 2006). In this study, 16S rRNA gene analysis was used to assess which of the microorganisms that have adapted to soils over the Nullarbor limestone can colonise chondrites. By examining the bacterial and archaeal populations within Nullarbor Plain soil and meteorites overlaying this soil, we shed new light on whether the structure of microbial communities in meteorites is determined by geochemical and niche factors (i.e., the composition

Table 4.1 | Sample List and Alpha Diversity

Sample Name	Group ID	Type	Shock	Weathering	Nseqs	Sobs*	Coverage*	Chao*,#	Inv. Simpson*,#	Shannon*
Watson 021	MA	H6	S4	W4	34871	2051 (N/A)	0.9704 (N/A)	3961 (N/A)	22.77 (N/A)	4.734 (N/A)
Watson 022	MB	L6	S4	W2	49758	2181 (19)	0.9626 (0.0006)	4935 (177)	23.7 (0.19)	4.592 (0.007)
Watson 019	MC	H6	S3	W1	62811	2702 (23)	0.9631 (0.0007)	5233 (177)	29.36 (0.34)	5.390 (0.009)
Watson 020	MD	L5	S2	W1	55066	8955 (46)	0.8044 (0.0015)	33057 (837)	57.28 (0.77)	6.747 (0.010)
Soil (Watson 021)	SA	Soil	-	-	-	-	-	-	-	-
Soil (Watson 022)	SB	Soil	-	-	38159	3144 (12)	0.9441 (0.0004)	7699 (156)	24.75 (0.10)	4.915 (0.004)
Soil (Watson 019)	SC	Soil	-	-	57753	12845 (54)	0.6973 (0.0017)	68819 (1679)	101.91 (1.66)	7.616 (0.010)
Soil (Watson 020)	SD	Soil	-	-	60281	15272 (57)	0.6316 (0.0018)	88505 (2075)	342.71 (5.45)	8.190 (0.009)

* Samples were subsampled to the library size of MA, which had the lowest numbers of sequences 34,871

Students t-test was conducted between the meteorite and the soil substrates on Inv. Simpson with a $p = >0.05$ for both. Standard deviations are given in brackets

and properties of the meteorites themselves) or by broader environmental factors operating in the Nullarbor Plain.

4.2 Methods

4.2.1 Field Sampling

Samples of meteorites and soil were collected on two consecutive days in 2015 during Monash University's annual expedition to the Nullarbor Plain. All meteorites, soil samples and thin sections are curated in the collection of the School of Earth, Atmosphere and Environment at Monash University. A total of four meteorites and associated soils were collected from two search locations that are ~8 km apart within the Nullarbor Plain, Australia (*Figure 4.1*). The two meteorites found at each search location (roughly ~1.4 km apart in both cases) were collected aseptically for microbial community/diversity analysis. The soil from directly beneath each meteorite was also collected in this manner. The properties of topsoil varied significantly between sample sites. Soils adjacent to meteorites were characterised by either (1) cryptogammic surfaces (ELDRIDGE AND GREENE, 1994) or (2) deflationary gibber surfaces, which are soils covered in a pavement of limestone pebbles and the occasional meteorite. Sampling cryptogammic surfaces would have artificially inflated the representation of prokaryotes associated with lichens in soil samples, where as sampling gibber surfaces would have artificially underrepresented the number of phototrophs and xerophiles. Ultimately, soil samples were collected from beneath the meteorites to create a uniform sampling method, although this may have resulted in underrepresentation of xerophiles and phototrophs compared to other soils in the region.

A sterile 10 mL centrifuge tube was used to collect a short push-core from the upper ~2 cm of the soil directly underneath each meteorite. We anticipated that soils collected from beneath meteorites would provide an analogue to the environmental conditions inside meteorites (i.e., low light flux and low evaporation). The meteorites were sub-sectioned in the field using a diamond-embedded dermal saw that was washed in 70% ethanol and an effort was made to avoid sectioning meteorite surfaces covered in soil (*Figure 4.2 C*). Sub-sectioning was done to expose cryptoendolithic and chasmoendolithic microbial communities while minimizing post-collection contamination. Any contaminant minerals or microorganisms introduced during processing in the field would most likely be indigenous to the Nullarbor Plain. Meteorites were handled as little as possible using nitrile gloves washed in 70% ethanol and the sub-sectioned meteorites were cut over autoclaved aluminium foil and deposited in sterile 50 mL centrifuge tubes that were sealed with paraffin film. Centrifuge tubes containing soil samples were also sealed with paraffin film. Both the meteorite and the soil samples were snap frozen in the field using a liquid-nitrogen dry shipper and transported frozen to the laboratory where they were stored at -20° C before DNA extraction.

4.2.2 Meteorite Sample Description

Meteorites were classified according to the rubric of Van Schmus and Wood (1967). Shock classifications were determined using Stoffler et al. (1991) and weathering classifications were obtained using the rubric outlined in Wlotzka (1993).

Watson 019 is a fragment of a L6 ordinary chondrite weighing 83 g. This single stone was found ‘face down’ with a fully intact fusion crust only on the side that did not face the ground (*Figure 4.2 B, C*). The sample is relatively unweathered, exhibiting a (W1) weathering profile, and shows signs of moderate shock including cross cutting melt veins (S3). *Watson 020* is a L5 ordinary chondrite that was found in three fragments, with a total mass of 134 g, over an area of ~20 m². The fragments were relatively fresh, showing a W1 weathering profile but minimal remaining fusion crust. *Watson 020* fragments have light shock textures (S2). The fragment chosen from *Watson 020* for 16S rRNA gene analysis contains a large vein of alteration minerals that cross cuts the sample. *Watson 021* is a single H7 ordinary chondrite, weighing 135 g (*Figure 4.2 A*). The sample has a large crack, lined with alteration minerals, that runs down its middle and only one third of its fusion crust remains intact. This meteorite shows near complete oxidation of its reduced metal and sulfide phases making this a

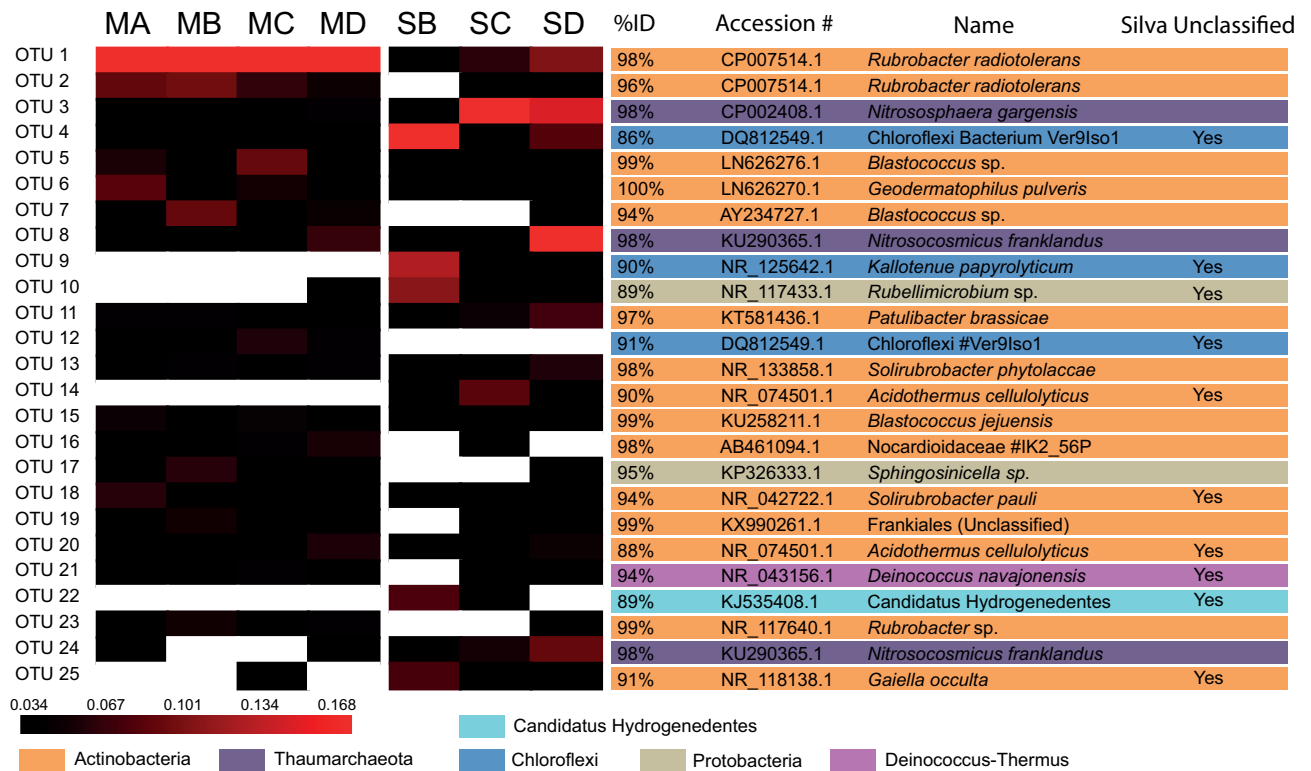


Figure 4.3 | Heatmap of OTU Abundance. Heatmap analysis of OTU abundance in meteorites and soil samples. Analysis performed for OTUs at a distance of ≤ 0.03 . The scale bar represents the fractional abundance of each OTU within each sample. The identity score, accession number, and the name of the nearest named isolate according to NCBI BLAST are indicated on the righthand side of the heatmap. OTUs that were classified no deeper than bacteria in the Silva database are also noted.

W4 chondrite. *Watson 021* is extensively shocked (S4), exhibiting globular silicate metal emulsions and shock veins that crosscut the sample. *Watson 022* is a single, 11.1-g oriented L6 ordinary chondrite. This sample shows extensive silicate/metal emulsions and crosscutting silicate veins indicating extensive shock (S4). The metal and troilite have experienced light weathering (W2).

The meteorite names used above are provisional, and subject to change. Meteorite classifications have been sent to the Meteoritic Bulletin and they await official naming and cataloguing. All samples of meteorites and soils described in this study have been given a two-character sample ID for ease of reference throughout this manuscript. Meteorites are given the prefix ‘M’, whereas soils are given the prefix ‘S’ (see *Table 4.1* for naming details).

4.2.3 DNA extraction and sequencing

DNA was extracted from the meteorite sub-sections and soil samples using a bead-beating cetyltrimethylammonium bromide (CTAB) based method coupled with column-based purification

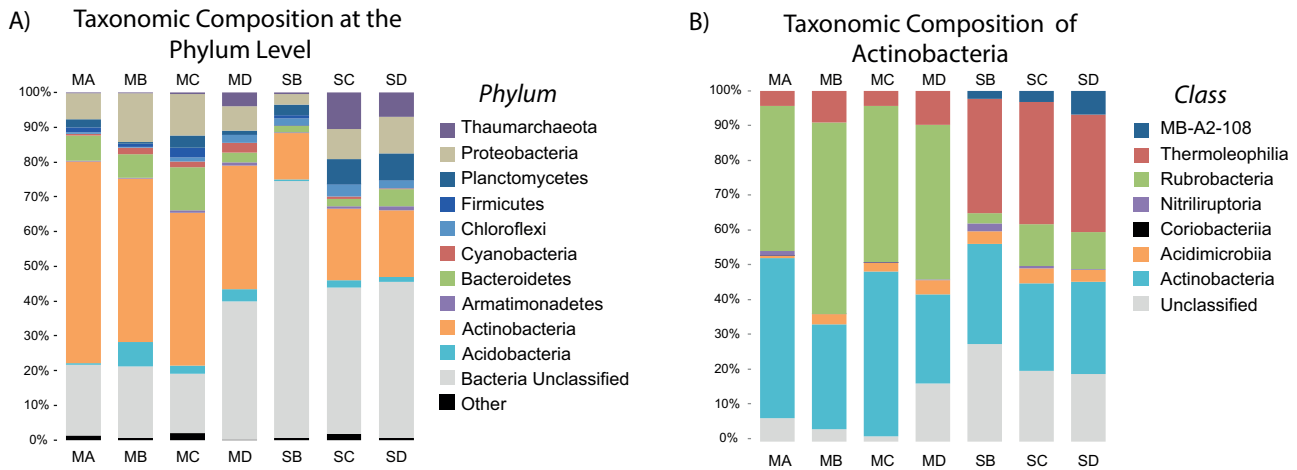


Figure 4.4 | Phyla and Actinobacteria Abundance of Meteorites and Soil This figure shows the relative abundance of different phyla and classes. **(a)** The major phyla classified according to the Silva taxonomy identification. ‘Other’ phyla include all phyla present at abundances less than 3%. ‘Bacteria Unclassified’ were OTUs that could not be classified below the domain Bacteria. **(b)** Taxonomic composition of the important soil phylum, Actinobacteria.

of nucleic acids using a PowerSoil® DNA isolation kit (MO BIO Laboratories Inc., Carlsbad, CA, USA) as per the manufacturer’s protocols (GAGEN *ET AL.*, 2010; GAGEN *ET AL.*, 2013). Less than 20 ng of DNA extracted from each sample was used as a template in a 50 µL PCR reaction to amplify the V6-V8 region of the 16S rRNA gene using primers 926f and 1392r (ENGELBREKTSON *ET AL.*, 2010). These primers target the domains Bacteria and Archaea and contain the Illumina specific adapter sequences (adapter sequences in capitals): 926F: 5’-TCGTCGGCAGCGTCAGATGTGTATAAGAGACAGaaactyaaakgaattgacgg-3’ and 1392wR: 5’-GTCTCGTGGGCTCGGGTCTC GTGGGCTCGGAGATGTGTATAAGAGACAGacgggcggtgtgtrc-3’. Libraries were prepared as outlined by Illumina (#15044223 Rev B) except that Q5 Hot Start High-Fidelity polymerase and PCR mastermix were used (New England Biolabs, Ipswich, MA, USA). PCR amplicons were purified using Agencourt AMPure XP beads (Beckman Coulter, Brea, CA, USA). Purified DNA was indexed with unique 8 bp barcodes using the Illumina Nextera XT v2 Index Kit sets A-D (Illumina San Diego, CA, USA) and the same PCR mastermix as previously. Indexed amplicons were pooled together in equimolar concentrations and sequenced on a MiSeq Sequencing System (Illumina) using paired-end sequencing with MiSeq Reagent Kit v3 (600 cycle) (MS-102-3003, Illumina) in accordance with the manufacturer’s protocol at the Australian Centre for Ecogenomics, The University of Queensland. Sequences have been submitted to the National Centre for Biotechnology Information Sequence Read Archive and can be accessed using the accession number SRP100888, or the BioProject number PRJNA377370.

4.2.4 Sequence Processing

Processing of DNA sequence data was done using MOTHUR v1.38.1 (SCHLOSS *ET AL.*, 2009) and only forward reads were used for analysis. Sequences were trimmed based on the quality score using a 'qwindowaverage' of 35, across a sliding window of 50, after which the PCR primer was removed.

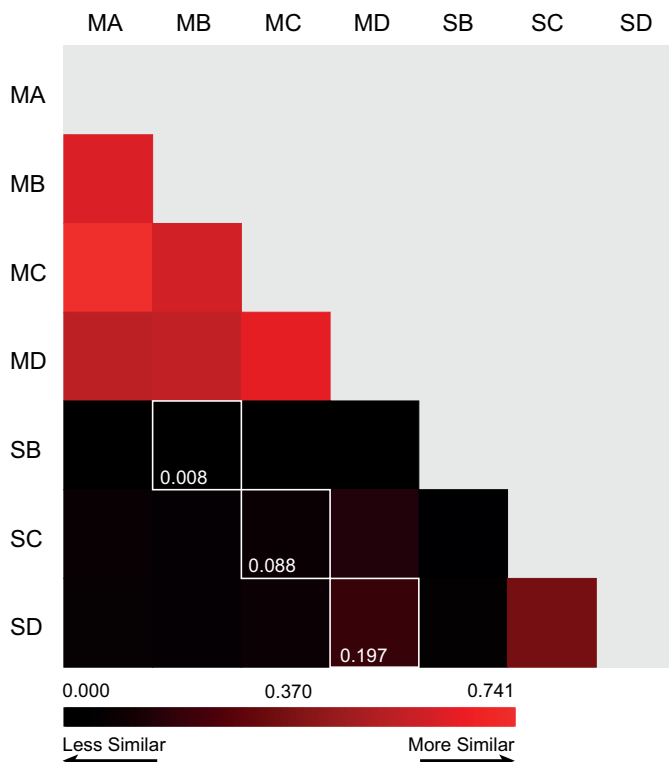


Figure 4.5 | Community Structure Dissimilarity. This calculation was made using Yue and Clayton (2005) indices at a clustering distance of ≤ 0.03 . The colours are scaled to the highest level of similarity between any two samples (red) and the lowest level of similarity (black). The white outline represents the direct comparison between the meteorite and its underlying soil.

Sequences were trimmed to 250 nt and any sequences shorter than 250 nt, or containing ambiguous bases and/or homopolymers in excess of 8 nt were also cut. Further sequence analysis was done as per Kozich et al. (2013), accessed online October 2016. The Silva reference database v123 (Quast et al., 2013) was used for taxonomic classification and alignment of sequences. Putative chimera were determined using UCHIME (EDGAR *ET AL.*, 2011) in MOTHUR (SCHLOSS *ET AL.*, 2009) and the Silva Gold reference database v123 (QUAST *ET AL.*, 2013) and were removed from further analysis. Anomalous taxa including Eukaryota, unknown classification, mitochondria, and chloroplasts, were also removed from the dataset. Sequences were clustered into OTUs (Operational Taxonomic Units) at a distance of ≤ 0.03 .

4.2.5 Sequence Analysis

Representative sequences from the most abundant 25 OTUs (Figure 4.3) were compared to publicly available sequences using Basic Logical Alignment Search Tool (BLAST) at the National Centre for Biotechnology Information (NCBI) excluding uncultured and environmental organisms. After 25 OTUs there were no abundant OTUs of interest, thus for the sake of brevity only the most abundant OTUs are discussed in detail. The dataset was subsampled 1000 times to the size of the smallest library

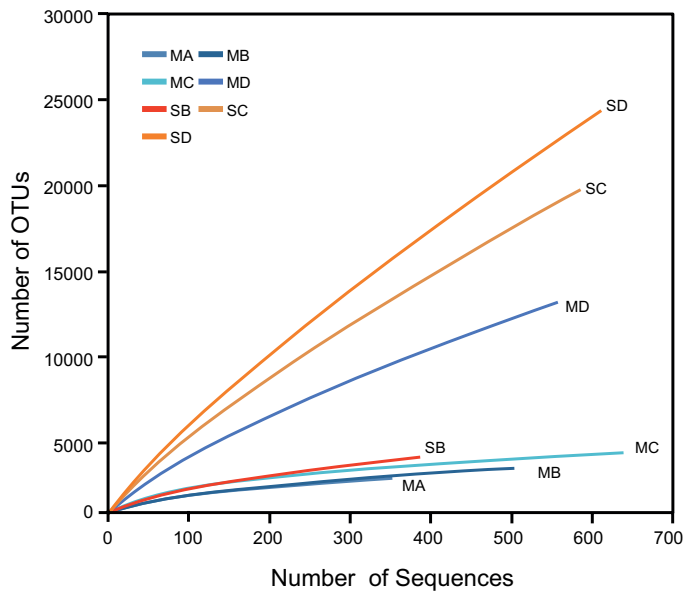


Figure 4.6 | Rarefaction Curve. Rarefaction analysis of all samples at a clustering distance of ≤ 0.03 . Warm colours are soil samples, cool colours are meteorites.

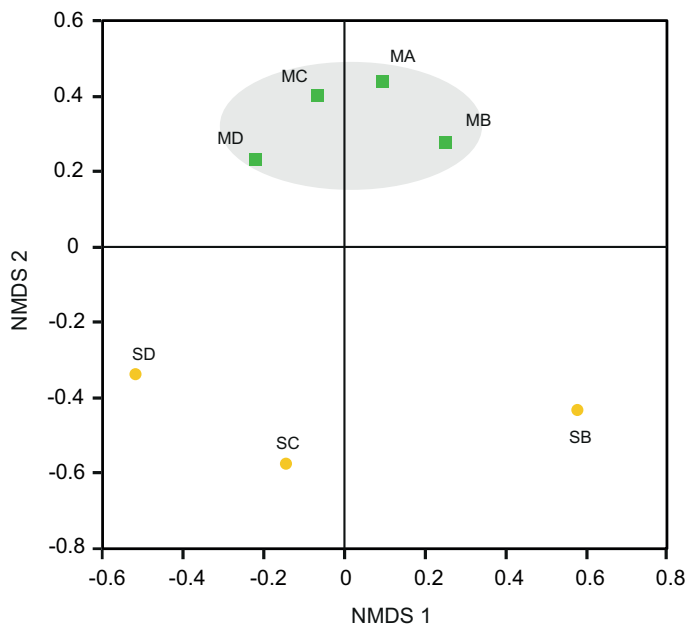


Figure 4.7 | Non-metric Multidimensional Scaling. NMDS plot for Nullarbor meteorite (MA, MB, MC, MD) and soil (SB, SC SD) samples based on the Yue and Clayton (2005) community structure. The stress value is 0.146 (a measure of fitness < 0.2 is considered good (LEVSHINA, 2015)).

to normalise the data before analysis (https://www.mothur.org/wiki/MiSeq_SOP, accessed online November 2016) (VAN HORN *ET AL.*, 2016; JIANG AND TAKACS-VESBACH, 2017). Further alpha and beta diversity analysis was conducted using MOTHUR (SCHLOSS *ET AL.*, 2009) as per the method in Kozich et al. (2013). Additional multivariate data analysis was conducted between the meteorite and soil substrates using Analysis of Molecular Variance (AMOVA) and Non-metric Multidimensional Scaling (NMDS) (EXCOFFIER *ET AL.*, 1992) in MOTHUR. Indicator species analysis was conducted using Linear Discriminant Analysis Effect Size (LEfSe) analysis (SEGATA *ET AL.*, 2011) to determine which OTUs correlated with which sample class. Student's t-test was used to correlate phylum and class OTU populations between the meteorites and the soil. Lastly, Silva classifications were searched for metal/sulfur cycling affiliated organisms.

4.3 Results

4.3.1 Major OTU Classification

DNA was recovered from all samples except for one of the soils, SA. Of the top 25 OTUs in all samples (*Figure 4.3*) only three were identified as Archaea. These were classified as Thaumarchaeota, a phylum that contains all the known Ammonia Oxidising Archaea (AOA) (PESTER *ET AL.*, 2011). These were major OTUs

in the soil samples but present only at low abundance in the meteorite samples (*Figure 4.4*). They demonstrated 98% 16S rRNA gene identity to the known ammonia oxidising Archaea, *Nitrososphaera gargensis* (OTU3) and *Nitrosocosmicus franklandus* (OTU8 and OTU24) (HATZENPICHLER *ET AL.*, 2008; LEHTOVIRTA-MORLEY *ET AL.*, 2016).

The dominant OTU in the meteorite samples (OTU1) demonstrated 98% 16S rRNA gene identity to *Rubrobacter radiotolerans* – #CP007514.1. This organism is an aerobic, heterotrophic thermophile (30° – 55° C) (EGAS *ET AL.*, 2014). We found this OTU to represent 27.3% ± 8.7% of total sequences in the meteorites, whereas it comprised only 1.6% ± 1.1% of the total abundance of sequences in soils. Another dominant OTU, OTU2, was present in all meteorites but was only found at low abundance in two of the soil samples (SC and SD). OTU2 shared 96% 16S rRNA gene identity with *R. radiotolerans*.

The availability of FeNi-alloys and troilite in the meteorites presents an opportunity for biogenic metal/sulfur cycling. As such, we used the Silva classification to search for common genus members that are known to contain species capable of iron or sulphur cycling metabolisms. We searched for: *Acidithiobacillus*, *Anaeromyxobacter*, *Caldivirga*, *Desulfovibrio*, *Gallionella*, *Geobacter*, *Leptospirillum*, *Shewanella*, *Sideroxydans*, *Sphaerotilus*, and *Thiobacillus*. Our search returned members of *Geobacter* (8 non-singleton unique OTUs) and *Desulfovibrio* (13 non-singleton unique OTUs). Out of these OTUs, the most abundant OTU was OTU71. The nearest named isolate to OTU71 was *Geobacter anodireducens* – #CP014963.1 (100% 16S rRNA gene identity across the region sequenced). *G. anodireducens* is able to reduce Fe(III) and sulfur with acetate as the electron donor (SUN *ET AL.*, 2014; SUN *ET AL.*, 2016). The most common *Desulfovibrio* was OTU501. The nearest named isolate to OTU501 shared 100% 16 rRNA gene identity across the region sequenced with *Desulfovibrio desulfuricans* – #KU921226.1, strains of which are known to reduce sulfate (MANGALO *ET AL.*, 2007). Refer to *Appendix: Table 1* for a full list of possible iron/sulfur cycling organisms found in this study. This list is not exhaustive and the 16S rRNA gene analysis is not a functional analysis of possible metabolisms. It is possible that some of the other species may cycle metal or sulfur, but it is outside the ability of this technique to discern.

4.3.2 Alpha Diversity Indices

Rarefaction analysis of 16S rRNA gene libraries clustered at <0.03 indicated that meteorite samples were sequenced with sufficient coverage (i.e., the rarefaction curves reach plateaus), whereas there remained diversity yet to be revealed by further sequencing from the soil samples, except for SB (see Figure 4.6). Good's coverage estimate for the percentage of species represented in a sample was generally higher for the meteorites (80–97%) than for the soils (63–94%) with the exception of SB and MD (see Table 4.1). The Chao species richness estimator predicted a much higher uncovered richness in the soils than the meteorite samples, with the exception of SB (see Table 4.1).

As indicated by the inverse Simpson index and Shannon index, there was generally greater species evenness in the soils than in the meteorites (see Table 4.1). Although species evenness in sample SB was considerably lower than that in the other two soils and sample MD, it showed markedly higher species evenness than the other three meteorite samples.

4.3.3 Beta Diversity

The use of Nonparametric Analysis of Molecular Variance (AMOVA) (EXCOFFIER *ET AL.*, 1992), using the Yue & Clayton (2005) index for community structure between the soils and the meteorite, confirmed that microbial community structure was different between the meteorites and the soils ($p < 0.05$).

The meteorites had community structures that were much more similar to each other, whereas those in the soils displayed more variation amongst themselves (see Figure 4.5). This was confirmed by NMDS analysis (BORG AND GROENEN, 2005), which revealed that the meteorite samples clustered together, away from each of the soil samples, which did not cluster closely to each other (Figure 4.7). We ran a Spearman's rank correlation coefficient analysis to establish which OTUs defined the two NMDS axes. The five major OTUs contributing to separation for axis NMDS 1 were: OTU8 (98% identity to *Nitrosocosmicus franklandus*) $p = 0.018$ for NMDS 1, OTU22 (89% identity to an uncultured *Candidatus Hydrogenedentes*, #KJ535408) $p = 0.021$ for NMDS 1, OTU25 (91% identity to *Gaiellaceae gaiella*) $p = 0.021$ for NMDS 1, OTU10 (89% identity to *Rubellimicrobium sp.*) $p = 0.021$ for NMDS 1, and OTU9 (90% identity to *Kallotenue papyrolyticum*) $p = 0.023$ for NMDS 1. For axis NMDS 2, the top five OTU contributions were: OTU1 (98% identity to *Rubrobacter radiotolerans*) $p = <0.001$ for

NMDS 2, OTU21 (94% identity to *Deinococcus navajonensis*) $p = 0.002$ for NMDS 2, OTU2 (96% identity to *Rubrobacter radiotolerans*) $p = 0.005$ for NMDS 2, OTU24 (98% identity to *Candidatus Nitrosocosmicus franklandus*) $p = 0.018$ for NMDS 2, and OTU18 (94% identity to *Patulibacter sp.*) $p = 0.031$ for NMDS 2. None of the OTUs associated with metal/sulfur cycling genera appeared to have a strong influence on the NMDS separation.

4.3.4 OTU Abundance

Actinobacteria accounted for $44.8\% \pm 9.4\%$ of the total number of identified sequences in the meteorite samples. This was by far the most abundant phylum identified in the meteorites. The next most abundant phyla in the meteorite samples were Proteobacteria ($10.0\% \pm 3.5\%$), Bacteroidetes ($7.6\% \pm 3.9\%$) and Acidobacteria ($3.4\% \pm 2.7\%$), with other phyla representing $<2.0\%$ each. Actinobacteria were dominant in the soils from our study ($17.7\% \pm 3.9\%$), albeit to a lesser extent than in the meteorites, followed by Proteobacteria ($7.4\% \pm 3.9\%$), Planctomycetes ($6.0\% \pm 2.5\%$) and Thaumarchaeota ($5.9\% \pm 5.2\%$), with other phyla present at $<3.0\%$ each.

The soils had a greater average abundance of unclassified bacteria ($53.7\% \pm 17.6\%$) compared to the meteorites ($23.6\% \pm 10.3\%$). BLAST analysis revealed that these “unclassified bacteria” were members of various phyla. Nine of these unclassified bacteria were represented in the most abundant 25 OTUs and overall they had poor identity scores compared to those OTUs that were identified from phylum or better. Two OTUs (OTU25 and OTU18) recorded poor identity scores with both Silva and BLAST. OTU25 was only distantly related (91% 16S rRNA gene identity) to the nearest named isolate, *Gaiella occulta* (ALBUQUERQUE ET AL., 2011), and demonstrated 96% identity to an uncharacterised organism that has been isolated from soil previously (DAVIS ET AL., 2011) and that is referred to as #Ellin7545. OTU18 was also only distantly related (94% 16S rRNA gene identity) to the nearest named isolate, *Solirubrobacter pauli* (FURLONG ET AL., 2002) (Figure 4.3). Different classes within the Actinobacteria are found at greater abundance in the meteorites and soils. Rubrobacteria dominated in the meteorites ($46.2\% \pm 5.8\%$ of the Actinobacteria in meteorites) whereas the class Thermoleophilia were dominant amongst the Actinobacteria in the soils ($33.7\% \pm 1.2\%$) (Figure 4.4 B).

4.3.5 OTU Correlations

Using Students' t-test, we found that the presence of Actinobacteria correlated strongly with the meteorites ($p = 0.005$) and Cyanobacteria were weakly correlated with meteorites as well ($p = 0.068$). The strongly correlated phyla differed in the soils: Planctomycetes ($p = 0.032$) and a weak correlation from Chloroflexi ($p = 0.066$). The phyla that did not correlate well with either meteorites or soil were Armatimonadetes ($p = 0.488$), Firmicutes ($p = 0.245$), Acidobacteria ($p = 0.285$), and Proteobacteria ($p = 0.379$). Rubrobacteria, Thermoleophilia and the candidate class, MB-A2-108, were significantly different between the meteorites and the soils (p values <0.001 , <0.001 , and 0.021 respectively). Rubrobacteria was the dominant class of Actinobacteria in the meteorites, whereas Thermoleophilia and MB-A2-108 were more strongly associated with the soils.

We used Linear Discriminant Analysis Effect Size (LEfSe) analysis to investigate which indicator species were associated with the meteorites or soils (SEGATA *ET AL.*, 2011). We found that most species did not correlate (i.e., $p > 0.05$) with either the soil or the meteorites. This also includes all the OTUs affiliated with metal/sulfur cycling isolates (*Appendix I: Table 1*). However, there were some notable exceptions in the top 25 OTUs used in previous beta diversity analysis. OTU1 and OTU2 (*R. radiotolerans*) correlated to the meteorites ($p = 0.034$), as did OTU5 (*Blastococcus sp.*) $p = 0.034$, OTU6 (*G. pulveris*) $p = 0.034$, OTU12 (*Chloroflexi*) $p = 0.028$, OTU15 (*B. jejuensis*) $p = 0.034$, OTU19 (*Frankiales*) $p = 0.034$, OTU21 (*D. navajonensis*) $p = 0.034$, and OTU23 (*Rubrobacter sp.*) $p = 0.032$. The OTUs associated with the soils were OTU4 (*Chloroflexi*) $p = 0.034$, OTU9 (*K. papyrolyticum*) $p = 0.019$, OTU14 (*A. cellulolyticus*) $p = 0.019$, and OTU25 (*G. gaiella*) $p = 0.028$ (*Appendix I: Table 1*).

4.4 Discussion

4.4.1 Meteorite Colonisation

Alpha diversity analyses (*Table 4.1*) indicate that the meteorites have poor species richness and evenness, suggesting that they have been colonised by a few successful niche organisms. This has also been observed in microbial communities of ignimbrites (a volcanic deposit) in the hyper-arid Atacama desert (WIERZCHOS *ET AL.*, 2013A). It would appear that species richness and structure is small in environments that select for multi-extremophiles. This is important for meteorites as they share many overlapping physical and chemical characteristics with ignimbrites, which likely lend themselves to

the same style of initial colonisation by microorganisms.

When a meteorite becomes a resident of the Nullarbor Plain it is colonised by environmental organisms derived (presumably) from soil as indicated by crossover species in the heat map (*Figure 4.3*). However, the soils have much greater species richness than the meteorites, indicating the microenvironment of the meteorites is unsuitable for some indigenous microbes. Indeed, the rarefaction curves (*Figure 4.6*) indicate that there considerable diversity within the soils that has not been accounted for whereas rarefaction curves for the meteorites generally plateaued.

Our AMOVA results show that, in spite of the presence of crossover species, the microbial community structures in meteorites and soils were significantly different, whereas all of the meteorites shared similar community structures (*Figure 4.5*). We attribute this difference in the soil to the establishment of distinctly different microenvironments within these samples. One caveat is that the soil samples were obtained from directly underneath the meteorites; such samples may have retained more moisture and experienced less environmental stress than soils that were more exposed to the atmosphere, allowing for a greater diversity of epilithic microorganisms. Despite the bias our sampling strategy may have introduced, there was still a large structural variation not only between the meteorites and the soils, but also between each of the soils. Thus, the lower structural variation reflected between the meteorite samples is probably due to chemical and/or physical homogeneity of the meteorites. The communities within soil and meteorite samples may have been similar initially, but are now structural different due to selective pressures (both geochemical and environmental). The meteorites in this study are chemically quite similar (all of our samples are L type ordinary chondrites), but they have quite varied physical characteristics. This would indicate that weathering, shock and even the degree of thermal-metamorphism that chondritic meteorites have undergone have little control on the composition of the microbial communities that inhabit them. Nonetheless, as previously discussed, ordinary chondritic meteorites are elementally and mineralogically quite homogeneous (DUNN *ET AL.*, 2010), which probably explains the low variability in microbial communities in the meteorites compared to Nullarbor soils and previous studies of volcanic rocks (KELLY *ET AL.*, 2010; KELLY *ET AL.*, 2011).

Weathering grade has been calibrated to the residency age of meteorites on the surface of Earth using radiometric dating methods (AL-KATHIRI *ET AL.*, 2005). Importantly, weathering grade and radiometric dates do not always correlate well for Nullarbor meteorites (JULL *ET AL.*, 2010). Thus, the

duration of residency of our four meteorite samples on the Nullarbor Plain, and the length of time available for microbial community structure to develop, cannot be determined from weathering grade alone (although, it would be possible to make reliable estimates in other deserts where weathering grade correlates strongly with residency age). Weathering grade does provide a relative estimate of the amount of oxidative weathering that has occurred in Nullarbor meteorites. However, our findings indicate that the current redox environment of the different meteorites does not result in a significantly different community structure (*Figure 4.5*). Tied intrinsically to the weathering grade of meteorites is their porosity. This porosity provides a range of microhabitats that could cater to microorganisms adapted to a range of different pH conditions (TAIT *ET AL.*, 2017), which could make them good substrates for a variety of microorganisms. However, we did not see any correlation with weathering or shock (two physical traits known to affect porosity). Meteorites are however dark in colour, resulting in a contrast in albedo compared to the white limestone and lightly coloured soil of the Nullarbor Plain, which could change the ambient temperatures of the rock (WIERZCHOS *ET AL.*, 2013B). Such dark meteorites may support the survival of microorganisms in cold environments such as Antarctica, and could play a similar role for putative life in other hostile environments within our solar system, such as at the surface of Mars. However, in the desert on Earth, a dark rock could reach thermally restrictive temperatures for mesophiles. It may be that thermophilic microorganisms, may be exploiting this thermal niche in the meteorite to obtain almost exclusive access to the films of water that form on hygroscopic alteration minerals (TAIT *ET AL.*, 2017). These minerals are the direct product of weathering in meteorites and are not found in abundance within the Nullarbor soil. Given the different weathering and shock grades of the meteorites we expected to see more scatter in the community structure of the meteorites, however this was not observed (*Figure 4.5*). In the absence of clear porosity driven separation in the meteorite community structure, other physical/chemical controls must be taking effect (i.e., hygroscopic mineral production, availability of native copper, fragmentation rate, competition with lichens). We interpret that it is the chemical homogeneity of the meteorites (i.e., they are all L type chondrites) and not their physical characteristics that drives the development of similar community structures for these meteorites.

It is possible that there is a nutritional advantage that causes the development of similar community structures in meteorites. Given the abundance of FeNi-alloys and FeS in these samples, the possibility of metal-cycling organisms was one that we explored. We found OTUs associated with known genera

that cycle iron and sulfur in both the soil and the meteorites. However, none of these OTUs was significantly associated with the meteorites (*Appendix I: Table 1*). The most abundant OTUs with similarity to known iron and sulfur cycling species were OTU71, and OTU501, which were most similar to known iron/sulfur and sulfur reducers, respectively. If the organisms forming these OTUs are indeed capable of iron and/or sulfur reduction, some abiotic oxidation and weathering of the meteorite would be required before these organisms could reduce the oxidized metals and sulfate, as most of the sulfur and iron in the meteorites is initially present in reduced phases (i.e., as Fe^0 , Fe^{2+} , and S^{2-}). These OTUs were not abundant in the libraries, and did not contribute significantly towards separation in the NMDS analysis, suggesting they are not key drivers shaping the community structure.

The iron and sulfur reducing organisms that are most similar to OTU71, and OTU501 are chemoorganotrophs. As such, some consideration should be given to discussing sources of organic carbon that are available to these organisms in the meteorites. The first possibility is that organic carbon is coming from other organisms. Many of the meteorites were found sitting on cryptogammic crusts, making the decay of lichens and associated algae the largest and most likely source of organic carbon accessible to these microorganisms. Indeed, we have found meteorites that are covered lichen in the Nullarbor. The other possibility is that these organisms obtain organic carbon from an exogenic source, such as the meteorite itself. Ordinary chondrites, such as those in this study, contain little organic matter. Given their history of thermal metamorphism, most carbon will have been devolatilised on the parent body or turned to kerogen or graphite. Nonetheless, Polycyclic Aromatic Hydrocarbons (PAH) and amino acids can still be found in small concentrations in ordinary chondrites (ZENOBİ ET AL., 1992).

Contrastingly, carbonaceous chondrites, which were not examined as part of this study, typically have not undergone high degrees of thermal metamorphism. Carbonaceous chondrites contain more organic material than ordinary chondrites; The Murchison CM2 meteorites organic inventory includes 1.45 wt% of macromolecular organic compounds and acetate in concentrations >300 ppm, as well as other organic compounds that could support heterotrophic metabolisms (SEPHTON, 2002). The carbon content of carbonaceous meteorites has been shown to support microorganisms under laboratory conditions (MAUTNER, 1997). Carbonaceous meteorites also contain native Fe(III) phases

(RUBIN, 1997), meaning that some of the metal cycling organisms affiliated with the OTUs found in this study could potentially use the native acetate and Fe(III) phases found within carbonaceous meteorites. Moreover, they would have no need for input of terrestrial organic matter nor would they have to wait for the meteorite to start weathering for Fe(III) to become available.

4.4.2 Comparison to Other Soils

The microbial communities in Nullarbor soil samples differ from those commonly found in pastoral and forested soils, which are dominated by Proteobacteria and Acidobacteria, with Actinobacteria being the third most abundant phylum (JANSSEN, 2006). The Nullarbor soils are instead dominated by Actinobacteria, which is consistent with previous observations from Australian arid deserts (HOLMES *ET AL.*, 2000), the arid Tataouine Desert (Tunisia) (CHANAL *ET AL.*, 2006), and the hyper-arid Atacama Desert (Chile) (NEILSON *ET AL.*, 2012). The dominant OTU and key indicator species in all four meteorites demonstrated 98% 16S rRNA gene identity with *R. radiotolerans*. The parent genus, *Rubrobacter*, has previously been reported to comprise 2.6% – 10.2% of the OTU abundance in soil samples from within the arid desert of the Sturt National Park, New South Wales (HOLMES *ET AL.*, 2000). The two major OTUs in the meteorites, OTU1 and OTU2, were most similar to *R. radiotolerans* indicating species level diversity within the *Rubrobacter* exists in the Nullarbor soil samples, as has been previously identified in Sturt National Park (HOLMES *ET AL.*, 2000). *R. radiotolerans* is a “multi-extremophile”, which can survive at high temperature and high UV, and endure radiation damage (EGAS *ET AL.*, 2014). Ordinary chondritic meteorites are significantly more depleted in radioactive elements, such as Th and U, than most crustal rocks on Earth (SHINOTSUKA AND EBIHARA, 1997). It is unlikely that *R. radiotolerans* is present in Nullarbor soils and meteorites because there is a source of ionizing radiation in the meteorites. A more likely explanation is that this radiation resistance is a fortunate side effect of DNA repair strategies associated with adaptation to desiccation and/or oxidative stress (EGAS *ET AL.*, 2014) in arid environments like the Nullarbor Plain.

Without functional gene analysis, we cannot tell with certainty whether OTU1 and OTU2 (which share 98% and 96% rRNA 16S gene identity respectively to *R. radiotolerans*) indeed have these traits. Such adaptations would be beneficial in the semi-arid and desiccating conditions of the Nullarbor Plain and the arid interior of Australia. The similarity between the communities from Sturt National Park and the Nullarbor Plain may be due to aeolian processes (i.e., dust storms) that are known to

transport microbial flora across Australia (DE DECKKER *ET AL.*, 2014).

A key identifier species (i.e, OTU8 and OTU24) in the soil samples were most closely related to a known AOA, *Nitrosocosmicus franklandus*, and it is possible that these and other Thaumarchaeota identified in the Nullarbor soil samples are ammonia oxidisers, given that AOAs are common in that phylum (PESTER *ET AL.*, 2011). Thus, they may play an important role in nitrogen cycling in the Nullarbor soils. Few OTUs closely related to known Ammonia Oxidising Bacteria (AOB) (e.g., Beta- and Gammaproteobacteria) (PURKHOLD *ET AL.*, 2000; PESTER *ET AL.*, 2011) were identified in this study. Also, a large proportion of the sequences from the soil samples were not closely related to any currently cultured species (e.g., the top 5 OTUs in soil sample SB were < 90% similar to any cultured species); thus, there remains much to be uncovered about Nullarbor soil microbial communities in the future. A note worth considering is that the soils sampled were directly beneath the meteorites and may not be representative of Nullarbor soil in the open. The meteorites shield the underlying soil from sunlight and serve as moisture traps; this may have led to a bias towards hypolithic organisms resulting in fewer sampled phototrophs or xerophilic organisms due to this microenvironmental difference. The meteorites we sampled were also small, and of similar size to cobbles found on the deflationary gibber surface of the Nullarbor Plain, which suggests that hypolithic organisms should already be common in these soil samples. However, the deeper nature of the cored soil profile (~2 cm) should mask any variation in microhabitat and reduce bias toward sampling hypolithic organisms.

4.4.3 Comparison to Volcanic Rocks

We found similar abundances of Actinobacteria in meteorites collected from the Nullarbor Plain to those previously reported by other workers during studies of volcanic (basaltic) glasses (KELLY *ET AL.*, 2010). Kelly et al. (2010) found that 43% of the sequences in basaltic glasses from Iceland were Actinobacteria followed by lesser abundances of Proteobacteria, Acidobacteria and Cyanobacteria. They attributed colonisation of basaltic glass to the liberation of bioessential elements (e.g., Fe, Mg, Ca) during weathering, which is rapid for basaltic glasses. This could create a nutritional advantage for certain organisms able to capitalise on the liberation of these cations. Meteorites commonly have a similar glassy coating called a 'fusion crust'. This crust is formed during ablative melting of the major silicate, sulfide and metal alloy minerals in meteors as they enter Earth's atmosphere. The melt quenches to form a silicate glass that is rich in Mn, K, Na and Al, with some Fe and Cr (GENGE AND

GRADY, 1999). Fusion crusts are weathered quickly due to their high reactivity with the atmosphere, surface and meteoric waters. As with basaltic glasses, oxidative weathering and reaction with carbonic acid in rain water combine to mobilise the elements needed to produce hygroscopic alteration minerals (e.g., carbonates, sulfates, Fe-(oxy)hydroxides and smectites) (TAIT *ET AL.*, 2017). Microbes that inhabit meteorites have been found just millimetres underneath fusion crusts in association with these alteration minerals (TAIT *ET AL.*, 2017) indicating that a similar process may be occurring in meteorites as has been observed in volcanic rocks in Iceland.

We did not find any significant trends between microbial ecology and the physical characteristics of meteorites (e.g., shock, weathering grade). Indeed all meteorites in this study were of the same chemical class of meteorite (i.e., they are L type ordinary chondrites) and come from the same parent body. It is not possible to distinguish between classes of ordinary chondrite (e.g., H, L, LL) by visual inspection in the field; thus, a higher number of samples may be needed to elucidate whether different microbial communities might colonize H or LL ordinary chondrites.

Understanding the chemical and physical properties of meteorites is important as they control the amount of porosity in the meteorite at any one time; porosity provides an upper limit for the amount of biomass in an endolithic community (PONTEFRACT *ET AL.*, 2016). Meteorites have variable amounts of porosity, which is retained from primary accretion of the parent body and modified by later impacts between asteroids (WILKISON *ET AL.*, 2003). Although the amount of porosity in ordinary chondrites has no observed correlation with shock, there is large scatter in the data that may hide such a trend (WILKISON *ET AL.*, 2003). In carbonaceous meteorites, the availability of primary porosity is inversely related to the amount of shock a meteorite has experienced (TAIT *ET AL.*, 2016). The opposite is true of impact basins on Earth, where crack networks from impacts are known to promote microbial diversity (PONTEFRACT *ET AL.*, 2016). Impacts do not adversely affect the bioavailability of elemental nutrients to microbial communities in shocked rocks on Earth (PONTEFRACT *ET AL.*, 2012). Given that similar impact process operated on meteorite parent bodies, it is likely that bioavailability of elemental nutrients will be similarly unaffected in meteorites. Mineral weathering is another important factor that will control microbial colonisation of meteorites. For instance, reaction-driven cracking during precipitation of secondary minerals can increase porosity and permeability within meteorites. Contrastingly, internal porosity can also be filled by the oxidative weathering products of troilite and

FeNi alloys (BLAND *ET AL.*, 2006), which may limit colonisation of pore spaces (TAIT *ET AL.*, 2017). It is worth noting that Actinobacteria was also the dominant microbial phylum in a study of shocked terrestrial rock found in impact basins on Earth (PONTEFRACT *ET AL.*, 2016), implying this phylum may have members that excel in endolithic microenvironments.

4.5 Conclusions

This study has found that microbial communities in samples of Nullarbor Plain soil are more diverse than those in meteorites, which are highly uniform in their species evenness and species richness despite having been found several kilometres apart and on soils with different microbial communities. Moreover, all meteorites were dominated by a single OTU classified as a member of the Actinobacteria, affiliating with *Rubrobacter radiotolerans*. The meteorites in this study are chemically similar L chondrites, but they have varied shock, weathering and thermal metamorphic histories. We could not discern, based on the small number of samples studied, whether these factors might contribute to development of different microbial populations. We did find OTUs affiliating with known iron and sulfur reducing genera, *Geobacter* and *Desulfovibrio*, but these were present in low abundance and did not contribute significantly to differences in community structure between meteorites and soils. Nonetheless, these organisms could potentially play a role in meteorite weathering. The chemical composition, and possibly the albedo of the meteorites, seems more likely to control community structure than the subtleties of their histories. This study has shown that microbes can exploit rock types and environments that are different from the soils that host parent communities. Specifically, once a community has taken hold in the new substrate, its structure will tend to reflect the environmental and chemical forcing of that habitat, rather than retain the structure of the parent soil community. This has consequences for any future sample return of exogenic meteorites from Mars as proposed by Tait et al. (2017). If meteorites returned from Mars were to contain evidence of a past putative biosphere, it could be that putative microorganisms in meteorites might not be indicative of the true complexity of the immediate environment.

4.6 Chapter 4 References

A

- Al-Kathiri, A., Hofmann, B.A., Jull, A.J.T., and Gnos, E. (2005). Weathering of meteorites from Oman: Correlation of chemical and mineralogical weathering proxies with ^{14}C terrestrial ages and the influence of soil chemistry. *Meteoritics & Planetary Science*, 40(8) 1215-1239.
- Albuquerque, L., França, L., Rainey, F.A., Schumann, P., Nobre, M.F., and da Costa, M.S. (2011). *Gaiella occulta* gen. nov., sp. nov., a novel representative of a deep branching phylogenetic lineage within the class Actinobacteria and proposal of Gaiellaceae fam. nov. and Gaiellales ord. nov. *Systematic and Applied Microbiology*, 34(8): 595-599.
- Australian Bureau of Meteorology (2015) Cook Weather station - 018110, (Years 1920-2010).

B

- Bennett III M. E., and McSween Jr H. Y. (2012) Revised model calculations for the thermal histories of ordinary chondrite parent bodies. *Meteoritics & Planetary Science*, 31: 783-792.
- Bland P. A., Zolensky M. E., Benedix G. K., and Sephton M. A. (2006) Weathering of chondritic meteorites. In: *Meteorites and the Early Solar System II*. edited by DS Lauretta and HY McSween, *University of Arizona Press*, Tucson, pp 943.
- Borg I., and Groenen P. (2005) *Modern Multidimensional Scaling: Theory and Applications*. Springer-Verlag, New York.
- Brown P. G., Assink J. D., Astiz L., Blaauw R., Boslough M. B., Borovička J., Brachet N., Brown D., Campbell-Brown M., Ceranna L. and others. (2013) A 500-kiloton airburst over Chelyabinsk and an enhanced hazard from small impactors. *Nature*, 503: 238-241.

C

- Cepilecha Z., Borovička J., Elford W. G., ReVelle D. O., Hawkes R. L., Porubčan V., and Šimek M. (1998) Meteor Phenomena and Bodies. *Space Science Reviews*, 84: 327-471.
- Chanal A., Chapon V., Benzerara K., Barakat M., Christen R., Achouak W., Barras F., and Heulin T. (2006) The desert of Tataouine: an extreme environment that hosts a wide diversity of microorganisms and radiotolerant bacteria. *Environmental Microbiology*, 8: 514-525.

D

- Davis K. E. R., Sangwan P., and Janssen P. H. (2011) Acidobacteria, Rubrobacteridae and Chloroflexi are abundant among very slow-growing and mini-colony-forming soil bacteria. *Environmental Microbiology*, 13: 798-805.

- De Deckker P., Munday C. I., Brocks J., O’Loingsigh T., Allison G. E., Hope J., Norman M., Stuut J.-B. W., Tapper N. J., and van der Kaars S. (2014) Characterisation of the major dust storm that traversed over eastern Australia in September 2009; a multidisciplinary approach. *Aeolian Research*, 15: 133-149.
- Dunn T. L., Cressey G., McSween Jr H. Y., and McCoy T. J. (2010) Analysis of ordinary chondrites using powder X-ray diffraction: 1. Modal mineral abundances. *Meteoritics & Planetary Science*, 45: 123-134.

E

- Edgar R. C., Haas B. J., Clemente J. C., Quince C., and Knight R. (2011) UCHIME improves sensitivity and speed of chimera detection. *Bioinformatics*, 27: 2194-2200.
- Egas C., Barroso C., Froufe H. J. C., Pacheco J., Albuquerque L., and da Costa M. S. (2014) Complete genome sequence of the Radiation-Resistant bacterium *Rubrobacter radiotolerans* RSPS-4. *Standards in Genomic Sciences*, 9: 1062-1075.
- Eldridge D. J. (1998) Soil crust lichens and mosses on calcretedominant soils at Maralinga in arid South Australia. *Journal of the Adelaide Botanic Garden*, 18: 9-24.
- Eldridge D. J., and Greene R. S. B. (1994) Microbiotic soil crusts - a review of their roles in soil and ecological processes in the rangelands of Australia. *Soil Research*, 32: 389-415.
- Engelbrektson A., Kunin V., Wrighton K. C., Zvenigorodsky N., Chen F., Ochman H., and Hugenholtz P. (2010) Experimental factors affecting PCR-based estimates of microbial species richness and evenness. *The ISME journal*, 4: 642-647.
- Englund B. (1976) Nitrogen Fixation by Free-Living Microorganisms on the Lava Field of Heimaey, Iceland. *Oikos*, 27: 428.
- Excoffier L., Smouse P. E., and Quattro J. M. (1992) Analysis of molecular variance inferred from metric distances among DNA haplotypes: application to human mitochondrial DNA restriction data. *Genetics*, 131: 479-491.

F

- Furlong M. A., Singleton D. R., Coleman D. C., and Whitman W. B. (2002) Molecular and culture-based analyses of prokaryotic communities from an agricultural soil and the burrows and casts of the earthworm *Lumbricus rubellus*. *Applied and Environmental Microbiology*, 68: 1265-1279.

G

- Gagen E. J., Denman S. E., Padmanabha J., Zadbuke S., Al Jassim R., Morrison M., and McSweeney C. S. (2010) Functional gene analysis suggests different acetogen populations in the bovine rumen and tammar wallaby forestomach. *Applied and Environmental Microbiology*, 76: 7785-7795.

- Gagen E. J., Huber H., Meador T., Hinrichs K. U., and Thomm M. (2013) Novel Cultivation-Based Approach To Understanding the Miscellaneous Crenarchaeotic Group (MCG) Archaea from Sedimentary Ecosystems. *Applied and Environmental Microbiology*, 79: 6400-6406.
- Genge M. J., and Grady M. M. (1999) The fusion crusts of stony meteorites: Implications for the atmospheric reprocessing of extraterrestrial materials. *Meteoritics & Planetary Science*, 34: 341-356.
- Gillieson D. S., Cochrane J. A., and Murray A. (1994) Surface hydrology and soil movement in an arid karst: the Nullarbor Plain, Australia. *Environmental Geology*: 125-133.
- Goede A., Harmon S., Atkinson T. C., and Rowe P. J. (1992) A giant late Pleistocene halite speleothem from Webbs Cave, Nullarbor Plain, south- eastern Western Australia. *Helictite: Journal of Australasian Cave Research*, 31: 3-6.

H

- Hatzenpichler R., Lebedeva E. V., Spieck E., Stoecker K., Richter A., Daims H., and Wagner M. (2008) A moderately thermophilic ammonia-oxidizing crenarchaeote from a hot spring. *Proceedings of the National Academy of Science*, 105: 2134-2139.
- Holmes A. J., Bowyer J., Holley M. P., O'Donoghue M., Montgomery M., and Gillings M. R. (2000) Diverse, yet-to-be-cultured members of the Rubrobacter subdivision of the Actinobacteria are widespread in Australian arid soils. *FEMS Microbiology Ecology*, 33: 111-120.
- Holmes A. J., Tujula N. A., Holley M., Contos A., James J. M., Rogers P., and Gillings M. R. (2001) Phylogenetic structure of unusual aquatic microbial formations in Nullarbor caves, Australia. *Environmental Microbiology*, 3: 256-264.

J

- Janssen P. H. (2006) Identifying the Dominant Soil Bacterial Taxa in Libraries of 16S rRNA and 16S rRNA Genes. *Applied and Environmental Microbiology*, 72: 1719-1728.
- Jiang X., and Takacs-Vesbach C. D. (2017) Microbial community analysis of pH 4 thermal springs in Yellowstone National Park. *Extremophiles*, 21: 135-152.
- Jull A. J. T., McHargue L. R., Bland P. A., Greenwood R. C., Bevan A. W. R., Kim K. J., LaMotta S. E., and Johnson J. A. (2010) Terrestrial ages of meteorites from the Nullarbor region, Australia, based on ^{14}C and ^{14}C - ^{10}Be measurements. *Meteoritics & Planetary Science*, 45: 1271-1283.

K

- Kelly L. C., Cockell C. S., Herrera-Belaroussi A., Piceno Y., Andersen G., DeSantis T., Brodie E., Thorsteinsson T., Marteinsson V., Poly F. and others. (2011) Bacterial Diversity of Terrestrial Crystalline Volcanic Rocks, Iceland. *Microbial Ecology*, 62: 69-79.

- Kelly L. C., Cockell C. S., Piceno Y. M., Andersen G. L., Thorsteinsson T., and Marteinson V. (2010) Bacterial diversity of weathered terrestrial Icelandic volcanic glasses. *Microbial Ecology*, 60: 740-752.
- Kelly L. C., Cockell C. S., Thorsteinsson T., Marteinson V., and Stevenson J. (2014) Pioneer Microbial Communities of the Fimmvörðuháls Lava Flow, Eyjafjallajökull, Iceland. *Microbial Ecology*, 68: 504-518.
- Kozich J. J., Westcott S. L., Baxter N. T., Highlander S. K., and Schloss P. D. (2013) Development of a dual-index sequencing strategy and curation pipeline for analyzing amplicon sequence data on the MiSeq Illumina sequencing platform. *Applied and Environmental Microbiology*, 79: 5112-5120.

L

- Lehtovirta-Morley L. E., Ross J., Hink L., Weber E. B., Gubry-Rangin C., Thion C., Prosser J. I., and Nicol G. W. (2016) Isolation of ‘Candidatus Nitrosocosmicus franklandus’, a novel ureolytic soil archaeal ammonia oxidiser with tolerance to high ammonia concentration. *FEMS Microbiology Ecology*, 92: fiw057.
- Levshina N. (2015) How to do Linguistics with R: Data exploration and statistical analysis. *John Benjamins Publishing Company*.
- Los Ríos A., Wierzbos J., Sancho L. G., and Ascaso C. (2003) Acid microenvironments in microbial biofilms of antarctic endolithic microecosystems. *Environmental Microbiology*, 5: 231-237.

M

- Mangalo M., Meckenstock R. U., Stichler W., and Einsiedl F. (2007) Stable isotope fractionation during bacterial sulfate reduction is controlled by reoxidation of intermediates. *Geochimica et Cosmochimica Acta*, 71: 4161-4171.
- Martin H. A. (1973) Palynology and Historical Ecology of Some Cave Excavations in the Australian Nullarbor. *Australian Journal of Botany*, 21: 283-316.
- Mautner M. N. (1997) Biological potential of extraterrestrial materials—1. Nutrients in carbonaceous meteorites, and effects on biological growth. *Planetary and Space Science*, 45: 653-664.
- Minster J.-F., and Allègre C. J. (1979) $^{87}\text{Rb}/^{87}\text{Sr}$ chronology of H chondrites: Constraint and speculations on the early evolution of their parent body. *Earth and Planetary Science Letters*, 42: 333-347.

N

- Neilson J. W., Quade J., Ortiz M., Nelson W. M., Legatzki A., Tian F., LaComb M., Betancourt J. L., Wing R. A., Soderlund C. A. and others. (2012) Life at the hyperarid margin: novel bacterial diversity in arid soils of the Atacama Desert, Chile. *Extremophiles*, 16: 553-566.

P

- Pester M., Schleper C., and Wagner M. (2011) The Thaumarchaeota: an emerging view of their phylogeny and ecophysiology. *Current Opinion in Microbiology*, 14: 300-306.
- Pontefract A., Osinski G. R., Cockell C. S., Southam G., McCausland P. J. A., Umoh J., and Holdsworth D. W. (2016) Microbial Diversity of Impact-Generated Habitats. *Astrobiology*, 16: 775-786.
- Pontefract A., Osinski G. R., Lindgren P., Parnell J., Cockell C. S., and Southam G. (2012) The effects of meteorite impacts on the availability of bioessential elements for endolithic organisms. *Meteoritics and Planetary Science*, 47: 1681-1691.
- Purkhold U., Pommerening-Röser A., Juretschko S., Schmid M. C., Koops H. P., and Wagner M. (2000) Phylogeny of all recognized species of ammonia oxidizers based on comparative 16S rRNA and amoA sequence analysis: implications for molecular diversity surveys. *Applied and Environmental Microbiology*, 66: 5368-5382.

Q

- Quast C., Pruesse E., Yilmaz P., Gerken J., Schweer T., Yarza P., Peplies J., and Glöckner F. O. (2013) The SILVA ribosomal RNA gene database project: improved data processing and web-based tools. *Nucleic Acids Research*, 41: D590-6.

R

- Rubin A. E. (1997) Mineralogy of meteorite groups. *Meteoritics*, 32: 231-247.

S

- Schloss P. D., Westcott S. L., Ryabin T., Hall J. R., Hartmann M., Hollister E. B., Lesniewski R. A., Oakley B. B., Parks D. H., Robinson C. J. and others. (2009) Introducing mothur: open-source, platform-independent, community-supported software for describing and comparing microbial communities. *Applied and Environmental Microbiology*, 75: 7537-7541.
- Schütte U. M. E., Abdo Z., Foster J., Ravel J., Bunge J., Solheim B., and Forney L. J. (2010) Bacterial diversity in a glacier foreland of the high Arctic. *Molecular Ecology*, 19: 54-66.
- Segata N., Izard J., Waldron L., Gevers D., Miropolsky L., Garrett W. S., and Huttenhower C. (2011) Metagenomic biomarker discovery and explanation. *Genome Biology*, 12: R60.
- Sephton M. A. (2002) Organic compounds in carbonaceous meteorites. *Natural Product Reports*, 19: 292-311.
- Shinotsuka K., and Ebihara M. (1997) Precise determination of rare earth elements, thorium and uranium in chondritic meteorites by inductively coupled plasma mass spectrometry — a comparative study with radiochemical neutron activation analysis. *Analytica Chimica Acta*, 338: 237-246.

- Stoffler D., Keil K., and Edward R. D. (1991) Shock metamorphism of ordinary chondrites. *Geochimica et Cosmochimica Acta*, 55: 3845-3867.
- Sun D., Cheng S., Wang A., Huang F., Liu W., and Xia X. (2016) Complete Genome Sequence of *Geobacter anodireducens* SD-1 T, a Salt-Tolerant Exoelectrogenic Microbe in Bioelectrochemical Systems. *Genome Announcements*, 4: e00415-16-1.
- Sun D., Wang A., Cheng S., Yates M., and Logan B. E. (2014) *Geobacter anodireducens* sp. nov., an exoelectrogenic microbe in bioelectrochemical systems. *International Journal of Systematic and Evolutionary Microbiology*, 64: 3485-3491.

T

- Tait A. W., Fisher K. R., Srinivasan P., and Simon J. I. (2016) Evidence for impact induced pressure gradients on the Allende CV3 parent body: Consequences for fluid and volatile transport. *Earth and Planetary Science Letters*, 454: 213-224.
- Tait A. W., Wilson S. A., Tomkins A. G., Gagen E. J., Stewart F. J., and Southam G. (2017) Evaluation of meteorites as habitats for terrestrial microorganisms: Results from the Nullarbor Plain, Australia, a Mars analogue site. *Geochimica et Cosmochimica Acta* (Accepted for publication 28th May 2017).
- Tetu S. G., Breakwell K., Elbourne L. D. H., Holmes A. J., Gillings M. R., and Paulsen I. T. (2013) Life in the dark: metagenomic evidence that a microbial slime community is driven by inorganic nitrogen metabolism. *The ISME journal*, 7: 1227-1236.

V

- Van Horn D. J., Wolf C. R., Colman D. R., Jiang X., Kohler T. J., McKnight D. M., Stanish L. F., Yazzie T., and Takacs-Vesbach C. D. (2016) Patterns of bacterial biodiversity in the glacial meltwater streams of the McMurdo Dry Valleys, Antarctica. *FEMS Microbiology Ecology*, 92: fiw148.
- Van Schmus W. R., and Wood J. (1967) A chemical-petrologic classification for the chondritic meteorites. *Geochimica et Cosmochimica Acta*, 31: 747-765.

W

- Webb J. A., and James J. M. (2006) Karst evolution of the Nullarbor Plain, Australia. *Geological Society of America Special Paper*, 404: 65-78.
- Wierzchos J., Davila A. F., Artieda O., Cámara-Gallego B., de los Ríos A., Nealson K. H., Valea S., Teresa García-González M., and Ascaso C. (2013a) Ignimbrite as a substrate for endolithic life in the hyper-arid Atacama Desert: Implications for the search for life on Mars. *Icarus*, 224: 334-346.

- Wierzchos J., de los Ríos A., and Ascaso C. (2013b) Microorganisms in desert rocks: the edge of life on Earth. *International Microbiology*, 15: 172-182.
- Wilkison S. L., McCoy T. J., McCamant J. E., Robinson M. S., and Britt D. T. (2003) Porosity and density of ordinary chondrites: Clues to the formation of friable and porous ordinary chondrites. *Meteoritics & Planetary Science*, 38: 1533-1546.
- Wlotzka F. (1993) A Weathering Scale for the ordinary chondrites. *Meteoritics*, 28: 460.

Y

- Yue J. C., and Clayton M. K. (2005) A Similarity Measure Based on Species Proportions. *Communications in Statistics - Theory and Methods*, 34: 2123-2131.

Z

- Zenobi R., Philippoz J.-M., Zare R. N., Wing M. R., Bada J. L., and Marti K. (1992) Organic compounds in the Forest Vale, H4 ordinary chondrite. *Geochimica et Cosmochimica Acta*, 56: 2899-2905.

Declaration for Thesis Chapter 5

Declaration by candidate

In the case of Chapter 5, the nature and extent of my contribution is as follows:

<i>Nature of contribution</i>	<i>Extent of contribution (%)</i>
Conceptualisation, field work, sample collection, Sample preparation, experimental execution, data interpretation, manuscript writing	77%

The following co-authors contributed to the work. If co-authors are students at Monash University, the extent of their contribution in percentage terms must be stated:

<i>Name</i>	<i>Nature of contribution</i>	<i>Extent of contribution (%)</i>
Siobhan A. Wilson	Supervisory Role	5%
Andrew G. Tomkins	Supervisory Role	5%
Emma J. Gagen	Experimental Design Advisor	5%
Amelia C. Y. Liu	FIB Data Collection	2%
Bree Morgan	Sulfate Experiment Advisor	2%
Suzanne D. Golding	CF-IRMS Data Collection	2%
Gordon Southam	Advisory Role	2%

The undersigned hereby certify that the above declaration correctly reflects the nature and extent of the candidate's and co-authors contributions to this work*.

Candidate's signature:



Date: 01/06/2017

Main supervisor's signature:

Date: 01/06/2017

*Note: Where the responsible author is not the candidate's main supervisor, the main supervisor should consult with the responsible author to agree on the respective contributions of the authors.

Chapter 5

Laboratory induced $\delta^{34}\text{S}$ biosignature in the Chelyabinsk LL5 chondrite: Using terrestrial microorganisms to refine tools for astrobiological exploration on the surface of Mars[†]

Alastair W. Tait¹, Siobhan A. Wilson¹, Andrew G. Tomkins¹, Emma J. Gagen², Amelia C. Y. Liu³, Bree Morgan^{1,4}, Suzanne D. Golding², and Gordon Southam²

¹School of Earth, Atmosphere & Environment, Monash University, Australia

²School of Earth & Environmental Sciences, The University of Queensland, Australia.

³Monash Centre for Electron Microscopy and School of Physics and Astronomy, Monash University, Australia.

⁴School of Geosciences, The University of Sydney, NSW 2006, Australia

[†] Submitted for publication in *Geochimica et Cosmochimica Acta*
17th February 2017

One of the greatest challenges facing astrobiological exploration of Mars and other planets is distinguishing between stable isotopic signatures caused by life and those isotopic fractionations caused by abiotic processes. Ideally, standard materials of known isotopic and elemental composition could be used to distinguish between such biotic and abiotic signatures, however this tool has not yet been satisfactorily developed. Ordinary and enstatite chondritic meteorites are the ideal standards on Mars because of their homogeneous stable sulfur isotope compositions and well-understood chemistry. Chondrites are also sterile, lacking microorganisms, when they fall to the surfaces of Earth, Mars and other planets. These characteristics make them ideal candidates for detection of isotopic biosignatures that have developed following their arrival at a planet's surface. In the martian context, positive detection of such biomarkers would reflect the activity of putative martian microorganisms. Because chondritic meteorites contain abundant reduced Fe and S in sulfide minerals, microorganisms that use sulfur in their metabolism may produce characteristic $\delta^{34}\text{S}$ biosignatures via processes such as sulfide oxidation. Here, we demonstrate through laboratory-based experiments that the organism *Acidithiobacillus ferrooxidans* is able to alter the iron sulfide mineral troilite (FeS) from the Chelyabinsk LL5 chondrite to induce a stable sulfur isotopic fractionation of $\Delta^{34}\text{S}_{\text{SO}_4-\text{FeS}} = 1.2 - 3.7\text{‰}$ (VCDT), which is preserved in the residual sulfate minerals. This result is similar in magnitude to the isotopic difference that we have measured between natural sulfate alteration products and troilite detected in two meteorites from the Nullarbor Plain, Australia: $\Delta^{34}\text{S}_{\text{SO}_4-\text{FeS}} = 2.2 - 6.7\text{‰}$ (VCDT) for meteorites that have been colonised by bacteria on Earth. This fractionation is consistent with microbial sulfur cycling, which produces a pool of ^{34}S -enriched aqueous sulfate from which alteration minerals may precipitate. During the course of our biotic experiments, *A. ferrooxidans* cells were commonly entombed beneath 1–20 μm thick crusts of goethite [$\text{FeO}(\text{OH})$], which is important because Fe-(oxy)hydroxide minerals are known to preserve fossil evidence of microbes over geological timescales on Earth. Additionally, focused Ion Beam – Scanning Electron Microscopy cross-sections through two experimental samples of Fe-(oxy)hydroxide efflorescences grown on meteorites revealed the presence of sulfate metabolite layers in the biotic samples; however, these were not present in the abiotic samples, providing another means of recognising the presence of sulfur-metabolising microbes in meteorites. Our findings suggest that the use of chondritic meteorites could provide a robust tool for mitigating ambiguity in detection of stable sulfur isotopic biosignatures on the surface of Mars.

5.1 Introduction

Environmental stable isotopes have been used to identify the influence of biological metabolisms in the formation of minerals since the 1940s (HORITA 2005). Our understanding of how metabolic processes fractionate stable isotopes has grown immensely since then, as have our analytical capabilities and our ability to explore the solar system. Stable isotope fractionation is a vital tool in our search for extraterrestrial life (DES MARAIS *ET AL.* 2008). One such isotope system used for biological identification is that of sulfur. Some chemolithoautotrophic organisms (e.g., *Acidithiobacillus ferrooxidans*) catalyse the oxidation of reduced sulfide phases as an energy source, imprinting their biological preference

for lighter isotopes in the residual weathering products (PISAPIA *ET AL.* 2007). Other microorganisms such as those recently identified from 16S rRNA analysis in Nullarbor meteorites (i.e., *Geobacter spp.* and *Desulfovibrio spp.*; (TAIT *ET AL.*, 2017A)) catalyze reduction of oxidised iron- and sulfur-phases. The Mars Science Laboratory (MSL) rover, Curiosity, which is currently exploring Mars, has the capability of measuring stable sulfur isotopes in trace atmospheric gases, such as SO₂ and H₂S, using the Sample Analysis at Mars (SAM) instrument suite (MAHAFFY *ET AL.* 2012). The quadrupole mass spectrometer that is part of SAM also has a limited capability to measure stable sulfur isotopes in minerals in the absence of mass spectrometric interferences (FRANZ *ET AL.* 2011). However, recognition of isotopic biosignatures is difficult in poorly characterised environments, such as the martian surface. Standard materials, with known elemental, mineralogical and isotopic compositions, can be used to reduce ambiguity in identifying biological processes and the distinctive geochemical signatures they produce. It would be ideal to find a standard material with a known stable sulfur isotope composition on the surface of Mars. This material would need to have a narrow range of $\delta^{34}\text{S}$ values, to not mask a biological fractionation and provide suitable sources of energy and nutrients for microorganisms. Tait et al. (2017b) proposed that ordinary chondritic meteorites at the martian surface could be used as a standard indicator for biological processes. This is because the range of $\delta^{34}\text{S}$ values of troilite (FeS), the dominant sulfide mineral in ordinary and enstatite chondrites, is smaller than the fractionations induced by many terrestrial organisms that metabolise and/or assimilate sulfur.

Studies of martian meteorites that have fallen to Earth (i.e., rocks ejected from the martian crust during impacts) have shown that they have -4.98‰ to +5.25‰ variability in the $\delta^{34}\text{S}$ values of sulfur bearing minerals (FARQUHAR *ET AL.* 2000), which could potentially mask biological fractionation of stable sulfur isotopes. In contrast, ordinary chondrites have a much narrower range of $\delta^{34}\text{S}$ values: $\delta^{34}\text{S} = -0.02\text{‰} \pm 0.06\text{‰}$ (GAO AND THIEMENS 1993). It is important to note that not all meteorites that are remnants from the formation of the early solar system have potential to be used as standards for biosignature detection. For instance, carbonaceous chondrites, which have been subjected to hydrous alteration and disequilibrium conditions, exhibit a broader range of stable sulfur isotopic compositions, $-5.7\text{‰} \leq \delta^{34}\text{S} \leq +1.1\text{‰}$ for pyrrhotite [Fe_{1-x}S] and pentlandite [(Fe,Ni)₉S₈] (McSWEEN *ET AL.* 1997), making it difficult to distinguish fractionation specific to biological processes. Consequently, carbonaceous chondrites will not be considered further in this study.

Ordinary and enstatite chondrites make up ~87% of Earth's known meteoritic inventory (based on entries in the Meteoritical Bulletin Database, 2016). However this excess of stony meteorites might not

be the same on Mars. Currently, iron meteorites make up the majority of finds on the surface of Mars; although stony-iron and achondrite classes have also been found (ASHLEY *ET AL.* 2011; SCHRÖDER *ET AL.* 2016). The meteorite populations at planetary surfaces are thought to be strongly influenced by the local rate of mineral weathering (SCHRÖDER *ET AL.* 2016), as well as their likelihood of surviving entry and impact given the composition of each planet's atmosphere (BLAND AND SMITH 2000). Chemical weathering of meteorites on Mars is likely very slow, with residence times thought to be on the order of $\sim 10^9$ years (BLAND AND SMITH 2000). Recent estimates by (SCHRÖDER *ET AL.* 2016) confirm that the weathering rate of stony meteorites at Meridiani Planum on Mars is 1 to 4 orders of magnitude slower than in Earth's Antarctica, where meteorites may persist for over 1 Myr. Additionally, because Mars lacks tectonics as a mechanism of crustal recycling, meteorites that have fallen to the planet's surface could have potentially been present during the Hesperian/Amazonian transition, 3.0 billion years ago. This is of significant astrobiological interest because this period bridges the transition from a Mars that had liquid water on its surface to the present desiccated environment (CARR AND HEAD 2010). Because meteorites weather in well characterised ways depending upon climatic conditions (JULL *ET AL.* 2010), they could prove to be useful as tools for understanding the evolution of Mars' lower atmosphere throughout time (ASHLEY 2011).

Tait et al. (2017b) demonstrate extensive colonisation of ordinary chondrites by terrestrial bacteria that are indigenous to the Nullarbor Plain, Australia. These organisms were typically associated with veins of hygroscopic Mg-calcite $[(\text{Ca},\text{Mg})\text{CO}_3]$ and gypsum $[\text{CaSO}_4 \cdot 2\text{H}_2\text{O}]$, as well as with 'pore spaces' filled with Fe-(oxy)hydroxide minerals. These minerals are common alteration products of chondritic meteorites (BLAND *ET AL.* 2006), and are known to preserve viable cells and fossil evidence of life on Earth (BLYTH *ET AL.* 2010). Formation of these minerals in meteorites can also entomb cells and paleobiofilms (*Chapter 3*) and may be able to record isotopic evidence of biological oxidation of troilite, or reduction of secondary sulfate by chemolithoautotrophic organisms. However, interpreting the stable sulfur isotope signature of the residual sulfate minerals is not straightforward. As such, we have identified five possible stable sulfur isotopic signatures that may be observed in sulfate alteration products of meteorites exposed to an extant biosphere (assuming similar fractionations for pyrite and troilite): (1) negligible fractionation of sulfur isotopes, $\Delta^{34}\text{S}_{\text{SO}_4-\text{FeS}} \cong 0\text{‰}$, during abiotic oxidation of troilite (BALCI *ET AL.* 2007); (2) a small negative or near-zero $\Delta^{34}\text{S}_{\text{SO}_4-\text{FeS}}$ value caused by biological oxidation of sulfur by chemolithoautotrophic metabolism (e.g., *Acidithiobacillus ferrooxidans*, $\Delta^{34}\text{S}_{\text{SO}_4-\text{FeS}_2} = 0.4 - -1.3\text{‰}$ (PISAPIA *ET AL.* 2007)); (3) a positive $\Delta^{34}\text{S}_{\text{SO}_4-\text{FeS}}$ value that is related to preferential

assimilation of $^{32}\text{SO}_4^{2-}$ by bacteria (CANFIELD 2001; JÄGER AND HUNZIKER 2012; KAPLAN AND RITTENBERG 1964); (4) a positive $\Delta^{34}\text{S}_{\text{SO}_4\text{-FeS}}$ value related to $^{32}\text{SO}_{2(\text{g})}$ degassing during sulfide oxidation by *Acidithiobacillus ferrooxidans*, which when coupled with an excess of ferrous iron triggers a change in metabolic mode that results in different isotopic signatures during the initial and main phases of microbial growth (e.g., $\Delta^{34}\text{S}_{\text{SO}_4(\text{initial})\text{-FeS}_2} = +4.0 \pm 1.7\text{‰}$, and $\Delta^{34}\text{S}_{\text{SO}_4(\text{main})\text{-FeS}_2} = -0.2 \pm 2.0\text{‰}$ (BRUNNER ET AL. 2008)); or (5) disproportionation of S^0 by *Acidithiobacillus ferrooxidans* under anaerobic conditions resulting in the production of H_2S (NG ET AL. 2000; OSORIO ET AL. 2013; VALDÉS ET AL. 2008). One important caveat is that most of these studies use pyrite [FeS_2] a common terrestrial sulfide mineral whereas meteorites contain troilite [FeS], which is rare on Earth. As such, little is known about stable sulfur isotope fractionation during troilite oxidation. For example, the variation $\Delta^{34}\text{S}_{\text{SO}_4\text{-FeS}}$ values between studies of stable sulfur isotope fractionation caused by *Acidithiobacillus ferrooxidans* has been attributed to stoichiometric and non-stoichiometric leaching of sulfur and iron from pyrite (BRUNNER ET AL. 2008; PISAPIA ET AL. 2007), which controlled by differences in bond strength between Fe–S (weak) and S–S (strong) bonds (RIMSTIDT AND VAUGHAN 2003). As troilite is a monosulfide mineral, strong ionic S–S bonds are not a factor influencing stable isotope fractionation.

Here, we build on previous research that shows a microbial role in the weathering of chondrites (TAIT ET AL., 2017B), to reveal that small but recognisable stable sulfur isotopic fractionations can be induced by chemolithoautotrophic bacteria on meteorites. To achieve this, we inoculated samples of the recently fallen Chelyabinsk chondrite, as well as samples of powdered troilite and pyrite, with the chemolithoautotrophic bacterium, *Acidithiobacillus ferrooxidans*, which is known to oxidize reduced iron and sulfur. Abiotic experiments were run in conjunction with the biotic experiments to serve as controls. Additional Fe-sulfate, with a distinct $\delta^{34}\text{S}$ value, was added to the medium in abiotic experiments to simulate mixing with contaminant sulfate on the surface of Mars. The $\delta^{34}\text{S}$ values of sulfate-bearing minerals and aqueous sulfate were measured to evaluate the magnitude of stable sulfur isotopic fractionation in both biotic and abiotic experiments. Our results show a measurable and diagnostic difference between the $\Delta^{34}\text{S}_{\text{SO}_4\text{-FeS}}$ values obtained from biotic and abiotic experiments, indicating that biological fractionation of stable sulfur isotopes can be detected in stony meteorites.

5.2 Methods

5.2.1 Experimental Design

5.2.1.1 Experimental Overview

The ultimate goal of this experiment is to induce an unequivocal $\delta^{34}\text{S}$ biosignature in the weathering products of an ordinary chondrite, and then to compare laboratory-based results with $\delta^{34}\text{S}$ values of sulfate-bearing weathering products in ordinary chondrites recovered from the Nullarbor Plain in southern Australia.

In order to produce an unequivocal $\delta^{34}\text{S}$ biosignature, we opted to design and execute a laboratory-based experiment under controlled conditions. This experiment required (1) a freshly fallen and gamma-sterilised ordinary chondrite, (2) a pure culture of an organism of known chemolithoautotrophic lifestyle, (3) a sulfate-poor culture medium that does not provide a source of energy to the selected organism or contribute largely to the final isotopic results, (4) parallel abiotic controls to identify and rule out abiotic processes from geomicrobial experiments, and (5) thorough characterisation of the $\delta^{34}\text{S}$ values of all sources of sulfur in the experiment. Details of experimental set up and descriptions of the analytical methods used in this study are described in detail below.

5.2.1.2 Meteorite and Sulfide Mineral Substrates

The Chelyabinsk LL5 chondrite, which fell to Earth over the Russian Federation in 2013, was selected as a substrate for culturing due to its fresh and unweathered nature. This meteorite contains minerals of interest to chemolithoautotrophic microorganisms, including 4.0 vol.% troilite, 1.3 vol.% FeNi alloys, and small inclusions of native copper (GALIMOV *ET AL.*, 2013). It also contains phosphorus within phosphate and phosphide minerals (e.g., chlorapatite, merrillite, and schreibersite) at an abundance of 0.10 wt.% (GALIMOV *ET AL.* 2013). The freshly fallen meteorite was used to ensure minimal alteration from biotic or abiotic weathering. This is important because meteorites, even those found in semi-arid and arid environments, may have been on Earth for up to 10^4 years and they are commonly heavily contaminated with terrestrial biota (TAIT *ET AL.* 2017B).

Two fragments of this meteorite, with a combined weight of approximately 100 g, were used in these experiments. Contact with water was avoided during preparation of meteorite specimens to limit the oxidation of the FeNi alloys and sulfide minerals, but in some instances, short periods of contact with

water could not be avoided. Samples were stored in 100% ethanol to minimise the effects of oxidation between steps in sample preparation. First, the meteorite was cut into 1.5-mm thick sections using a diamond wire saw that was cooled with 100% ethanol. The thick sections were polished using 12 μm silicon carbide powder in water slurry. These were then sonicated in 100% ethanol for 1 min. A final polishing step was done using 0.5 μm sandpaper, after which the samples were cut into approximately equal sized portions (5 mm \times 5 mm \times 1 mm) using a wire saw. Note, the heavily shocked (S4) nature of the Chelyabinsk meteorite meant that it would often break apart during preparation, which made uniform sizing an impossible task. Each sample was visually inspected for the presence of troilite and FeNi alloys on the polished side and any samples that did not contain visible troilite were not used in experiments. All meteorite pieces selected for use in experiments were sonicated in ethanol for a further 5 min to remove any debris before being stored in 100% ethanol prior to experimentation to minimise oxidation. In addition to the polished sections, crushed meteorite fragments were also used in some experiments.

Samples of synthetic troilite (99.9% purity, Sigma-Aldrich) and naturally occurring pyrite were crushed and sieved to $\leq 150 \mu\text{m}$ for separate use in parallel experiments. The sieved mineral samples were sealed in polystyrene containers under a humidity free 100% N_2 atmosphere. Prior to their use in experiments the mineral powders were sterilised by exposure to a 50 kGy dose of gamma radiation from a ^{60}Co source.

Approximately 10 mg of carbonate–gypsum vein material was collected from two meteorites, *Ooldea 006* and *Ooldea 007*, which were recovered from the Nullarbor Plain in Australia, during 2013 and 2014, for stable sulfur isotope analysis. These samples were analysed for comparison with experimentally obtained $\delta^{34}\text{S}$ values. *Ooldea 006*, a H3 ordinary chondrite weighing 113 g, has a moderate weathering profile (W3) and a light shock (S2). *Ooldea 007* is a H3 ordinary chondrite that was found as a single stone weighing 135 g. It has a highly weathered profile (W4) and a moderate shock grade of (S3). A full description of these meteorites can be found online at the Meteoritical Bulletin Database. Petrological classifications of chondrites are based on Van Schmus and Wood (1967). For weathering classification see Wlotzka (1993), and for shock classification see Stoffler et al. (1991).

5.2.1.3 Model Organism

The organism *Acidithiobacillus ferrooxidans* (Catalogue numbers: DSMZ 14882, NCIB 8455, ATCC 23270) (KELLY AND WOOD 2000; TEMPLE AND COLMER 1951) is a gram-negative chemolithoautotrophic

bacterium that forms medium rods of 1.0–2.0 μm in length. The microorganism was chosen for this study because of its iron- and sulfur-oxidising pathways. *A. ferrooxidans* has previously been suggested to have model metabolic pathways for a putative martian biosphere (BAUERMEISTER *ET AL.* 2013), and it has been used in previous meteorite weathering studies relating to early Earth research (GRONSTAL *ET AL.* 2009). This organism can also switch its metabolic mode to use ferrous iron as an energy source, instead of sulfide, which can result in different sulfur pools being generated within an experiment, and associated fractionations of $\Delta^{34}\text{S}_{\text{SO4(initial)}-\text{FeS}_2} = +4.0 \pm 1.7\text{‰}$ (BRUNNER *ET AL.* 2008). The stable sulfur isotopic fractionations produced by *A. ferrooxidans* are well outside the range of $\delta^{34}\text{S}$ values of ordinary chondrites ($\delta^{34}\text{S} = -0.02\text{‰} \pm 0.06\text{‰}$) and enstatite chondrites ($\delta^{34}\text{S} = -0.27\text{‰} \pm 0.07\text{‰}$) (GAO AND THIEMENS 1993). Thus, we hypothesise *A. ferrooxidans* should produce a recognisable stable sulfur isotopic biosignature in the sulfate mineral alteration products of meteorites. The metabolic versatility of this organism could result in other unexpected isotopic signatures. For instances, *A. ferrooxidans* is also known to assimilate aqueous sulfate for use in cell functions (TUOVINEN *ET AL.* 1975; VALDÉS *ET AL.* 2003); however, the magnitude of stable sulfur isotope fractionation between organosulfur and aqueous sulfate has not previously been reported for this species. Although sulfur assimilation in general is believed to result in small to negligible $\Delta^{34}\text{S}$ values (CANFIELD 2001). Some strains of *A. ferrooxidans* (e.g., NASF-1) can use S^0 as an electron acceptor to make H_2S under anaerobic conditions (NG *ET AL.* 2000; OSORIO *ET AL.* 2013; VALDÉS *ET AL.* 2008), although the isotopic fractionation associated with this metabolic pathway in *A. ferrooxidans* have yet to be recorded, dissimilatory processes normally result in large, positive $\Delta^{34}\text{S}$ values (CANFIELD 2001).

5.2.1.4 Experimental Setup

The experiment was run over 4 weeks, with sampling conducted at time steps of 24 hrs, 48 hrs, 1 week, 2 weeks and 4 weeks. The overall experiment contained 36 individual experiments in 5 mL Petri dishes, across two parallel experimental lines: a biotic line (18 experiments) and an abiotic line (18 experiments). Each of these two series (i.e., biotic and abiotic experiments) consisted of 9 polished meteorite thick sections (~1.0 g each), 2 meteorite fragments (~2.0 g each), 3 specimens of synthetic troilite powder (~0.5 g each), and 3 specimens of natural pyrite powder (~0.5 g each). Incubations also included and 1 blank containing only medium (or in the case of the biotic blank, medium inoculated with culture). All experiments were incubated at 28°C. Replicate experiments (e.g., some of the 9 polished meteorite thick sections) were conducted so that some could be sampled at each time step for

SEM analysis (which is destructive).

Prior to the start of the experiment, meteorite thick sections, meteorite fragments and powdered mineral specimens were placed into small Petri dishes and weighed. Following this, the approximate sulfur content of each experimental specimen was calculated. This was done using the modal mineral abundance for the Chelyabinsk meteorite reported by Dunn et al. (2010), or from stoichiometry using the formulae of troilite and pyrite in the case of powdered mineral specimens. Refer to *Appendix II: Table 1* for a list of absolute masses of meteorite, sulfide minerals and calculated masses of sulfur available in each experiment.

Meteorite thick sections were analysed using FIB-SEM to examine the growth of efflorescences and to investigate how microbes etch FeNi-alloy and troilite grains. $\delta^{34}\text{S}$ values of sulfate-bearing alteration minerals in efflorescences were obtained using Isotope Ratio Mass Spectrometry (IRMS). The meteorite fragment samples were embedded in epoxy and cross-sectioned to examine internal alteration textures. Mineralogical and isotopic results from the sulfide powder experiments (pure pyrite and troilite) were used to assess the reproducibility of the experiment given the large amount of literature on the behaviour of *A. ferrooxidans* cultured on pure sulfide samples (e.g., (FOWLER AND CRUNDWELL 1999; PISAPIA ET AL. 2007)). The use of powdered samples of pure sulfide minerals also provides a useful comparison with meteorite specimens, which contain much lower abundances of sulfide minerals with low surface area exposure.

5.2.1.5 Media and Culturing

An important design decision was to minimise the amount of media-derived sulfate in the Basal Salt Medium (BSM) used in the experiment. Sulfate is necessary for the growth of *A. ferrooxidans* and cannot be entirely removed from the cultivation medium. However, it was important to avoid external sources of sulfur (i.e., ‘contamination’, that could obscure biologically-mediated sulfur isotope signatures in secondary sulfate minerals). As such, microbes were cultivated in a modified DSMZ 882 medium, in which the BSM salts were replaced (1:1 molar substitution on the basis of cations) with chloride and phosphate-bearing alternatives to minimise the potential for sulfate contamination. Complications arose because *A. ferrooxidans* is not halo-tolerant and it almost completely loses the ability to oxidise iron in 0.4 M NaCl medium (KIEFT AND SPENCE 1988). As such, phosphate alternatives were used preferentially over chloride salts when designing the medium.

The BSM was prepared in two parts. Part A consisted of 450 mL of 18.2 MΩ cm Milli-Q water,

0.052 g of NH_4Cl , 0.008 g of $\text{MgHPO}_4 \cdot 3\text{H}_2\text{O}$, 0.027 g of KH_2PO_4 , 0.735 g of $\text{CaCl}_2 \cdot 2\text{H}_2\text{O}$, and 2 mL of the DSMZ 882 trace element solution. The pH of the medium was adjusted to a value of 2.1 using 1 M HCl before sterilising in an autoclave at 122°C for 30 min. Part B consisted of 50 mL 18.2 MΩ cm Milli-Q water and 2.5 g of $\text{FeSO}_4 \cdot 7\text{H}_2\text{O}$ adjusted to pH 2.1 using 1 M HCl before being filter (0.45 μm) sterilised.

For culturing, a 1 mL aliquot of *A. ferrooxidans* culture containing $\sim 10^6$ cells mL^{-1} was transferred into 100 mL of fresh medium containing 9:1 mixtures of Part A + Part B and incubated at 28° C for three weeks. This enrichment procedure was performed three times in a series to acclimatise the culture to the sulfate poor medium.

5.2.1.6 Sulfur Mixing

Because aqueous sulfate could not be completely removed from the medium due to the biological requirements of *A. ferrooxidans*, the sulfate in the medium was treated as a ‘contaminant’ and used to introduce a linear mixing trend for $\delta^{34}\text{S}$ into the experiment. Soil and regolith can make their way into meteorites via the network of cracks that develop as they weather (TAIT ET AL. 2017B). In the Nullarbor Plain, mechanical admixtures of contaminant limestone and the carbonate mineral products of biologically mediated meteorite weathering can produce a linear mixing trend in $\delta^{13}\text{C}$ – F^{14}C space (TAIT ET AL. 2017 B). Because sulfate minerals are common in martian regolith (DEHOUCK ET AL. 2012; MCLENNAN ET AL. 2014; WILSON AND BISH 2012), it is important to assess how contamination of this nature will affect $\delta^{34}\text{S}$ results. Thus, abiotic experiments were inoculated with 4.5 mL of Part A of the modified medium and 0.5 mL of Part B. Part B of the medium was introduced into the abiotic experiments to simulate sulfate contamination on the surface of Mars. The mass of “foreign” sulfate (i.e., melanterite, $\text{FeSO}_4 \cdot 7\text{H}_2\text{O}$, from the medium) in the abiotic samples is $\sim 10\times$ that in the biotic samples. This amount was chosen to develop a clear mixing trend between the $\delta^{34}\text{S}$ values of sulfate produced by oxidative weathering of the substrate and contaminant sulfate from the medium. Biotic experiments were inoculated with 4.5 mL of Part A of the modified medium and 0.5 mL of *A. ferrooxidans* culture (cultured in Part A + Part B solutions). The *A. ferrooxidans* culture contained 1.40×10^7 cells mL^{-1} . The mean amount of sulfate in the media compared to total mass of sulfur in meteorite experiments was 3.0 ± 1.6 wt.% for the biotic experiments. Thus, we hypothesise that the resulting $\delta^{34}\text{S}$ values of sulfate minerals produced in the biotic experiments should predominantly reflect biological fractionation of stable sulfur isotopes. The abiotic meteorite experiments contained

4.5 mL of Part A solution and 0.5 mL of Part B solution; the average amount of contaminant sulfur in the overall sulfur budget was thus 21.3 ± 16.9 wt.%. This is similar to the relative abundance of sedimentary carbonate contamination found in meteorites collected from the Nullarbor Plain (TAIT *ET AL.* 2017B), which means that it is a plausible level of contamination from regolith. Refer to *Appendix II: Table 1* for a more detailed breakdown of the mass ratios of sulfur introduced into biotic and abiotic experiments via the medium versus the substrate.

5.2.2 Analytical Methods

5.2.2.1 Cell Counting

Aliquots of approximately 50 μ L of supernatant were drawn from each biological sample at each time step to monitor cell counts. A LIVE/DEAD® BacLight™ Bacterial Viability Kit, (ThermoFisher) was used for cell enumeration according to the manufacturer's instructions in a Petroff-Hausser Counting Chamber with a depth of 20 μ m. Samples were viewed at the Monash Micro Imaging (MMI) platform using an Olympus PROVIS AX70 Widefield Microscope under bright field and fluorescence modes. Initial cell counts were back calculated based on the starting concentration of the inoculum.

5.2.2.2 Dissolved Sulfate Concentrations

A 50 μ L aliquot of supernatant was centrifuged at $9,800 \times g$ for 3 min. The solid phase was used for mineralogical analysis (see below) and aqueous sulfate concentrations were analysed using the turbidimetric method of Laskov et al. (2007). Briefly, the supernatant of each system (50 μ L of sample; dilution dependant) was added to 250 μ L of an acidified 0.08 M barium chloride [$\text{BaCl}_2 \cdot 2\text{H}_2\text{O}$] gelatine solution in a 96-well microplate. Samples were continuously agitated for 1 hr before being analysed using a wavelength of 450 nm with a Multiskan™ GO Microplate Spectrophotometer (ThermoFisher) using v3.2 of the SkanIt™ software. Aqueous sulfate concentrations were calculated against a calibration curve produced using range of standard ammonium sulfate [$(\text{NH}_4)_2\text{SO}_4$] dilutions.

5.2.2.3 Scanning Electron Microscopy

Meteorite samples taken from experiments at all time steps were analysed using a JEOL 7001F Field Emission Gun - Scanning Electron Microscope (FEG-SEM) at the Monash Centre for Electron

Microscopy (MCEM). Both biotic and abiotic experiments underwent chemical fixation with 2% glutaraldehyde solution followed by an ethanol dehydration series (15 minutes in each of 25%, 50%, 75%, 100%, 100%, and 100% ethanol) and replacement of ethanol with CO_2 by critical point drying (CPD) on a Bal-Tec CPD 030. Samples were Pt-coated and examined with Back Scattered Electron (BSE) imaging and Secondary Electron Imaging (SEI) using accelerating voltages from 1–15 kV at a working distance of ~10 mm.

Some samples were cross-sectioned to examine the interfaces between the original meteoritic material or sulfide minerals and their alteration products. These samples were fixed with 2.5% glutaraldehyde in a 0.1 M sodium cacodylate buffer for 2 hrs before being washed three times in the 0.1 M sodium cacodylate buffer, followed by staining with 1%_(aq) osmium tetroxide. Following this, samples were washed with distilled water and taken through a dehydration series with acetone (30, 50, 70, 90, 3×100%) before the acetone was progressively replaced with EPON ‘hard’ resin in acetone (25, 50, 75, 100% EPON) and then hardened for 48 hrs at 60°C. Epoxied samples were cross-sectioned using a water-cooled saw and machine-polished to a 0.25 μm finish. Cross-sectioned samples were Pt-coated and vacuum-desiccated prior to examination with light microscopy and SEM analysis.

5.2.2.4 Focused Ion Beam – Scanning Electron Microscopy

For the Focused Ion Beam (FIB) analysis, one sample from each of a biotic and an abiotic polished meteorite experiment was chosen: *Meteorite 17* (48 hours, abiotic), and *Meteorite 12* (1 week, biotic). These two samples were selected because they exhibited discrete and spatially localised efflorescences that coated grains of FeNi alloys and troilite. FIB analysis enabled us to investigate the interface between the reduced minerals and the oxide layer to assess the extent to which *A. ferrooxidans* cells and/or biofilms are preserved in alteration minerals.

A single efflorescence with a diameter of ~50 μm was chosen to be sectioned on each sample. Prior to sectioning, the area of interest was covered in a 1- μm thick layer of Pt to reduce charging and aid in maintaining the integrity of delicate secondary Fe-(oxy)hydroxide minerals. The FIB cross-section analysis was conducted using a Quanta 3DFEG (FEI Company, Hillsboro, USA) dual beam instrument using Ga^+ ions and an accelerating voltage of 30 kV. BSE images were taken using an accelerating voltage of 15 kV and beam currents ranging from 53 pA to 11 nA. Energy Dispersive X-ray (EDX) spectroscopy maps were obtained after sectioning on the JEOL 7001F FEG-SEM using an Oxford Instruments Aztec analysis system and an 80 mm² silicon drift detector. Operating

conditions of 4–15 kV and 4.5–11 nA were used. A dwell time of 200 μ s was used for mapping and drift stabilization was enabled. Element maps were processed using the Aztec™ analysis software by Oxford Instruments. Maps were processed to remove window and pulse pileup artefacts. Images collected using lower accelerating voltages were pixel binned twice.

5.2.2.5 Powder X-ray Diffraction

Mineral phase identification was conducted on 12 samples in order to identify sulfur-bearing alteration phases. Alteration minerals in efflorescences were mechanically extracted from meteorites

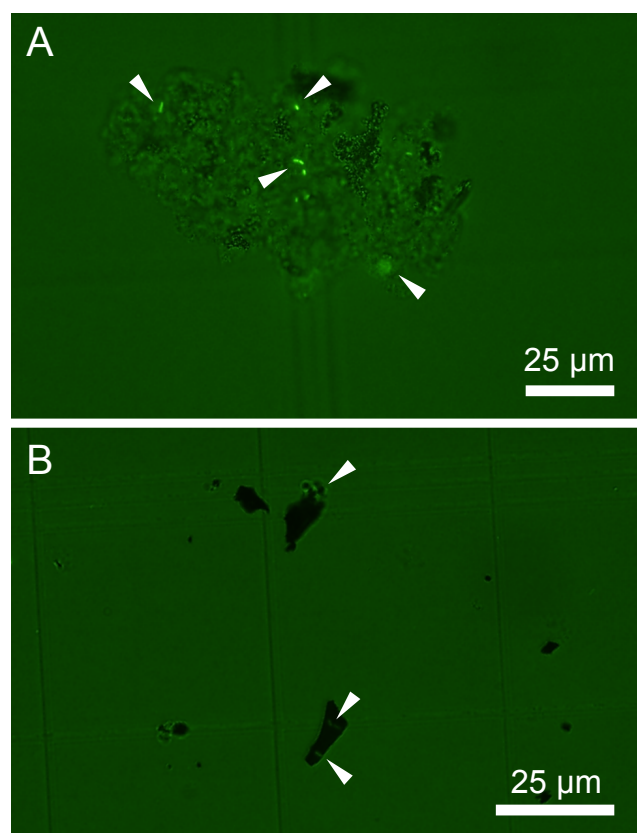


Figure 5.1 | UV Microscopy of *A. ferrooxidans*. These two fluorescent light micrographs were taken on a UV petrographic microscope using a Petroff-Hausser counting chamber. Microbes were stained with Syto 9, and were photographed at the 1-week time step. **(A)** This image is from the supernatant of a meteorite slice experiment. Notice *A. ferrooxidans* cells (white arrows) colonizing a large suspended sulfate grain (XRD inferred mineralogy). **(B)** This image is of the supernatant collected from a pyrite experiment. It shows *A. ferrooxidans* cells attached to grains of pyrite (white arrowheads). The dim cells in this image are due to prolonged UV bleaching during counting.

using a glass slide rather than a metal spatula to avoid sulfur and metal contamination of samples. Each sample was prepared as a 100% ethanol slurry and mounted onto a zero-background plate prior to analysis. Powder X-ray diffraction (XRD) patterns were collected at the Monash X-ray Platform using a Bruker D8 Advance Eco X-Ray Diffractometer with an automatic sample loader. XRD patterns were collected using a Cu X-ray tube operating at 40 kV and 25 mA. Data were collected over a 2θ range of 3–140° with a step size of 0.02° step⁻¹ and generally with a dwell time of 2 s step⁻¹, although longer dwell times of 4 s step⁻¹ were used for smaller samples. Mineral phases were identified using the International Center for Diffraction Data (ICDD) Powder Diffraction File 2 (PDF-2) database and DIFFRACplus EVA v.2 software from Bruker.

5.2.2.6 Continuous Flow - Isotope Ratio Mass Spectrometry (CF-IRMS) for $\delta^{34}\text{S}$

The $\delta^{34}\text{S}$ values of experimentally produced

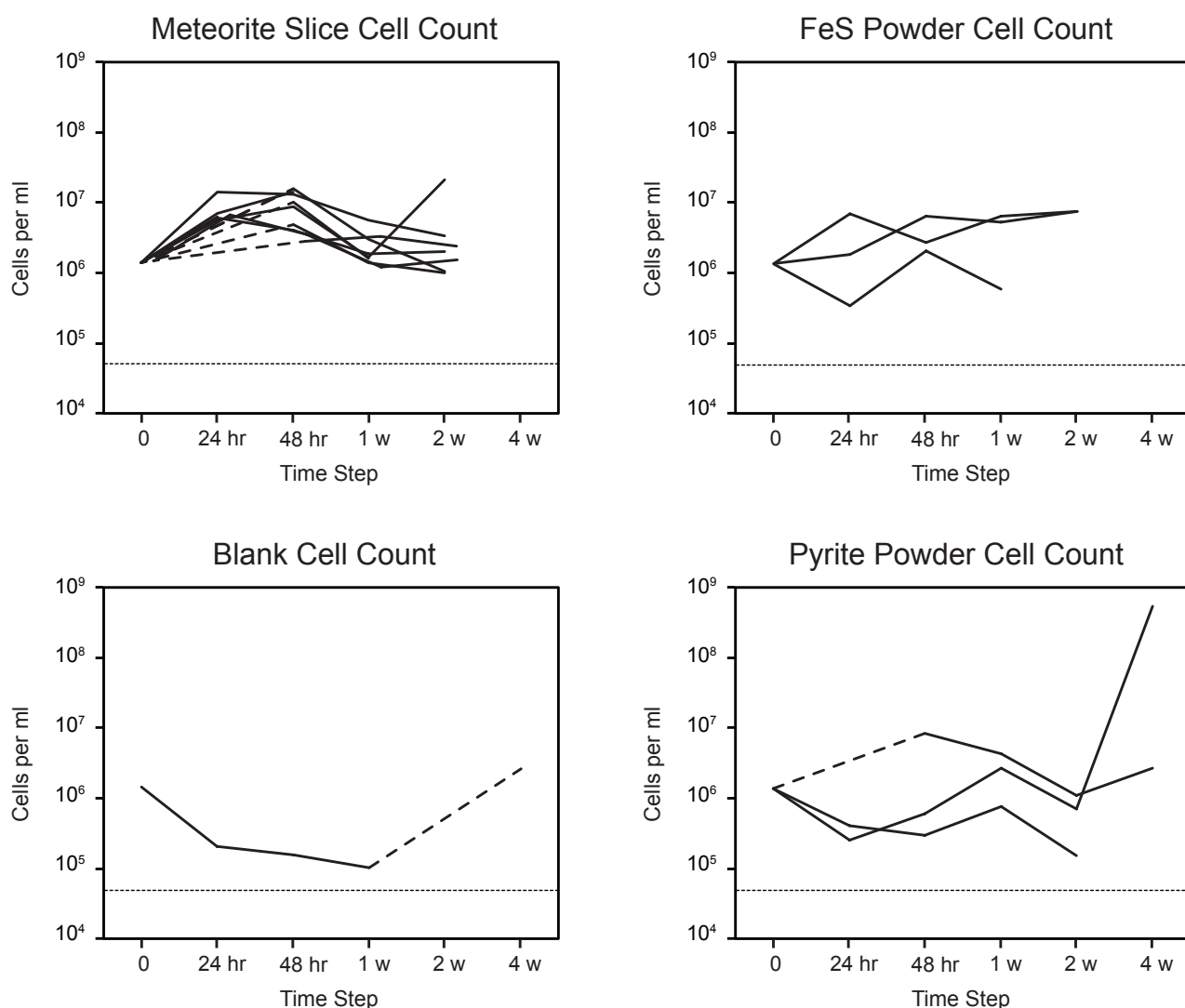


Figure 5.2 | Cell Counts in Supernatant. These four graphs show the concentration of cells mL^{-1} in the supernatant at each time step. Dashed lines represent a missing time step. The dotted line at the bottom of each graph is the minimum number of cells that can be counted in the chamber.

alteration minerals were obtained from the same samples used for XRD analysis. Samples of the initial reservoirs of sulfur were also analysed: the Chelyabinsk meteorite, synthetic troilite, pyrite and the $\text{FeSO}_4 \cdot 7\text{H}_2\text{O}$ used in the medium. In addition to the experimental samples, the carbonate–gypsum veins from two Nullarbor Plain meteorites (*Ooldea 006* and *Ooldea 007*) were selected for measurement of $\delta^{34}\text{S}$ values. Aqueous sulfate was only extracted successfully from the supernatant of one experiment, *Meteorite 11*, as BaSO_4 using the gravimetric method from Rayment and Higginson (1992). Stable sulfur isotope compositions were measured at the Stable Isotope Geochemistry Laboratory, School of Earth Sciences, at The University of Queensland using an Isoprime Continuous Flow – Stable Isotope Ratio Mass Spectrometer (CF-IRMS) coupled to an Elemental Analyser (EA). Stable sulfur isotope data are reported in per mil (‰) relative to Vienna Canyon Diablo Troilite (VCDT) with international standards IAEA-S1, S3 and NBS127 ($\delta^{34}\text{S}$ values are -0.30, -32.3 and

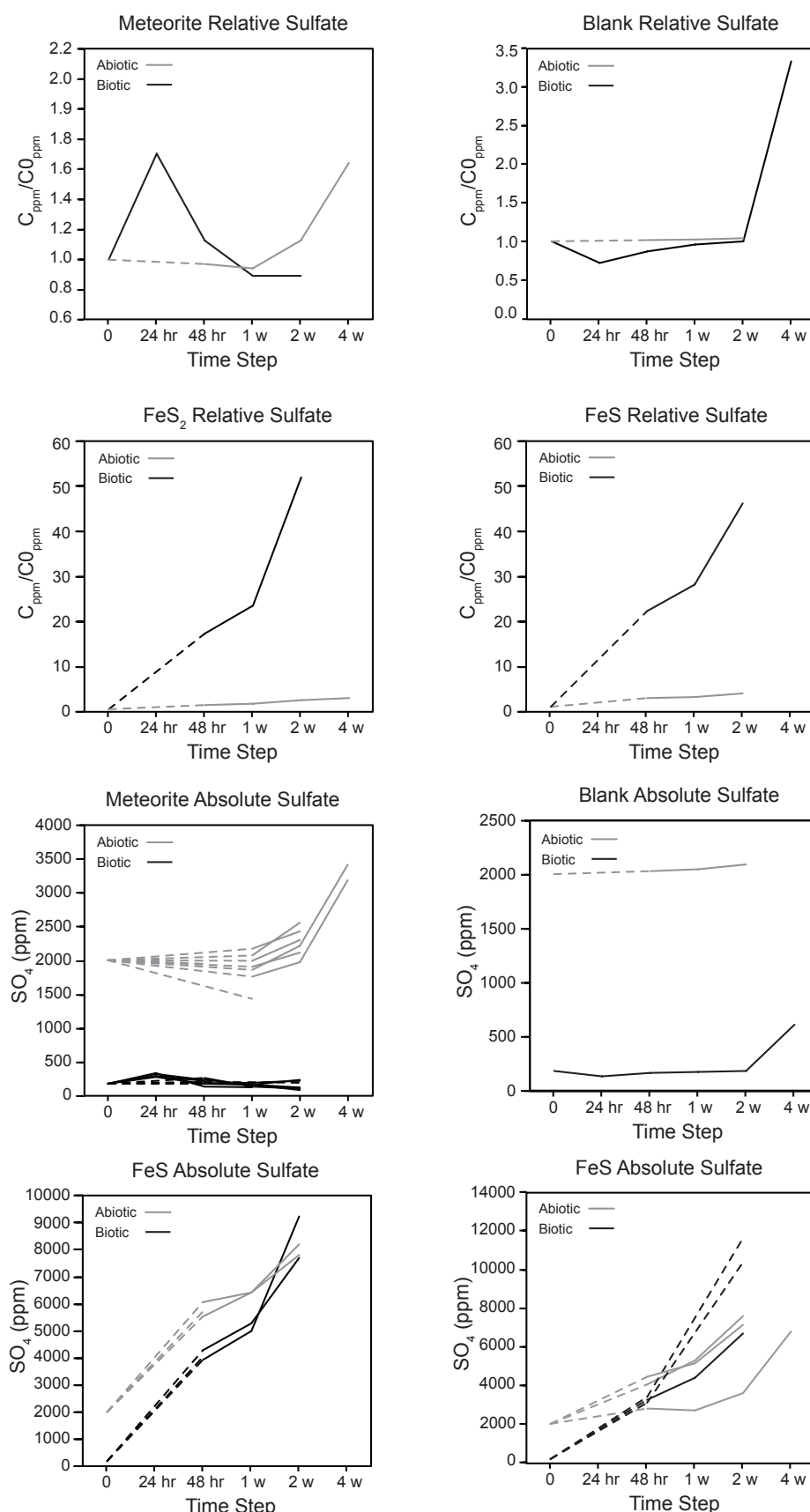


Figure 5.3 | Sulfate Analysis. Dissolved sulfate concentrations in each treatment throughout the experiments. The top four subfigures show the relative change in sulfate concentration compared to starting concentrations (biotic = 183.3 ppm, abiotic = 2006.3 ppm). Dotted lines represent missing data between measurements. The four upper subfigures plot average sulfate concentration for replicate experiments at each time step. The four bottom subfigures show the absolute concentration of sulfate for all experiments. Not all samples have week 4 data due to drying out.

+20.3‰ respectively) used to normalize the sample measurements via a 3-point calibration. Precision is $\pm 0.3\text{‰}$ at 1 standard deviation. Because this technique combusts all sulfur-bearing minerals in a sample together to produce SO_2 gas, the $\delta^{34}\text{S}$ values reported may reflect the compositions of multiple mineral phases in some cases.

5.3 Results

5.3.1 Cell-Counting and UV-Microscopy

During cell counting, we were able to make several observations about the bacteria in the supernatant. The meteorite incubations produced suspended grains of secondary sulfate minerals, such as gypsum and jarosite (confirmed by XRD analysis, see *Appendix II: Table 2*), that had numerous large communities of *A. ferrooxidans* attached to them (*Figure 5.1 A*), and in some cases, bacteria appeared to be trapped inside the mineral grains. There were no visible alteration minerals in the troilite and the pyrite experiments, and while cells were observed on the sulfide grains, these were far fewer than were observed on suspended sulfate grains in the meteorite experiments (*Figure 5.1 B*).

Cell counts in all meteorite experiments (using both fragments and polished thick sections) displayed a growth phase over the first 48 h, followed by a plateau in cell counts before a slow decrease (*Figure 5.2*). Overall their growth curve in the fluid phase is chaotic. In contrast, cell counts in the pyrite experiments increased over the first 48 hrs, with *Pyrite 32* finishing at 5.32×10^8 cells mL^{-1} . The troilite experiments showed an overall increase in cell counts from 1.40×10^6 cells mL^{-1} to finish on $\sim 7.80 \times 10^6$ cells mL^{-1} by week 3. Towards the end of the experiment, as samples began to dry out, there was less supernatant remaining which resulted in an apparent amplification of cell concentrations in this fluid. This is particularly noticeable in the blank and pyrite experiments (*Figure 5.2*). Surprisingly, cells were not dead in the blank experiments after 4 weeks, although they were smaller in size indicating nutrient stress. Abiotic controls remained free of microbial contamination throughout the experiment. One biotic meteorite treatments, Meteorite 4, developed contamination with what appeared to be a fungus; the results of this experiment were discarded from our final analysis.

5.3.2 Aqueous sulfate concentration

Sulfate concentrations for all experimental treatments throughout the 4-week incubation experiments are presented in (*Figure 5.3*). The initial sulfate concentrations for the biotic and abiotic experiments

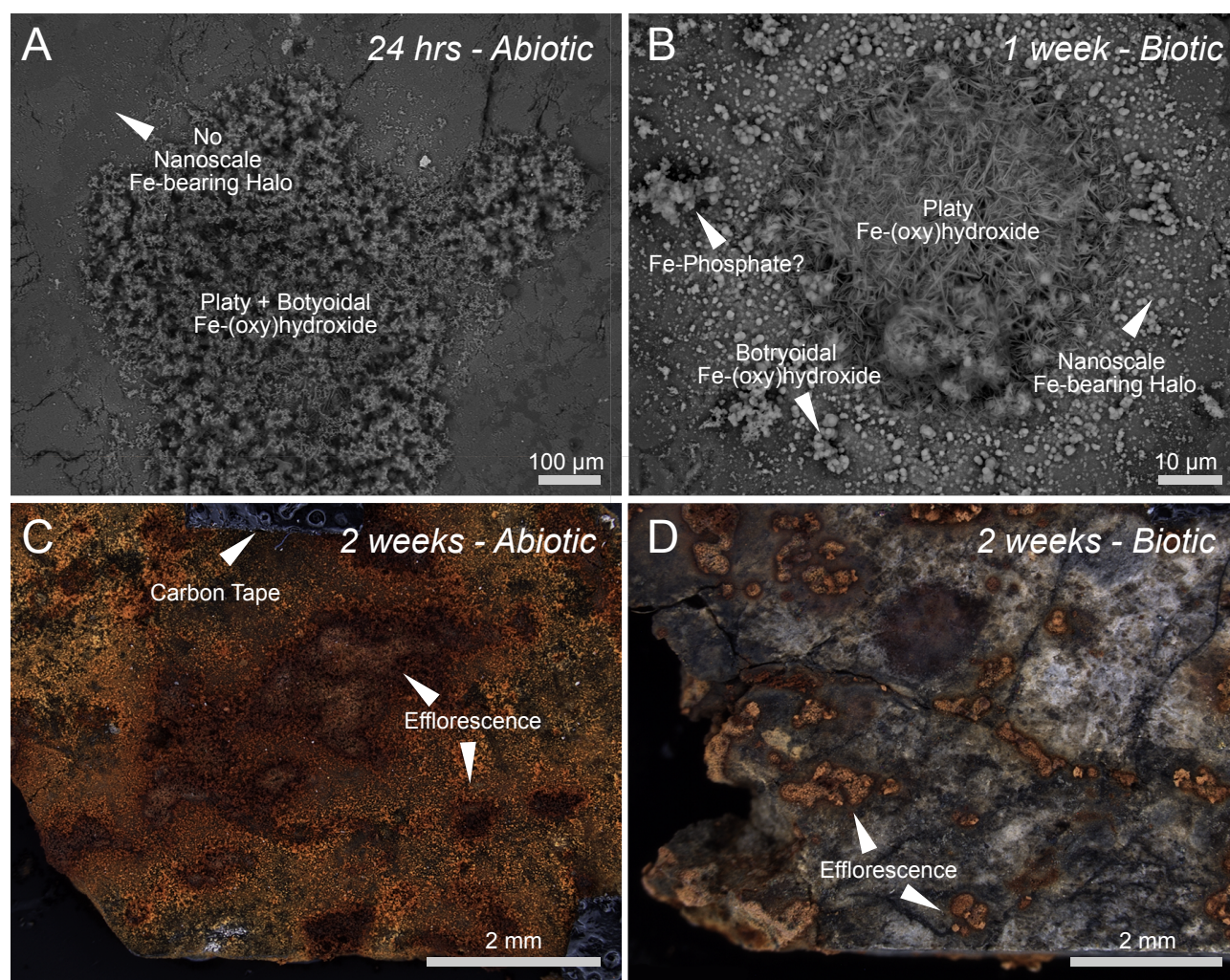


Figure 5.4 | Fe-(oxy)hydroxide Efflorescence and Surface Variation. These BSE and petrographic microscope images show polished sections of the Chelyabinsk meteorite from abiotic and biotic experiments at different time steps. **(A)** BSE image of an efflorescence at 24 hrs on *Meteorite 09*, an abiotic sample. The efflorescence is characterized by platy and botryoidal Fe-(oxy)hydroxides covering a FeS or FeNi grain. **(B)** An efflorescence on *Meteorite 12*, a biotic experiment, at one week. It is much thicker than the abiotic efflorescence and characterized by a core of predominantly platy material, surrounded by botryoidal Fe-(oxy)hydroxides and a halo of Fe-bearing nanoparticles. **(C)** A petrographic image of *Meteorite 11*, an abiotic experiment, at 2 weeks. Detrital Fe-(oxy)hydroxides and Fe-phosphates cover the thick section. What were once discrete efflorescences, have grown to coat most of the surface. **(D)** A petrographic image from the biotic *Meteorite 06* experiment at 2 weeks. The surface is relatively clear of efflorescences except for at the surfaces of FeNi-alloy and troilite grains, which bear extensive efflorescences. Although efflorescences are more numerous in biotic experiments, they are smaller than the abiotic ones.

were 183 ppm and 2006 ppm, respectively, with this difference being due to the mixing-trend experiments. Biotic experiments containing meteorite samples displayed a rapid increase in sulfate concentrations to 1.8 \times starting concentrations in the first 24 h of incubation. This was followed by an equally rapid decrease in sulfate to 1.1 \times the starting concentration at 48 h, where it plateaued and slowly decreased to $\sim 0.9\times$ starting concentration by the end of the experiment. In contrast, in abiotic

meteorite experiments sulfate concentrations initially remained relatively stable near the starting concentrations, before gradually increasing to 1.7× starting concentrations between 1 and 4 weeks. Results differed greatly between the meteorite and powdered sulfide experiments. The powdered troilite and pyrite experiments produced essentially the same trends. At the end of the biotic sulfide mineral experiments (i.e., after 4 weeks), they had yielded 60× more sulfate in solution than was initially present. Conversely, in this same time period sulfate concentrations in the abiotic experiments had only increased to 4× the initial starting concentration. Sulfate concentrations in the blank control experiments, which lacked a substrate, did not vary considerably throughout the abiotic experiments, but decreased to 0.7× starting concentration in the initial 24 hrs in the biotic experiments, before rising sharply to 3.3× starting concentration after 4 weeks.

Following 4 weeks of experimentation many of the experiments had dried out, meaning that no supernatant could be collected for sulfate analysis. Additionally, a technical issue resulted in missing data for the 24 h time step for several treatments.

5.3.3 Scanning Electron Microscopy on Mineral and Meteorite Surfaces

SEM images show textural differences between the biotic and abiotic polished meteorite specimens, which are related to the growth of Fe-(oxy)hydroxide efflorescences over FeNi alloy and troilite grains (*Figure 5.4*). These efflorescences are characterised by a central mound of platy Fe-(oxy)hydroxide minerals surrounded by a rim of botryoidal Fe-(oxy)hydroxides, and halos of nanoscale grains of Fe-bearing material. Intermixed with the Fe-(oxy)hydroxide crystals in the efflorescences are grains of phosphate minerals and biofilm. EDX analysis indicates that some of the efflorescences contain low abundances of sulfur but others do not; however, no crystalline sulfur-bearing mineral phases, such as jarosite $[\text{KFe}^{3+}_3(\text{OH})_6(\text{SO}_4)_2]$ or rozenite $[\text{Fe}^{2+}\text{SO}_4 \cdot 4\text{H}_2\text{O}]$, were observed by XRD in these samples, suggesting this sulfur must be present in a phase that is either poorly ordered or present in small quantities that are not detectable by XRD (<1 wt.%).

In contrast, abiotic samples formed fewer efflorescent crusts over polished grains of FeNi alloys and troilite (*Figure 5.4 A*). Their central mounds are a mixture of botryoidal and platy Fe-(oxy)hydroxides and phosphates; they are also thinner than their counterparts from the biotic experiments and were more homogenous in crystal habit (*Figure 5.4 B*). These efflorescences also contain fewer botryoidal grains of Fe-(oxy)hydroxides and, unlike the biotic samples, do not possess halos of Fe-(oxy)hydroxide nanoparticles at the surface of the meteorite samples. As in the biotic samples, while no sulfate

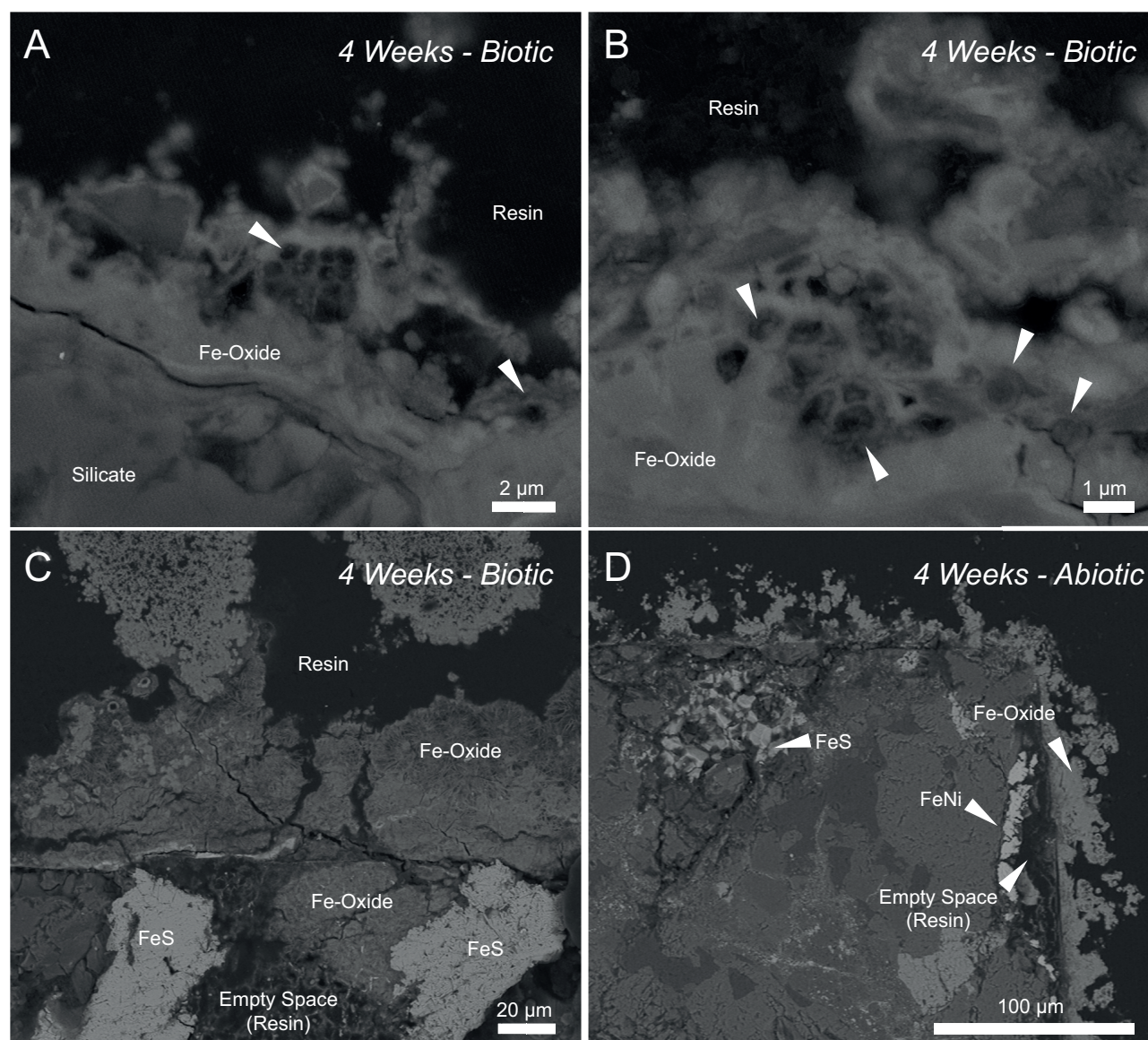


Figure 5.5 | SEM Images of Meteorite Cross-Sections. These BSE images were taken at the 4-week time step from biotic and abiotic samples that were Os stained and impregnated with resin. They show cross-sections through the meteorites and their weathering products. **(A, B)** Both images are of *Meteorite 20*. They show epilithic micro-colonies of *A. ferrooxidans* encased and fossilized within a layer of Fe-(oxy)hydroxide minerals. Arrows point to cells. **(C)** This image shows an efflorescence in cross section from *Meteorite 04*, a biotic experiment. Notice the efflorescence formed on a troilite grain that later was etched away to leave an empty space that is now filled with resin. **(D)** This is an image of *Meteorite 05*, an abiotic experiment. It shows troilite and FeNi-alloy grains that have been etched by the acidic media. As in the biotic samples, efflorescence can be seen forming over the grain, which is being etched away to leave a void.

minerals were found with XRD, EDX analyses showed a diffuse sulfur signature in association with the efflorescences (*Figure 5.4 A*).

Not all exposed grains of reduced sulfide phases developed efflorescences. This observation holds for both the biotic and abiotic experiments, but we are unsure why some grains formed efflorescences whereas others did not. In both the biotic and abiotic samples, thin crusts of Fe-(oxy)hydroxides that had formed over some troilite grains were cracked open during sample preparation for microscopy,

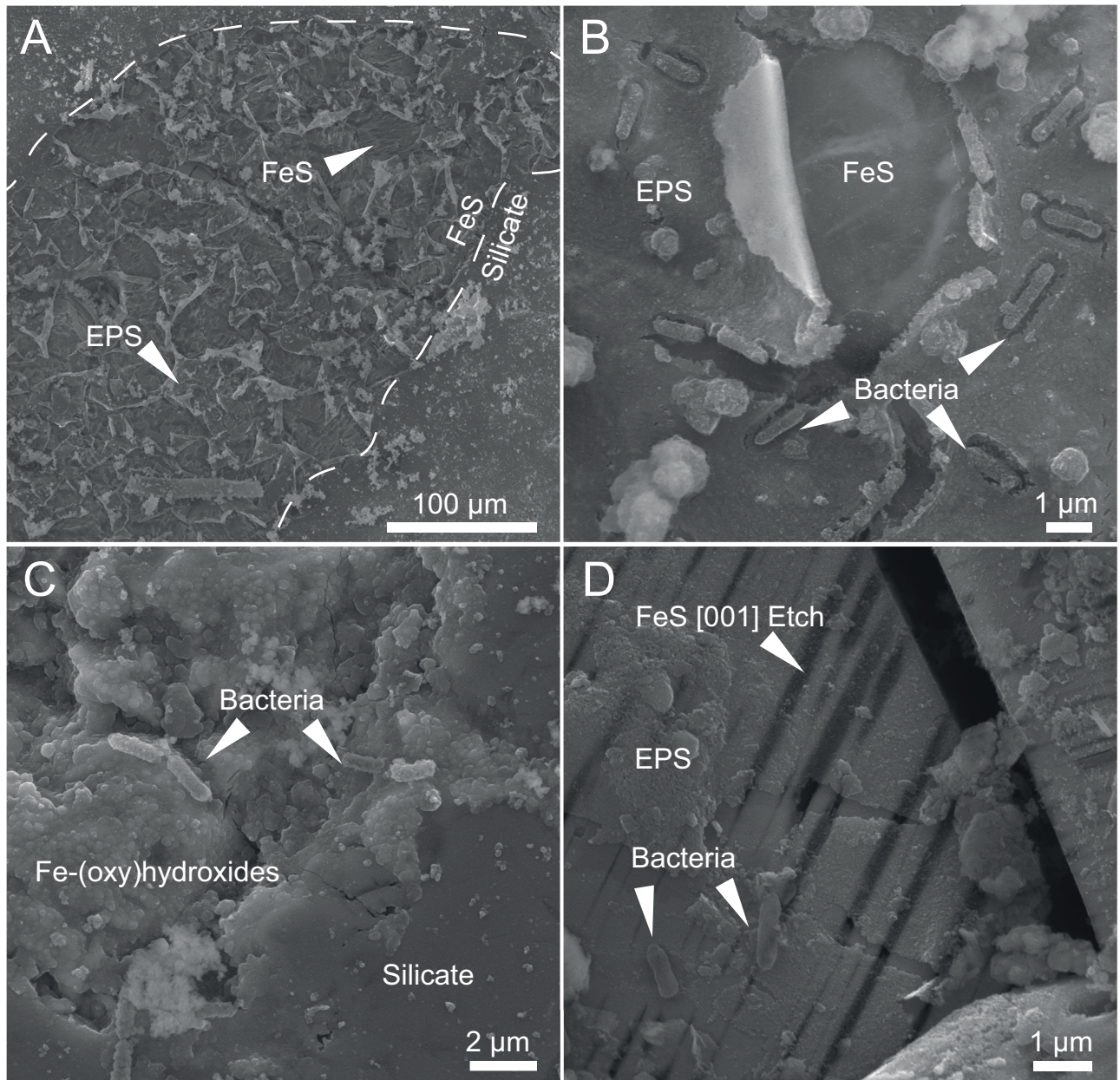


Figure 5.6 | Mineral-Microbe Spatial Relationships. These secondary electron images (SEI) are of *Meteorite 08*, from a biotic experiment, after 4 weeks. **(A)** A large FeS grain (dotted line) is covered in EPS, which has peeled back in places. This EPS does not extend to the silicate minerals surrounding the troilite grain. The sulfide grain is extensively etched. **(B)** This micrograph is from the same sulfide grain in *(A)*. It shows the EPS peeling back to expose the troilite underneath. *A. ferrooxidans* cells can be seen embedded in the mineralized biofilm. **(C)** This shows a pitted and weathered FeNi-alloy grain surrounded by silicate minerals. From the polished surface of the silicate grain it is clear that the metal alloy grain has become recessed by $\sim 2\ \mu\text{m}$. The grain is covered in Fe-(oxy)hydroxide grains and bacteria that are covered in the same material. **(D)** This shows a troilite grain with etched [001] planes. It is covered by a thin film of EPS and a few bacteria.

allowing the grains underneath to be viewed. These crusts appear to have had the effect of promoting etching of the reduced grains, possibly by concentrating and immobilising the sulfuric acid generated by weathering at the mineral interface (*Figure 5.5 C, D*). Curiously, in these same samples some of the efflorescent crusts appeared to have the opposite effect, protecting reduced grains from further

acid attack by providing an impermeable barrier once the acid generated by the initial reaction was neutralised. Both these textures could be seen in the same sample, indicating what ever the cause that drove the different textures was extremely localised.

Efflorescent crusts formed within as little as 24 hrs, but were more common in the experiments after 1 week. By week 2, the abiotic samples were almost completely covered in platy or botryoidal grains of Fe-(oxy)hydroxides and phosphates (*Figure 5.4 C*). The small efflorescences that were initially restricted to the surfaces of FeNi alloy and troilite grains were either overgrown or had spread beyond the surface footprint of these grains. Very different textures were observed in the biotic samples from 2 weeks onward: they had comparatively unaltered surfaces, marked only by a few detrital grains of Fe- and Ca-phosphates, while efflorescence growth had slowed or ceased (*Figure 5.4 D*).

Samples from the biotic experiments all showed *A. ferrooxidans* cells on grains of reduced phases. At 24 hrs, FeNi alloys and troilite grains showed localised etching and many reduced grains had been consumed, leaving behind corrosion pits coated in dried EPS. Evidence of silicate dissolution could be seen around the edges of these pits. Cells can occasionally be seen within the web of EPS and more may be present deeper within the etched pits (see resin cross section results). Many troilite grains showed geometric pitting or dissolution along the [001] twinning plane (ZURFLUH *ET AL.* 2013) (*Figure 5.6 D*) and were covered sparsely by EPS. By 4 weeks some troilite grains were covered in a diffuse layer of cells connected by their biofilm (*Figure 5.6 A, B, D*), which had shrunk and peeled back in places during sample preparation to reveal the troilite below. Extensive geometric pitting of troilite could also be seen after 4 weeks; however, not every grain was pitted to the same extent, with some appearing less altered than others. Interestingly, there were very few cells on the less altered troilite. Many of the surfaces of troilite grains were recessed by the end of the experiment and some cells were starting to be covered in a mineral precipitate (*Figure 5.6 C*).

5.3.4 Cross Sections Through Meteorite Samples

Following incubation, the experimental samples were cross-sectioned for inspection of efflorescence interiors using SEM. At 4 weeks, there were notable differences between the thickness of efflorescences on meteorites incubated in biotic ($n = 8$, median = $71.7 \pm 74.3 \mu\text{m}$) versus abiotic ($n = 7$, median $30.23 \pm 26.7 \mu\text{m}$) media, with the crust being, on average, twice as thick in biotic treatments. Additionally, in the biotic samples, epilithic micro-colonies of *A. ferrooxidans* were seen encased in Fe-(oxy)hydroxides (*Figure 5.5 A,B*). These cells appear to have been cut tangentially. Cells were not observed at the base

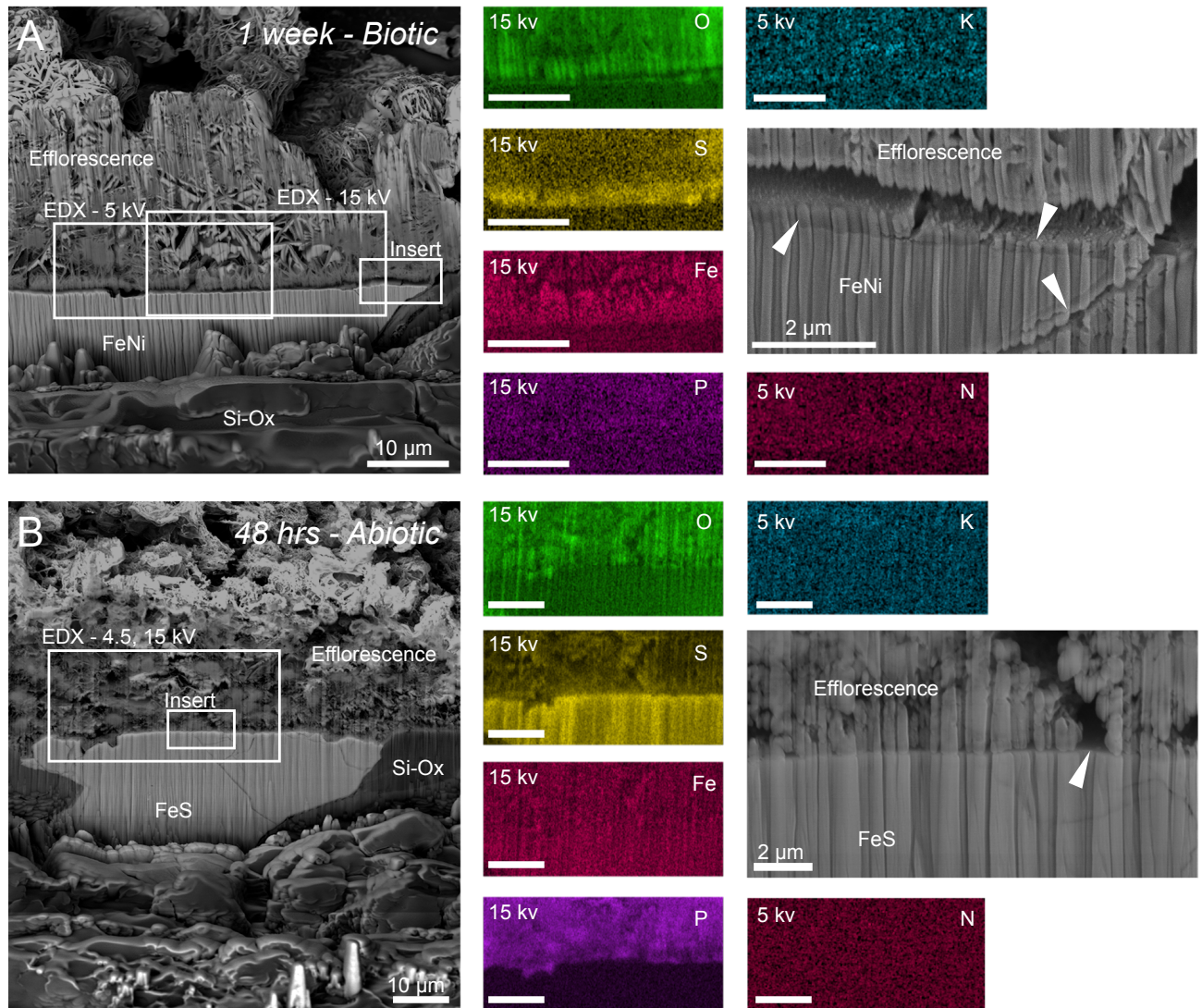


Figure 5.7 | Focused Ion Beam cross-section and SEM EDX maps. These images show meteorite samples from one biotic and one abiotic experiment. Each sample had a Focused Ion Beam (FIB) trench cut through an efflorescence into the underlying substrate. Both images were tilted to 38° from the EDX detector. These BSE images were horizontally compressed to adjust for the 50° tilt used on the SEM whilst EDX mapping. Displayed in both images are quantitative element maps of elements (i.e., O, S, Fe, P, N, and K) that include a semi-quantitative measure of elemental abundance in wt.%. Both 5 kV and 15 kV accelerating voltages were used; images collected at 5 kV were binned twice. Vertical striations are FIB cutting artefacts due to the uneven specimen surface. **(A)** This image shows the biotic sample, *Meteorite 12*, at 1 week. The underlying substrate is FeNi-alloy. A distinct gap can be seen at the interface between the FeNi-alloy grain and efflorescence, indicated by a sulfur- and oxygen-rich interlayer (insert: arrows). A thin layer containing elevated phosphorus, potassium and nitrogen is also observed at this interface. **(B)** SEM micrograph of the abiotic sample, *Meteorite 17*, at 48 hrs. The underlying substrate is troilite. There is no gap at the interface between the FeS grain and the efflorescence and the contact between them is very sharp. There is no oxidized interlayer (insert: arrowheads). The efflorescence in the abiotic sample is more phosphorus-rich than the biotic sample. No noticeable potassium or nitrogen layer exists in the abiotic efflorescence.

of the Fe-(oxy)hydroxide efflorescences where the phase forms an interface between the troilite and FeNi grains.

It would appear that, in both biotic and abiotic samples, efflorescences initially grew at the FeNi alloy

and/or troilite grain surfaces, but the continued etching of the chemically reduced interface eventually left voids beneath (*Figure 5.5 C, D*). Grains of reduced phases deep within the meteorite samples (i.e., 500 μm from the surface) were sometimes etched away as well. This did not happen to all grains, only to those connected to the surface of the sample by crack networks were corroded. Altered grains that appeared isolated in cross-section were probably connected to cracks present beneath the surface of the sample or that had been cut away. Unfortunately, much of the material at the contact between reduced grains and oxidation products was displaced during polishing, indicating the weathering products were soft. Therefore, FIB-SEM was used to study this interface.

5.3.5 Focused Ion Beam - Scanning Electron Microscopy

Use of the FIB-SEM allowed for cross-sections to be made through efflorescences with a higher acuity and higher specificity than with a wire saw. Because the alteration minerals covering efflorescent crusts were not indicative of the mineral substrate underneath, we exhumed different substrates for the biotic sample, *Meteorite 12* (FeNi alloy), and the abiotic sample, *Meteorite 17* (troilite). EDX maps revealed that the biotic sample (*Figure 5.7 A*) had a complex elemental composition at the interface between the FeNi grain and its alteration products. The contact between the troilite grain in the abiotic sample and the overlying efflorescence had a much simpler and more homogenous elemental composition in the elements measured (e.g., O, P, K, N, S, Fe) (*Figure 5.7 B*). However, in the biotic experiment there was a void of $\sim 1\ \mu\text{m}$ height that ran along the interface between the FeNi grain and efflorescence; no such gap was seen in the abiotic sample. A 100–300-nm thick layer of oxygen rich material lines the edges of the gap in the biotic sample. The abundance of oxygen appears to be greater on the FeNi side of the gap where small perforations can be seen on the surface of the interlayer near the void space (*Figure 5.7 A*). This more oxidised layer does not exist in the abiotic sample. Also, where Fe-(oxy)hydroxide crystals have grown into each other to create a gap, the troilite grain appears smooth, which differs from the irregular surface of the FeNi grain the biotic sample (*Figure 5.7 B*). A 2- μm thick sulfur-rich layer can be seen above the FeNi grain in the biotic sample. This sulfur-rich layer is not present in the abiotic sample, despite the substrate being a troilite grain and being treated with the 10 \times enrichment of sulfate compared to the initial medium. In the biotic sample, very low abundances of biologically important phosphorus, potassium and nitrogen are detected in EDX maps in the sulfur-bearing layer. Phosphorus, which was introduced in the culture medium, gives a strong EDX signal in the abiotic sample and it is more homogeneously distributed throughout the efflorescence compared to the

Table 5.1| $\delta^{34}\text{S}$ Values for Experimental Precipitates and Substrates

<i>S Bearing Phase²</i>	<i>Material ID</i>	<i>Biotic/ Abiotic</i>	<i>Type</i>	<i>Time Step</i>	$\delta^{34}\text{S}_{\text{VCDT}} \%$	<i>Weight (mg)</i>	<i>f_{Std}</i>	<i>f_{Sulf}</i>
Gypsum	Meteorite 14	Biotic	Efflorescence	Week 4	1.5	3.70	-	-
Gypsum	Meteorite 18	Biotic	Efflorescence	Week 4	4.0	3.15	-	-
Rhombochase	Meteorite 07	Abiotic	Efflorescence	Week 4	-0.1	2.00	0.83	0.17
x	Meteorite 13	Abiotic	Efflorescence	Week 4	-1.2	3.00	0.35	0.65
S ⁰ , Troilite, Melanterite, Iron Sulfate Hydroxide	Troilite 28	Biotic	Efflorescence	Week 4	18.7	1.25	-	-
Gypsum	Ooldea 006	Natural	Vein Material	-	2.1	6.50	-	-
Gypsum	Ooldea 007	Natural	Vein Material	-	6.8	6.70	-	-
S ⁰ , Melanterite	Troilite 28	Biotic	Evaporite	Week 4	16.8	2.50	-	-
Gypsum, Jarosite, Rozenite, Woodhouseite	Troilite 27	Abiotic	Evaporite	Week 4	13.2	0.60	0.73	0.27
Gypsum, Rozenite	Troilite 28	Biotic	Pellet	Week 2	17.8	0.65	-	-
x	Pyrite 33	Abiotic	Pellet	Week 2	14.6	0.37	0.70	0.40
Barium Sulfate	Meteorite 07	Abiotic	BaSO ₄	Week 2	-1.3	0.34	0.30	0.70
Pyrite	Pyrite	-	Standard	-	21.8	0.17	-	-
Troilite	Troilite	-	Standard	-	18.7	0.35	-	-
Melanterite	Melanterite	-	Standard	-	-2.0	0.70	-	-
Troilite	Chelyabinsk	-	Standard	-	0.3	6.00	-	-

¹Precision for $\delta^{34}\text{S}$ is $\pm 0.3 \%$ at 1 standard deviation. International standards IAEA-S1, S3 and NBS127 were used for calibration using a 3-point normalization.

²The "x" denotes that no XRD sample was run for that sample.

localized and low-abundance layer in the biotic sample. It is important to note that the EDX spectra of phosphorus and platinum (used to coat the top of the sample, but not the FIB-cut face) suffer from some peak overlap. Although not ideal, we are using spatial relationships to constrain detection of platinum versus phosphorus. No obvious layer enriched in nitrogen or potassium was detected in the efflorescence examined in the abiotic sample. Unfortunately, our analysis did not resolve the presence of carbon because the protective window on the EDX detector limits its sensitivity to elements of low atomic number.

5.3.6 Powder X-Ray Diffraction

XRD results showed that the samples chosen for stable sulfur isotope analysis contained common minerals associated with low pH weathering and acid mine drainage environments, including lepidocrocite [$\gamma\text{-FeO}(\text{OH})$], ferrihydrite [$\text{Fe}_{10}^{3+}\text{O}_{14}(\text{OH})_2 \cdot n\text{H}_2\text{O}$] (MICHEL ET AL. 2010), goethite,

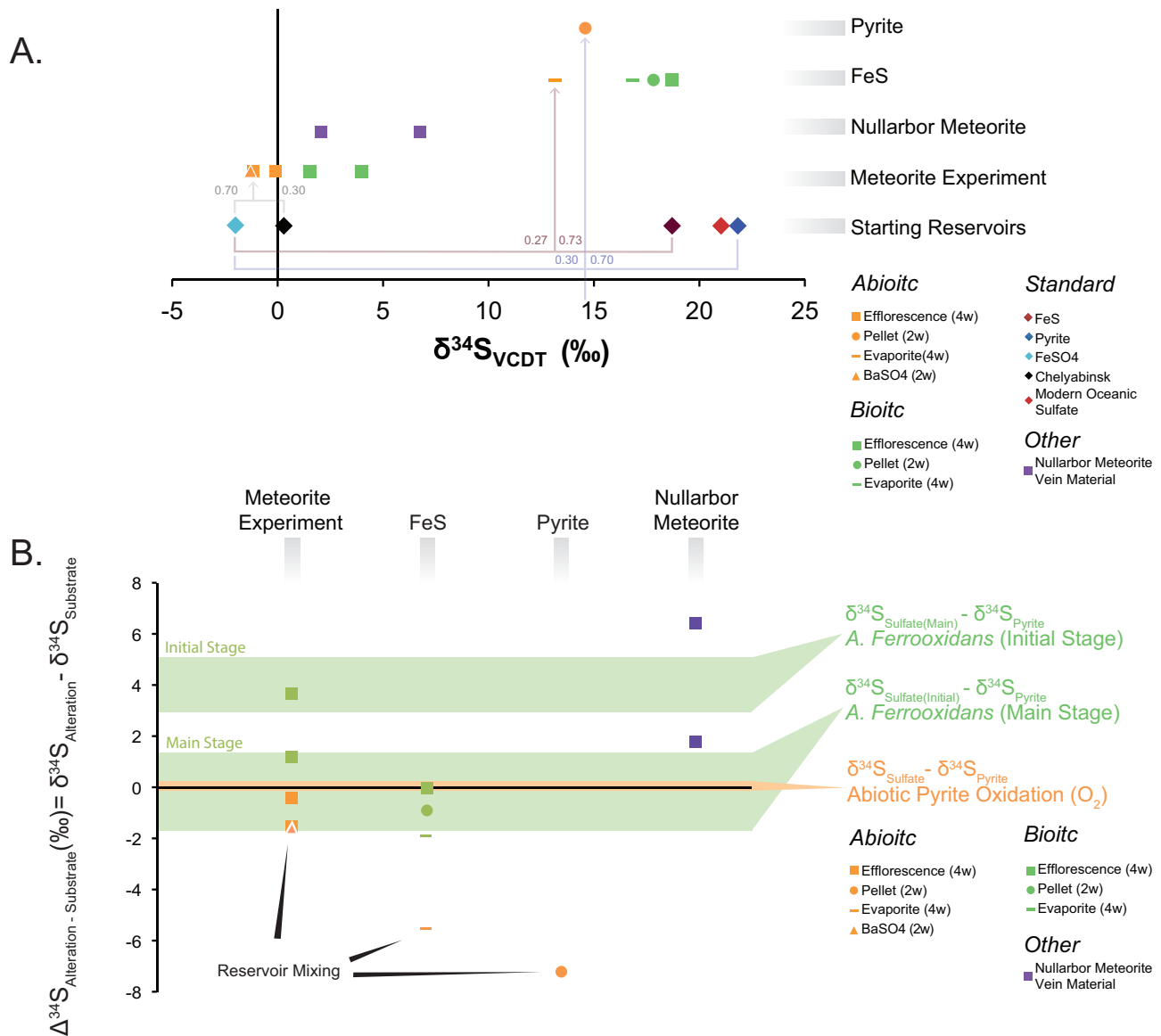


Figure 5.8 | $\delta^{34}\text{S}$ results. This figure shows the $\delta^{34}\text{S}$ results from the CF-IRMS analysis. Not all samples gave results due to their small size. **(a)** The bottom row of values shows the starting isotopic reservoirs, whereas the upper rows show results from biotic (Green) and abiotic (orange) experiments. The abiotic values in the meteorite experiment plot close together, the symbols are efflorescence (Square), BaSO₄ (triangle with white outline). The biotic meteorite experiment produces positive fractionation away from the starting reservoir (chondritic troilite), indicating biological sulfur assimilation. In all abiotic experiments, abiotic oxidation of the substrate resulted in a negative fractionation. Linear mixing trends between reservoirs and fractional contributions to sulfate in alteration minerals are indicated. **(b)** Isotopic differences between alteration products and substrates used in experiments (e.g., meteoritic troilite, synthetic troilite powder, pyrite powder). The green shaded fields are the fractionation ranges of sulfates produced during the ‘initial’ and ‘main’ stages of biotic pyrite leaching experiments in Brunner et al. (2008). The orange field is the abiotic oxidation of pyrite by O₂ (BALCI ET AL. 2007). Note that the abiotic fractionations do not plot in the field for abiotic sulfide oxidation. This is the result of reservoir mixing with ‘contaminant’ sulfate (i.e., melanterite in the medium).

gypsum and jarosite (KARATHANASIS AND THOMPSON 1995) (*Appendix II: Table 2*). A variety of other sulfate and phosphate minerals were also produced, including: archerite $[(\text{K},\text{NH}_4)\text{H}_2\text{PO}_4]$, rhomboclase $[\text{HFe}^{3+}(\text{SO}_4)_2 \cdot 4\text{H}_2\text{O}]$, melanterite $[\text{FeSO}_4 \cdot 7\text{H}_2\text{O}]$, pentahydrate $[\text{MgSO}_4 \cdot 5\text{H}_2\text{O}]$, anhydrite $[\text{CaSO}_4]$, voltaite $[\text{K}_2\text{Fe}^{2+}_5\text{Fe}^{3+}_3\text{Al}(\text{SO}_4)_{12} \cdot 18\text{H}_2\text{O}]$, kieserite $[\text{MgSO}_4 \cdot \text{H}_2\text{O}]$, sabieite $[(\text{NH}_4)\text{Fe}^{3+}(\text{SO}_4)_2]$, and rozenite. Melanterite and archerite, which were used in the medium, were observed to re-precipitate as experiments dried out. Every experiment – both biotic and abiotic – produced one or more sulfur-bearing mineral phase(s) (*Appendix II: Table 2*).

Residual troilite was also detected in some of the samples collected for XRD and $\delta^{34}\text{S}$ analysis (*Meteorite 2, Meteorite 7, Meteorite 11, Troilite 28*). Other substrate minerals that were detected were: forsterite $[\text{Mg}_2\text{SiO}_4]$, ferrosilite $[(\text{Fe}^{2+},\text{Mg})_2\text{Si}_2\text{O}_6]$, anorthite $[\text{CaAl}_2\text{Si}_2\text{O}_8]$ and albite $[\text{NaAlSi}_3\text{O}_8]$, but not all in the same sample. A broad, intense asymmetric peak was detected in some of the biotic samples at $\sim 11.8^\circ 2\theta$. This peak corresponds to the (020) peak of gypsum and brushite $[\text{CaHPO}_4 \cdot 2\text{H}_2\text{O}]$. These minerals are isostructural and have been found to coexist in experiments using *A. ferrooxidans* previously (LI ET AL. 2013). The breadth of the peak and the low intensity of our patterns (which were collected from minute amounts of powder) make it difficult to distinguish between these minerals. None of the abiotic meteorite experiments contained gypsum or brushite. Also, many of the experiments yielded very little material for XRD, thus our patterns commonly had low counts and low signal to noise ratios. This meant that some phases could only be tentatively identified where present at minor abundance.

5.3.7 Stable Sulfur Isotopes

Stable sulfur isotope measurements were obtained successfully for 16 samples, including: five efflorescences from substrate surfaces, two samples of evaporite minerals collected from the walls of Petri dishes containing experimental substrates, two pellets (separated by centrifugation), one BaSO_4 sample precipitated from aqueous sulfate, three samples of unaltered sulfide minerals, the melanterite used in the medium, and two natural carbonate–gypsum vein samples from Nullarbor meteorites (see *Table 5.1*). Supernatant sulfate samples (as BaSO_4) and pellet samples were taken at the penultimate time step, week 2. Of these samples, only a single BaSO_4 sample gave a $\delta^{34}\text{S}$ result due to the abundance of sulfate minerals and the concentration of aqueous sulfate being below detection on the MultiskanTM GO instrument. Samples of evaporite minerals (dried material in the Petri dish) and alteration products (efflorescences) removed from the surfaces of reduced mineral substrates were

taken at the end of the experiments in Week 4. Not all experiments developed evaporites at the edges of Petri dishes, and the experiments using pyrite did not form any visible alteration crusts that could be sampled from this substrate for analysis.

Troilite from the Chelyabinsk meteorite gave a $\delta^{34}\text{S}$ value of 0.3‰, consistent with the previously reported value of 0.31‰ (IGNATIEV *ET AL.* 2013), indicating that the Chelyabinsk troilite is somewhat more enriched in ^{34}S than troilite in most ordinary chondrites (GAO AND THIEMENS 1993). The synthetic troilite and natural pyrite substrates, and the melanterite used in the medium, gave $\delta^{34}\text{S}$ values of 18.7‰, 21.8‰, and -2.0‰ respectively (see *Figure 5.8 A* and *Table 5.1*). The sulfate-bearing alteration products of meteorites ($n = 4$) gave distinctly different $\delta^{34}\text{S}$ values for the biotic experiments (1.5‰ and 4.0‰) and abiotic experiments (-0.1‰ and -1.2‰). The mean isotopic difference, $\Delta^{34}\text{S}_{\text{SO}_4-\text{FeS}}$, between the biotic samples and Chelyabinsk troilite is 2.8‰. The abiotic experiments give a mean $\Delta^{34}\text{S}_{\text{SO}_4-\text{FeS}}$ value of -0.7‰ (*Figure 5.8 B*).

$\delta^{34}\text{S}$ values could not be obtained from all experiments that used pyrite and troilite, as contamination from the powdered substrate could overprint the alteration signature. The alteration products from one biotic troilite experiment recorded a $\delta^{34}\text{S}$ value of 16.8‰, which corresponds to $\Delta^{34}\text{S}_{\text{SO}_4-\text{FeS}} = -1.9‰$. The evaporite sample from the abiotic troilite experiment gave a $\delta^{34}\text{S}$ value of 13.2‰, which reflects a $\Delta^{34}\text{S}_{\text{SO}_4-\text{FeS}}$ value of -5.5‰. Only one sample from the pyrite experiments yielded a $\delta^{34}\text{S}$ value, a pellet sample from an abiotic pyrite experiment, which gave a $\delta^{34}\text{S}$ value of 14.6‰ and a $\Delta^{34}\text{S}_{\text{SO}_4-\text{FeS}_2}$ value of -7.2‰.

$\delta^{34}\text{S}$ values from natural carbonate–gypsum vein samples in *Ooldea 006* ($\delta^{34}\text{S} = 2.6‰$) and *Ooldea 007* ($\delta^{34}\text{S} = 6.7‰$) were similar in magnitude to the $\delta^{34}\text{S}$ values from biotic meteorite experiments. As the *Ooldea* meteorites used in this study are H chondrites we can use the $\delta^{34}\text{S}$ value for troilite in H chondrites from Gao and Thiemens (1993) of -0.02‰, $n = 4$ to calculate an isotopic difference of $\Delta^{34}\text{S}_{\text{SO}_4-\text{FeS}} = 2.6‰$ for *Ooldea 006* and $\Delta^{34}\text{S}_{\text{SO}_4-\text{FeS}} = 6.7‰$ for *Ooldea 007*.

5.4 Discussion

5.4.1 Fossilisation of Bacteria During Sulfide Oxidation

SEM images of cross-sections through biotic samples commonly show epilithic micro-colonies of *A. ferrooxidans* at the surface of *Meteorite 20* (*Figure 5.5 A, B*). In thick section, these cells appear as hollow shapes with light coloured cell walls under BSE (owing to the Os stain and their association

with Fe-bearing minerals). For this reason, we are confident they are micro-colonies of *A. ferrooxidans*. What is important from a preservation standpoint is that the microcolonies are commonly entombed under >1- μm thick coating of Fe-(oxy)hydroxides (Figure 5.5 A, B). It may be that many of the cells have been coated in Fe-(oxy)hydroxide minerals, which would explain why SEM images of the meteorite surfaces show very few microbes. Consistent with previous studies that show iron oxides preserve microfossils on geological time scales (PRESTON ET AL. 2011), our data suggest that meteorites may also have the capacity to preserve microfossils of environmental bacteria in Fe-(oxy)hydroxide coatings.

Fewer *A. ferrooxidans* cells were observed at the surface of experimental substrates than were expected based on cell counting, possibly because they were pelagic or on the surfaces of suspended grains (e.g., Figure 5.1). The apparent scarcity of *A. ferrooxidans* cells on the surfaces of sulfide grains is not uncommon in culture experiments (YU ET AL. 2001) and our SEM images shed light on this, with cross-sectioned samples showing bacteria buried within 1–20 μm thick crusts of Fe-(oxy)hydroxide minerals (Figure 5.5 A, B).

Thicker Fe-(oxy)hydroxide efflorescences were produced in biotic experiments compared to the abiotic counterparts and they do not seem to contain any microorganisms at the surface or at depth. This may be an artefact of our sample preparation given that some efflorescent crusts suffered loss of material during polishing at the interface between the oxidised and reduced minerals, which is where we would expect microbes to be present. However, FIB prepared cross-sections did not reveal textures that could be associated with microbes either (Figure 5.7 A), and although EDX revealed the presence of a metabolite-rich layer, this may have been associated with a biofilm. The volume ratio of Fe-(oxy)hydroxide to organisms is quite high in the meteorite samples, which is why the bacterial population did not appear that numerous on troilite grains at the end of the experiment, despite grains showing numerous etch pits and mineral coatings (Figure 5.4 B, D). A large amount of mineral weathering product is to be expected given the low energy gain from iron oxidation under acidic conditions ($\Delta G^\circ = -8.7 \text{ kJ mol}^{-1}$; (POPA ET AL. 2012). We can also estimate the maximum number of cells that could cover the meteorite thick sections by multiplying the surface area of the meteorite slice ($\sim 0.5 \text{ cm}^2$) by the proportional abundance of FeNi alloy and troilite (JAROSEWICH 1990), and dividing that value by the surface area of a cell ($\sim 2 \mu\text{m} \times \sim 0.5 \mu\text{m} = \sim 1 \mu\text{m}^2$). The estimated number of cells that each meteorite slice could support as a monolayer on the surface of the metal and troilite grains is $\sim 3.2 \times 10^6$. Based on the cell counts in the media, 10^6 – $10^8 \text{ cell mL}^{-1}$ (Figure 5.2), most of the cells in

the experiment would have been pelagic.

It is worth pointing out that the efflorescences exist in both the biotic and abiotic samples (*Figure 5.4*), so the efflorescences themselves are not a diagnostic biogenic feature. The efflorescences are quite porous, which would allow for ingress of culture medium (water) and abiotic mineral growth without microbes being required. Where microbes are present on troilite grains at the week 4 sampling interval (*Figure 5.6*), they formed thin, ~1- μm thick, biofilms and extensive coatings of EPS, and although they etched the sulfides, they did not form large efflorescences (*Figure 5.6 A, B*). Also, many of the pits left behind by oxidative weathering of troilite started to infill with Fe-(oxy)hydroxides and the microbes within the pits became coated with mineral precipitates (*Figure 5.6 C*). This could mark a shift to higher pH within the medium as a result of buffering by silicate mineral dissolution. *A. ferrooxidans* starts to develop precipitates on its surface and becomes increasingly unable to diffuse H^+ across its membrane when the pH becomes >2.3 (LIU *ET AL.* 2009). Thus, a change in pH conditions could trigger fossilisation of *A. ferrooxidans* by Fe-(oxy)hydroxides. This could also be evidence of a shift in metabolism towards iron oxidation with the excess of ferrous Fe^{2+} in the media (BRUNNER *ET AL.* 2008). Experiments were not agitated during the 4 weeks, so the possibility of localized pH conditions exists. This could help to explain why some *A. ferrooxidans* cells were encased in and hidden beneath a layer of Fe-(oxy)hydroxide, whereas others were beginning to develop precipitates and still others formed thin biofilms on sulfide grains, all within the same sample.

5.4.2 Elemental and Mineralogical Biosignatures in Biotic Experiments

The turbidimetric sulfate concentration data (*Figure 5.3*) for the biotic meteorite experiments show a decrease in the amount of sulfate after the 24 hr time step. This sulfate was either precipitated as sulfate minerals or assimilated as organosulfur. Production of aqueous sulfate had slowed after this time, indicating a change in the metabolism of *A. ferrooxidans* to favour oxidation ferrous iron (BRUNNER *ET AL.* 2008), which is associated with both troilite and FeNi alloy minerals. Our images from the FIB cross-section (*Figure 5.7*) of an Fe-(oxy)hydroxide efflorescence from a biotic meteorite sample show complex, heterogeneous stratification of S, O, K, N, and P associated with the surface of the FeNi grain and the overlying efflorescence. The efflorescence examined in the abiotic sample had no such layering or concentration of bioessential elements and it is relatively homogeneous in its elemental distribution. Similarly complex layers, showing elemental and isotopic heterogeneity, have been observed in other experiments involving the oxidation of pyrite using *A. ferrooxidans*, and this feature

is thought to be related to biological alteration (PISAPIA *ET AL.* 2007). The presence of these elements could indicate that small amounts of S^0 , sulfate or intermediate species were forming at the interface of the metal/sulfide grains. If these phases are crystalline, they appear to be below the detection limits of our XRD analysis, which is expected for analysis of very small samples. Bioleaching studies have also shown that in acidic conditions (such as those present in our experiment) native sulfur can crystallise, become suspended (i.e., transported) and form layers on the surfaces of metal-sulfide grains (e.g., (ROHWERDER *ET AL.* 2003)). This is comparable to what we observe for the FeNi alloy grain. This layering of sulfur can hinder leaching kinetics in the absence of microbes and in their presence, if the microbes are obstructed from attaching to the sulfide grains. Similarly, an increase the population of sulfur oxidising bacteria can cause this sulfur layer to be oxidised due to the increased production of aqueous Fe^{3+} (FOWLER AND CRUNDWELL 1999). Thus, these metabolite layers likely reflect the initial abiotic build up of S^0 while cell counts were still quite low. Once cell counts increased, and the ratio of aqueous $\text{Fe}^{3+}:\text{S}$ increased, the bacteria may have then been able to oxidise and/or assimilate the elemental sulfur layer which resulted in no further S^0 stratification. This heterogeneity does not exist in the abiotic samples, lending strength to our interpretation that there was a higher Fe:S ratio in the biotic meteorite samples due to regeneration of aqueous Fe^{3+} . We interpret this sulfur stratification feature to be a product of direct microbial sulfide oxidation at the beginning of the experiment (*Figure 5.3*) before S^0 and Fe^{2+} were readily available in solution, and before sufficient cell counts were able to drive oxidation and Fe^{3+} regeneration. This biologically mediated sulfur efflorescence was quickly encased by Fe-(oxy)hydroxides and fewer sulfate minerals were produced, which is consistent with the dominance of Fe-(oxy)hydroxides in the samples (*Appendix II: Table 2*).

Our SEM images and XRD analysis show no obvious stoichiometric gypsum or other sulfates in the FIB-sectioned meteorite efflorescence, in either the biotic or abiotic samples. Complicating matters, is that brushite and gypsum share a solid solution with each other, marked by a miscibility gap where they form ardelite (a mineral that was not detected in our experiments) (PINTO *ET AL.* 2012). Pinto et al. (2012) also observed asymmetry in the (020) peak of synthetic phases along the gypsum–brushite solid solution. Given the similar shape of the (020) peak of brushite/gypsum in our XRD patterns, we infer that our samples may contain an intermediate phase in this solid solution. The presence of brushite and phases along the brushite–gypsum solid solution is consistent with the high concentration of phosphate in the medium and EDX observations of phosphate minerals. The presence of sulfate minerals in the lower layers of the efflorescence covering the FeNi grain suggests that sulfur was

being leached from nearby sulfide grains or what little sulfate was available from the medium was being oxidised and precipitated on the FeNi grain at the start of the experiment.

5.4.3 Stable Sulfur Isotope Mixing in Abiotic Experiments

The fractional contribution of sulfate from each reservoir can be calculated using eq. 1. This approach assumes there are only two isotopically distinct reservoirs for sulfur in the experiments. It also assumes no fractionation (or at least negligible fractionation) occurs during oxidation of troilite or pyrite, which means this approach cannot be used for biotic treatments. As such, the results of this calculation (*Table 5.1*) should be considered approximate estimates of the amount of mixing in the abiotic samples.

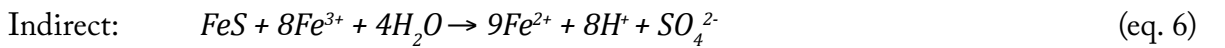
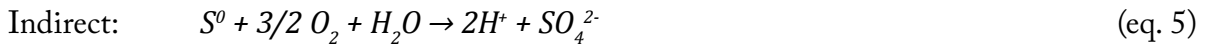
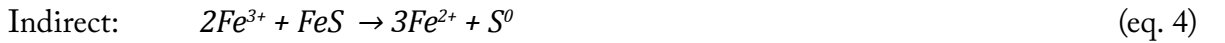
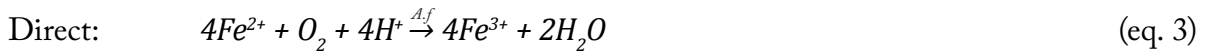
$$\begin{aligned}\delta^{34}S_{Alt} &= f_{Sulfide} \cdot \delta^{34}S_{Sulfide} + f_{Media} \cdot \delta^{34}S_{Media} \\ \delta^{34}S_{Alt} &= f_{Sulfide} \cdot \delta^{34}S_{Sulfide} + (1 - f_{Sulfide}) \cdot \delta^{34}S_{Media} \\ \delta^{34}S_{Alt} &= f_{Sulfide} (\delta^{34}S_{Sulfide} - \delta^{34}S_{Media}) + \delta^{34}S_{Media} \\ f_{Sulfide} &= (\delta^{34}S_{Alt} - \delta^{34}S_{Media}) / (\delta^{34}S_{Sulfide} - \delta^{34}S_{Media})\end{aligned}\tag{eq.1}$$

The median fractional mass of sulfate sourced from the meteorite, pyrite or troilite in abiotic experiments, $f_{Sulfide}$, is 0.72 ± 0.21 (*Table 5.1*). Thus, most of the sulfur in alteration minerals comes from oxidation of the substrate minerals and not the medium. The BaSO₄ sample obtained from an abiotic meteorite experiment gives an $f_{Sulfide}$ value of 0.30, which is likely due to background sulfate in the medium. It is significant, that 30% of the sulfur budget of the bulk supernatant was supplied by weathering of meteorite sulfides at the 2-week time step. The $f_{Sulfide}$ value for an efflorescence removed from a meteorite gave $f_{Sulfide} = 0.83$. This indicates the vast majority of the sulfur in the alteration minerals comes from the meteoritic substrate and not from sulfur introduced in the medium. It is important to consider that the abiotic samples contained 10× times the concentration of sulfate in the starting medium relative to the biotic samples. Thus, their $f_{Sulfide}$ values should be lower than those from biotic samples, indicating greater input of sulfur from ‘contaminant’ melanterite.

5.4.4 Isotopic $\delta^{34}S$ Biosignatures

A. ferrooxidans can catalyse the oxidation of sulfide minerals such as troilite and pyrite either directly or indirectly (JENSEN 1995; SAND ET AL. 1999; SILVERMAN 1967). Direct oxidation involves attachment

of cells to a troilite grain and the use of dissolved oxygen as an electron acceptor, which catalyses the oxidation of sulfur (eq. 3; (JENSEN 1995)) or Fe (eq. 4; (SAND ET AL. 1999)). Direct oxidation proceeds through enzymatic activity with no detectable intermediate sulfur species (i.e., no thiosulfate or sulfite) (SAND ET AL. 1999). Indirect oxidation is the abiotic process by which Fe^{3+} cations act as electron acceptors for reduced Fe and S in troilite, generating Fe^{2+} and/or S^0 (eq. 5; (JENSEN 1995; SAND ET AL. 1999)). Further indirect oxidation converts S^0 into sulfate (SO_4^{2-}) and Fe^{3+} leaches Fe^{2+} from sulfide minerals (eq. 6 and 7; (SAND ET AL. 1999)). These products go on to be oxidized to Fe^{3+} and SO_4^{2-} . The bacteria do not need to be attached to the substrate for this to happen.



It would appear that the oxidation pathway has had an effect on the fractionation of stable sulfur isotopes in this experiment. The biotic troilite experiments produced alteration minerals with small $\Delta^{34}\text{S}_{\text{SO}_4\text{-FeS}}$ values of 0.0 to -1.9‰, which is within the reported range of fractionations produced by *A. ferrooxidans* (PISAPIA ET AL. 2007). Contrastingly, the sulfate mineral products of biotic meteorite experiments give positive $\Delta^{34}\text{S}_{\text{SO}_4\text{-FeS}}$ values of 1.2 to 3.7‰ (Figure 5.8 B). Here we will explore the possible explanations for this dichotomy.

5.4.4.1 The Null Hypothesis

The first idea to explore is that no biological fractionation has taken place. The initial $\delta^{34}\text{S}$ of the melanterite used in the low sulfate media is $\delta^{34}\text{S}_{\text{SO}_4} = -2.0 \pm 0.3\text{‰}$ (Table 5.1), whereas the initial $\delta^{34}\text{S}$ of the meteoritic troilite is $\delta^{34}\text{S}_{\text{FeS}} = 0.3 \pm 0.3\text{‰}$. The $\delta^{34}\text{S}$ results for the abiotic meteorite experiments plot between these two values indicating a mixing trend. This is to be expected as there is negligible fractionation (i.e., $\epsilon_{\text{SO}_4\text{-FeS}_2} = -0.1 \pm 0.2\text{‰}$) of stable sulfur isotopes during abiotic oxidation of pyrite (assuming this holds true for troilite as well) (BALCI ET AL. 2007). The $\delta^{34}\text{S}$ values observed in biotic experiments do not plot between these values, but are in fact more positive than the $\delta^{34}\text{S}$ value of either sulfur reservoir that was initially introduced in the system. This is hard to explain abiotically,

suggesting that this is a biotic fractionation.

5.4.4.2 Sulfur Assimilation

Once in solution, either native sulfur or sulfate can be assimilated by *A. ferrooxidans* for use in building organic molecules (e.g., cysteine and methionine) rather than for energy generation (CANFIELD 2001). Given the decrease in aqueous sulfate observed over the course of the biotic meteorite experiments, *A. ferrooxidans* likely obtained most of its energy from Fe^{2+} oxidation. A full understanding of sulfate assimilation by *A. ferrooxidans* is not available; however, a bioinformatics study of the sulfate assimilation pathway in *A. ferrooxidans* suggests that the organism assimilates sulfate via the APS (adenosine-t'-phosphosulfate) pathway (VALDÉS ET AL. 2003). Valdés et al (2003) also found tentative evidence of a PAPS (phosphoadenosine-5'-phosphosulfate) 'like' metabolite, but they speculate its use is for sulfation of extracellular proteins that may help the cell adhere to substrates. However, sulfur assimilation is generally known to provide only a small isotopic fractionation (CANFIELD 2001). This is because sulfur makes up a small fraction of the overall cell weight (e.g., *Escherichia coli* = 9 fg S cell⁻¹ (FAGERBAKKEM ET AL. 1996)). Using the starting cell number of 1.4×10^7 cells mL⁻¹ and the starting average sulfur content in the initial 5 mL of media (0.0003 g of S; Appendix II: Table 1) we find that the mass of sulfur in cells reflects only 0.02% of sulfur in the experiment, with 99.98% of the initial mass of sulfur present in the low sulfur media. Therefore, it is unlikely that the stable sulfur isotope signature observed in our biotic meteorite experiments was produced by sulfur assimilation.

5.4.4.3 Degassing of Isotopically Light $^{32}\text{SO}_2$, Build up of Ferrous Iron and a Switch Metabolic Mode

Most biologically mediated sulfur oxidation happens via the direct method (YU ET AL. 2001). Thus, limited supply of accessible sulfur will affect the lifestyle of *A. ferrooxidans*. Planktonic *A. ferrooxidans* would likely have to rely on indirect leaching of the troilite (eq.5) in meteorite samples to obtain Fe^{2+} and S^0 for energy, which are quickly oxidized to Fe^{3+} , sulfate and thiosulfate [$\text{S}_2\text{O}_3^{2-}$] by *A. ferrooxidans*. LL chondrites such as the Chelyabinsk meteorite also contain FeNi alloys at an abundance of ~2.44 wt.% (JAROSEWICH 1990); these are not present in the synthetic sulfide powders used in our experiments. Indirect leaching of the FeNi alloys would also create an excess of Fe^{2+} , making the ratio of biologically available Fe:S in the meteorite experiments quite large compared to the 1:1 ratio in the troilite powder; this results in an overabundance of Fe compared to S for the meteorite experiments.

This is important because *A. ferrooxidans* is not an obligate S oxidiser and preferentially metabolises reduced Fe species over reduced sulfur species (YARZÁBAL *ET AL.* 2004). Not only does *A. ferrooxidans* prefer to oxidise iron, but the organism is known to “sense” changes in water chemistry and can start to preferentially oxidise Fe^{2+} over the initially abundant S^{2-} , S^0 (BRUNNER *ET AL.* 2008). In the model proposed by Brunner et al. (2008), native sulfur is produced by oxidation of pyrite as per (eq.5) during the initial stage of the experiment. Here it is catalysed by *A. ferrooxidans* to make hydrogen sulfite (eq.8):



Now, the system has several oxidised sulfur pools in addition to the original pools of sulfide in meteoritic troilite and sulfate introduced in the medium by dissolution of melanterite. The hydrogen sulfite can then go on and be catalysed by *A. ferrooxidans* to make thiosulfate or it can react with acid in the system to make sulfur dioxide. Isotopically light sulfur dioxide is preferentially degassed and leaves the system resulting in an increased production of isotopically heavy sulfate during the initial phases of the experiment (eq.9) (BRUNNER *ET AL.* 2008) .



Brunner et al. (2008) found that degassing of sulfur dioxide and biotic oxidation of native sulfur and intermediaries during the initial stage of their experiment yielded relatively large stable sulfur isotope fractionations of $\Delta^{34}\text{S}_{\text{SO4(initial)}-\text{FeS}_2} = +4.0 \pm 1.7\text{‰}$. These values are similar in magnitude to the fractionations in our biotic meteorite experiments, $\Delta^{34}\text{S}_{\text{SO4}-\text{FeS}} = +1.1 - +3.7\text{‰}$ (Table 5.1). During the later stage of pyrite oxidation, Brunner et al. (2008) found that oxidation of ferrous iron became the dominant metabolism used by *A. ferrooxidans*. This resulted in less degassing of sulfur dioxide and a negligible stable sulfur isotopic fractionation $\Delta^{34}\text{S}_{\text{SO4(main)}-\text{FeS}_2} = -0.2 \pm 2.1\text{‰}$. Note, that the isotopic difference come close to overlapping within error of each other, meaning these two leaching modes may be indistinguishable in our meteorites samples for $\delta^{34}\text{S}_{\text{SO}_4} \sim 2.0\text{‰}$. This may explain why there is a decrease in the concentration of aqueous sulfate from 1.7 times the starting SO_4^{2-} value at 24 hrs to 0.9 times the starting value of SO_4^{2-} at the end of the biotic meteorite experiments, compared to the abiotic meteorite experiments which steadily grew over time (Figure 5.3). This is compatible with

Brunner et al. (2008) model that the initial stage of the experiment is defined by microbially catalysed sulfur oxidation, whereas the main phase is defined by iron oxidation. This would also explain why Fe-(oxy)hydroxide crusts were more likely to develop after 1 week (*Figure 5.4*). Additionally, our FIB results, which show a concentrated layer of sulfur at the surface of the FeNi grain, indicate that sulfur was in excess during the initial formation of this efflorescence. Based on these two lines of evidence and the stable isotope results, it is highly likely that microorganisms were using sulfur intermediaries for energy during the initial stage of the experiment, some of which reacted with acid to produce isotopically light sulfur dioxide, which enriched the aqueous sulfate and minerals in ^{34}S . By the main stage of the experiment commencing after 24 hours (based on SO_4^{2-} decrease) the microorganisms were metabolising iron, as evident by the excessive development of Fe-(oxy)hydroxide crusts.

5.4.4.4 Reduction of Native Sulfur in Anoxic Microenvironments

Another possible explanation for the heavy stable isotopic signature in the residue efflorescences of the biotic meteorite experiments is dissimilatory reduction of S^0 to H_2S by *A. ferrooxidans* under anaerobic conditions (NG ET AL. 2000; OSORIO ET AL. 2013; VALDÉS ET AL. 2008). The fractionation factor for dissimilatory sulfur reduction is not yet known for *A. ferrooxidans*, but in other species such as *Desulfovibrio desulfuricans* this process can create large fractionations up to $\Delta^{34}\text{S}_{\text{Sulfide-Sulfate}} = +46\text{‰}$ (CANFIELD 2001; CANFIELD AND TESKE 1996). Although our experiments were run under aerobic conditions, such reactions could still have taken place within anoxic microenvironments. Many reactions, both biotic and abiotic, were consuming oxygen within the experiments, including those already discussed (eq. 3, 4, and 6). This could have led to hypoxia within self-contained microenvironments such as those depicted in (*Figure 5.5 C*), forcing a metabolic switch in *A. ferrooxidans*. However, the efflorescences that cap grains of troilite and FeNi alloy were porous and cracked, so it is unlikely that sulfur reduction would have been an efficient process under these conditions. Another unlikely possibility is that a large redox gradient existed within the biofilm at the mineral/microbe interface, which could have created anaerobic conditions sufficient to facilitate the reduction of S^0 to H_2S .

5.4.5 Comparisons of Experimental Meteorite Results to Nullarbor Finds

To understand the $\delta^{34}\text{S}$ isotope data for the vein material from Nullarbor Plain meteorites (i.e., *Ooldea 006*; $\delta^{34}\text{S} = 2.6\text{‰}$ and *Ooldea 007*; $\delta^{34}\text{S} = 6.7\text{‰}$), it is important to discuss the possible sources of

sulfur in the system and the processes that may be fractionating stable sulfur isotopes. Firstly, abiotic oxidation of troilite in the meteorites yields a negligible fractionation (assuming the value, $\epsilon_{\text{SO}_4\text{-FeS}_2} = -0.1\text{‰} \pm 0.2\text{‰}$, for pyrite holds for troilite; (BALCI *ET AL.* 2007) that should produce $\delta^{34}\text{S}$ values of $\sim 0\text{‰}$ in the sulfate alteration products. If the interiors of the meteorites were contaminated by sulfate from the environment we should see a linear mixing trend, provided that the contaminant phase has a distinct $\delta^{34}\text{S}$ value. Previous studies have shown that the sulfate in the Nullarbor Plain region originates from oceanic aerosols (JAMES 1991). The $\delta^{34}\text{S}$ signature of modern oceanic sulfate is $+21\text{‰}$ (VCDT) (CLARK AND FRITZ 1997), which also does not match the $\delta^{34}\text{S}$ signature of carbonate–gypsum veins in the Nullarbor meteorites. Another possibility is the presence of sulfate reducing microorganisms, which can fractionate stable sulfur isotopes creating large enrichments in ^{34}S , resulting in $\delta^{34}\text{S}$ values of $+2.0\text{‰}$ to $+42.0\text{‰}$ (DETMERS *ET AL.* 2001). Such sulfur cycling organisms (e.g. *Desulfovibrio spp.*) have been found in small quantities in Nullarbor meteorites (*Chapter 4*; Tait et al., 2017a).

If we assume that all sulfur in the gypsum was sourced from oxidation of sulfide minerals in Nullarbor meteorites, using starting $\delta^{34}\text{S}$ values from Gao and Thiemens (1993), we obtain $\Delta^{34}\text{S}_{\text{SO}_4\text{-FeS}}$ values of 2.2‰ for *Ooldea 006* and 6.7‰ for *Ooldea 007*. These values are very similar to those found in our biotic meteorite experiments, which we interpret to be the signature of sulfur oxidation by *A. ferrooxidans*, during initial FeS leaching prior to ferrous oxidation metabolism (e.g., Brunner et al. (2008)). The higher $\Delta^{34}\text{S}_{\text{SO}_4\text{-FeS}}$ value in *Ooldea 007* could reflect minor input of foreign sulfate from the Nullarbor ($\delta^{34}\text{S} \cong +21\text{‰}$) or the dissimilatory reduction of sulfate (originally oxidised from the FeS) by members of *Desulfovibrio spp.* (TAIT *ET AL.*, 2017A), or similar sulfur/iron cycling microorganisms. Calcite contamination is known to occur in Nullarbor meteorite vein material, which can affect stable carbon isotopes (TAIT *ET AL.*, 2017B). However, sulfate minerals were not detected in Nullarbor regolith from the Ooldea region via XRD analysis (TAIT *ET AL.*, 2017B). This indicates that if sulfate minerals are present in the regolith, their abundance is below the detection limit of the analysis (approximately <1 wt.% for most phases), meaning that contaminant sulfate minerals are not likely to be a significant source of sulfur input to the interiors of meteorites in the Nullarbor Plain. However, it could affect results if a sulfur-bearing phase existed in our samples at a concentration below the detection limit of our XRD analyses.

We interpret the following based on the $\delta^{34}\text{S}$ results for the Nullarbor Plain meteorites: (1) the results are not consistent with primary meteorite sulfur signatures; (2) they do not reflect abiotic oxidation of troilite; (3) the $\delta^{34}\text{S}$ values from meteorites do not reflect an oceanic sulfate signature or substantial

sulfate contamination from the environment; (4) the $\delta^{34}\text{S}$ values of gypsum from Nullarbor meteorites more closely reflect those found in our biotic meteorite experiments. The $\delta^{34}\text{S}$ values observed in Nullarbor meteorites most likely reflect a metabolic process similar to those observed in Brunner et al. (2008) or dissimilatory sulfur reduction (e.g., by *Desulfovibrio spp.*). Thus, it is most likely that sulfate alteration minerals in Nullarbor meteorites record a stable sulfur isotope fractionation caused by microbial sulfur cycling. As such, we propose that the results from the Nullarbor meteorite carbonate–gypsum veins represent a distinct isotopic biosignature.

5.4.6 Using Meteorites on Mars for Biomarker Detection

Our experiment has shown that it is possible for Fe- and S-oxidizing bacteria to produce several distinct stable sulfur isotopic fractionations between the sulfate alteration products and primary sulfide minerals in chondritic meteorites. Importantly, the same organism may produce different stable sulfur isotopic fractionations under conditions where sulfur is readily available or a limiting nutrient. The fractionations observed in our study are relatively small and negative, $\Delta^{34}\text{S}_{\text{SO}_4\text{--FeS}} = -1.9\text{‰}$ for the biotic powdered troilite experiment (stoichiometric Fe:S ratio, no sulfur limitation) versus $\Delta^{34}\text{S}_{\text{SO}_4\text{--FeS}} = 1.2 - 3.7\text{‰}$ for the biotic meteorite experiment (non-stoichiometric Fe:S ratio, sulfur-limited conditions). Despite their small magnitude, these isotopic differences are still much larger than the range of $\delta^{34}\text{S}$ values observed in most ordinary chondritic meteorites, $\delta^{34}\text{S} = -0.02\text{‰} \pm 0.06\text{‰}$ (GAO AND THIEMENS 1993). We have shown that a sulfur oxidation signature in sulfate-limited conditions is detectable in meteorites collected from the Nullarbor Plain, which have been colonised and altered by environmental microorganisms.

Tait et al. (2017b) proposed that stable S isotopes in chondritic meteorites might be used to detect isotopic biosignatures produced during colonization by a possible martian biosphere. This method relies on the narrow range of $\delta^{34}\text{S}$ values of troilite in ordinary chondrites. It could be used to detect stable sulfur isotopic biosignatures in meteorites so long as two conditions are met: (1) the biological fractionation falls outside the range of $\delta^{34}\text{S}$ values of the troilite in meteorites and (2) any abiotic processes capable of fractionating sulfur isotopes relative to the starting isotopic composition of meteoritic sulfur are extensively examined and tested. With a growing body of knowledge about environmental conditions on Mars (e.g., mineralogy of regolith, atmospheric composition and palaeoenvironmental conditions), they could be constrained prior to sample return by in situ experiments.

Under conditions of low environmental sulfate contamination, it may be possible to reliably detect

biological fractionation of stable sulfur isotopes in meteorites on Mars. For instance, in the case of abiotic oxidation of sulfide minerals to sulfate phases, the fractionation should be negligible (BALCI *ET AL.* 2007), implying that larger stable sulfur isotope fractionations could be related to biological processes. However, the $\delta^{34}\text{S}$ values of surrounding reservoirs for sulfur would also need to be analysed to reliably demonstrate biogenicity and rule out other causes of stable sulfur isotope fraction. Contamination of meteorites by sulfate minerals from regolith or dust could occur on Mars via sedimentary processes (e.g., burial, aeolian or hydrological transport). Mechanical mixing of sulfate minerals produced from two isotopically distinct reservoirs for sulfur can create a mixing trend in stable sulfur isotope data. As our abiotic experiments have shown, this can be detected in the sulfate alteration products of meteorites. The elevated concentration of ‘contaminant’ sulfate introduced as melanterite in the medium used in the abiotic experiments (*Figure 5.8*) did not hinder the detection of an isotopic biosignature. Because the concentration of melanterite was an order of magnitude lower in the biological experiments it was possible to identify stable sulfur isotope fractionations associated with biological processes such as assimilatory sulfate reduction. The only situations where this may present an issue for biosignature detection would be if the contaminant had a similar $\delta^{34}\text{S}$ value to meteoritic troilite or if the $\Delta^{34}\text{S}_{\text{SO}_4\text{-FeS}}$ biosignature were to fall between the $\delta^{34}\text{S}$ values of the meteorite ($\sim 0\%$) and the contaminant. However, if the contaminant phase is mineralogically distinct and present in regolith, its contribution to the sulfur budget of the meteorite can be calculated from modal abundances of background minerals using quantitative XRD, a capability available through the MSL’s CheMin instrument (BISH *ET AL.*, 2013; VANIMAN *ET AL.*, 1998). This approach has been demonstrated for stable carbon isotopes by identifying phases that are not meteoritic in origin but exist in the nearby soil (TAIT *ET AL.* 2017B). This allows the provenance of the sulfate to be determined. Thus, using the isotopic composition of meteoritic sulfur as a standard, biological fractionation can be separated from fractionation produced by abiotic processes, even in contaminated samples.

5.5 Conclusions

Chondritic meteorites on the martian surface represent chemical and isotopic standards, which could provide unambiguous evidence of a biosphere (should one have existed) on Mars. We have demonstrated the feasibility of using meteorites as standards for detection of isotopic biomarkers, which relies upon the narrow range of $\delta^{34}\text{S}$ compositions of troilite in all ordinary and enstatite chondrites (FARQUHAR *ET AL.* 2007). Our experimental results show that meteorites can be used as

a tool to remove ambiguity associated with detection of biologically mediated isotope fractionations in environments where geochemical context is still being established. Given the magnitude of the biogenic fractionation of sulfur isotopes in experiments and meteorite vein material (e.g., $\Delta^{34}\text{S}_{\text{SO}_4\text{-FeS}} = +6.7\text{‰}$), this could even be detected by low-resolution mass spectrometers, such as those found on MSL (FRANZ *ET AL.* 2011). If we apply this tool to chondritic meteorites at the surface of Mars, it is quite possible that we could start to record sulfur isotope fractionations to unambiguously interpret martian environmental process, and perhaps search for hints of a martian biosphere.

5.6 Chapter 5 References

A

- Ashley J. W. (2011) Meteorites on Mars as Planetary Research Tools with Special Considerations for Martian Weathering Processes: *Arizona State University*. 343 p.
- Ashley J. W., Golombek M. P., Christensen P. R., Squyres S. W., McCoy T. J., Schröder C., Fleischer I., R J. J. J., Herkenhoff K. E., and Parker T. J. (2011) Evidence for mechanical and chemical alteration of iron-nickel meteorites on Mars: Process insights for Meridiani Planum. *Journal of Geophysical Research*, 116: E00F20.

B

- Balci N., Shanks Iii W. C., Mayer B., and Mandernack K. W. (2007) Oxygen and sulfur isotope systematics of sulfate produced by bacterial and abiotic oxidation of pyrite. *Geochimica et Cosmochimica Acta*, 71: 3796-3811.
- Bauermeister A., Rettberg P., and Flemming H.-C. (2013) Growth of the acidophilic iron-sulfur bacterium *Acidithiobacillus ferrooxidans* under Mars-like geochemical conditions. *Planetary and Space Science*: 1-11.
- Bland P., and Smith T. B. (2000) Meteorite accumulations on Mars. *Icarus*, 144: 21-26.
- Bland P. A., Zolensky M. E., Benedix G. K., and Sephton M. A. (2006) Weathering of chondritic meteorites. In: Meteorites and the Early Solar System II. edited by DS Lauretta and HY McSween, *University of Arizona Press*, Tucson, pp 943.
- Blyth A. J., Watson J. S., Woodhead J., and Hellstrom J. (2010) Organic compounds preserved in a 2.9 million year old stalagmite from the Nullarbor Plain, Australia. *Chemical Geology*, 279: 101-105.
- Brunner B., Yu J.-Y., Mielke R. E., MacAskill J. A., Madzunkov S., McGenity T. J., and Coleman M. (2008) Different isotope and chemical patterns of pyrite oxidation related to lag and exponential growth phases of *Acidithiobacillus ferrooxidans* reveal a microbial growth strategy. *Earth and Planetary Science Letters*, 270: 63-72.

C

- Canfield D. E. (2001) Biogeochemistry of sulfur isotopes. In: Reviews in Mineralogy and Geochemistry. edited by JW Valley and DR Coles, *Mineralogical Society of America*, Washington, DC, USA, pp 607-636.
- Canfield D. E., and Teske A. (1996) Late Proterozoic rise in atmospheric oxygen concentration inferred from phylogenetic and sulphur-isotope studies. *Nature*, 382: 127-132.
- Carr M. H., and Head III J. W. (2010) Geologic history of Mars. *Earth and Planetary Science Letters*, 294: 185-203.
- Clark I. D., and Fritz P. (1997) Environmental isotopes in hydrogeology. *CRC press*.

D

- Dehouck E., Chevrier V., Gaudin A., Mangold N., Mathé P. E., and Rochette P. (2012) Evaluating the role of sulfide-weathering in the formation of sulfates or carbonates on Mars. *Geochimica et Cosmochimica Acta*, 90: 47-63.
- Des Marais D. J., Nuth Iii J. A., Allamandola L. J., Boss A. P., Farmer J. D., Hoehler T. M., Jakosky B. M., Meadows V. S., Pohorille A., Runnegar B. and others. (2008) The NASA Astrobiology Roadmap. *Astrobiology*, 8: 715-730.
- Detmers J., Brüchert V., Habicht K. S., and Kuever J. (2001) Diversity of sulfur isotope fractionations by sulfate-reducing prokaryotes. *Applied and Environmental Microbiology*, 67: 888-894.
- Dunn T. L., Cressey G., McSween Jr H. Y., and McCoy T. J. (2010) Analysis of ordinary chondrites using powder X-ray diffraction: 1. Modal mineral abundances. *Meteoritics & Planetary Science*, 45: 123-134.

F

- Fagerbakkem K. M., Heldal M., and Norland S. (1996) Content of carbon, nitrogen, oxygen, sulfur and phosphorus in native aquatic and cultured bacteria. *Aquatic Microbial Ecology*, 10: 15-27.
- Farquhar J., Kim S.-T., and Masterson A. (2007) Implications from sulfur isotopes of the Nakhla meteorite for the origin of sulfate on Mars. *Earth and Planetary Science Letters*, 264: 1-8.
- Farquhar J., Savarino J., Jackson T. L., and Thiemens M. H. (2000) Evidence of atmospheric sulphur in the martian regolith from sulphur isotopes in meteorites. *Nature*, 404: 50-52.
- Fowler T. A., and Crundwell F. K. (1999) Leaching of zinc sulfide by *Thiobacillus ferrooxidans*: Bacterial oxidation of the sulfur product layer increases the rate of zinc sulfide dissolution at high concentrations of ferrous ions. *Applied and Environmental Microbiology*, 65: 5285-5292.
- Franz H. B., Mahaffy P. R., Kasprzak W., Lyness E., and Raaen E. (2011) Measuring sulfur isotope ratios from solid samples with the Sample Analysis at Mars instrument and the effects of dead time corrections. *42nd Lunar Planetary Science Conference*.

G

- Galimov E. M., Kolotov V. P., Nazarov M. A., Kostitsyn Y. A., Kubrakova I. V., Kononkova N. N., Roshchina I. A., Alexeev V. A., Kashkarov L. L., Badyukov D. D. and others. (2013) Analytical results for the material of the Chelyabinsk meteorite. *Geochemistry International*, 51: 522-539.
- Gao X., and Thiemens M. H. (1993) Variations of the isotopic composition of sulfur in enstatite and ordinary chondrites. *Geochimica et Cosmochimica Acta* (ISSN 0016-7037), 57: 3171-3176.
- Gronstal A., Pearson V., Kappler A., Dooris C., Anand M., Poitrasson F., Kee T. P., and Cockell C. S. (2009) Laboratory experiments on the weathering of iron meteorites and carbonaceous chondrites by iron-oxidizing bacteria. *Meteoritics & Planetary Science*, 44: 233-247-15.

H

- Horita J. (2005) Some perspectives on isotope biosignatures for early life. *Chemical Geology*, 218: 171-186.

I

- Ignatiev A. V., Velivetskaia T. A., Kiyashko S. I., and Grokovsky V. I. (2013) The first data of oxygen, sulfur, and carbon isotope compositions in meteorite Chelyabinsk. *The Annual Meteoritical Society Meeting*.

J

- Jäger E., and Hunziker J. C. (2012) Lectures in isotope geology. *Springer Science & Business Media*.
- James J. M. (1991) The sulfate speleothems of Thampanna Cave, Nullarbor Plain, Australia. *Helictite: Journal of Australasian Cave Research*, 291: 19-23.
- Jarosewich E. (1990) Chemical analyses of meteorites: A compilation of stony and iron meteorite analyses. *Meteoritics*, 25: 323-337.
- Jensen A. (1995) Ferrous sulphate oxidation using *Thiobacillus ferrooxidans*: A review. *Process Biochemistry*, 30: 225-236.
- Jull A. J. T., McHargue L. R., Bland P. A., Greenwood R. C., Bevan A. W. R., Kim K. J., LaMotta S. E., and Johnson J. A. (2010) Terrestrial ages of meteorites from the Nullarbor region, Australia, based on ^{14}C and ^{14}C - ^{10}Be measurements. *Meteoritics & Planetary Science*, 45: 1271-1283.

K

- Kaplan I. R., and Rittenberg S. C. (1964) Microbiological fractionation of sulphur isotopes. *Journal of General Microbiology*, 34: 195-212.
- Karathanasis A. D., and Thompson Y. L. (1995) Mineralogy of iron precipitates in a constructed acid mine drainage wetland. *Soil Science Society of America Journal*, 59: 1773-1781.
- Kelly D. P., and Wood A. P. (2000) Reclassification of some species of *Thiobacillus* to the newly designated genera *Acidithiobacillus* gen. nov., *Halothiobacillus* gen. nov. and *Thermithiobacillus* gen. nov. *International Journal of Systematic and Evolutionary Microbiology*, 50: 511-516.
- Kieft D. T. L., and Spence S. D. (1988) Osmoregulation in *Thiobacillus ferrooxidans*: Stimulation of iron oxidation by proline and betaine under salt stress. *Current Microbiology*, 17: 255-258.

L

- Laskov C., Herzog C., Lewandowski J., and Hupfer M. (2007) Miniaturized photometrical methods for the rapid analysis of phosphate, ammonium, ferrous iron, and sulfate in pore water of freshwater sediments. *Limnology and Oceanography: Methods*, 5: 63-71.
- Li L., Lv Z., and Yuan X. (2013) Effect of l-glycine on bioleaching of collophanite by *Acidithiobacillus ferrooxidans*. *International Biodeterioration & Biodegradation*, 85: 156-165.
- Liu J.-y., Xiu X.-x., and Cai P. (2009) Study of formation of jarosite mediated by *thiobacillus ferrooxidans* in 9K medium. *PROEPS*, 1: 706-712.

M

- Mahaffy P. R., Webster C. R., Cabane M., Conrad P. G., Coll P., Atreya S. K., Arvey R., Barciniak M., Benna M., Bleacher L. and others. (2012) The Sample Analysis at Mars Investigation and Instrument Suite. *Space Science Reviews*, 170: 401-478.
- McLennan S. M., Anderson R. B., Bell Iii J. F., Bridges J. C., Calef Iii F., Campbell J. L., Clark B. C., Clegg S., Conrad P., Cousin A. and others. (2014) Elemental Geochemistry of Sedimentary Rocks at Yellowknife Bay, Gale Crater, Mars. *Science*, 343: 1244734.
- McSween H. Y., Riciputi L. R., and Paterson B. A. (1997) Fractionated sulfur isotopes in sulfides of the Kaidun meteorite. *Meteoritics & Planetary Science*, 32: 51-54.
- Michel F. M., Barrón V., Torrent J., Morales M. P., Serna C. J., Boily J.-F., Liu Q., Ambrosini A., Cismasu A. C., and Brown G. E. (2010) Ordered ferrimagnetic form of ferrihydrite reveals links among structure, composition, and magnetism. *Proceedings of the National Academy of Sciences of the United States of America*, 107: 2787-2792.

N

- Ng K. Y., Sawada R., Inoue S., Kamimura K., and Sugio T. (2000) Purification and some properties of sulfur reductase from the iron-oxidizing bacterium *Thiobacillus ferrooxidans* NASF-1. *Journal of Bioscience and Bioengineering*, 90: 199-203.

O

- Osorio H., Mangold S., Denis Y., Nancucheo I., Esparza M., Johnson D. B., Bonnefoy V., Dopson M., and Holmes D. S. (2013) Anaerobic sulfur metabolism coupled to dissimilatory iron reduction in the extremophile *Acidithiobacillus ferrooxidans*. *Applied and Environmental Microbiology*, 79: 2172-2181.

P

- Pinto A. J., Carneiro J., Katsikopoulos D., Jiménez A., and Prieto M. (2012) The link between brushite and gypsum: Miscibility, dehydration, and crystallochemical behavior in the $\text{CaPO}_4 \cdot 2\text{H}_2\text{O}$ – $\text{CaSO}_4 \cdot 2\text{H}_2\text{O}$ system. *Crystal Growth & Design*, 12: 445-455.

- Pisapia C., Chaussidon M., Mustin C., and Humbert B. (2007) O and S isotopic composition of dissolved and attached oxidation products of pyrite by *Acidithiobacillus ferrooxidans*: Comparison with abiotic oxidations. *Geochimica et Cosmochimica Acta*, 71: 2474-2490.
- Popa R., Smith A. R., Popa R., Boone J., and Fisk M. (2012) Olivine-Respiring Bacteria Isolated from the Rock-Ice Interface in a Lava-Tube Cave, a Mars Analog Environment. *Astrobiology*, 12: 9-18.
- Preston L. J., Shuster J., Fernández-Remolar D., Banerjee N. R., Osinski G. R., and Southam G. (2011) The preservation and degradation of filamentous bacteria and biomolecules within iron oxide deposits at Rio Tinto, Spain. *Geobiology*, 9: 233-249.

R

- Rayment G. E., and Higginson F. R. (1992) Australian laboratory handbook of soil and water chemical methods. Inkata Press, Melbourne.
- Rimstidt J. D., and Vaughan D. J. (2003) Pyrite oxidation: a state-of-the-art assessment of the reaction mechanism. *Geochimica et Cosmochimica Acta*, 67: 873-880.
- Rohwerder T., Gehrke T., Kinzler K., and Sand W. (2003) Bioleaching review part A. *Applied Microbiology and Biotechnology*, 63: 239-248.

S

- Sand W., Gehrke T., Jozsa P. G., and Schippers A. (1999) Direct versus indirect bioleaching. In: Biohydrometallurgy and the Environment Toward the Mining of the 21st Century - Proceedings of the International Biohydrometallurgy Symposium, *Elsevier*, pp 27-49.
- Schröder C., Bland P. A., Golombek M. P., Ashley J. W., Warner N. H., and Grant J. A. (2016) Amazonian chemical weathering rate derived from stony meteorite finds at Meridiani Planum on Mars. *Nature Communications*, 7: 13459.
- Silverman M. P. (1967) Mechanism of bacterial pyrite oxidation. *Journal of Bacteriology*, 94: 1046-1051.
- Stoffler D., Keil K., and Edward R. D. (1991) Shock metamorphism of ordinary chondrites. *Geochimica et Cosmochimica Acta*, 55: 3845-3867.

T

- Tait A. W., Gagen E. J., Wilson S. A., Tomkins A. G., and Southam G. (2017a) Microbial populations of stony meteorites: Substrate controls on first colonisers. *Frontiers in Microbiology* (Accepted for publication, 19th May 2017).
- Tait A. W., Wilson S. A., Tomkins A. G., Gagen E. J., Stewart F. J., and Southam G. (2017b) Evaluation of meteorites as habitats for terrestrial microorganisms: Results from the Nullarbor Plain, Australia, a Mars analogue site. *Geochimica et Cosmochimica Acta* (Accepted for publication 28th May 2017).

Temple K. L., and Colmer A. R. (1951) The autotrophic oxidation of iron by a new bacterium: *Thiobacillus ferrooxidans*. *Journal of Bacteriology*, 62: 601-611.

Tuovinen O. H., Kelley B. C., and Nicholas D. J. D. (1975) The uptake and assimilation of sulphate by *Thiobacillus ferrooxidans*. *Archives of Microbiology*, 105: 123-127.

V

Valdés J., Pedroso I., Quatrini R., Dodson R. J., Tettelin H., Blake R., Eisen J. A., and Holmes D. S. (2008) *Acidithiobacillus ferrooxidans* metabolism: from genome sequence to industrial applications. *BMC Genomics*, 9: 597.

Valdés J., Veloso F., Jedlicki E., and Holmes D. (2003) Metabolic reconstruction of sulfur assimilation in the extremophile *Acidithiobacillus ferrooxidans* based on genome analysis . *BMC Genomics*, 4: 51.

Van Schmus W. R., and Wood J. (1967) A chemical-petrologic classification for the chondritic meteorites. *Geochimica et Cosmochimica Acta*, 31: 747-765.

W

Wilson S. A., and Bish D. L. (2012) Stability of Mg-sulfate minerals in the presence of smectites: Possible mineralogical controls on H₂O cycling and biomarker preservation on Mars. *Geochimica et Cosmochimica Acta*, 96: 120-133.

Wlotzka F. (1993) A Weathering Scale for the ordinary chondrites. *Meteoritics*, 28: 460.

Y

Yarzabal A., Appia-Ayme C., Ratouchniak J., and Bonnefoy V. (2004) Regulation of the expression of the *Acidithiobacillus ferrooxidans* rus operon encoding two cytochromes c, a cytochrome oxidase and rusticyanin. *Microbiology* (Reading, England), 150: 2113-2123.

Yu J.-Y., McGenity T. J., and Coleman M. L. (2001) Solution chemistry during the lag phase and exponential phase of pyrite oxidation by *Thiobacillus ferrooxidans*. *Chemical geology*, 175: 307-317.

Z

Zurfluh F. J., Hofmann B. A., Gnos E., and Eggenberger U. (2013) “Sweating meteorites”—Water-soluble salts and temperature variation in ordinary chondrites and soil from the hot desert of Oman. *Meteoritics & Planetary Science*, 48: 1958-1980.

Chapter 6

Meteorites as a universal habitat: A summary of microbial colonisation on Earth and applications for Mars and beyond

Alastair W. Tait¹

¹School of Earth, Atmosphere & Environment, Monash University, Australia

6.1 Introduction

Prior to the work presented in this thesis, little was known about the relationship between microorganisms and meteorites. Previous work has largely been restricted to development of theoretical view points on this relationship, such as considering meteorites as a source for pre-biotic chemicals in aid of abiogenesis (PASEK AND LAURETTA 2008; PEARCE AND PUDRITZ 2016), or as carrying agents in lithopanspermia (BURCHELL 2004). This latter idea reached public attention with the controversial identification of martian ‘nanobacteria’ in meteorites from Mars (McKAY *ET AL.*, 1996). Studies of meteorites have generally considered terrestrial microorganisms to be undesirable contaminants that could complicate unrelated analysis (STEELE *ET AL.* 2000). One study reports culturing a model microorganism, *Acidithiobacillus ferrooxidans*, on iron meteorites and carbonaceous chondrites from the perspective of early Earth research (GRONSTAL *ET AL.* 2009). Another cultivated soil microbes and plants in pulverised meteorites, suggesting they could be used to produce soils for future space settlement (MAUTNER 1997). My thesis has used geochemical and geomicrobiological approaches to explore meteorites as microbial habitats in their own right. This final chapter provides an overview of how microorganisms colonise meteorites on Earth and speculates on how this could occur on Mars. Finally, this chapter discusses avenues for future research and applications that emerge from viewing meteorites as microbial habitats.

6.1.1 Summary of Terrestrial Microbial Colonisation of Chondrites

The primary goal of this research has been to establish a terrestrial baseline for microbial colonisation of meteorites so that they may be used as standard substrates for biomarker detection on other planets, particularly Mars. This is important because it helps to improve our understanding of how meteorite–microbe interactions work on Earth before applying this knowledge to planets where (bio) geochemical element cycling is less understood. Meteorites were collected from the Nullarbor Plain, Australia for geochemical and ecological study. The Nullarbor Plain was employed here as a Mars analogue because (1) the terrain has not changed in ~1 Ma (WEBB AND JAMES 2006), (2) it has a thin deflationary surface very similar to parts of the surface of Mars, (3) it is a semi-arid desert with little vegetation, and (4) it experiences large diurnal humidity and temperature swings similar to those on Mars, which are ideal for the development of many weathering minerals.

In Chapter 4 we showed that the soils of the Nullarbor are quite unique from each other in terms

of bacterial and archaeal community structure, despite the homogenous karst terrain. The soils have poor species membership and structure, being dominated primarily by Actinobacteria rather than Proteobacteria and Acidobacteria, which make up the majority of communities in forested and pastoral soils (JANSSEN 2006). The results of Chapter 4 show that when an ordinary chondrite falls to the Nullarbor Plain on Earth, it is colonised by community members from nearby soil (or possibly rainwater). However, with time the community structure inside the meteorites develops poor community evenness, indicating that environmental forcing inside the meteorites favours organisms that are best able to capitalise on that geochemical niche. Soil communities differ geographically (JANSSEN 2006), so some soils are expected to contain organisms that are better suited to life inside meteorites. For instance, a community originating in volcanic soil might have higher community evenness after colonising a meteorite than those from soil developed over the Nullarbor limestone karst.

Chapter 2 investigated the weathering processes that start once meteorites have fallen to Earth and how they influence microbial activity. It is well known that abiological weathering drives oxidation of FeNi-alloys and iron-sulfide minerals (e.g., (BLAND *ET AL.* 2006)). Atmospheric water vapour, meteoric precipitation and occasional floods all contribute to the ingress of water into the interiors of meteorites, allowing carbonic acid in water and sulfuric acid sourced from sulfide oxidation to etch and dissolve silicate minerals. This liberates Ca, Mg, Fe, Na and other cations that can react with dissolved inorganic carbon, sulfate and silica to produce hygroscopic weathering minerals such as carbonates, sulfates, Fe-(oxy)hydroxides and smectites. Precipitation of these alteration minerals typically leads to large volume increases, resulting in reaction-driven cracking. This enhances permeability and the penetration of water and vapour deeper into the meteorite.

Many of the alteration minerals in chondrites are hygroscopic, and in Chapter 2 we show that carbonate–gypsum vein material can adsorb up to 3 % of its mass in H₂O at mineral surfaces. This suggests that water adsorbed to the surfaces of hygroscopic minerals in meteorites is retained during the day even at lower relative humidity (RH). Thus, bioessential water is likely scavenged mainly at night when temperatures drop and RH approaches 100%, but this can happen at lower RH as well (WILSON AND BISH 2011). This creates a ‘humidity oasis’ within meteorites compared to their dry exteriors, where surface water will evaporate when subjected to the hot daytime temperatures of the

Nullarbor Plain. This results in meteorites with an oxidised, weathered core and a reduced outer rim.

The majority of environmental microbes in Nullarbor meteorites are found on these hygroscopic alteration minerals (Chapters 2 and 3). The most likely scenario is that they are utilising these minerals for a source of water. Many of the mineral grains that host microbial colonies also show acid etch pits and extensive coverage by extracellular polymeric substances (EPS). Grains of hygroscopic minerals without microbes or EPS do not have such etch marks, indicating the organisms have an acidic EPS (JONES 2010). EPS is also known to trap moisture, which would facilitate survival of microorganisms in meteorites. Microbes could also be colonising hygroscopic carbonate minerals as a way of buffering acidity without having to expend energy (STEINHAUER *ET AL.* 2010). The microbes likely also benefit from liberation of aqueous species needed for metabolism and biomass production during partial dissolution of hygroscopic minerals by films of water. Indeed, Chapter 5 shows $\delta^{34}\text{S}$ isotopic evidence that *A. ferrooxidans* and environmental microbes found in Nullarbor meteorites oxidise sulfate produced by weathering of meteorites for their own enzymatic utility. Chapter 3 shows that microorganisms can be entombed and preserved within the weathering products of meteorites. The Mg-calcite $[(\text{Mg},\text{Ca})\text{CO}_3]$ and gypsum $[\text{CaSO}_4 \cdot 2\text{H}_2\text{O}]$ admixture, which makes up the vein material in meteorites, has potential to preserve organic compounds for millions of years (BLYTH *ET AL.* 2010). Indeed, NASA's robotic missions on Mars have targeted sulfates, carbonates and smectites for their biopreservation potential; these are the typical secondary minerals that occur inside meteorites.

The experiments reported in Chapter 5 showed that when the chemolithoautotrophic organism, *A. ferrooxidans*, is cultivated on freshly fallen LL chondritic material, it will oxidise sulfur first but as Ferrous iron builds up in media, from the leaching of FeNi-alloys a metabolism switch occurs where the organisms prefers to catalyse iron for energy. This preference for Fe over S oxidation has previously been predicted using gene analysis (YARZÁBAL *ET AL.* 2004). The consequence is that *A. ferrooxidans* imparted an isotopic biosignature from the initial stages of the leaching process, which lead to multiple intermediary sulfur speciation, and $^{32}\text{SO}_2$ degassing. This resulted in a positive $\delta^{34}\text{S}$ biosignature. We also found a similar heavy $\delta^{34}\text{S}$ isotope signature in the alteration products of two Nullarbor meteorites. Indicating some level of biogenic sulfur/metal cycling had taken place.

6.1.2 Application to the Search for Life on Mars

Although establishing a terrestrial baseline occupied the majority of work in this thesis, the ultimate goal was to develop a feasible way of reducing ambiguity in detecting chemical and isotopic biosignatures in environments where geochemical context is still being established, such as the surface of Mars. The classic way to remove uncertainty in geomicrobiology experiments is by using a standard substrate of known chemical and/or isotopic composition. Chapters 1, 2, and 5 suggest that meteorites make very good standard substrates owing to their narrow ranges of mineralogical and isotopic composition. Indeed, this is why meteorites are commonly used as chemical baselines in geochemistry (e.g., Vienna Canyon Diablo Troilite (VCDT) as a stable sulfur isotope standard, CI elemental normalisation). Ordinary chondrites have been found on the surface of Mars (SCHRÖDER *ET AL.* 2016) and could be analysed in situ with rover instrumentation, or targeted for sample return, to test for the fingerprints of life beyond Earth. The mechanisms by which this could be achieved using rover instrumentation are discussed in Chapter 2. Here, I present how the terrestrial observations gathered in this thesis can be applied to our current understanding of Mars, and how putative microorganisms might colonise or have colonised meteorites on Mars.

Mars predominantly has a basaltic crust (CARR AND HEAD 2010). The composition of martian meteorites indicates that this basalt is comprised of varying proportions of mainly orthopyroxene $[(\text{Fe,Mg})_2\text{Si}_2\text{O}_6]$, augite $[(\text{Ca,Na})(\text{Mg,Fe,Al,Ti})(\text{Si,Al})_2\text{O}_6]$, pigeonite $[(\text{Mg,Fe,Ca})(\text{MgFe})\text{Si}_2\text{O}_6]$, olivine $[(\text{Mg,Fe})_2\text{SiO}_4]$, plagioclase $[(\text{Na,Ca})(\text{Si,Al})_4\text{O}_8]$, and pyrrhotite $[\text{Fe}_{1-x}\text{S}]$. This mafic composition is similar in many ways to that of chondrites, including the list of possible electron donors that could be used by chemolithoautotrophic organisms (e.g., Fe, Ni and S in FeNi-alloys and sulfides). If there is currently an extant deep subterranean biosphere on Mars (e.g., Michalski et al. (2013)), it could comprise chemolithoautotrophic organisms that are well adapted for life in meteorites because there are likely no alternative energy sources beneath the surface. Michalski et al. (2013) proposed that a putative biosphere could be using H^+ and CH_4 generated by serpentinisation reactions in deep underground aquifers. Recent discoveries on Mars hint at episodic release of groundwater from crater walls (OJHA *ET AL.* 2015), although some scientists disagree with this conclusion (DUNDAS *ET AL.* 2015). Such groundwater seeps could transport members of a deep biosphere into a meteorite at the surface of Mars.

Mars has not had large standing bodies of water at its surface for a long time (~3 Ga; (CARR AND HEAD 2010)). Some meteorites currently on Mars could have fallen to its surface as far back as the Hesperian/Noachian transition, ~3.7 billion years ago (BLAND AND SMITH 2000; SCHRÖDER *ET AL.* 2016). Given the long residence time of stony meteorites on the martian surface, it is more likely that meteorites would preserve evidence of life from the past than extant life. Because meteorites fall to the martian surface at different times, they could record ecological snapshots through the history of Mars, in a similar fashion to caves on Earth, trapping megafauna unfortunate enough to fall into them (AYLIFFE *ET AL.* 2008). As observed in Chapter 3, microbes could be entombed in layers of alteration minerals. Combined with the potential of meteorites to record climatic transitions on Mars (ASHLEY *ET AL.* 2011A), they could be used as both astrobiological and paleoenvironmental tools.

Other mechanisms might transport and mobilise water at the surface of Mars. For instance, rampart craters show evidence of impact heating of subterranean ice (WOHLETZ AND SHERIDAN 1983). Some meteorites would be buried beneath rampart ejecta, but would rarely be re-exposed to allow rover analysis. However, long-lived hydrothermal systems produced by large impacts (ABRAMOV AND KRING 2005; OSINSKI *ET AL.* 2013) could provide brines carrying biota to the surface. Another way organisms and water could enter into meteorites is via burial by sand dunes; such dunes are thought to have once covered the meteorites on Meridiani Planum (ASHLEY *ET AL.* 2011A). Given the atmospheric pressure at the current surface, a layer of regolith ~1 m deep or more could keep water ice stable for $10^2 - 10^3$ years (BRYSON *ET AL.* 2008). Deeper cover by regolith could allow water ice to last over major obliquity changes on Mars ~400 ka (BRYSON *ET AL.* 2008). With the migration of sand dunes and the cycling of H₂O into the regolith, a buried meteorite could collect a large amount of water ice within regolith, which could contribute to the internal weathering of a meteorite long after the sand dune has migrated away.

Once inside the meteorites, microbes would find similar mineralogy to the subterranean basalt as previously discussed. However, the chances of survival would be slim today, depending on extremophilic adaptations to low atmospheric pressure, oxidative stress from perchlorate salts and extremely dry conditions. Chapter 4 shows that a few niche organisms dominate the community structure inside meteorites on Earth. I would expect this trend to also exist on Mars, if microorganisms evolved there, as only extremophiles with the right adaptations could make use of a meteorite as a habitat

in this setting. If the putative organisms were iron or sulfur-oxidisers, they could metabolise and utilise reduced Fe, Ni and S in minerals for energy. Abiotic and biotitic weathering of meteorites also produces sulfate minerals, which could provide electron acceptors for possible sulfate reducing organisms as well.

The low albedo of many meteorites means that they would absorb heat better than the surrounding regolith (WIERZCHOS *ET AL.* 2013), which could make temperature conditions inside meteorites less extreme. Water vapour from the atmosphere would be adsorbed or absorbed to the hygroscopic weathering minerals as discussed in Chapter 2, albeit to a lesser extent than on Earth (given that the partial pressure of H₂O gas on Mars is 1/10,000th of that on Earth; resulting in a total precipitation potential of 10 μm (MALTAGLIATI *ET AL.* 2011). Organisms could use these hygroscopic minerals to obtain water in the desiccating martian environment. This would be more likely to have happened in the past when the martian atmosphere was thicker.

Over time, the alteration minerals in meteorites would grow to form thick efflorescences, entombing the microorganisms and biofilms, as discussed in Chapter 3. The remains of these organisms would be preserved in minerals, protected from oxidising salts such as perchlorates and the atmosphere. Although UV degradation could break down organic biomolecules into a kerogen-like material, this would depend on the size of the meteorite.

Many of the processes described above would be identical for colonisation and preservation of hypothetical microorganisms in basaltic rocks on Mars. Our familiarity with the elemental and isotopic compositions of chondritic meteorites, gained from extensive study on Earth, is what makes them valuable and deserving of our attention on Mars.

The Mars Science Laboratory (MSL) rover, Curiosity, is partway through its mission to assess the habitability of the martian surface. Its largest payload is the Science Analysis at Mars (SAM) suite of instruments, which can perform chemical, and isotope analysis of pyrolysed samples of the atmosphere and solids. However, what is relevant to my thesis is that the Quadrupole Mass Spectrometer (QMS) in the suite can be used to measure stable sulfur isotope ratios in soils as SO₂ following pyrolysis in the SAM oven. The instrument has a low resolution for $\delta^{34}\text{S}$, giving measurement errors on the order

of $\pm 8.6\text{‰}$ (FRANZ *ET AL.* 2011). Although this is not ideal for measurement of small stable sulfur isotope fractionations caused by assimilatory sulfur reduction, it could be used to measure the larger fractionations associated with dissimilatory sulfur reduction, which can be as high as $\Delta^{34}\text{S}_{(\text{Sulfate-Sulfide})} +46\text{‰}$ (CANFIELD AND TESKE 1996). If evidence of near-complete oxidation of sulfide minerals in a meteorite were identified on Mars, it would be possible to drill into the meteorite and employ the CheMin instrument to identify alteration phases and remnant troilite, which could affect the $\delta^{34}\text{S}$ value of the sample. Providing no troilite remains, this sample could then be passed into SAM for analysis. If no microbial mediated alteration of S-bearing minerals had taken place, the $\delta^{34}\text{S}$ value should be $\sim 0 \pm 8.6\text{‰}$. However, if there is a detectable increase in heavier ^{34}S in the sample relative meteoritic troilite, this could be interpreted as evidence for dissimilatory sulfur reduction or a similar biological process (i.e., $^{32}\text{SO}_2$ escape during sulfur oxidation (BRUNNER *ET AL.* 2008)). If stable sulfur isotopic signatures that are consistent with biological processes were observed in meteorites, these meteorites could then be targeted for sample return and further analysis on Earth.

6.1.3 Future Research Directions and Applications

The research presented in this thesis focused on sulfur isotope biosignatures and fossilisation of microorganisms in chondrites. But other biosignatures, such biogenic trace organics, and the use of other isotope systems should be examined in order to cast a wider net over indicators of known biological processes on Earth. Future work could also concentrate on understanding biosignatures found in other types of meteorites (e.g., carbonaceous and iron meteorites) and those produced by different metabolisms (e.g., heterotrophy).

6.1.3.1 Functional Gene Analysis

The 16S rRNA gene analysis employed here is useful for understanding the ecology and diversity of organisms in a community, but does not shed light on the function of organisms. The technique did find OTUs affiliated with known iron- and sulfur-reducing organisms *Geobacter spp* and *Desulfovibrio spp*, within the meteorites found on the Nullarbor. However to be certain of their metabolism functional gene analysis would be required to examine whether there are indeed chemolithoautotrophic organisms utilising sulfur or iron in meteorites for their metabolism. This could be done with a polymerase chain reaction (PCR) approach by amplifying previously identified genes associated with sulfur oxidation

such as the *soxB* gene (TOURNA *ET AL.* 2014). Other useful metabolisms to explore for include iron oxidation or reduction and sulfur reduction. By comparing results for meteorites and soils, we could have a better understanding of whether microbes are using meteorites as a source of energy and nutrients, or merely as a source of water – like an environmental lifeboat.

6.1.3.2 Putative Heterotrophic Metabolisms on Mars

Much of this thesis has focused on chemolithoautotrophic organisms for reasons discussed in Chapters 2 and 5. However, little attention has been paid to the possibility of heterotrophy on Mars. Heterotrophic organisms cannot fix inorganic sources of carbon, relying on organic sources instead. As a consequence, they require autotrophs to fix inorganic carbon for them, and thus would have evolved after the chemolithoautotrophs. It is possible that a putative biosphere on Mars might have been sufficiently complex to support heterotrophs, but life would need to have persisted for some time for this capability to evolve. Previous experiments have shown that carbonaceous meteorites – specifically Murchison (CM2) – contains ~1.5 wt.% macromolecular organic carbon as well as smaller molecules such as abundant acetate, amino acids, and sugars (SEPHTON 2002). This has led some researchers to hypothesise that meteorites delivered important ingredients for the origin of life on Earth (PASEK AND LAURETTA 2008; PEARCE AND PUDRITZ 2016). Others have shown that the organics in carbonaceous meteorites can support the growth of heterotrophic microorganisms (MAUTNER 1997). Thus, meteorites could make good habitats for possible heterotrophic life on Mars.

6.1.3.3 Carbonaceous Meteorites on Mars

Carbonaceous meteorites, as mentioned in Chapter 2, have highly variable $\delta^{34}\text{S}$ values that make them unsuitable for detection of readily interpretable sulfur isotope biosignatures using the methods laid out in this thesis. But, if they could be found on the surface of Mars, they would still be of use as a standard for organic molecules. Carbonaceous meteorites and micrometeorites on the martian surface are probably the greatest reservoir of organic matter on the surface of Mars today. Indeed, carbonaceous meteorites are believed to be a source of contamination in organic analysis carried out on rover missions (MING *ET AL.* 2014). Return of a carbonaceous meteorite from Mars to Earth would provide an unprecedented look at how organics degrade (or are preserved) in the martian environment (e.g., ionizing radiation, perchlorate oxidation, oxidative digenesis) (BENNER *ET AL.* 2000; KMINEK

2006; KOUNAVES *ET AL.* 2014). It would be useful to juxtapose our detailed understanding of the organic inventories of terrestrially resident organic meteorites with those resident on Mars (SEPHTON 2002). Given that many biological organic molecules overlap with meteorite organic molecule inventories (e.g., amino acids, sugars), we could use this similarity to understand how putative biological organics in the martian environment behave.

6.1.3.4 Iron Meteorites on Mars

The vast majority of meteorites found on Mars thus far have been iron meteorites, although a small number of stony meteorites have been reported (ASHLEY 2015; SCHRÖDER *ET AL.* 2016). The lack of porosity in iron meteorites (CONSOLMAGNO AND BRITT 1998) and the absence of silicate minerals (that can weather to produce the abundant hygroscopic minerals found in ordinary chondrites) could be a hindrance to organisms seeking to colonise such meteorites on Mars. Some of the iron meteorites found on Mars show evidence of hydrous alteration (ASHLEY *ET AL.* 2011A), indicating they may record evidence of past climatic histories on Mars (ASHLEY *ET AL.* 2011B). Moreover many of the iron meteorites found on Mars appear to have hollowed out interiors (e.g., Mackinac Island, Shelter Island) (ASHLEY *ET AL.* 2011A). Chapter 2 discusses the idea of a humidity oasis within chondrites, causing their interiors to be more oxidised and weathered compared to their exteriors. The same thing could be happening to the meteorites on Mars. Despite the lack of silicates to make hygroscopic minerals, Fe^0 could bind with Cl^- species sourced from the regolith to make lawrencite $[\text{FeCl}_2]$, a highly hygroscopic salt (ZURFLUH *ET AL.* 2013). Such hygroscopic minerals could be driving a weathering front from the regolith up into the meteorite, given that the regolith is known to control cycling of much of the planet's water vapour (AUDOUARD *ET AL.* 2014). Such hygroscopic weathering surfaces are prime places to look for life (DAVILA *ET AL.* 2010), and the redox gradient could provide energy for chemolithoautotrophic organisms as discussed in Chapter 2.

6.1.3.5 Application to the Study of Life on Early Earth

The meteorite flux to Earth during the Hadean and Achaean eons was much greater than today (ABRAMOV AND MOJZSIS 2009; JOHNSON AND BOWLING 2014). It is thought that life developed on Earth over the same time period (NUTMAN *ET AL.* 2016) and that all life on our planet stems from chemolithoautotrophic and thermophilic organisms (DI GIULIO 2001) that utilized inorganic gasses

and minerals around hydrothermal systems. Reduced minerals precipitate from the fluids released from modern deep ocean vents, renewing redox potential at the sea floor. In this sense, the FeNi alloy and sulfide minerals found in meteorites are similar to those found at deep ocean vents, and can act as electron donors for organisms with sulfur (SIEVERT *ET AL.* 2008) or iron-based metabolisms. As such, the abundant provision of meteorites and micrometeorites to the early Earth could have played a role in the development of these deep sea metabolisms in the past by providing an additional source of electron donors (GRONSTAL *ET AL.* 2009).

6.1.3.6 Applications to Asteroid Mining

The corporate world is now looking towards space for future resources (LEWICKI *ET AL.* 2013). Two main commodities have been identified (SONTER 1997): (1) Water, for use as rocket fuel, oxygen, radiation shielding, and electrical power and (2) Platinum Group Elements (PGEs) which have a variety of uses but are rare on Earth, and largely engineered out of our technology due to their high price. Companies such as Planetary Resources™ and Deep Space Industries™ aim to establish the space water market first, to refuel satellites and drive further expansion. If this were successful PGE mining would soon follow.

Microbes have only recently been used in terrestrial mining to catalyse the leaching of metals from ore by the production of acid from sulfide oxidation (ROHWERDER *ET AL.* 2003). Prior to their use, large volumes of acid were used to accelerate the leaching process. In the future, space mining will have to look at novel ways to leach metals from asteroid materials, and like ore bodies on Earth, different asteroids will need different extraction processes. Transporting large quantities of highly concentrated acid into space may not be economically viable. Sulfuric acid [H_2SO_4] can be produced by the oxidation of troilite [FeS] in meteorites; chemolithoautotrophic Fe and S oxidisers such as those used in Chapter 5 could catalyse this reaction by the introduction of space deployed bioleaching tanks. As the space water market is likely to be established before the mining of PGEs, space-derived water could be harvested from volatile rich asteroids and hydrolysed to make O_2 and H_2 (SONTER 1997). The oxygen could be used as an electron acceptor in conjunction with chemolithoautotrophic organisms to leach metals from chondritic meteorites such as PGEs, which partition into the FeNi alloys (HIRATA AND NESBITT 1997), in equilibrated bodies. If CO_2 cannot be obtained from PGE-rich meteorites, organic rich volatiles such as those found in carbonaceous asteroids could provide a

source of carbon for microbial biomass instead (MAUTNER 1997). This thesis provides perhaps the most detailed examination of how chemolithoautotrophic organisms can facilitate the leaching of iron and nickel in chondritic material (Chapter 5), as well as a glimpse of the buffering effect silicates could play in neutralizing the acid generated (Chapter 2). In the future, understanding how microbes can live in chondritic material may be vital to a commercial space economy.

6.2 Concluding Remarks

The ultimate result of this thesis is to establish a new branch of astrobiology, which is the interaction of extra-terrestrial materials with an extant biosphere. Much of the literature surrounding the connection between life and meteorites has focused on three main areas: (1) the transfer of life between planets via panspermia, (2) the passive role of meteorites in delivering organic molecules to the pre-biotic Earth, and (3) the role of meteorites in bringing about mass extinction through asteroid impacts. However, this thesis demonstrates that it is almost certain that meteorites have interacted with Earth's microbial biosphere throughout its history, and still do today. Ancient meteorite–biosphere interactions could provide a research opportunity for exploring the evolution of microbial metabolisms on Earth.

Because meteorites are ubiquitous throughout the solar system, we can use what we learn from hypothetical biosphere–meteorite interactions on other planets, such as Mars, in an effort to find putative life beyond Earth. We have sufficient understanding of the age of the martian surface and the rates at which meteorites weather to determine whether a putative biosignature in a chondritic meteorite on Mars was produced 3.5 billion years ago, when Mars was last wet, or during modern interaction with seasonal brine. Meteorites on Mars are ‘witness plates’ to the environment around them, and maybe even a putative-biosphere. In order to fit meteorites into existing work on the effort to find ‘special regions’ on Mars where life could exist (BEATY *ET AL.* 2006; RUMMEL *ET AL.* 2014), meteorites would fit the criteria of ‘uncertain regions’ at this time. This makes meteorites the one isotopic and chemical constant with which to test ideas of microbial colonisation throughout martian history.

Field-based and experimental results presented in this thesis demonstrate that stable sulfur isotopic biosignatures are detectable in meteorites from the Nullarbor Plain (Chapter 5). Our ^{16}S phylogenetic analysis has shown that organisms that have close affiliation with iron and sulfur cycling bacteria

live in these meteorites (Chapter 4). We have also shown that the weathering products of chondritic meteorites make them more habitable over time (Chapter 2): hygroscopic minerals adsorb bioavailable water to their surfaces in desiccating environments and oxidation of reduced minerals affords more diverse energy sources for chemolithotrophs and possibly even heterotrophic microorganisms (Chapter 2). The silicate, oxide, carbonate and sulfate weathering products of chondritic meteorites can trap fossil microorganisms (Chapter 3) and organics for potentially millions of years. No other known environment on Mars – that is accessible to rovers – contains sulfate, clay, and carbonate minerals, redox gradients, and a supply of organics within hundreds of micrometres of each other.

6.3 Chapter 6 References

A

- Abramov O., and Kring D. A. (2005) Impact-induced hydrothermal activity on early Mars. *Journal of Geophysical Research*, 110: E12S09.
- Abramov O., and Mojzsis S. J. (2009) Microbial habitability of the Hadean Earth during the late heavy bombardment. *Nature*, 459: 419-422.
- Ashley J. W. (2015) The Study of Exogenic Rocks on Mars — an Evolving Subdiscipline in Meteoritics. In: *Elements*, pp 10-11.
- Ashley J. W., Golombek M. P., Christensen P. R., Squyres S. W., McCoy T. J., Schröder C., Fleischer I., R J. J. J., Herkenhoff K. E., and Parker T. J. (2011a) Evidence for mechanical and chemical alteration of iron-nickel meteorites on Mars: Process insights for Meridiani Planum. *Journal of Geophysical Research: Biogeosciences* (2005–2012), 116.
- Ashley J. W., Huss G. R., Chappelow J. E., Golombek M. P., Velbel M. A., Ruff S. W., Schoder C., Farrand W. H., Durda D. D., Bland P. A. and others. (2011b) The scientific rationale for studying metoerites found on other worlds. In: *Visions and Voyages for Planetary Science in the Decade 2013-2022*. *National Academies Press*, pp 400.
- Audouard J., Poulet F., Vincendon M., Milliken R. E., Jouglet D., Bibring J. P., Gondet B., and Langevin Y. (2014) Water in the Martian regolith from OMEGA/Mars Express. *Journal of Geophysical Research: Planets*, 119: 1969-1989.
- Ayliffe L. K., Prideaux G. J., Bird M. I., Grün R., Roberts R. G., Gully G. A., Jones R., Fifield L. K., and Cresswell R. G. (2008) Age constraints on Pleistocene megafauna at Tight Entrance Cave in southwestern Australia. *Quaternary Science Reviews*, 27: 1784-1788.

B

- Beaty D. W., Carr M., Abell P., Barnes J., Boston P. J., Brinckerhoff W., Charles J., Delory G., Head J. W., Heldmann J. L. and others. (2006) Findings of the Mars Special Regions Science Analysis Group. *Astrobiology*, 6: 677-732.
- Benner S. A., Devine K. G., Matveeva L. N., and Powell D. H. (2000) The missing organic molecules on Mars. *Proceedings of the National Academy of Sciences of the United States of America*, 97: 2425-2430.
- Bland P., and Smith T. B. (2000) Meteorite accumulations on Mars. *Icarus*, 144: 21-26.
- Bland P. A., Zolensky M. E., Benedix G. K., and Sephton M. A. (2006) Weathering of chondritic meteorites. In: *Meteorites and the Early Solar System II*. edited by DS Lauretta and HY McSween, *University of Arizona Press*, Tucson, pp 943.
- Blyth A. J., Watson J. S., Woodhead J., and Hellstrom J. (2010) Organic compounds preserved in a 2.9 million year old stalagmite from the Nullarbor Plain, Australia. *Chemical Geology*, 279: 101-105.

- Brunner B., Yu J.-Y., Mielke R. E., MacAskill J. A., Madzunkov S., McGenity T. J., and Coleman M. (2008) Different isotope and chemical patterns of pyrite oxidation related to lag and exponential growth phases of *Acidithiobacillus ferrooxidans* reveal a microbial growth strategy. *Earth and Planetary Science Letters*, 270: 63-72.
- Bryson K., Chevrier V., Sears D., and Ulrich R. (2008) Stability of ice on Mars and the water vapor diurnal cycle: Experimental study of the sublimation of ice through a fine-grained basaltic regolith. *Icarus*, 196: 446-458.
- Burchell M. J. (2004) Panspermia today. *International Journal of Astrobiology*, 3: 73-80.

C

- Canfield D. E., and Teske A. (1996) Late Proterozoic rise in atmospheric oxygen concentration inferred from phylogenetic and sulphur-isotope studies. *Nature*, 382: 127-132.
- Carr M. H., and Head J. W. (2010) Geologic history of Mars. *Earth and Planetary Science Letters*, 294: 185-203.
- Consolmagno G. J., and Britt D. T. (1998) The density and porosity of meteorites from the Vatican collection. *Meteoritics & Planetary Science*, 33: 1231-1241.

D

- Davila A. F., Duport L. G., Melchiorri R., Jänchen J., Valea S., de los Ríos A., Fairén A. G., Möhlmann D., McKay C. P., Ascaso C. and others. (2010) Hygroscopic salts and the potential for life on Mars. *Astrobiology*, 10: 617-628.
- Di Giulio M. (2001) The universal ancestor was a thermophile or a hyperthermophile. *Gene*, 281: 11-17.
- Dundas C. M., Diniega S., and McEwen A. S. (2015) Long-term monitoring of martian gully formation and evolution with MRO/HiRISE. *Icarus*, 251: 244-263.

F

- Franz H. B., Mahaffy P. R., Kasprzak W., Lyness E., and Raaen E. (2011) Measuring sulfur isotope ratios from solid samples with the Sample Analysis at Mars instrument and the effects of dead time corrections. *42nd Lunar Planetary Science Conference*.

G

- Gronstal A., Pearson V., Kappler A., Dooris C., Anand M., Poitrasson F., Kee T. P., and Cockell C. S. (2009) Laboratory experiments on the weathering of iron meteorites and carbonaceous chondrites by iron-oxidizing bacteria. *Meteoritics & Planetary Science*, 44: 233-247-15.

H

Hirata T., and Nesbitt R. W. (1997) Distribution of platinum group elements and rhenium between metallic phases of iron meteorites. *Earth and Planetary Science Letters*, 147: 11-24.

J

Janssen P. H. (2006) Identifying the Dominant Soil Bacterial Taxa in Libraries of 16S rRNA and 16S rRNA Genes. *Applied and Environmental Microbiology*, 72: 1719-1728.

Johnson B. C., and Bowling T. J. (2014) Where have all the craters gone? Earth's bombardment history and the expected terrestrial cratering record. *Geology*: G35754.1.

Jones B. (2010) Microbes in caves: agents of calcite corrosion and precipitation. *Geological Society*, 336: 7-30.

K

Kminek G. (2006) The effect of ionizing radiation on the preservation of amino acids on Mars. *Earth and Planetary Science Letters*, 245: 1-5.

Kounaves S. P., Chaniotakis N. A., Chevrier V. F., Carrier B. L., Folds K. E., Hansen V. M., McElhoney K. M., O'Neil G. D., and Weber A. W. (2014) Identification of the perchlorate parent salts at the Phoenix Mars landing site and possible implications. *Icarus*, 232: 226-231.

L

Lewicki C., Diamandis P., Anderson E., Voorhees C., and Mycroft F. (2013) Planetary Resources—The Asteroid Mining Company. *New Space*, 1: 105-108.

M

Maltagliati L., Montmessin F., Fedorova A., Korablev O., Forget F., and Bertaux J. L. (2011) Evidence of water vapor in excess of saturation in the atmosphere of Mars. *Science*, 333: 1868-1871.

Mautner M. N. (1997) Biological potential of extraterrestrial materials—1. Nutrients in carbonaceous meteorites, and effects on biological growth. *Planetary and Space Science*, 45: 653-664.

Michalski J. R., Cuadros J., Niles P. B., Parnell J., Rogers A. D., and Wright S. P. (2013) Groundwater activity on Mars and implications for a deep biosphere. *Nature Geoscience*, 6: 133-138.

Ming D. W., Archer P. D., Glavin D. P., Eigenbrode J. L., Franz H. B., Sutter B., Brunner A. E., Stern J. C., Freissinet C., McAdam A. C. and others. (2014) Volatile and Organic Compositions of Sedimentary Rocks in Yellowknife Bay, Gale Crater, Mars. *Science*, 343: 1245267-1245267.

N

- Nutman A. P., Bennett V. C., Friend C. R. L., Van Kranendonk M. J., and Chivas A. R. (2016) Rapid emergence of life shown by discovery of 3,700-million-year-old microbial structures. *Nature*, 537: 535-538.

O

- Ojha L., Wilhelm M. B., Murchie S. L., McEwen A. S., Wray J. J., Hanley J., Massé M., and Chojnacki M. (2015) Spectral evidence for hydrated salts in recurring slope lineae on Mars. *Nature Geoscience*, 8: 829-832.
- Osinski G. R., Tornabene L. L., Banerjee N. R., Cockell C. S., Flemming R., Izawa M. R. M., McCutcheon J., Parnell J., Preston L. J., Pickersgill A. E. and others. (2013) Impact-generated hydrothermal systems on Earth and Mars. *Icarus*, 224: 347-363.

P

- Pasek M., and Lauretta D. S. (2008) Extraterrestrial flux of potentially prebiotic C, N, and P to the early earth. *Origins of life and evolution of the biosphere: The journal of the International Society for the Study of the Origin of Life*, 38: 5-21.
- Pearce B., and Pudritz R. (2016) Meteorites and the RNA World: A Thermodynamic Model of Nucleobase Synthesis within Planetesimals. *Astrobiology*, 16: 853-872.

R

- Rohwerder T., Gehrke T., Kinzler K., and Sand W. (2003) Bioleaching review part A. *Applied Microbiology and Biotechnology*, 63: 239-248.
- Rummel J. D., Beaty D. W., Jones M. A., Bakermans C., Barlow N. G., Boston P. J., Chevrier V. F., Clark B. C., de Vera J.-P. P., Gough R. V. and others. (2014) A New Analysis of Mars “Special Regions”: Findings of the Second MEPAG Special Regions Science Analysis Group (SR-SAG2). *Astrobiology*, 14: 887-968.

S

- Schröder C., Bland P. A., Golombek M. P., Ashley J. W., Warner N. H., and Grant J. A. (2016) Amazonian chemical weathering rate derived from stony meteorite finds at Meridiani Planum on Mars. *Nature Communications*, 7: 13459.
- Sephton M. A. (2002) Organic compounds in carbonaceous meteorites. *Natural Product Reports*, 19: 292-311.

- Sievert S. M., Hügler M., Taylor C. D., and Wirsén C. O. (2008) Sulfur Oxidation at Deep-Sea Hydrothermal Vents. In: Microbial Sulfur Metabolism, *Springer Berlin Heidelberg*, pp 238-258.
- Sonter M. J. (1997) The technical and economic feasibility of mining the near-earth asteroids. *Acta Astronautica*, 41: 637-647.
- Steele A., Goddard D. T., Stapleton D., Toporski J. K. W., Peters V., Bassinger V., Sharples G., Wynn-Williams D. D., and McKay D. S. (2000) Investigations into an unknown organism on the martian meteorite Allan Hills 84001. *Meteoritics & Planetary Science*, 35: 237-241.
- Steinhauer E. S., Omelon C. R., and Bennett P. C. (2010) Limestone corrosion by neutrophilic sulfur-oxidizing bacteria: A coupled microbe-mineral system. *Geomicrobiology Journal*, 27: 723-738.

T

- Tourna M., Maclean P., Condron L., O'Callaghan M., and Wakelin S. A. (2014) Links between sulphur oxidation and sulphur-oxidising bacteria abundance and diversity in soil microcosms based on soxB functional gene analysis. *FEMS Microbiology Ecology*, 88: 538-549.

W

- Webb J. A., and James J. M. (2006) Karst evolution of the Nullarbor Plain, Australia. *Geological Society of America Special Paper*, 404: 65-78.
- Wierzchos J., de los Ríos A., and Ascaso C. (2013) Microorganisms in desert rocks: the edge of life on Earth. *International Microbiology*, 15: 172-182.
- Wilson S. A., and Bish D. L. (2011) Formation of gypsum and bassanite by cation exchange reactions in the absence of free-liquid H₂O: Implications for Mars. *Journal of Geophysical Research*, 116: E09010.
- Wohletz K. H., and Sheridan M. F. (1983) Martian rampart crater ejecta - Experiments and analysis of melt-water interaction. *Icarus* (ISSN 0019-1035), 56: 15-37.

Y

- Yarzabal A., Appia-Ayme C., Ratouchniak J., and Bonnefoy V. (2004) Regulation of the expression of the *Acidithiobacillus ferrooxidans* rus operon encoding two cytochromes c, a cytochrome oxidase and rusticyanin. *Microbiology* (Reading, England), 150: 2113-2123.

Z

Zurfluh F. J., Hofmann B. A., Gnos E., and Eggenberger U. (2013) “Sweating meteorites”—Water-soluble salts and temperature variation in ordinary chondrites and soil from the hot desert of Oman. *Meteoritics & Planetary Science*, 48: 1958-1980.

Appendix I

Data processing and analysis commands used in
MOTHUR for Chapter 4.

Appendix I: Table 1| Indicator Species list and Iron/Sulfur Cycling Species

Top 25 OTUs							
<i>OTU</i>	<i>%ID</i>	<i>#Accession</i>	<i>BLAST Identity</i>	<i>LogMaxMean[§]</i>	<i>Class[★]</i>	<i>LDA[*]</i>	<i>p Value</i>
OTU1	98%	CP007514.1	<i>Rubrobacter radiotolerans</i>	5.174	Meteorite	4.818	0.034
OTU2	96%	CP007514.1	<i>Rubrobacter radiotolerans</i>	4.693	Meteorite	4.370	0.034
OTU3	98%	CP002408.1	<i>Nitrososphaera gargensis</i>	4.576	-	-	-
OTU4	86%	DQ812549.1	Chloroflexi Bacterium Ver9Iso1	4.700	Soil	4.427	0.034
OTU5	99%	LN626276.1	<i>Blastococcus</i> sp.	4.425	Meteorite	3.926	0.034
OTU6	100%	LN626270.1	<i>Geodermatophilus pulveris</i>	4.388	Meteorite	3.969	0.034
OTU7	94%	AY234727.1	<i>Blastococcus</i> sp.	4.301	-	-	-
OTU8	98%	KU290365.1	<i>Nitrosocosmicus franklandus</i>	4.056	-	-	-
OTU9	90%	NR_125642.1	<i>Kallotenue papyrolyticum</i>	4.497	Soil	4.236	0.019
OTU10	89%	NR_117433.1	<i>Rubellimicrobium</i> sp.	4.395	-	-	-
OTU11	97%	KT581436.1	<i>Patulibacter brassicae</i>	3.844	-	-	-
OTU12	91%	DQ812549.1	Chloroflexi #Ver9Iso1	3.997	Meteorite	3.571	0.028
OTU13	98%	NR_133858.1	<i>Solirubrobacter phytolaccae</i>	3.878	-	-	-
OTU14	90%	NR_074501.1	<i>Acidothermus cellulolyticus</i>	4.053	Soil	3.789	0.019
OTU15	99%	KU258211.1	<i>Blastococcus jejuensis</i>	4.000	Meteorite	3.553	0.034
OTU16	98%	AB461094.1	Nocardiodaceae #IK2_56P	3.884	-	-	-
OTU17	95%	KP326333.1	<i>Sphingosinicella</i> sp.	3.937	-	-	-
OTU18	94%	NR_042722.1	<i>Solirubrobacter pauli</i>	3.980	-	-	-
OTU19	99%	KX990261.1	Frankiales (Unclassified)	3.933	Meteorite	3.650	0.034
OTU20	88%	NR_074501.1	<i>Acidothermus cellulolyticus</i>	3.758	-	-	-
OTU21	94%	NR_043156.1	<i>Deinococcus navajonensis</i>	3.929	Meteorite	3.550	0.034
OTU22	89%	KJ535408.1	Candidatus Hydrogenedentes	4.176	-	-	-
OTU23	99%	NR_117640.1	<i>Rubrobacter</i> sp.	3.917	Meteorite	3.706	0.032
OTU24	98%	KU290365.1	<i>Nitrosocosmicus franklandus</i>	3.964	-	-	-
OTU25	91%	NR_118138.1	<i>Gaiellaceae gaiella</i>	4.147	Soil	3.887	0.028
Possible Metal/Sulfur Cycling OTUs							
<i>OTU</i>	<i>%ID</i>	<i>#Accession</i>	<i>BLAST Identity</i>	<i>LogMaxMean[§]</i>	<i>Class[★]</i>	<i>LDA[*]</i>	<i>p Value</i>
OTU71	100%	CP014963.1	<i>Geobacter anodireducens</i>	3.421	-	-	-
OTU264	100%	NR_074979.1	<i>Geobacter lovleyi</i>	2.864	-	-	-
OTU501	100%	KU921226.1	<i>Desulfovibrio desulfuricans</i>	2.489	-	-	-
OTU712	100%	KU201952.1	<i>Desulfovibrio</i> sp.	2.196	-	-	-
OTU730	100%	EU190359.2	<i>Desulfovibrio intestinalis</i>	2.237	-	-	-
OTU884	99%	NR_075011.1	<i>Geobacter metallireducens</i>	2.116	-	-	-
OTU1164	99%	HQ395074.1	<i>Desulfovibrio vulgaris</i>	2.050	-	-	-
OTU1518	100%	NR_028775.1	<i>Geobacter thiogenes</i>	1.860	-	-	-
OTU1812	98%	CP002297.1	<i>Desulfovibrio vulgaris</i>	1.766	-	-	-
OTU2077	99%	AF443593.1	<i>Desulfomicrobium</i> sp	1.503	-	-	-
OTU2350	98%	LC008330.1	<i>Geobacter</i> sp.	1.591	-	-	-
OTU2784	97%	GU176294.1	<i>Desulfovibrio</i> sp	1.725	-	-	-
OTU2886	96%	LC186051.1	<i>Desulfovibrio</i> sp	1.445	-	-	-
OTU4867	97%	LC008330.1	<i>Geobacter</i> sp.	1.202	-	-	-
OTU4868	96%	LC186051.1	<i>Desulfovibrio</i> sp	1.230	-	-	-
OTU7045	99%	EU190359.2	<i>Desulfovibrio</i> sp	1.178	-	-	-
OTU7098	95%	KJ459867.1	<i>Desulfovibrio desulfuricans</i>	1.418	-	-	-
OTU10078	97%	LC008330.1	<i>Geobacter</i> sp.	0.761	-	-	-
OTU10079	96%	NR_075011.1	<i>Geobacter metallireducens</i>	0.743	-	-	-
OTU12162	96%	KU201952.1	<i>Desulfovibrio</i> sp.	1.157	-	-	-
OTU12175	98%	EF055877.1	<i>Desulfovibrio</i> sp.	1.157	-	-	-
OTU12259	98%	NR_029364.2	<i>Desulfovibrio longreachensis</i>	1.002	-	-	-

* LDA = Linear Discriminant Analysis, is the effect size.

§ LogMaxMean = Is the log of the greatest class mean.

★ Class = Refers to either the meteorite or soil sample type being examined by Lefse.

Sequence Processing Commands

```
screen.seqs(fasta=MetBact.trim.pcr.trim.fasta, minlength=250, maxambig=0,
maxhomop=8)
```

```
list.seqs(fasta=MetBact.trim.pcr.trim.good.fasta)
```

```
get.seqs(group=MetBact.groups, accnos=MetBact.trim.pcr.trim.good.accnos)
```

```
unique.seqs(fasta=MetBact.trim.pcr.trim.good.fasta)
```

```
summary.seqs(fasta=MetBact.trim.pcr.trim.good.unique.fasta, processors=8)
```

```
count.seqs(name=MetBact.trim.pcr.trim.good.names, group=MetBact.pick.
groups)
```

```
summary.seqs(fasta=MetBact.trim.pcr.trim.good.unique.fasta,
count=MetBact.trim.pcr.trim.good.count_table)
```

```
align.seqs(fasta=MetBact.trim.pcr.trim.good.unique.fasta, reference=silva.
seed_v123.align)
```

```
summary.seqs(fasta=MetBact.trim.pcr.trim.good.unique.align,
count=MetBact.trim.pcr.trim.good.count_table)
```

```
screen.seqs(fasta=MetBact.trim.pcr.trim.good.unique.align, count=MetBact.
trim.pcr.trim.good.count_table, summary=MetBact.trim.pcr.trim.good.
unique.summary, minlength=250, start=28465, end=36000)
```

```
filter.seqs(fasta=MetBact.trim.pcr.trim.good.unique.good.align,
vertical=T)
```

```
unique.seqs(fasta=MetBact.trim.pcr.trim.good.unique.good.filter.fasta,  
count=MetBact.trim.pcr.trim.good.good.count_table)
```

```
pre.cluster(fasta=MetBact.trim.pcr.trim.good.unique.good.filter.unique.  
fasta, count=MetBact.trim.pcr.trim.good.unique.good.filter.count_table,  
diffs=2)
```

```
chimera.uchime(fasta=MetBact.trim.pcr.trim.good.unique.good.filter.unique.  
precluster.fasta, reference=silva.gold.align)
```

```
remove.seqs(fasta=MetBact.trim.pcr.trim.good.unique.good.filter.unique.  
precluster.fasta, count=MetBact.trim.pcr.trim.good.unique.good.filter.  
unique.precluster.count_table accnos=MetBact.trim.pcr.trim.good.unique.  
good.filter.unique.precluster.ref.uchime.accnos)
```

```
classify.seqs(fasta=MetBact.trim.pcr.trim.good.unique.good.filter.unique.  
precluster.pick.fasta, count=MetBact.trim.pcr.trim.good.unique.good.  
filter.unique.precluster.pick.count_table, reference=silva.seed_v123.  
align, taxonomy=silva.seed_v123.tax, cutoff=80)
```

```
remove.lineage(fasta=MetBact.trim.pcr.trim.good.unique.good.filter.  
unique.precluster.pick.fasta, count=MetBact.trim.pcr.trim.good.unique.  
good.filter.unique.precluster.pick.count_table, taxonomy=MetBact.trim.  
pcr.trim.good.unique.good.filter.unique.precluster.pick.seed_v123.wang.  
taxonomy, taxon=Chloroplast-Mitochondria-Eukaryota-unknown;)
```

```
cluster.split(fasta=MetBact.trim.pcr.trim.good.unique.good.filter.unique.  
precluster.pick.pick.fasta, count=MetBact.trim.pcr.trim.good.unique.good.  
filter.unique.precluster.pick.pick.count_table, taxonomy=MetBact.trim.
```



```
pcr.trim.good.unique.good.filter.unique.precluster.pick.seeed_v123.wang.  
pick.taxonomy, splitmethod=classify, taxlevel=4, cutoff=0.15)
```

```
make.shared(list=MetBact.trim.pcr.trim.good.unique.good.filter.unique.  
precluster.pick.pick.an.unique_list.list, count=MetBact.trim.pcr.  
trim.good.unique.good.filter.unique.precluster.pick.pick.count_table,  
label=0.03)
```

```
classify.otu(list=MetBact.trim.pcr.trim.good.unique.good.filter.unique.  
precluster.pick.pick.an.unique_list.list, count=MetBact.trim.pcr.  
trim.good.unique.good.filter.unique.precluster.pick.pick.count_table,  
taxonomy=MetBact.trim.pcr.trim.good.unique.good.filter.unique.precluster.  
pick.seeed_v123.wang.pick.taxonomy, label=0.03)
```

```
get.oturep(method=abundance,list=MetBact.trim.pcr.trim.good.unique.good.  
filter.unique.precluster.pick.pick.an.unique_list.list, count=MetBact.  
trim.pcr.trim.good.unique.good.filter.unique.precluster.pick.pick.  
count_table, fasta=MetBact.trim.pcr.trim.good.unique.good.filter.unique.  
precluster.pick.pick.fasta)
```

```
system(mv MetBact.trim.pcr.trim.good.unique.good.filter.unique.precluster.  
pick.pick.an.unique_list.shared MetBact.an.shared)
```

```
system(mv MetBact.trim.pcr.trim.good.unique.good.filter.unique.precluster.  
pick.pick.an.unique_list.0.03.cons.taxonomy MetBact.an.cons.taxonomy)
```

OTU Analysis

```
count.groups(shared=MetBact.an.shared)
```

```
rarefaction.single(shared=MetBact.an.shared, calc=sobs, freq=100)
```

```
summary.single(shared=MetBact.mian.shared, calc=nseqs-bootstrap-sobs-  
coverage-invsimpson-simpson-shannon-chao, subsample=T)  
heatmap.bin(shared=MetBact.an.shared, scale=linear, numotu=25)
```

```
heatmap.sim(phylip=MetBact.an.thetayc.0.03.lt.dist)mimi  
heatmap.sim(phylip=MetBact.an.jclass.0.03.lt.dist)
```

```
dist.shared(shared=MetBact.an.shared, calc=thetayc-jclass, subsample=T,  
processors=8)
```

```
sub.sample(shared=MetBact.an.shared)
```

```
nmds(phylip=MetBact.an.thetayc.0.03.lt.ave.dist)
```

```
corr.axes(shared=MetBact.an.0.03.subsample.shared, axes=MetBact.  
an.thetayc.0.03.lt.ave.nmds.axes, label=0.03)
```

```
amova(phylip=MetBact.an.jclass.0.03.lt.dist, design=MetBact.design)
```

```
amova(phylip=MetBact.an.thetayc.0.03.lt.dist, design=MetBact.design)
```


Appendix II

Additional data tables from Chapter 5.

Appendix II: Table 1| Substrate Sample Weights and Initial Sulfur Content

<i>Material</i>	<i>ID Number</i>	<i>Substrate</i>	<i>Experiment</i>	<i>Mass (g)</i>	<i>Sulfide Mass (g)</i>	<i>Sulfur Mass (g)</i>	<i>C/Co*</i>
Meteorite	1	Polished	Abiotic	1.160	0.045	0.016	5.7
Meteorite	3	Polished	Abiotic	2.184	0.085	0.031	10.8
Meteorite	5	Polished	Abiotic	1.620	0.063	0.023	8.0
Meteorite	7	Polished	Abiotic	0.637	0.025	0.009	3.1
Meteorite	9	Polished	Abiotic	1.337	0.052	0.019	6.6
Meteorite	11	Polished	Abiotic	0.313	0.012	0.004	1.5
Meteorite	13	Polished	Abiotic	1.665	0.065	0.024	8.2
Meteorite	15	Polished	Abiotic	0.968	0.038	0.014	4.8
Meteorite	17	Polished	Abiotic	1.554	0.061	0.022	7.7
Meteorite	2	Polished	Biotic	1.493	0.058	0.021	73.7
Meteorite	4	Polished	Biotic	0.807	0.031	0.011	39.8
Meteorite	6	Polished	Biotic	0.720	0.028	0.010	35.5
Meteorite	8	Polished	Biotic	0.343	0.013	0.005	16.9
Meteorite	10	Polished	Biotic	0.370	0.014	0.005	18.3
Meteorite	12	Polished	Biotic	0.613	0.024	0.009	30.2
Meteorite	14	Polished	Biotic	1.070	0.042	0.015	52.8
Meteorite	16	Polished	Biotic	1.149	0.045	0.016	56.7
Meteorite	18	Polished	Biotic	0.775	0.030	0.011	38.2
<i>Mean</i>	-	-	-	<i>1.043</i>	<i>0.041</i>	<i>0.015</i>	<i>23.3</i>
<i>Std.</i>	-	-	-	<i>0.524</i>	<i>0.020</i>	<i>0.007</i>	<i>21.6</i>
Meteorite	19	Chip	Abiotic	1.571	0.079	0.029	10.0
Meteorite	21	Chip	Abiotic	1.934	0.097	0.035	12.3
Meteorite	20	Chip	Biotic	2.463	0.123	0.045	155.6
Meteorite	22	Chip	Biotic	1.961	0.098	0.036	124.0
<i>Mean</i>	-	-	-	<i>1.982</i>	<i>0.099</i>	<i>0.036</i>	<i>75.5</i>
<i>Std.</i>	-	-	-	<i>0.367</i>	<i>0.018</i>	<i>0.007</i>	<i>75.4</i>
FeS	23	Powder	Abiotic	0.624	0.624	0.228	78.9
FeS	25	Powder	Abiotic	0.583	0.583	0.213	73.8
FeS	27	Powder	Abiotic	0.559	0.559	0.204	70.7
FeS	24	Powder	Biotic	0.524	0.524	0.191	662.9
FeS	26	Powder	Biotic	0.545	0.545	0.199	689.4
FeS	28	Powder	Biotic	0.620	0.620	0.226	784.3
<i>Mean</i>	-	-	-	<i>0.576</i>	<i>0.576</i>	<i>0.210</i>	<i>393.3</i>
<i>Std.</i>	-	-	-	<i>0.041</i>	<i>0.041</i>	<i>0.015</i>	<i>351.6</i>
FeS ₂	29	Powder	Abiotic	0.422	0.422	0.226	78.3
FeS ₂	31	Powder	Abiotic	0.452	0.452	0.242	83.9
FeS ₂	33	Powder	Abiotic	0.448	0.448	0.239	83.1
FeS ₂	30	Powder	Biotic	0.553	0.553	0.296	1019.2
FeS ₂	32	Powder	Biotic	0.474	0.474	0.253	873.6
FeS ₂	34	Powder	Biotic	0.459	0.459	0.245	846.0
<i>Mean</i>	-	-	-	<i>0.468</i>	<i>0.468</i>	<i>0.250</i>	<i>497.4</i>
<i>Std.</i>	-	-	-	<i>0.045</i>	<i>0.045</i>	<i>0.024</i>	<i>459.0</i>
FeSO ₄ ·7H ₂ O	35	Aqueous	Abiotic (Blank)	0.025	-	0.0029	1
FeSO ₄ ·7H ₂ O	36	Aqueous	Biotic (Blank)	0.003	-	0.0003	1

*C = Measured concentration of sulfate, C₀ = Initial sulfate concentration (See text for absolute value).

Appendix II: Table 2 | Powder XRD Phase Analysis Results

Mineral	Formula	Meteorite 02	Meteorite 14	Meteorite 18	Meteorite 07	Meteorite 11	FeS 25 (PelI)	FeS 27	FeS 27 (Evp)	FeS 28	FeS 28 (PelI)	FeS 28 (Evp)	FeS ₂ 30 (PelI)
		LC, CSB	LC, CSB	LC, CSB	LC, TP	LC						TP	TP
Archertite ^v K _{0.75} (NH ₄) _{0.25} H ₂ (PO ₄)													
Brushite/Gypsum Ca(HPO ₄)·2(H ₂ O) / Ca(SO ₄)·2(H ₂ O)		X	X	X		X	X						
Rhombooclase HFe ³⁺ (SO ₄) ₂ ·4(H ₂ O)					X								
Albite NaAlSi ₃ O ₈													
Alunite KAl ₃ (SO ₄) ₂ (OH) ₆									X				
Ammonium jarosite (NH ₄)Fe ³⁺ ₃ (SO ₄) ₂ (OH) ₆									X				
Anhydrite Ca(SO ₄)													X
Anorthite CaAl ₂ Si ₂ O ₈				X									
Collinsite Ca ₂ Mg _{6.75} Fe ²⁺ _{0.25} (PO ₄) ₂ ·2(H ₂ O)												X	
Ferrhydrite Fe ₁₀ ³⁺ O ₁₄ (OH) ₂ ·~H ₂ O]							X						
Ferrosilite Fe ²⁺ MgSi ₂ O ₆		X	X	X	X	X							
Forsterite Mg ₂ (SiO ₄)		X	X	X	X								
Goethite Fe ³⁺ O(OH)		X	X	X	X	X	X	X		X	X	X	X
Gypsum Ca(SO ₄)·2(H ₂ O)									X				
Hydronium jarosite (H ₃ O)Fe ³⁺ ₃ (SO ₄) ₂ (OH) ₆							X					X	
Iron Sulfate Hydroxide Fe(OH)(SO ₄)													
Jarosite KFe ³⁺ ₃ (SO ₄) ₂ (OH) ₆							X						X
Kieserite Mg(SO ₄)·(H ₂ O)								X					X
Lepidocrocite Fe ³⁺ O(OH)		X	X	X	X		X	X		X	X		
Maghemite Fe ³⁺ ₂ O ₃		X	X	X									
Melanterite ^v Fe ²⁺ (SO ₄)·7(H ₂ O)										X			
Pentahydrate Mg(SO ₄)·5(H ₂ O)							X						
Rhombooclase HFe ³⁺ (SO ₄) ₂ ·4(H ₂ O)					X								
Rozenite Fe ²⁺ (SO ₄)·4(H ₂ O)							X		X		X	X	X
Sabieite (NH ₄)Fe ³⁺ (SO ₄) ₂													X
Sulfur S								X					
Troilite FeS		X			X	X				X	X		
Volatite K ₂ Fe ²⁺ ₅ Fe ³⁺ ₃ Al(SO ₄) ₁₂ ·18(H ₂ O)									X				X
Woodhouseite CaAl ₃ (PO ₄)(SO ₄)(OH) ₆													

LC = Low Counts, CSB = Compositional Strain Broadening, TP = Tentative Phase
PelI = Pellet, Evp = Evaporite
^vPhase is recrystallised salt used in media

